

VOLUME V

SUBSYSTEM AND TECHNICAL ANALYSES

NASA CR-66139

BOOK 5

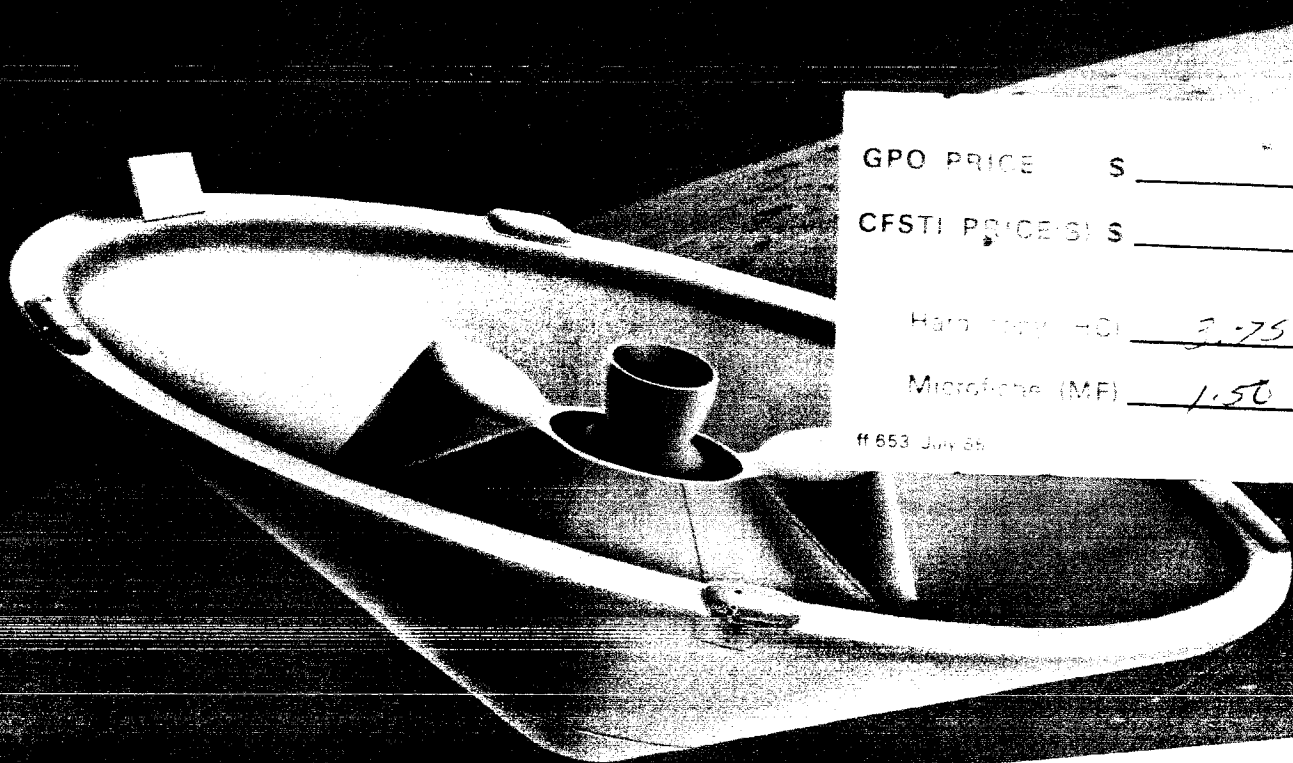
# ATTITUDE CONTROL and PROPULSION



## MARS PROBE

FINAL REPORT

CONTRACT NO. NAS 1-5224



GPO PRICE \$ \_\_\_\_\_  
CFSTI PRICE(S) \$ \_\_\_\_\_  
Hard copy (HC) 2.75  
Microfilm (MF) 1.50

ff 653 July 85

## BOOK INDEX

VOLUME I SUMMARY

VOLUME II PROBE/LANDER, ENTRY FROM THE APPROACH  
TRAJECTORY

Book 1 System Design

Book 2 Mission and System Specifications

VOLUME III PROBE, ENTRY FROM ORBIT

Book 1 System Design

Book 2 Mission, System and Component Specifications

Book 3 Development Test Programs

VOLUME IV STERILIZATION

VOLUME V SUBSYSTEM AND TECHNICAL ANALYSES

Book 1 Trajectory Analysis

Book 2 Aeromechanics and Thermal Control

Book 3 Telecommunications, Radar Systems and Power

Book 4 Instrumentation

Book 5 Attitude Control and Propulsion

Book 6 Mechanical Subsystems

COMPARATIVE STUDIES OF CONCEPTUAL  
DESIGN AND QUALIFICATION PROCEDURES  
FOR A MARS PROBE/LANDER

FINAL REPORT  
VOLUME V SUBSYSTEM AND TECHNICAL ANALYSES

Book 5 ATTITUDE CONTROL AND PROPULSION

Prepared by

SPACE SYSTEMS DIVISION  
AVCO CORPORATION  
Lowell, Massachusetts

AVSSD-0006-66-RR  
Contract NAS 1-5224

11 May 1966

Prepared for

NATIONAL AERONAUTICS AND SPACE ADMINISTRATION  
LANGLEY RESEARCH CENTER  
LANGLEY STATION  
Hampton, Virginia 23365

## PREFACE

The results of Mars Probe/Lander studies, conducted over a 10-month period for Langley Research Center, NASA, are presented in detail in this report. Under the original contract work statement, studies were directed toward a direct entry mission concept, consistent with the use of the Saturn IB-Centaur Launch Vehicle, wherein the landing capsule is separated from the spacecraft on the interplanetary approach trajectory, some 10 to 12 days before planet encounter. The primary objectives of this mission were atmospheric sampling by the probe/lander during entry and terrain and atmosphere physical composition measurement for a period of about 1 day after landing.

Studies for this mission were predicated on the assumption that the atmosphere of Mars could be described as being within the range specified by, NASA Mars Model Atmospheres 1, 2, 3 and a Terminal Descent Atmosphere of the document NASA TM-D2525. These models describe the surface pressure as being between 10 and 40 mb. For this surface pressure range a payload of moderate size can be landed on the planet's surface if the entry angle is restricted to be less than about 45 degrees.

Midway during the course of the study, it was discovered by Mariner IV that the pressure at the surface of the planet is in the 4 to 10 mb range, a range much lower than previously thought to be the case. The results of the study were re-examined at this point. It was found that retention of the direct entry mission mode would require much shallower entry angles to achieve the same payloads previously attained at the higher entry angles of the higher surface pressure model atmospheres. The achievement of shallow entry angles (on the order of 20 degrees), in turn, required sophisticated capsule terminal guidance, and a sizeable capsule propulsion system to apply a velocity correction close to the planet, after the final terminal navigation measurements.

Faced with these facts, NASA/LRC decided that the direct entry from the approach trajectory mission mode should be compared with the entry from orbit mode under the assumption that the Saturn 5 Launch Vehicle would be available. Entry of the flight capsule from orbit allows the shallow angle entry (together with low entry velocity) necessary to permit higher values of  $M/C_D A$ , and hence entry weight in the attenuated atmosphere.

It was also decided by LRC to eliminate the landing portion of the mission in favor of a descent payload having greater data-gathering capacity, including television and penetrometers. In both the direct entry and the entry from orbit cases, ballistic atmospheric retardation was the only retardation means considered as specifically required by the contract work statement.

Four months had elapsed at the time the study ground rules were changed. After this point the study continued for an additional five months, during which

period a new design for the substantially changed conditions was evolved. For this design, qualification test programs for selected subsystems were studied. Sterilization studies were included in the program from the start and, based on the development of a fundamental approach to the sterilization problem, these efforts were expanded in the second half of the study.

The organization of this report reflects the circumstance that two essentially different mission modes were studied -- the first being the entry from the approach trajectory mission mode and the other being the entry from orbit mission mode -- from which two designs were evolved. The report organization is as follows:

Volume I, Summary, summarizes the entire study for both mission modes.

Volume II reports on the results of the first part of the study. This volume is titled Probe/Lander, Entry from the Approach Trajectory. It is divided into two books, Book 1 and Book 2. Book 1 is titled System Design and presents a discursive summary of the entry from the approach trajectory system as it had evolved up to the point where the mission mode was changed. Book 2, titled Mission and System Specifications, presents, in formal fashion, specifications for the system. It should be understood, however, that the study for this mission mode was not carried through to completion and many of the design selections are subject to further tradeoff analysis.

Volume III is composed of three books which summarize the results of the entry from orbit studies. Books 1 and 2 are organized in the same fashion as the books of Volume II, except that Book 2 of Volume III presents component specifications as well. Book 3 is titled Development Test Programs and presents, for selected subsystems, a discussion of technology status, test requirements and plans. This Book is intended to satisfy the study and reporting requirements concerning qualification studies, but the selected title is believed to describe more accurately the study emphasis desired by LRC.

Volume IV presents Sterilization results. This information is presented separately because of its potential utilization as a more fundamental reference document.

Volume V presents, in six separate books, Subsystem and Technical Analyses. In order (from Book 1 to Book 6) they are:

- Trajectory Analysis
- Aeromechanics and Thermal Control
- Telecommunications, Radar Systems and Power
- Instrumentation
- Attitude Control and Propulsion
- Mechanical Subsystems

Most of the books of Volume V are divided into separate discussions of the two mission modes. Table of Contents for each book clearly shows its organization.

## CONTENTS

### INTRODUCTION

#### ATTITUDE CONTROL PROBE/LANDER, ENTRY FROM THE APPROACH TRAJECTORY

1.0	Introduction and Summary .....	1
1.1	Scope of Study .....	1
1.2	Mission Profile and Attitude Control System Requirements .....	1
1.3	Alternatives Considered .....	2
1.4	Reference Design Summary .....	2
2.0	Performance Requirements and Analysis .....	5
2.1	$\Delta V$ Accuracy Requirements versus Entry Angle .....	5
2.1.1	Flight Capsule Speedup Maneuver .....	5
2.1.2	Flight Spacecraft Slowdown Maneuver .....	7
2.2	Alternate Approaches .....	7
2.2.1	Orientation to Thrust Attitude .....	10
2.2.2	Terminal Guidance .....	10
2.3	Achievable Performance of Spin-Only Configuration .....	10
2.3.1	Description of Operation .....	11
2.3.2	Error Analysis .....	11
2.4	Achievable Performance of Active ACS Configuration .....	12
2.4.1	Description of Operation .....	12
2.4.2	Error Analysis .....	19
2.5	Achievable Performance of Active ACS System with Terminal Guidance .....	22
2.5.1	Description of Operation .....	22
2.5.2	Error Analysis .....	23
2.6	Achievable Performance of Active ACS Plus Spin System .....	24
2.6.1	Description of Operation .....	24
2.6.2	Error Analysis .....	25

## CONTENTS (Cont'd)

3.0	Selection of Reference Design Concept for 1971 Mission..	26
3.1	Criteria and Constraints .....	26
3.1.1	Basic Function.....	26
3.1.2	Criteria .....	26
3.1.3	Constraints .....	27
3.2	Comparison of Concepts and Selection of Reference Concept .....	28
3.2.1	Spin-Only System .....	28
3.2.2	Active ACS .....	29
3.2.3	Active ACS with Terminal Guidance .....	29
3.2.4	Active ACS Plus Spin System .....	29
3.2.5	Selection of Reference Concept .....	29
3.3	Intrasystem Tradeoffs For Reference Concept .....	30
3.3.1	Gyros .....	30
3.3.2	Control Logic .....	30
3.3.3	Limit Cycle .....	30
3.3.4	Reaction System.....	31
4.0	Reference Attitude Control System Description .....	32
4.1	General Description .....	32
4.2	Sensor and Electronics Subsystem .....	32
4.3	Reaction Control Subsystem .....	36
4.4	Spin Subsystem .....	43
4.5	Packaging .....	45
4.6	Alignment Subsystem .....	47
ATTITUDE CONTROL PROBE, ENTRY FROM ORBIT		
5.0	Introduction and Summary .....	48
5.1	Scope of Study .....	48
5.2	Mission Profile and Attitude Control Requirements .....	48

## CONTENTS (Cont'd)

5.2.1	Separation To Thrusting .....	48
5.2.2	Thrusting .....	48
5.2.3	Thrusting to Entry .....	48
5.2.4	Entry to Parachute Deployment .....	49
5.2.5	Parachute Descent .....	49
5.3	Alternatives Considered .....	49
5.3.1	Spin-Only System .....	49
5.3.2	Active ACS With Spin .....	50
5.3.3	Active ACS - Cold Gas .....	50
5.3.4	Active ACS With Gimballing .....	50
5.3.5	Active ACS - Cold Gas and Hot Gas .....	50
5.4	Reference Design Summary .....	50
6.0	Performance Requirements and Analysis .....	54
6.1	$\overline{AV}$ Accuracy Requirements .....	54
6.1.1	Entry-Range Dispersions .....	54
6.1.2	Entry-Angle Dispersion .....	54
6.1.3	Effect of Velocity Magnitude .....	56
6.2	TV Camera Orientation Requirements .....	56
6.3	Descent Acceleration Measurement Requirements ...	56
6.4	Wind Measurement Requirements .....	56
6.5	Alternate Approaches .....	57
6.5.1	Candidate Techniques by Mission Phase .....	57
6.5.2	Synthesis of Alternate Systems .....	58
6.6	Achievable Performance of Active ACS Plus Spin Configuration .....	60
6.6.1	Description of Operation .....	60
6.6.2	Error Analysis .....	62
6.7	Achievable Performance of Active ACS Configuration.	64
6.7.1	Description of Operation .....	64
6.7.2	Error Analysis .....	65

## CONTENTS (Cont'd)

6.8 Achievable Performance with Rate Damping .....	69
6.8.1 Description of Operation .....	69
6.8.2 Performance and Error Analysis .....	69
7.0 Selection of Reference Design Concept for 1971 Mission ...	81
7.1 Criteria and Constraints .....	81
7.1.1 Basic Function .....	81
7.1.2 Criteria .....	81
7.1.3 Basic Constraints .....	82
7.2 Comparison of Concepts and Selection of Reference Concept .....	83
7.2.1 Spin-Only System .....	83
7.2.2 Active ACS With Spin .....	83
7.2.3 Active ACS (Cold-Gas Reaction System) .....	84
7.2.4 Active ACS With Gimballing .....	84
7.2.5 Active ACS (Cold-Gas and Hot Gas) .....	84
7.2.6 Selection of Reference Concept .....	84
7.3 Intrasystem Tradeoffs for Reference Concept .....	86
7.3.1 Sensor and Electronics Subsystem .....	86
7.3.2 Reaction Control Subsystem for Attitude Control .....	86
7.3.3 Thrust Vector Control System .....	91
8.0 Reference Attitude Control System Description .....	111
8.1 Introduction .....	111
8.2 Sensor and Electronics Subsystem .....	111
8.2.1 Inertial Reference System .....	111
8.2.2 Sentry Gyro System .....	115
8.3 Reaction Control Subsystem .....	116
8.3.1 Cold-Gas System for Attitude Control .....	116
8.3.2 Hot-Gas System for TVC .....	119

## CONTENTS (Concl'd)

8.4 Packaging .....	124
8.5 TV Stable Platform .....	125
9.0 Propulsion System .....	128
9.1 Introduction and Summary .....	128
9.1.1 Scope .....	128
9.1.2 Primary Performance and Design Constraints ...	128
9.1.3 Design Summary .....	129
9.2 Probe, Entry from the Approach Trajectory .....	130
9.2.1 Performance Requirements .....	130
9.2.2 Design Requirements and Constraints .....	131
9.2.3 Solid versus Liquid Propellant Engines .....	132
9.2.4 Reference System Design .....	135
9.3 Probe, Entry From Orbit .....	136
9.3.1 Performance Requirements .....	136
9.3.2 Design Requirements and Constraints .....	139
9.3.3 Solid versus Liquid Propellant Engines .....	139
9.3.4 Reference System Design .....	139

## APPENDIXES

A Separation Dynamics .....	143
B Analytical Methods Used in Evaluation of Spin System .....	149
C Direct Entry Terminal Guidance Velocity Requirements ....	155
D Reference Design Cold-Gas System Sizing Calculation .....	167
E Solid Propellant System Sizing Calculations .....	175
F Monopropellant Hydrazine System Sizing Calculations.....	179
G Bipropellant Hydrazine-Nitrogen Tetroxide System Calculations .....	189
H Flexure Gimbal System Sizing Calculations .....	195
I Cold-Gas System Sizing Calculations .....	203
J Gimbal Angle Coordinate Transformation for Camera Pointing .....	207
K Computation of Reaction Control System Impulse Requirements .....	213
L Reference Design Solid Propellant System Sizing Calculations .....	221

## ILLUSTRATIONS

Figure 1	Allowable Thrust Application Angle Error .....	6
2	Allowable Thrust Application Angle Error For Selected Velocity Errors .....	8
3	Entry Angle Dispersion When Thrust Is Applied At The Insensitive Angle .....	9
4	Spin-Thrust System Accuracy .....	14
5	Precession Cone Central Angle Versus Spin Rate .....	15
6	Precession Cone Half Angle Versus Spin Rate .....	16
7	Spin-Thrust System Errors .....	17
8	Entry Angle of Attack As A Function Of Entry Angle For Various Lead Times .....	18
9	Attitude Control Subsystem Schematic .....	20
10	Mathematical Model Of Attitude Control System .....	33
11	Cold-Gas Reaction Control System .....	37
12	Conventional Vent - Fill System .....	38
13	Total Impulse/Tank Weight Versus Molecular Weight .....	41
14	Attitude Control System Package .....	46
15	Performance of ACS .....	55
16	$\Delta V$ Pointing Error Versus Spin Rate .....	63
17	Rate Damping Control Loop .....	70
18	Dynamics of Controller and Reaction Control System .....	72
19	Nozzle Thrust Requirements Versus Solution Time (Rate Damping Of Capsule On Parachute) .....	73
20	Impulse Requirements Versus Gust Velocity (per Gust) (Rate Damping of Capsule on Parachute) .....	74

## ILLUSTRATIONS (Cont'd)

Figure 21	Reaction Control System Weight Versus Solution Time (Rate Damping of Capsule On Parachute) .....	75
22	Nozzle Requirements Versus Solution Time (Rate Damping During Early Entry) .....	77
23	Impulse Requirements Per Axis Versus Solution Time (Rate Damping During Early Entry) .....	78
24	Reaction Control System Weight Versus Solution Time (Rate Damping During Early Entry) .....	79
25	Evaluation of Candidate Systems .....	85
26	Total Impulse/Tank Weight Versus Molecular Weight .....	88
27	Cold-Gas Reaction System .....	89
28	Conventional Vent - Fill System .....	90
29	Solid Propellant Open Centered TVC System .....	93
30	Monopropellant Hydrazine System .....	96
31	Bipropellant $N_2H_4$ - $N_2O_4$ System .....	98
32	Flexure Gimbal TVC Basic Configuration .....	100
33	Flexure Gimbal TVC System .....	101
34	Cold-Gas (Nitrogen) TVC System .....	103
35	Alternate TVC System Parametric Evaluation .....	106
36	Attitude Control System Block Diagram .....	112
37	Reaction Control System Schematic Layout .....	118
38	Solid Propellant Open Centered TVC System .....	121
39	Two-Way Solenoid Valve .....	123
40	TV Camera Platform .....	126

# ILLUSTRATIONS (Cont'd)

Figure A-1	Offsets in Separation System .....	144
A-2	Offsets in Resultant Spring Forces .....	145
B-1	Spin Thrust System Errors .....	150
C-1	$\Delta V$ Versus In-Plane Displacement, $\gamma_E = -90$ Degrees, $\Delta V$ Applied Perpendicular to Capsule Velocity Vector....	156
C-2	$\Delta V$ Versus Change in Entry Angle, $\gamma_E = -90$ Degrees, $\Delta V$ Applied Perpendicular to Capsule Velocity Vector....	157
C-3	$\Delta V$ Versus In-Plane Displacement, $\gamma_e = -50$ degrees $\Delta V$ Applied Perpendicular to Capsule Velocity Vector....	159
C-4	$\Delta V$ Versus Out-Of-Plane Displacement, $\gamma_e = -50$ degrees, $\Delta V$ Applied Perpendicular To Orbital Plane .....	160
C-5	$\Delta V$ Versus Change In Entry Angle, $\gamma_e = -50$ Degrees, $\Delta V$ Applied Perpendicular To Capsule Velocity Vector...	161
C-6	$\Delta V$ Versus Change In Entry Angle, $\gamma_e = -50$ Degrees, $\Delta V$ Applied Perpendicular To Orbital Plane .....	162
C-7	$\Delta t$ Versus $\Delta V$ , $\gamma_e = -90$ Degrees, $\Delta V$ Applied Perpendicular To Capsule Velocity Vector .....	163
C-8	$\Delta t$ Versus $\Delta V$ , $\gamma_e = -50$ Degrees, $\Delta V$ Applied Perpendicular To Capsule Velocity Vector .....	164
C-9	$\Delta t$ Versus $\Delta V$ , $\gamma_e = -50$ Degrees, $\Delta V$ Applied Perpendicular To Orbital Plane .....	165
F-1	Monopropellant-Hydrazine Propellant Flow Rate To Thrust Ratio versus Area Ratio Thrust Coefficient Versus Area Ratio .....	180
F-2	Monopropellant-Hydrazine Nozzle Weight Versus Propellant Flow Rate .....	181
F-3	Monopropellant-Hydrazine Chamber Weight Versus Propellant Flow Rate .....	182

## ILLUSTRATIONS (Concl'd)

Figure F-4	Propellant Tank Weight To Volume Ratio Versus Propellant Volume .....	184
F-5	Adiabatic Expulsion Process Ratio of $\text{GN}_2$ Pressure Vessel Weight To Propellant Volume Versus Charging Pressure .....	186
G-1	Bipropellant Rocket Motor Weight Versus Thrust .....	192
H-1	Flexure Gimbal Deflection Geometry .....	196
J-1	Four Gimbal System Transformation .....	208
J-2	Camera Line Of Sight Transformation .....	209
J-3	Local Vertical Transformation .....	210

## TABLES

Table	I	Attitude Control System Characteristics .....	3
	II	Sequence of Operation .....	4
	III	Parameter Values For Spin-Thrust Accuracy Analysis .....	13
	IV	Weight And Volume Summary Of Sensors And Electronics (Integrated Circuits) .....	36
	V	Summary Of Required Impulse .....	39
	VI	Reaction Control System Weight Summary .....	43
	VII	Spin Rocket Vacuum Performance Summary .....	44
	VIII	Nominal Spin Rocket Design Summary .....	44
	IX	Attitude Control System Characteristics .....	52
	X	Sequence of Operation .....	53
	XI	Major ACS Combinations .....	58
	XII	Characteristics of Active ACS Plus Spin System (Attitude Control System) .....	61
	XIII	Characteristics Of Active ACS Plus Spin System (Spin System) .....	61
	XIV	Summary Of Inertial Reference System Characteristics .....	66
	XV	Summary of Cold Gas Reaction System Characteristics .....	67
	XVI	Summary Of Hot Gas Reaction System Characteristics .....	68
	XVII	Comparison Of Gust Velocity To Maximum Rate .....	71
	XVIII	Weight Summary For Reaction Control System Used For Rate Damping During Early Entry .....	80

# TABLES (Concl'd)

Table	XIX	Solid Propellant System Weight Breakdown .....	94
	XX	Monopropellant Hydrazine System Weight Breakdown .....	95
	XXI	Bipropellant $N_2H_4$ - $N_2O_4$ System Weight Breakdown .....	97
	XXII	Flexure Gimbal TVC System Weight Breakdown .....	102
	XXIII	Cold Gas $GN_2$ TVC System Weight Breakdown .....	104
	XXIV	Total Impulse Summary .....	116
	XXV	Cold Gas Nitrogen Reaction Control Subsystem Weight Summary .....	119
	XXVI	Solid Propellant System Weight Summary .....	124
	XXVII	Summary Of Propulsion System Characteristics (Entry From The Approach Trajectory) .....	137
	XXVIII	Summary Of Propulsion System Characteristics (Entry From Orbit) .....	142
	C-1	Terminal Guidance Influence Coefficients .....	166
	K-1	Total Impulse Summary .....	217

## GLOSSARY OF TERMS

**Planetary Vehicle:** The Planetary Vehicle (PV) is defined as the composite Flight Spacecraft (FS) and Flight Capsule (FC) integrally attached and operated up to separation in the vicinity of the selected planet.

### **Flight Capsule Terminology:**

#### **a. Peculiar to Entry from Approach Trajectory Case**

Specific terminology is used at the operational stages of separation and/or deployment. The Flight Capsule is attached to the Flight Spacecraft by the forward and aft sections of the FC to FS adapter. Operation of the sterilization canister lid separation mechanism followed by the operation of the separation system on the FC to FS adapter, results in the Separated Vehicle. Attitude control and propulsion maneuvers are performed to place the Separated Vehicle on a preselected planetary impact trajectory. After these maneuvers, the propulsion and attitude control system (ACS) electronics assembly is separated and the resultant Entry Vehicle cruises to and enters the planet atmosphere. After entry, the entry shell (including the ACS reaction subsystem and spin/despin rockets) is separated and the Suspended Capsule descends through the atmosphere with the parachute. At a preselected time during descent, a separation mechanism operation extends the Landed Capsule from the parachute by use of a tether. At impact, the Landed Capsule is separated from the tether for landed operations.

#### **b. Peculiar to Entry from Orbit Trajectory Case**

The Flight Capsule is attached to the Flight Spacecraft by the forward and aft sections of the FC to FS adapter. Operation of the sterilization canister lid separation mechanism followed by the operation of the separation system on the FC to FS adapter, results in the Separated Vehicle. Attitude control, propulsion and thrust vector control maneuvers are performed to deorbit the Separated Vehicle and place it on a preselected planetary impact trajectory. After the propellants have been expelled to perform these maneuvers, the resultant Entry Vehicle cruises to and enters the planet atmosphere. After entry, the entry shell (including the ACS and TVC reaction subsystems) is separated and the Suspended Capsule descends through the atmosphere with the parachute.

Additional terminology used in this Book are as follows:

CC&S: Central Computer and Sequencer

TVC: Thrust Vector Control

ACS: Attitude Control System

IRS: Inertial Reference System, which includes an inertial platform and a digital computer

SENTRY: Body-mounted rate gyros used for ACS deactivation in certain failure modes.

DSIF: Deep-Space Instrumentation Facility

JPL: Jet Propulsion Laboratory

$\Delta V$ : Incremental velocity applied to the capsule to de-orbit and/or place it on an impact trajectory. (A bar over the symbol,  $\overline{\Delta V}$ , refers to the vector quantity.)

## ACKNOWLEDGMENT

The conduct of the study and technical preparation of this report involved the participation and close coordination of many people, all of whose contributions were important to the end results.

It is impractical to single out each individual, but the major contributors to the study, reflected in the material presented in this Book, are as follows:

### Responsible Manager

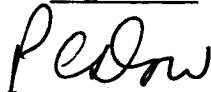
P. C. Dow

### Major Contributors

<u>Name</u>	<u>Sections</u>
L. E. Ceglowski	1, 2, 3, 4, 5, 6, 7, 8
E. C. Graves	1, 2, 3, 4, 6, 7
D. P. Fields	2
J. P. Vullo	1, 2, 3, 4
L. J. Fusegni	4, 7, 8
N. A. Taylor	7
R. Barnes	9

### Approved by

Signature



P. C. Dow

Title

Manager  
Guidance, Control, and Communications  
Department

## INTRODUCTION

This book discusses the attitude control and propulsion requirements for the Mars Probe/Lander. The book is divided into three parts: the first part covers attitude control for entry from the approach trajectory (Sections 1-4); the second part deals with attitude control for entry from orbit (Sections 5-8); the third part treats the propulsion system for both missions (Section 9). Detailed analyses are contained in the Appendixes.

Both the entry from the approach trajectory and entry from orbit missions, require a velocity increment to place the capsule on a trajectory which will impact the planet. This in turn requires a propulsion system and some means of attitude control to apply the imparted velocity in the desired direction. Attitude control is also desirable to control the orientation of the capsule before it enters the planetary atmosphere in order to improve communications and also to provide a suitable angle of attack at the time of entry.

The requirements placed on both the attitude control and propulsion systems are quite different for the two missions. Entry from the approach trajectory requires very precise control of the direction of the applied capsule incremental velocity, due to the requirement to achieve shallow entry angles with a minimum dispersion, while at the same time accelerating the capsule to obtain sufficient communications lead time. The propulsion requirements are modest, since only a small incremental velocity is required at the large separation range selected.

Entry from orbit places much less stringent requirements on the attitude control system since the control of the direction of the applied velocity is less critical. The velocity required for this case, however, is more than an order of magnitude greater than that required for entry from the approach trajectory, so that the propulsion system must furnish proportionately greater total impulse.

A closed-loop cold-gas attitude control system was chosen for both missions to give the capsule complete flexibility in accomplishing the necessary orientation maneuvers and, in the entry from the approach trajectory case, to meet the pointing accuracy requirements. An inertial platform is used for attitude reference for the entry from orbit mission, because it is required to furnish gimbal angle commands to the television camera during parachute descent. For attitude control while thrusting during the deorbit maneuver, a hot-gas reaction control system is used.

Both missions make use of a solid propellant rocket motor, using an existing sterilizable propellant. For entry from the approach trajectory the Titan vernier rocket was chosen; for entry from orbit a design similar to the Surveyor main retromotor was selected.

# ATTITUDE CONTROL PROBE/LANDER, ENTRY FROM THE APPROACH TRAJECTORY

## 1.0 INTRODUCTION AND SUMMARY

### 1.1 SCOPE OF STUDY

Attitude control is required to orient and maintain the capsule in the proper attitude for thrusting, then to place and maintain the vehicle in the proper attitude for entry. Several alternative concepts of attitude control have been evaluated in terms of their performance and other criteria, and a reference attitude control system (ACS) has been selected. The reference system has been designed in sufficient detail so that an accurate assessment can be made of its performance, size, weight, volume, power requirements, development status, reliability, and ability to meet environmental criteria.

### 1.2 MISSION PROFILE AND ATTITUDE CONTROL SYSTEM REQUIREMENTS

The planetary vehicle is on a fly-by trajectory as it approaches Mars. The capsule must be separated from the flight spacecraft (FS) and placed on an impact trajectory before encounter.

The capsule must also arrive at the entry point with sufficient lead time to permit communication with the spacecraft to continue for a reasonable period of time before it is interrupted by the capsule passing over the horizon. This means that at the time of separation either the spacecraft must be slowed down or the capsule must be speeded up. The capsule must be propelled with an incremental velocity to impact the planet; this maneuver can also include the velocity change necessary to obtain the desired communication lead time. The capsule must be placed in the proper attitude for its fixed total-impulse propulsion system to apply the desired velocity change and the capsule must be maintained in that attitude while thrusting. This orientation can take place before separation, using attitude control on the spacecraft, or after separation, using the capsule attitude control system. After thrusting it is desirable to reorient the capsule so that the angle of attack at entry is small. Since the entry vehicle is aerodynamically stable, no attitude control during entry is required. Although low entry angles of attack are preferred, large angles are acceptable if the capsule is spin-stabilized at low spin rates. However, it is not desirable for the capsule to be tumbling at entry thus raising the requirement for some form of control after thrusting and prior to entry. The most stringent requirement on the ACS is that of maintaining the capsule orientation while thrusting. The requirement stems from the desire to minimize entry angle and landing point dispersion, and is made more severe if communication lead time must be obtained by capsule speedup.

### 1.3 ALTERNATIVES CONSIDERED

Four ACS concepts were considered. The first is a spin-stabilization system in which the spacecraft orients to the proper attitude for capsule thrusting, separation occurs, the capsule is spun up by spin rockets, thrusting occurs, and the vehicle is despun before entry. The pointing accuracy (i. e., the uncertainty in the direction of the applied incremental velocity vector) is about 0.4 degree using this approach. However, if a communication lead time of 3 hours must be obtained by capsule speedup rather than spacecraft slowdown, a pointing accuracy of better than 0.25 degree is required for some expected operating conditions. The requirement for a spacecraft orientation maneuver is also a drawback to this approach.

A second alternative is the use of an active attitude control system. This approach using gyros on the capsule which are referenced to the spacecraft attitude before separation, permits the orientation maneuvers to be performed by the capsule itself rather than by the spacecraft, and can maintain attitude during thrusting to achieve a pointing accuracy, which is acceptable with 3-hour lead times. The active ACS can also orient and maintain attitude for entry. A variation of this approach is to use spin stabilization to maintain attitude during cruise until entry, after the active ACS performs the orientation to entry attitude. This approach eliminates the long term operation of the ACS in a limit cycle mode for several days, which would result in increased gas consumption and gyro drift. This active ACS plus spin system is the reference design selected. Another alternative to achieve greater accuracy is the use of on-board celestial sensing to control the entry conditions by terminal guidance. However this technique adds considerably to the weight and complexity of the whole system and its much greater accuracy is not warranted, at least for these early missions.

### 1.4 REFERENCE DESIGN SUMMARY

The design selected makes use of a combination of active attitude control using a gyro-controlled cold-gas reaction system together with spin stabilization which is accomplished by solid propellant spin rockets. The angular rates of the capsule are measured by three body-mounted rate gyros; the outputs of these gyros are electronically integrated so that angular position as well as angular rate is available. This information is used by the control logic to operate the valves of the cold-gas reaction control system. This system provides three-axis control in couples by means of 12 nozzles. Spin stabilization is provided by two redundant groups of solid propellant rockets. Normally only one group is required for spin stabilization, but if the primary operational mode of the ACS fails, both sets of spin rockets will be used in the backup mode for adequate control during thrusting for the incremental velocity. (In this case, it is necessary to despin prior to entry, and a third set of rockets is provided for that purpose.)

The gyros and electronics are turned on and allowed to warm up while the vehicle is attached to the spacecraft. During this time the ACS is checked out; this also provides an opportunity to trim the drift of the gyros and integrators. After the capsule is separated from the spacecraft, the reaction control system is activated and realigns the capsule to the spacecraft reference attitude, correcting for any disturbances which occurred during separation. The capsule is then oriented so that its thrust axis is aligned to the desired direction for the incremental applied velocity and maintained in that direction during thrusting. The capsule is then reoriented to have zero-angle of attack at entry and is spun up by one set of spin rockets to maintain this attitude for the remainder of its trajectory, until entry. Finally the propulsion and ACS electronics assembly are jettisoned to reduce the weight of the entry vehicle.

Some of the significant characteristics of the ACS are contained in Table I. A sequence of operations is shown in Table II.

TABLE I  
ATTITUDE CONTROL SYSTEM CHARACTERISTICS

• <u>Orientation Uncertainty</u>	0.23 degree (1-sigma)
• <u>Maximum Operating Time</u>	
Active Control	15 minutes
Spin Stabilization	12 days
• <u>Weight</u>	90 pounds
• <u>Stored Impulse</u>	764 lb-sec, cold gas
• <u>Limit Cycle Amplitude</u>	0.1 degree
• <u>Spin Stabilization</u>	Solid Propellant Rockets

TABLE II  
SEQUENCE OF OPERATION

• Prior to Separation

Verify ACS Operation

Trim Gyro and Integrator Drift

Establish Angular Commands

• Separation to Thrusting

Activate Reaction Control

Nullify Separation Rates

Orient to Thrusting Attitude

• Thrusting

Maintain Attitude During Thrusting

• Thrust Termination to Entry

Orient for Entry Conditions

Spin Stabilize

Jettison ACS Electronics Assembly

## 2.0 PERFORMANCE REQUIREMENTS AND ANALYSIS

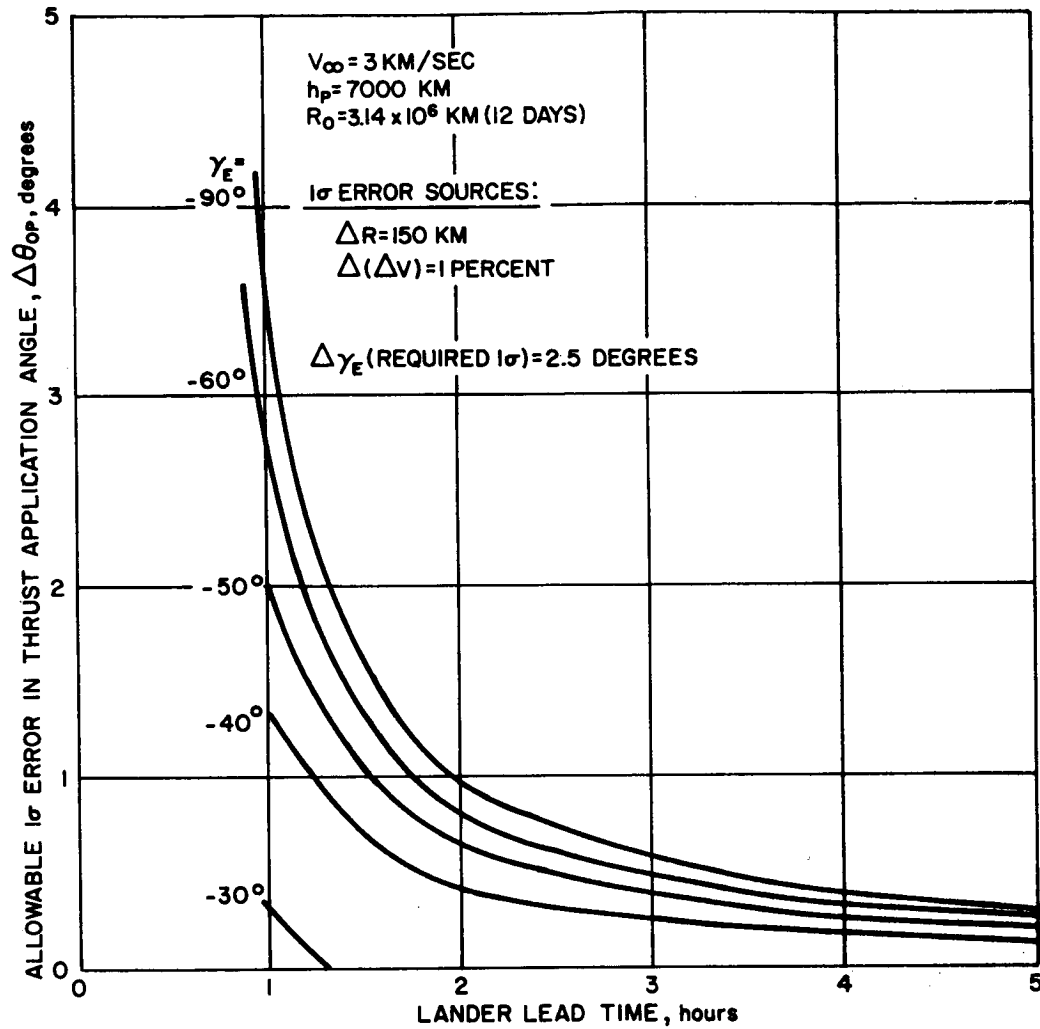
### 2.1 $\Delta V$ ACCURACY REQUIREMENTS VERSUS ENTRY ANGLE

The accuracy with which the incremental velocity ( $\Delta V$ ) must be applied, both in magnitude and direction, is determined by the allowable dispersion in entry angle. The accuracy of the direction of the imparted velocity increment is a function of ACS performance, while the accuracy in its magnitude depends on the propulsion system. With the spacecraft on a fly-by trajectory, it is necessary to impart a velocity change to the capsule to place it on an impact course. It is also necessary to provide an additional incremental velocity between spacecraft and capsule to obtain the necessary communication lead time. This can be done either by speeding up the capsule or by decelerating the spacecraft. If capsule speedup is selected, this maneuver can be combined with the incremental velocity change required to place it on an impact trajectory. In the following paragraphs the incremental velocity accuracy requirements with capsule speedup and spacecraft slowdown will be determined. First, the entry angle dispersion requirements should be stated. It is a design requirement of the system that the dispersion in impact point be no more than 500 km. This corresponds to a variation in entry angle of approximately 7.5 degrees, and this tolerance is essentially constant over the range of trajectory parameters considered. Furthermore, the entry angle must be between -30 and -50 degrees to satisfy the parachute deployment conditions.

#### 2.1.1 Flight Capsule Speedup Maneuver

Detailed analyses have been carried out to show which trajectory parameters are important in determining the thrust pointing accuracy required, and the results are presented in Section 3.0, Book 1, Volume V. These analyses show that entry-angle dispersion is virtually independent of separation range and periapsis altitude, but the dispersion increases rapidly with increasing lead time\* and with increasing approach velocities. The hyperbolic approach velocity can be minimized by proper choice of launch period. The effect of lead time and entry angle on ACS pointing accuracy requirements can be seen in Figure 1 in which the lead time is obtained by capsule speedup. This figure shows the allowable error in capsule thrust application angle as a function of lead time for a range of entry angles. The nominal separation conditions are also stated, and the figure is based on an allowable entry angle dispersion of 2.5 degrees (one sigma). It is also based on a position uncertainty at the time of separation of 150 kilometers and an uncertainty in velocity increment of 1 percent. (The position uncertainty is due principally to uncertainty in

\* Lead time is defined as the difference between the time of capsule entry into the planetary atmosphere and flight spacecraft periapsis passage.



85-0792

Figure 1 ALLOWABLE THRUST APPLICATION ANGLE ERROR

the ephemeris of Mars. This is a very significant contributor to entry-angle dispersion and if reduced by improved ephemeris data can greatly ease the ACS pointing accuracy requirements.) These are the only important error sources affecting entry dispersion other than pointing accuracy and are the expected nominal values.

From this figure it can be seen that to achieve a lead time of 3 hours the allowable error in thrust application angle is 0.38 degree for an entry angle of -50 degrees, and 0.25 degree for an entry angle of -40 degrees, and at -30 degrees entry angle the desired dispersion is unachievable even with a perfect ACS.

Figure 2 shows the effect of entry angle on pointing angle accuracy requirements for different values of uncertainty in the separation velocity increment. It can be seen that at -40 degrees entry angle the allowable pointing error increases from 0.25 degree with a 1 percent velocity error to 0.29 degree with a velocity error of 1/4 percent. Or if the pointing error is fixed at 0.25 degree, the entry angle can become about 3 degrees more shallow by reducing the velocity error from one percent to 1/4 percent.

#### 2.1.2 Flight Spacecraft Slowdown Maneuver

The desired lead time can be obtained by flight spacecraft slowdown instead of capsule speedup. In this case lead time is not a factor in selection of the direction of the separation velocity. That is, the thrust application angle can be chosen so that errors in the direction of the applied thrust will have a minimum effect on entry-angle dispersion. The allowable pointing error in this case can be greatly increased (to about 5 degrees) with consequent easing of the requirements imposed on the ACS. Dispersion is slightly more sensitive to errors in the magnitude of the separation velocity. Figure 3 shows that the velocity error should be kept below about 0.85 percent, for a pointing error of 0.23 degree and entry angle of -30 degrees. In summary, it can be seen that lead-time requirements together with the shallow entry angles required impose severe constraints on the ACS accuracy. The ACS requirements can be relaxed by the use of spacecraft slowdown, by improved ephemeris data, or by terminal guidance.

### 2.2 ALTERNATE APPROACHES

Two alternatives exist in the design of the system for orienting the capsule to the proper thrusting attitude, and the choice has an important influence on the design of the ACS. Another design alternative is the use of terminal guidance on the capsule. This, too, has an important effect on ACS design. These alternatives are discussed in the following paragraphs.

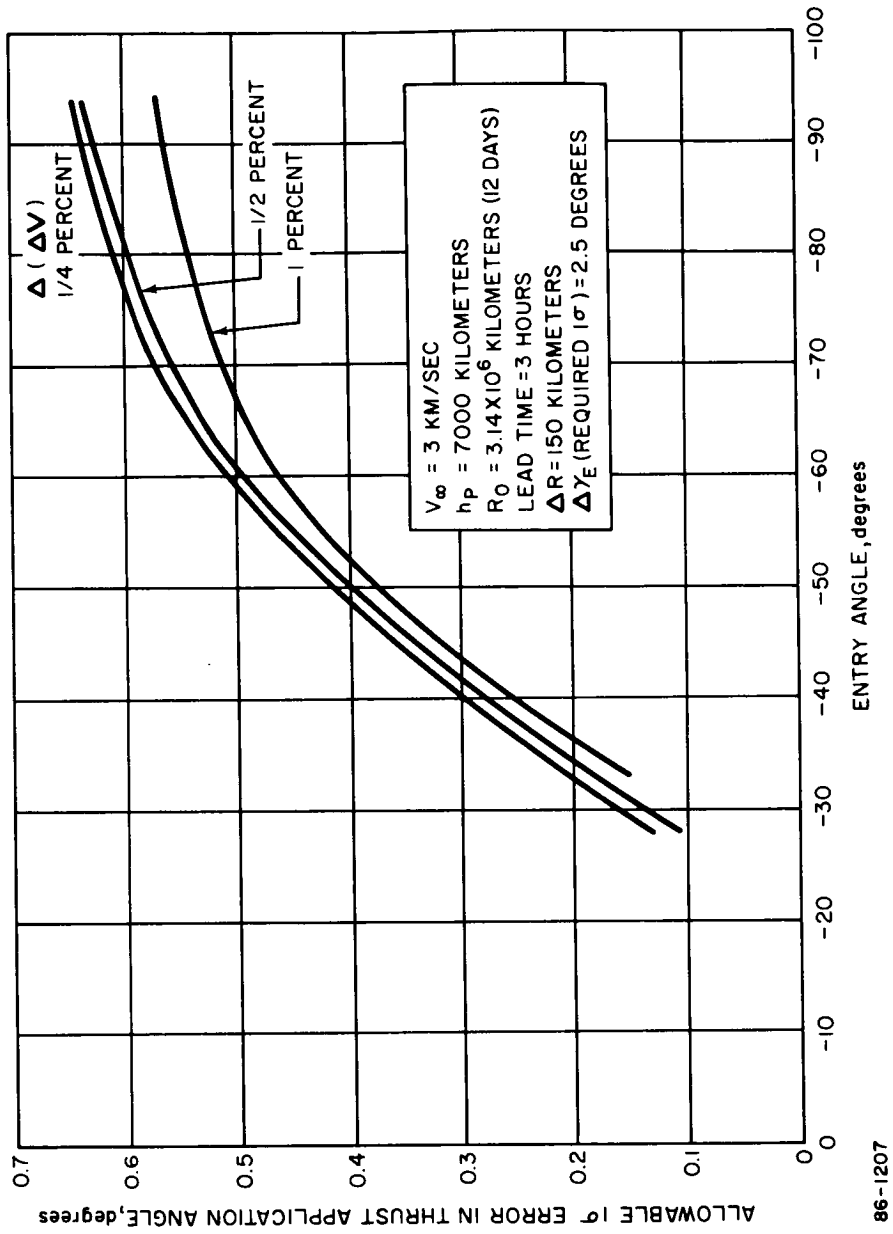


Figure 2 ALLOWABLE THRUST APPLICATION ANGLE ERROR FOR SELECTED VELOCITY ERRORS

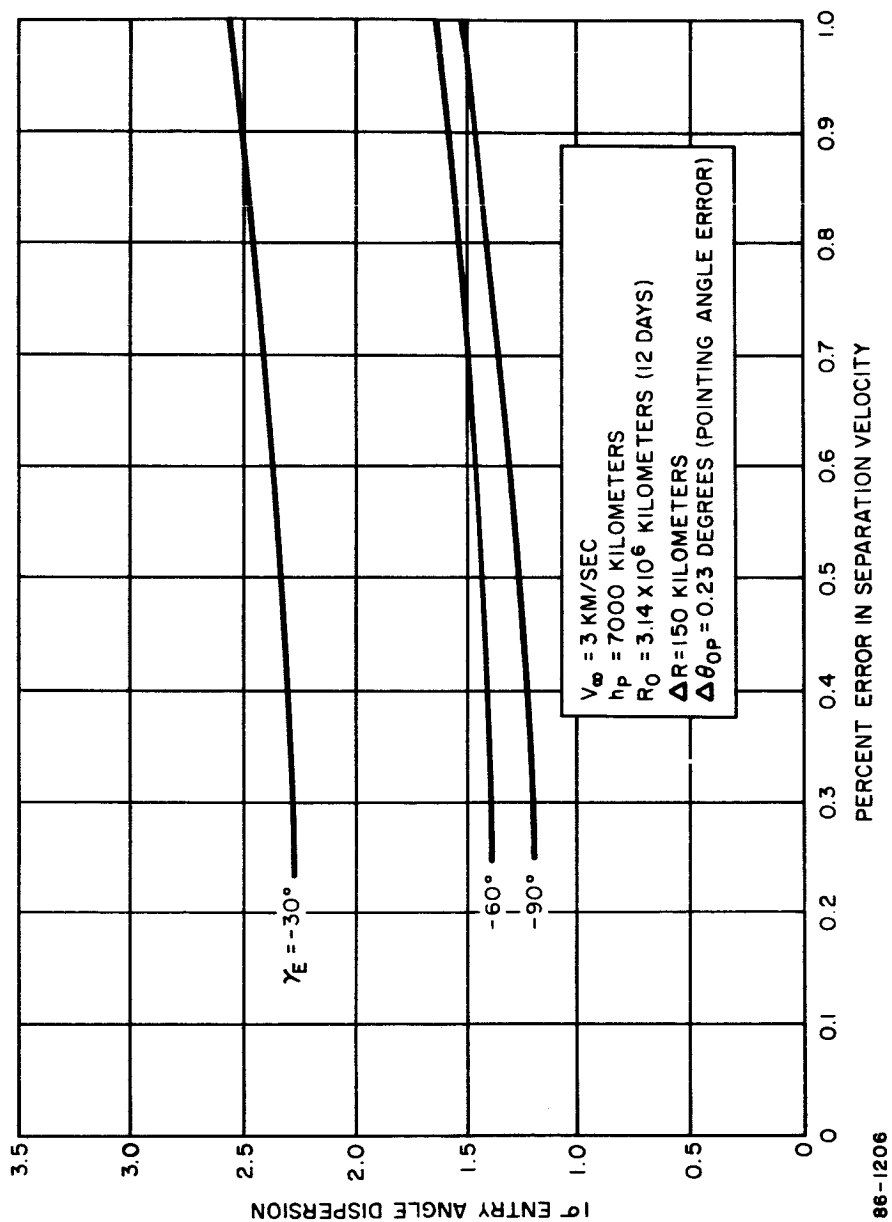


Figure 3 ENTRY ANGLE DISPERSION WHEN THRUST IS APPLIED AT THE INSENSITIVE ANGLE

### 2.2.1 Orientation to Thrust Attitude

An important option in the flight sequence which has a direct impact on the design of the ACS is whether or not to perform a spacecraft pre-separation maneuver designed to provide the required thrust application angle for the capsule. Such a maneuver is required if a simple spin system is used for stabilization while thrusting. If the spacecraft maneuver is not used, the ACS must perform a capsule orientation maneuver after separation. In this case an active attitude control system is required. It will be shown later that a spin system cannot meet the dispersion requirements if lead time must be obtained by capsule speed up. Consequently the spacecraft pre-separation maneuver is only beneficial to the design of the capsule ACS if it is also possible to obtain communications lead time by slowing down the spacecraft. In this case the simple spin system can be used.

### 2.2.2 Terminal Guidance

From the discussion in Section 2.1 and the following sections it will be clear that even the performance of the closed-loop active ACS is marginal in meeting the accuracy requirements. If a communication lead time of at least 3 hours must be obtained by capsule speedup and if no improvement in Mars ephemeris data is obtained, then the active ACS will not permit entry angles shallower than about -40 degrees in order to meet dispersion requirements. If shallower angles become a requirement, it may be necessary to employ terminal guidance on the capsule. Such a system would include, in addition to the ACS, a precision planet tracker, sun tracker, computer, and possibly a star tracker to make a navigation fix at a range of about 30,000 km from Mars. A velocity correction would then be performed using the ACS and propulsion system to correct to the desired trajectory. The additional weight of such a system would be about 100 pounds plus the weight of additional propellant required which amounts to 100-200 pounds depending on the range from the planet at which the velocity correction is made. A terminal guidance system would greatly ease the demands on ACS accuracy for thrusting after separation, and may in fact be strongly desirable for missions in which better control of impact point location is required. In this sense it is an attractive approach since it provides growth potential for more ambitious future missions. However it must be regarded as a less attractive choice for the present mission than reducing the entry angle dispersions at the time of separation.

## 2.3 ACHIEVABLE PERFORMANCE OF SPIN-ONLY CONFIGURATION

Four attitude control concepts will be discussed, their operation described, and the performance which is achievable defined. The first, a spin-only configuration, is described in this section. The following three sections describe an active ACS, an active ACS with terminal guidance and an active ACS plus a spin system.

### 2.3.1 Description of Operation

The sequence of events for the spin-thrust system is as follows:

- a. Orient spacecraft to required thrusting attitude
- b. Electrical and mechanical separation from the FS
- c. Delay to provide vehicle clearance
- d. Spin-up capsule
- e. Fire  $\Delta V$  rocket
- f. De-spin (if required) just prior to entry to improve angle of attack convergence.

The capsule relies upon spin-stabilization to hold attitude accurately during thrusting and throughout cruise to entry. Since the vehicle is spinning about its axis of maximum moment of inertia, it has asymptotic stability; any structural damping present will cause the precession half-cone angle to decrease with time.

### 2.3.2 Error Analysis

The first step in analyzing the spin-thrust system errors is to determine the attitude error existing before spinup. The 1-sigma attitude error sources and contributions are:

Flight Spacecraft Sensor Error	0.144 degree*
Flight Spacecraft Limit Cycle	0.066 degree**
Flight Capsule Mounting Accuracy	0.167 degree
Capsule Tipoff Angle Before Spinup	0.204 degree***

Assuming statistical independence of the error sources the attitude error before spin-up is 0.31 degree (1 sigma).

\* This includes the optical sensor error together with the gyro sensor errors which occur during the maneuver of the spacecraft to the thrusting orientation.

\*\* Assumes uniform distribution.

\*\*\* See Appendix A. The principal contributor to this error is the 0.0833 inch (1-sigma) error in c.g. position. The error in spring force resultant was estimated as about 0.03 inch (1 sigma) so that the c.g. position error dominates. A separation distance of the order of 4 feet was assumed to be required to assure clearance.

Next it is necessary to determine the attitude and  $\Delta V$  pointing error after spinup. Using the parameter values listed in Table III, the accuracy and precession characteristics were investigated. The method of combining the spin-thrust system errors is detailed in Appendix B.

A curve of spin-thrust system performance in achieving the desired  $\Delta V$  pointing accuracy as a function of spin rate and tip-off angle is shown in Figure 4. From this figure it can be seen that with a spin rate of 40 rpm and a tip-off angle of 0.30 degrees, the  $\Delta V$  pointing error is nearly 0.40 degree. Figures 5 and 6, describe the characteristics of the precession cone after thrusting for the  $\Delta V$  correction. The geometry of the situation is outlined on Figure 7. From this it can be determined that the vehicle thrust axis will be within 1 or 2 degrees of the applied velocity vector making the entry angle of attack quite predictable. However, although it is predictable it is a dependent variable, dependent on other considerations such as communications lead time. Therefore a large angle of attack at entry is possible.

A curve of angle of attack at entry versus entry angle for communication lead times from 1 to 5 hours and approach velocity of 3 km/sec is shown in Figure 8. It shows that as the entry angle varies from -20 degrees to -90 degrees the angle of attack ranges from -15 degrees to a value exceeding 60 degrees, depending upon the lead time desired.

Because of the possibility of a large entry angle of attack, with spin rates as high as 40 - 50 rpm, a despin maneuver to a lower spin rate may be required just prior to entry. The advantage of a low spin rate is that angle of attack convergence is improved, thus ensuring a low angle of attack during most of the atmospheric trajectory. This in turn improves integrated heating and increases the altitude at which Mach 1.3 is reached, for parachute deployment. The effect of spin during entry is fully discussed in Section 7.3, Book 2, Volume V.

## 2.4 ACHIEVABLE PERFORMANCE OF ACTIVE ACS CONFIGURATION

The next attitude control system to be discussed uses active control from separation to entry.

### 2.4.1 Description of Operation

The operation of the active ACS is as follows:

- a. Nullify tipoff rates due to separation from the FS and realign the capsule to the spacecraft reference attitude.

TABLE III

PARAMETER VALUES FOR SPIN-THRUST ACCURACY ANALYSIS

Parameter	Definition	Value
W	Weight	1430 pounds
$I_T$	Transverse moment of inertia	409 slug-ft <sup>2</sup>
$I_X$	Roll moment of inertia	530 slug-ft <sup>2</sup>
X	Distance of plane of spin rockets from vehicle c. g.	13 inches
R	Radius of spin rocket circle	85 inches
L	Distance of thrust rocket aft of vehicle c. g.	56 inches
N	Number of spin rockets	10
T	Thrust duration	5 seconds
$V_o$	Perturbation velocity	100 ft/sec
$\sigma_{\Delta X_S}$	Spin rocket location error	0.042 inch
$\sigma_{\Delta k_S}$	Spin rocket total impulse error (normalized)	0.01
$\sigma_{\Delta \xi_S}$	Spin rocket angular misalignment	0.167 degree
$\sigma_{\Delta X_T}$	Thrust rocket location error	0.042 inch
$\sigma_{\Delta c_g}$	c. g. location error off vehicle centerline	0.0833 inch
$\sigma_{\Delta \xi_T}$	Thrust rocket angular misalignment	0.167 degree
$\sigma_{\Delta k_T}$	Thrust rocket total impulse error (normalized)	0.01
$\sigma_{\Delta m}$	Vehicle mass error	0
$\sigma_{a_o}$	Initial attitude error at separation	0.2 degree

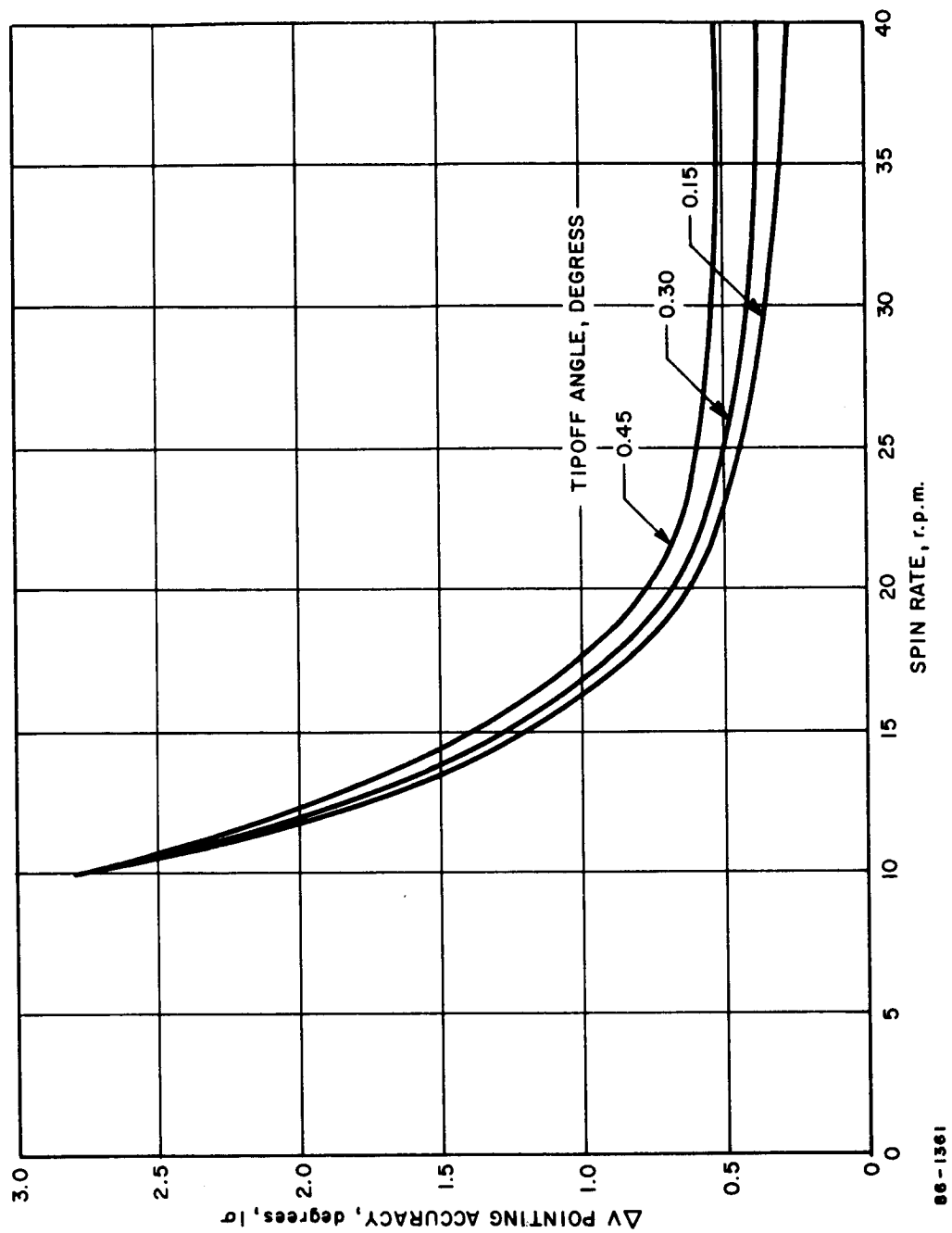
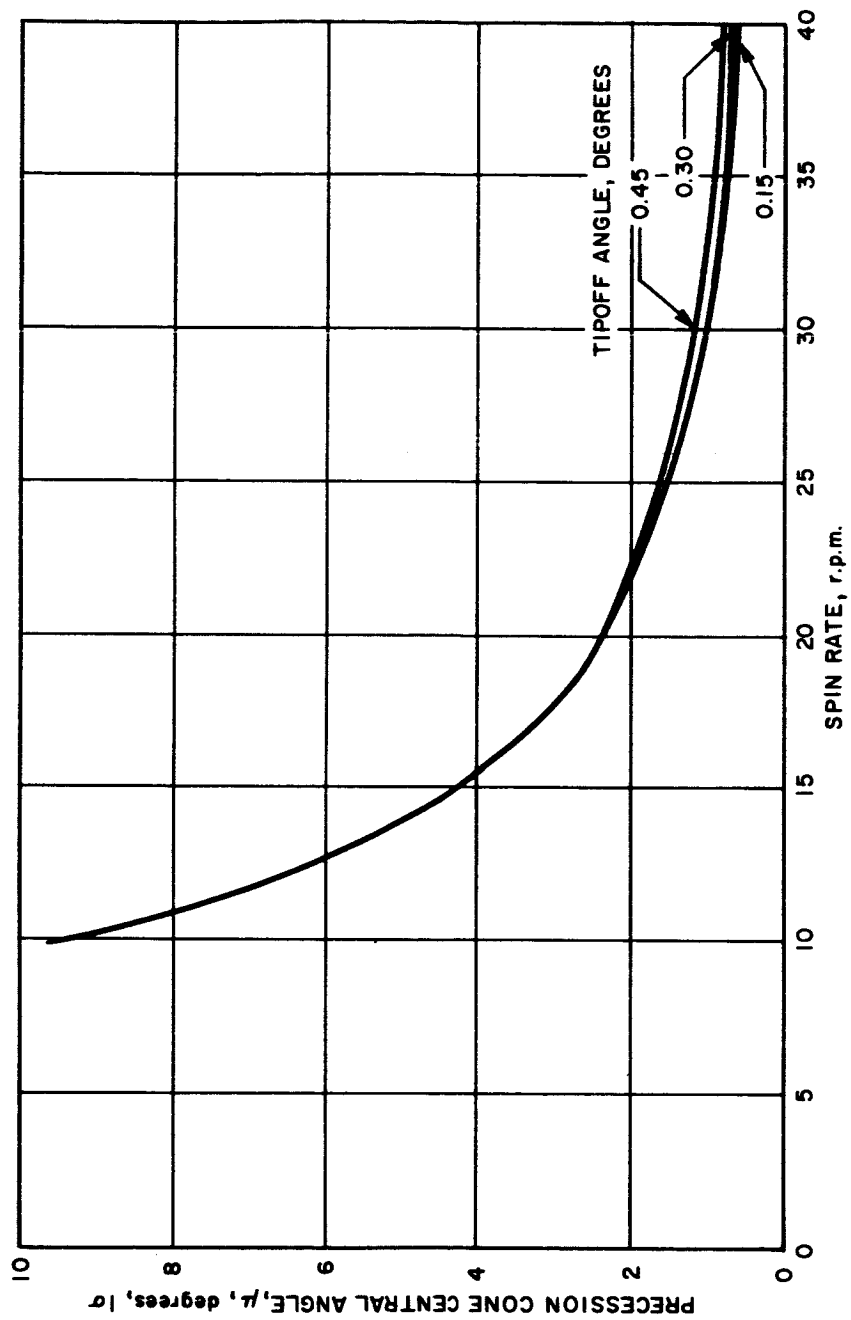
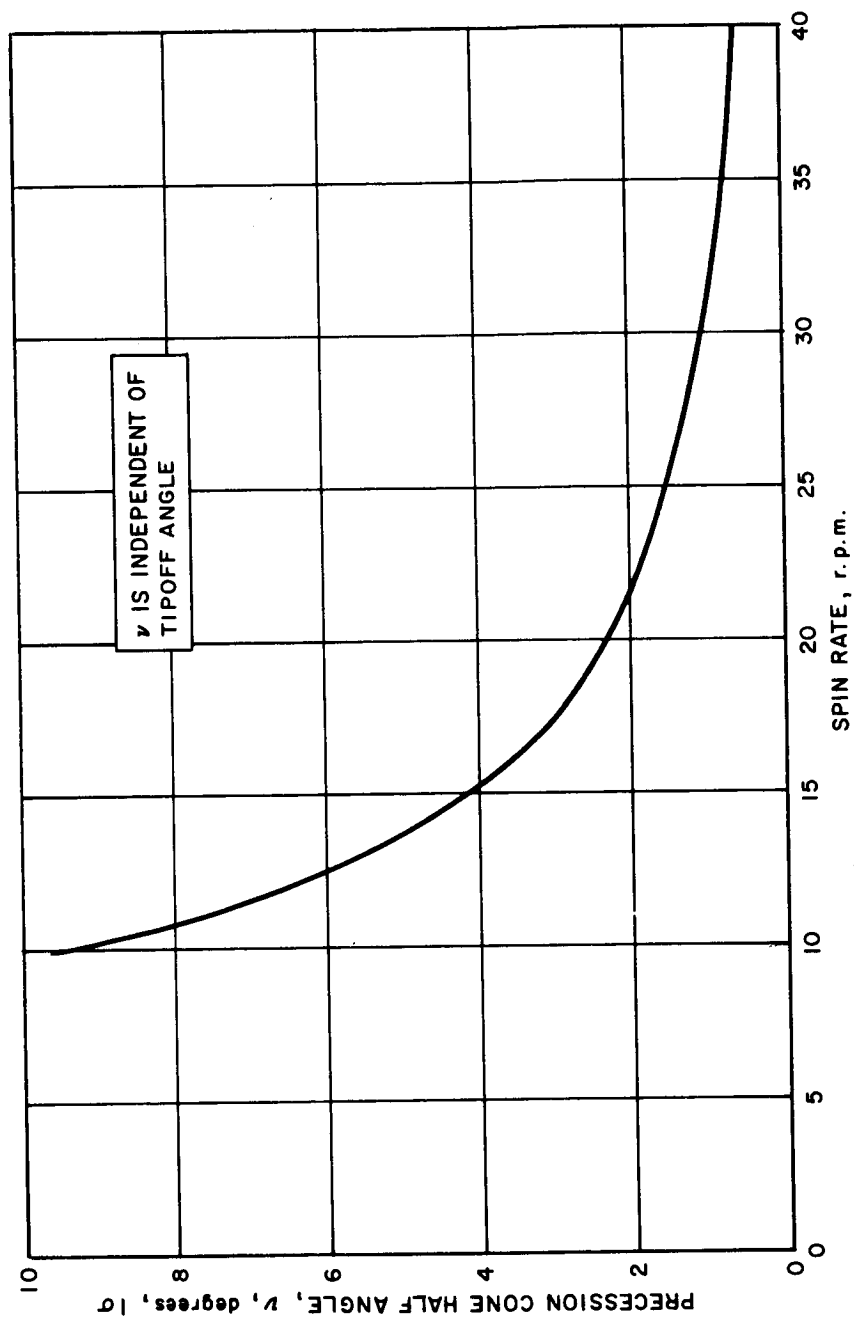


Figure 4 SPIN-THRUST SYSTEM ACCURACY



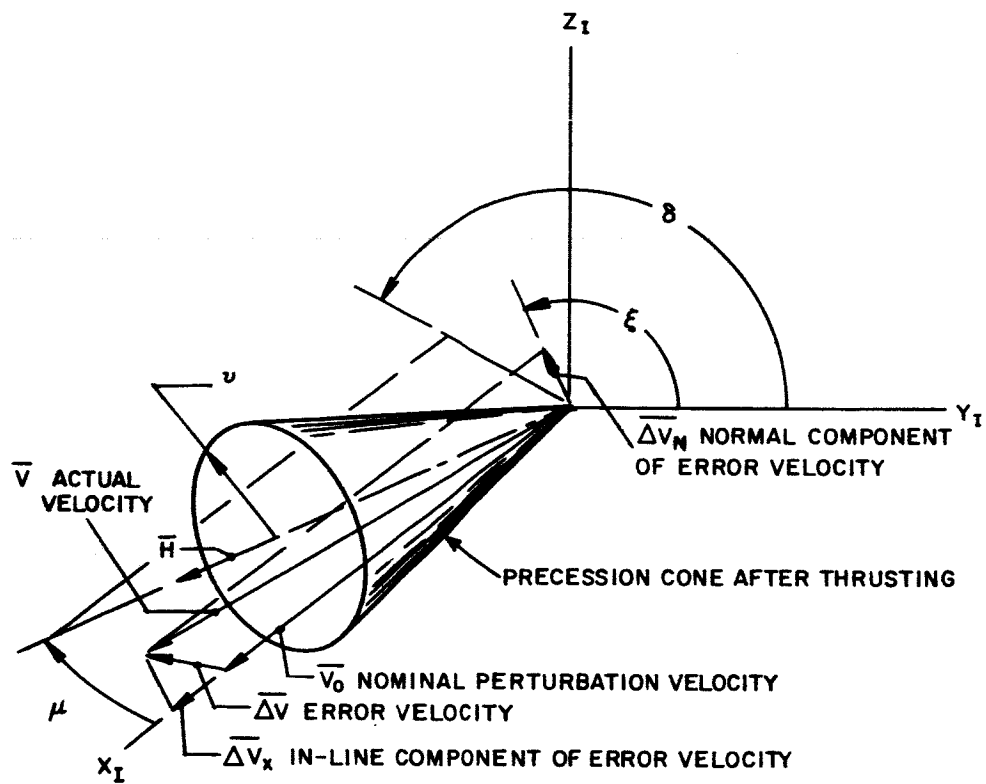
66-1362

Figure 5 PRECESSION CONE CENTRAL ANGLE VERSUS SPIN RATE



86-1363

Figure 6 PRECESSION CONE HALF ANGLE VERSUS SPIN RATE



86-1364

Figure 7 SPIN-THRUST SYSTEM ERRORS

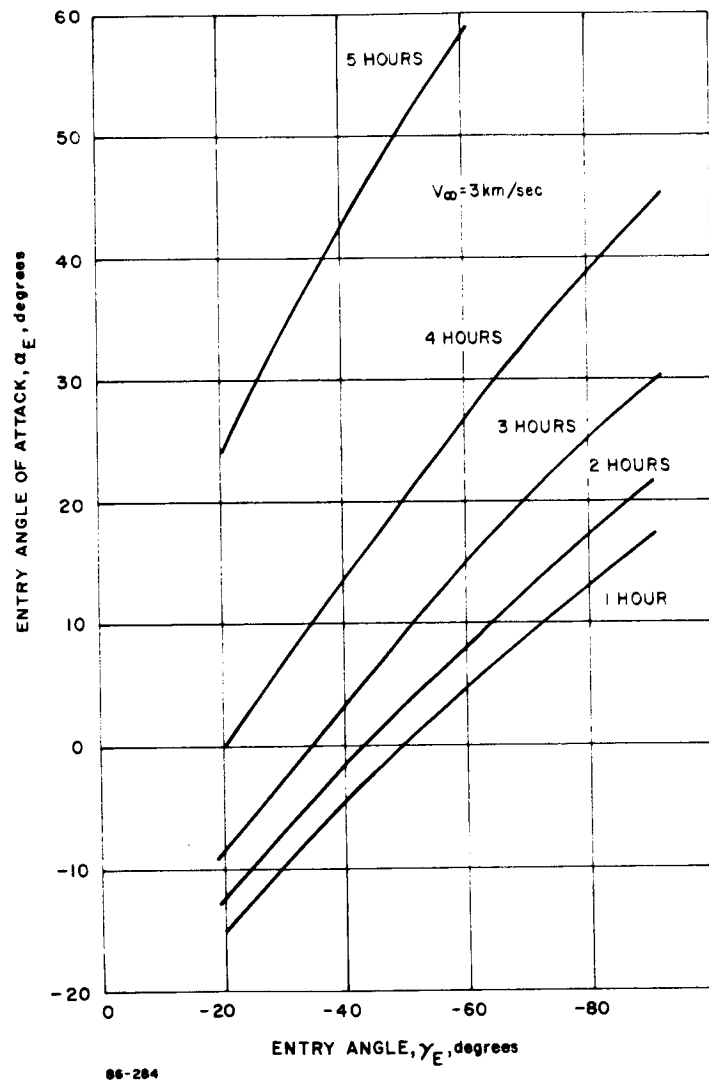


Figure 8 ENTRY ANGLE OF ATTACK AS A FUNCTION OF ENTRY ANGLE FOR VARIOUS LEAD TIMES

- b. Maneuver the capsule thrust axis into a preselected attitude with respect to the spacecraft reference attitude for thrust application.
- c. Provide thrust vector control during thrusting.
- d. Maneuver the entry vehicle to the attitude required for entry or communications.
- e. Maintain attitude during cruise to entry with the reaction control system.

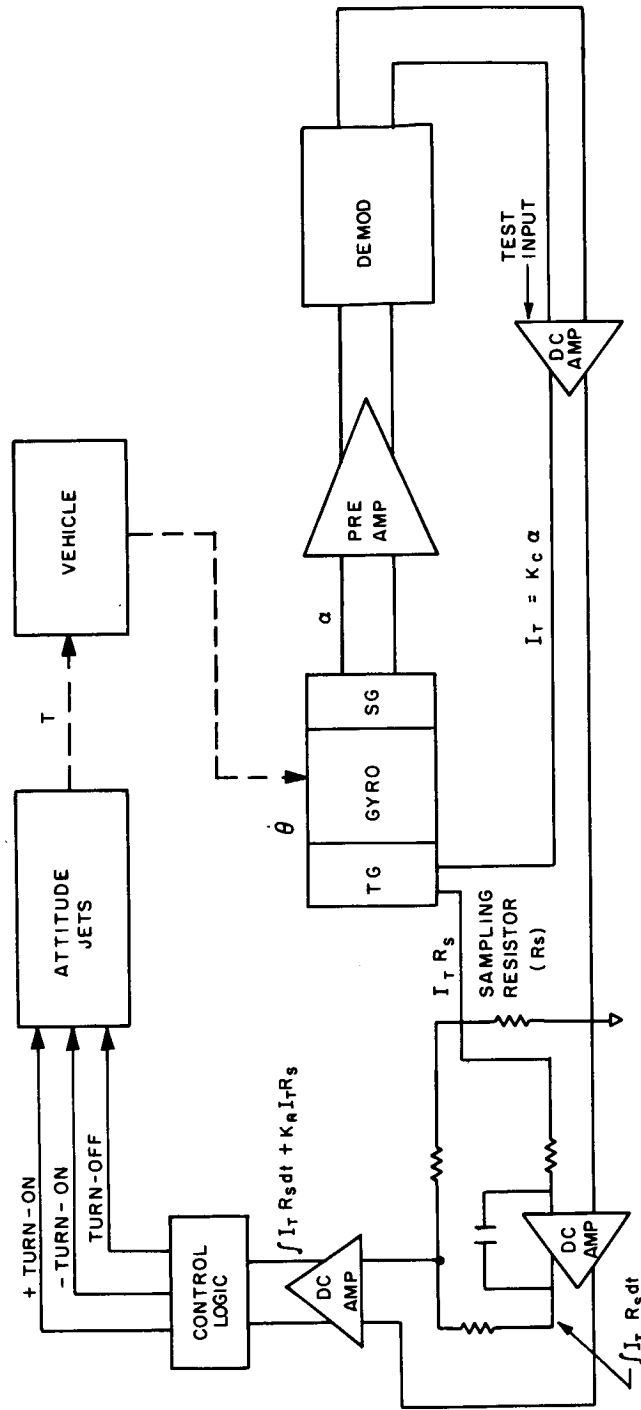
#### 2.4.2 Error Analysis

The performance and error analysis is based on the schematic shown in Figure 9. Rate information is provided by the gyro subsystem. Angular memory is provided by electronic integrators operating on signals derived from the gyro capture currents. The two gyros have their input axes normal to the longitudinal axis (pitch and yaw gyros) will be installed with their output axes parallel to the longitudinal axis. Therefore, the axial acceleration will not react on the gyro gimbal mass unbalance and anisoeasticities to cause acceleration-induced drift rates in these two gyros, which control the direction of the thrust vector.

A high-gain gyro capture loop is used so that the gyro output angle is kept small enough to avoid significant off-null accuracy degradation in the gyro torquer. The total error in the computation of the vehicle pitch and yaw attitude angles may then be estimated as follows for the 1-sigma values:

Torquer scale factor stability	0.05 percent
Torquer nonlinearity	0.02 percent
Wheel power frequency	0.01 percent
DC voltage reference uncertainty	0.02 percent
Integrator nonlinearity	0.05 percent
Sampling resistor	0.02 percent

Assuming the errors to be statistically independent the combined standard deviation is 0.08 percent. This estimate applies to an angular rotation not accompanied by reversals in direction. If oscillatory motion is also present, then the following rectification errors apply to the angular amplitude of the oscillation:



85-1782

Figure 9 ATTITUDE CONTROL SUBSYSTEM SCHEMATIC

Torquer asymmetry	0.01 percent
Difference between + dc and - dc	0.01 percent
Integrator rectification	0.02 percent

The overall contribution is 0.025 percent.

In addition to the nonlinearity errors, the integrators have a drift rate which may be expressed in terms of the input signal required to maintain a zero output. This effect may be limited to an equivalent input error of 0.001 percent of the maximum input, if thermal control of critical circuit elements is provided. Thus, if the integrator is scaled for gyro torquing rates up to 10,000 deg/hr, the integrator drift will be 0.1 deg/hr. Sensitivity to acceleration in the pitch and yaw gyros is avoided by suitable gyro orientation. Therefore, the total drift rate for these gyros is 0.05 deg/hr (1 sigma).

The total 1-sigma attitude error,  $\sigma_{\Delta\theta}$  accumulated during a time,  $t$ , during which the flight capsule rotates through an angle  $\theta$  and oscillates with an angular amplitude  $\theta_0$  may be estimated from the equation:

$$\sigma_{\Delta\theta}^2 = (0.0008\theta)^2 + (0.00025\theta_0)^2 + (0.05 t)^2 + (0.1 t)^2$$

where  $\theta$ ,  $\theta_0$  and  $\sigma_{\Delta\theta}$  are in degrees and  $t$  is in hours. This equation may be evaluated for the various phases of the velocity correction sequence with the results:

<u>Phase</u>	<u>Duration</u>	<u>Nominal Turning Angle (degrees)</u>	<u>Cumulative Sensor Error (1 sigma) (degrees)</u>
Ejection	1 minute	0	0.00195
Orientation (for thrust)	6 minutes	180	0.144
Thrust	5 seconds	0	0.144
Orientation (for entry)	3 minutes	90	0.16

The system pointing accuracy while thrusting is then determined by:

Flight Spacecraft Sensor Error	0.053 degree *
Flight Spacecraft Limit Cycle	0.066 degree
Capsule Sensor Error	0.144 degree
Capsule Limit Cycle	0.066 degree
Capsule Mounting Accuracy	0.167 degree
Gyro Package Alignment	0.090 degree

The pointing accuracy during thrusting is then 0.26 degree (1 sigma).

This accuracy estimate represents a worst case condition. If the orientation for thrusting were 90 degrees, with a duration of three minutes, the cumulative capsule sensor error becomes 0.072 degree (1 sigma) and the resulting  $\Delta V$  pointing accuracy during thrusting is 0.23 degree (1 sigma). A reduction in pointing error of only 0.03 degree is realized.

After the orientation for entry the system will operate in a limit cycle mode until entry. Gyro drift rates, however, will cause excessive errors in the ACS. For a drift rate of 0.05 degree per hour (1 sigma) and a time to entry of 12 days the angular degradation is 14.4 degrees (1 sigma).

## 2.5 ACHIEVABLE PERFORMANCE OF ACTIVE ACS SYSTEM WITH TERMINAL GUIDANCE

### 2.5.1 Description of Operation

Future missions requiring better accuracy may necessitate a terminal guidance maneuver. The impact on the attitude control system will be in the form of additional sensors to provide optical fixes, increased fuel requirements, and/or auxiliary thrusters.

A preliminary analysis was done to determine the attitude control requirements for a terminal maneuver. The results indicate that the attitude control system weight will increase by 65 pounds to correct for a 500-km impact error at a range of 25,000 km. This is in addition to 30 pounds for instrumentation required to determine the value of the correction and the thruster and fuel required to provide the velocity correction.

---

\* This spacecraft sensor error is smaller than the value given in section 2.3.2 because no spacecraft orientation is required in this case.

The pointing requirements for the velocity correction are minimum during the terminal maneuver and can easily be met by the attitude control system used during the separation events. The major increase in the attitude control system weight is due to the cold-gas requirements for the reaction control system during the engine thrusting.

Because of failure mode possibilities, a desirable implementation of the attitude control events would be as follows:

1. Separate from flight spacecraft and null separation rates.
2. Reorient the capsule for velocity vector correction.
3. Stabilize during thrust application.
4. Reorient for correct entry angle.
5. Spin-up capsule for stabilization during cruise to entry.
6. Despin for terminal navigation maneuvers.
7. Establish the correct celestial reference frame.
8. Make navigation measurements.
9. Compute velocity correction.
10. Reorient for velocity correction.
11. Make velocity correction.
12. Reorient for entry.
13. Spin for entry stabilization.

#### 2.5.2 Error Analysis

An analysis was performed to determine the effect of a terminal maneuver on the ACS design for an impact point error correction. The terminal guidance velocity requirements are discussed in Appendix C. Due to geometric considerations, the use of DSIF alone for terminal guidance information is not considered practicable. Therefore, terminal corrections must be the result of on-board navigation equipment.

The instrumentation used in the ACS just after separation will also be utilized during the terminal maneuvers. The navigation measurements for another  $\Delta V$  will require additional instrumentation to gather the necessary data. This instrumentation will include a precision planet tracker, a sun tracker, a computer, and possibly a star tracker. Using a typical performance characteristic for these instruments that can be expected in 1971, and assuming that the radius of Mars is known to 0.1 percent, a terminal maneuver cannot be executed until the range has been reduced to 30,000 km if the impact point error is to be limited to 50 km. This is due to the fact that at longer ranges, the error associated with the navigation instrumentation exceeds 50 km.

Assuming a terminal maneuver at 25,000 km, the velocity increment required for a 500-km correction will vary from 360 ft/sec for  $\gamma_e = -90$  degrees to 280 ft/sec for  $\gamma_e = -50$  degrees. Using the derived influence coefficients, the applied velocity correction error can be 30 ft/sec before the impact point error reaches 50 km. This can be translated into an attitude error during the terminal maneuver thrusting mode of approximately 5 degrees. Since the ACS will be capable of maintaining vehicle attitude of 1 degree or better if the thruster characteristics are similar to those of the thruster used at separation, the attitude control error contribution can be neglected.

As a result of the additional control needed for terminal guidance, the ACS will require additional equipment such as extra spin and despin rockets and additional capacity in the cold-gas reaction system. The weight for this additional equipment will be 65 pounds. Furthermore, the navigation instrumentation will add another 30 pounds. This, of course, is all in addition to the existing equipment and the propulsion system required for the velocity correction of 280-360 ft/sec.

## 2.6 ACHIEVABLE PERFORMANCE OF ACTIVE ACS PLUS SPIN SYSTEM

This system is the same as that described in Section 2.4 except that stabilization during cruise is obtained by spin instead of active attitude control.

### 2.6.1 Description of Operation

The sequence of operations for this concept is as follows:

- a. System turn-on and warmup,
- b. System drift trimming,
- c. System checkout,

- d. Electrical and mechanical separation from the spacecraft,
- e. Activate reaction system and realign Separated Vehicle to reference attitude,
- f. Orient vehicle thrust axis to desired  $\Delta V$  vector,
- g.  $\Delta V$  thrust applied, three-axis control maintained,
- h. Reorient capsule bus so that vehicle is aligned for desired entry angle of attack,
- i. Spin stabilize, and
- j. Eject the ACS.

#### 2.6.2 Error Analysis

The error analysis for the active ACS during thrusting is identical to that described in paragraph 2.4.2 for the active ACS only, giving a pointing accuracy during thrusting of between 0.23 and 0.26 degree (1 sigma), depending on the magnitude of the orientation maneuver required prior to thrusting.

After thrusting the vehicle is oriented for the entry attitude and is then spun up to 10 rpm. Any initial transverse angular rate will cause the capsule to precess (a coning motion) up to entry. The magnitude of the cone half-angle will be less than 2 degrees. Since the entry vehicle is spinning about its axis of maximum moment of inertia, it possesses asymptotic stability; any structural damping present will cause the precession half-cone angle to decrease. Thus the angle of attack at entry can be controlled and made nominally zero, within 2 degrees.

### 3.0 SELECTION OF REFERENCE DESIGN CONCEPT FOR 1971 MISSION

#### 3.1 CRITERIA AND CONSTRAINTS

##### 3.1.1 Basic Function

The ACS is required to perform the following basic functions:

- a. Orient the capsule thrust axis to the proper attitude for application of the separation velocity
- b. Stabilize the capsule during thrusting.
- c. Reorient the capsule after thrusting to maintain proper attitude for communications or entry.

Some of these basic functions may not be required, depending on the detailed capsule design concept, or some may be desirable but not essential. Specifically, the orientation of the capsule is not required if the orientation is performed by the spacecraft before separation. Stabilization of the capsule during thrusting is required in all cases. Reorientation and maintenance of proper attitude before entry is not essential, but if not done, may place additional demands on other subsystems, and is therefore a proper function for a tradeoff evaluation.

##### 3.1.2 Criteria

In performing the basic functions the ACS should meet certain criteria as follows:

###### 3.1.2.1 Performance

The control of the thrust application angle should be such as to effect entry angle dispersion of less than 2.5 degrees (one sigma), and the ACS should perform other orientation maneuvers as required. This requires attitude control during thrusting with an accuracy of 0.25 degrees (one sigma) for an entry angle of -40 degrees (see Paragraph 2.1.1).

###### 3.1.2.2 Reliability

The ACS components shall meet performance specifications with a reliability of 0.987 percent at 90 percent confidence level. Back up failure modes should be provided in the event of failure of a critical part of the subsystem. Existing qualified components will be used where applicable.

### 3.1.2.3 Environmental Criteria

The ACS must withstand:

- a. Flight capsule static accelerations of 15g axial and 7.5g lateral. Capsule dynamic loads which can be simulated by a 3-g rms axial and 2-g rms lateral vibration input to a flight configuration on a hard mount using a sine sweep 1 minute/octave from 2 to 100 cps.
- b. Nominal earth transportation and handling loads.
- c. Earth storage at  $80^{\circ}\text{F} \pm 30^{\circ}\text{F}$  for 2 years.

### 3.1.2.4 Sterilization

The system must undergo three high-temperature sterilization cycles within a period of 3 months. Sterilization conditions of  $295^{\circ}\text{F} \pm 2^{\circ}\text{F}$  for 24-hours duration are to be attained inside the motor where temperature lag is greatest. No inspection by disassembly is permitted after sterilization.

### 3.1.2.5 Other Desirable Criteria

Other criteria may be desirable, but not at the expense of those already presented. The system should be light in weight. It should be flexible in its use; that is, it should readily accommodate changes in other subsystems or changes in requirements or mission details. The subsystem should have a minimum effect on design requirements of other subsystems. It should have growth potential for use on later more sophisticated missions.

### 3.1.3 Constraints

Design requirements include the following basic constraints:

- a. The capsule c.g. location will be known within 0.0833 inch (1 sigma).
- b. The  $\Delta V$  thrust rocket will be located to within 0.042 inch (1 sigma).
- c. The  $\Delta V$  thrust misalignment will be no greater than 0.09 degree (1 sigma) with the capsule gyro reference axis.
- d. The velocity change sequence shall be accomplished within 15 minutes after separation.

- e. Exhaust products from ACS thrust nozzles or rockets must be gaseous only.
- f. Flight spacecraft sensor error is 0.053 degree (1 sigma) from the spacecraft reference axes.
- g. Flight capsule mounting accuracy is 0.167 degree (1 sigma) with respect to the reference axes of the spacecraft.
- h. The ACS may be mounted such that ejection mechanism for the rocket motor shall also eject all or part of the ACS package.
- i. Location of the ACS components shall be such as to minimize blocking of the VHF communication antenna with respect to the spacecraft.

### 3.2 COMPARISON OF CONCEPTS AND SELECTION OF REFERENCE CONCEPT

Four ACS concepts have been described; these are: (1) the spin-only configuration, (2) the active ACS, (3) the active ACS with terminal guidance, and (4) the active ACS plus spin system. Each of these concepts is compared in the following paragraphs, weighed against the criteria, and the reference concept is selected.

#### 3.2.1 Spin-Only System

The performance and error analysis shows that spin rates of 30 to 40 rpm must be achieved before the  $\Delta V$  pointing accuracy begins to level off. These asymptotes are 0.25, 0.36, and 0.50 degrees for the tipoff angles 0.15, 0.30, and 0.45 degrees, respectively; the 0.30 tipoff angle representing a nominal case.

Maneuvers are required by the spacecraft to attain the proper attitude for thrusting. These orientation maneuvers must be made using gyros for attitude reference. As a consequence, the spacecraft pointing accuracy is lower than that achievable with optical (Sun-Canopus) sensors. The causes an increase in initial errors. When combined with the other static errors they form the asymptote approached with increasing spin rate.

Thus, the required nominal  $\Delta V$  pointing accuracy of 0.25 degree (1 sigma) is not realizable for a 0.3-degree tipoff angle. At shallower entry angles or higher approach velocities, the spin system is even more inadequate.

This is the simplest and lightest system; however, the requirement to maneuver the spacecraft may be a disadvantage. Although the required pointing accuracy is not met if a 3-hour lead time must be obtained by

speedup of the capsule, its performance is adequate with reduced lead times.

### 3.2.2 Active ACS

This system uses an active ACS for orientation, to maintain attitude during thrusting, to orient for entry attitude, and to maintain attitude during cruise. Adequate pointing accuracy can be realized for lead times less than 3 hours and entry angles of -40 degrees or steeper. No spacecraft maneuver is required. It is flexible and has growth potential, but is heavier, more complex and less reliable than a spin only system. It is also difficult to achieve proper alignment between the spacecraft attitude reference and the gyro reference on the capsule. This concept maintains cruise attitude by reaction control. Due to the long time during cruise the total impulse required becomes excessive and attitude error due to gyro drift becomes so large that the benefits to be gained by active attitude control during cruise are questionable.

### 3.2.3 Active ACS with Terminal Guidance

The use of terminal guidance permits almost any reasonable degree of accuracy to be achieved and easily meets performance requirements. For more sophisticated missions in the future it may be a desirable choice. At the present time it represents a complex, unproven technique, a significant weight penalty, and a complication to the mission by requiring maneuvers for navigation fixes and large velocity changes while rather close to encounter.

### 3.2.4 Active ACS Plus Spin System

This is the same as the active system discussed in paragraph 3.2.2, except that spin stabilization is used during cruise. The same comments apply except that much better control of the entry angle of attack is possible by use of spin stabilization, specifically 2 degrees compared to 14 degrees (see paragraphs 2.4.2 and 2.6.2).

### 3.2.5 Selection of Reference Concept

The concept which has been selected is the active ACS with spin. This choice was dictated by the stringent pointing accuracy requirements imposed by a lead time of 3 hours together with the desire to avoid the complication of spacecraft orientation and slowdown maneuvers. If these maneuvers should be permitted, the spin-only system would be the preferred choice.

The concept of active ACS with terminal guidance was not selected because of its complexity, impact on other systems, and weight penalty. The active

ACS plus spin is marginally adequate, but use of shallower entry angles will result in more stringent pointing requirements, thus forcing the use of terminal guidance unless better ephemeris data is obtained, or spacecraft orientation and slowdown maneuvers are permitted. The selected concept has an important failure mode provision. If the active ACS fails before separation, the spacecraft can (in an emergency mode) perform the required orientation maneuver, and the spin rockets can be used to spin up the capsule, thus using a spin-only mode as a failure mode. The spin rockets used for stabilization after thrusting in the normal mode will not provide a sufficiently high spin rate for attitude stabilization while thrusting in the failure mode. Therefore, additional spin rockets are provided for this purpose.

### 3.3 INTRASYSTEM TRADEOFFS FOR REFERENCE CONCEPT

For the active ACS with spin, there were various tradeoffs made within the design of the ACS itself. A discussion of these aspects is the subject of this section.

#### 3.3.1 Gyros

The gyro proposed for the ACS is the Kearfott Alpha gyro similar to that used by JPL on the Mariner flights. Some characteristics may be varied to meet mission requirements, but basically it will be the same design as the JPL gyro which has been proven in space flight. Since the gyro was designed for space flight, it meets some of the unique requirements for this application; among these are the ability to be sterilized by soak at high temperature, the ability to withstand vacuum environments for long periods of time, and excellent long-term drift stability. The foregoing were major factors in the choice of this gyro.

#### 3.3.2 Control Logic

The control logic was selected to optimize performance in both the stabilization and orientation modes and the limit cycle mode. Linear switching lines are used; i.e., the valve actuation signals are a linear combination of the first two components of the state vector (attitude error and error rate). Deadband and hysteresis are included to provide satisfactory limit-cycle performance. Since fast settling time was not a requirement during orientations, angular rate is limited to a maximum of 1 deg/sec during this phase.

#### 3.3.3 Limit Cycle

Limit-cycle characteristics were chosen so as to maintain a required accuracy. Since stabilization during cruise is provided by the spin system,

a low duty cycle was not a factor. The limit-cycle amplitude will be less than 0.1 degree with a limit-cycle rate of less than 0.3 deg/sec.

#### 3.3.4 Reaction System

The reaction control system selected is a cold-gas system with gaseous nitrogen as the propellant. Three-axis control is provided in couples. Pitch and yaw thrust levels are dictated by the disturbing torques during the thrust interval, and are six pounds per nozzle. The roll nozzles are sized on a basis of the requirement to null separation rates. A thrust level of 0.3 pound per nozzle was found to be satisfactory.

If the system were filled prior to sterilization, a double penalty on pressure vessel weight would be imposed: Vessel material strength would be degraded while at the same time internal gas pressure would rise significantly at the elevated temperature. To avoid this situation, a fill system has been devised that allows filling the tanks after sterilization. It consists of a filter, a normally closed solenoid valve, and a capillary tube sealed at the sterilization canister outlet and attached to a sterile propellant supply. Following the sterilization cycle, the pressure vessel is filled, after which the solenoid valve is closed, and the tube is pinched and weld-sealed outside the canister providing a redundant seal.

Gaseous nitrogen was selected for the propellant since it gives reasonable weights and volume while providing adequate performance. Other propellants may have volume advantages for comparable system weights; however, their use is not warranted since the volume constraint does not appear limiting, and additional costs and handling complexities are imposed by their use.

## 4.0 REFERENCE ATTITUDE CONTROL SYSTEM DESCRIPTION

### 4.1 GENERAL DESCRIPTION

The design selected makes use of a combination of active attitude control (a gyro controlled cold-gas reaction system) and spin stabilization, which is accomplished by solid propellant spin rockets. The angular rates of the capsule are measured by three body-mounted rate gyros; the outputs of these gyros are electronically integrated so that angular position as well as angular rate is available. This information is used by the control logic to operate the valves of the cold-gas reaction control system. This system provides three-axis control in couples by means of 12 nozzles. Spin stabilization is provided by two redundant groups of solid propellant rockets. Normally only one group is required for spin stabilization, but if the primary operational mode of the ACS fails, both sets of spin rockets will be used in the backup mode. (In this case it is necessary to despin prior to entry, and a third set of rockets is provided for that purpose.)

The gyros and electronics will be turned on and allowed to warm up while the vehicle is attached to the spacecraft. During this time the ACS will be checked out; this also provides an opportunity to trim the drift of the gyros and integrators. Next the capsule is separated from the spacecraft, the reaction control system is activated and realigns the capsule to the spacecraft reference attitude, correcting for any disturbances which occurred during separation. The capsule is then oriented so that its thrust axis is aligned to the desired  $\Delta V$  direction and maintained in that direction during thrusting. The capsule is then reoriented to have zero-angle of attack at entry and is spun up by one set of spin rockets to maintain this attitude for the remainder of its trajectory until entry. Finally, the propulsion and ACS electronics assembly are jettisoned to reduce the weight of the entry vehicle.

### 4.2 SENSOR AND ELECTRONICS SUBSYSTEM

A schematic of the attitude control system is shown in Figure 9 while the mathematical model is illustrated in Figure 10.

The gyro proposed for the attitude control system is the Kearfott Alpha gyro similar to the gyro used by JPL on the Mariner flights. The gyro characteristics may be varied to meet the requirements of the ACS, but basically will be the same design as the JPL gyro which has been proven in space flight. Some of the characteristics that may be altered are the gyro gain, the characteristic time, and the gyro heater voltage. These will be modified to be compatible with the present requirements. Since the gyro was designed for space flight, it meets some of the unique requirements for this application; among them are the ability to be sterilized by soak at high temperature; the ability to withstand vacuum environments for long periods; and excellent drift stability over long periods of time.

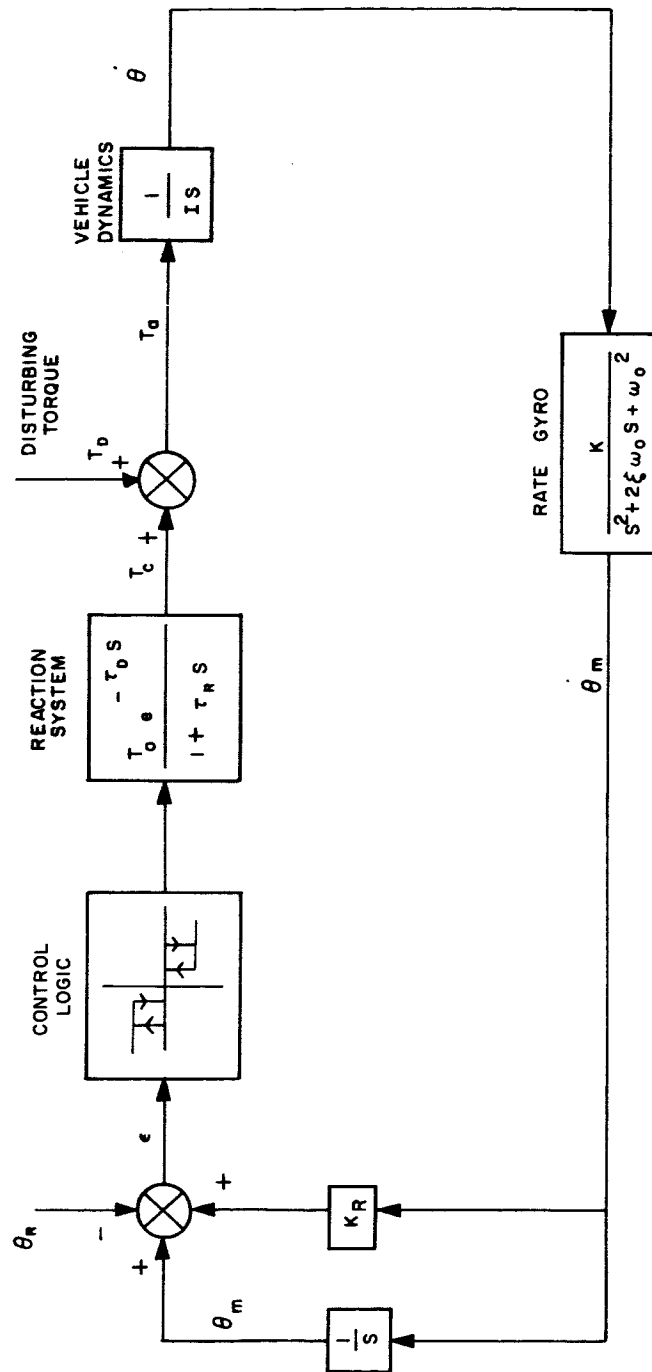


Figure 10 MATHEMATICAL MODEL OF ATTITUDE CONTROL SYSTEM

85-1785

The electronics required for the control of the gyro sensor consist of an amplifier-demodulator to close the gyro loop, an electronic temperature controller, and a precision inverter. The gyro-loop amplifier demodulator is a standard design using integrated circuit electronics. The gyro-loop dynamics are adjusted by the gain of the amplifier to meet the requirements of the control loop. For a gyro-loop natural frequency of 100 rad/sec and a damping ratio of 0.6, the amplifier gain is approximately 1.0 ampere/volt for the Kearfott Alpha-type gyro. The sensitivity of the rate-gyro loop is determined by the gyro torque motor sensitivity (deg/sec/ma) and the value of the sensing resistor (used in the torque motor circuit).

The temperature controller will maintain the gyro to within 0.5°F of the operating temperature by using a bridge-type circuit to proportionally control the power to the heater. The close control is required to maintain the low values of gyro drift rates. The Alpha gyro is provided with a two-stage heater. The high-power heater is used for the initial warmup of the gyro and the low-power heater is used to maintain the gyro temperature. The operating characteristics of the gyro temperature controller will be a function of the environment of the gyro. That is, the radiated heat loss will determine the required temperature controller performance. To minimize the radiated heat losses, the gyro package is enclosed in a covered package. In this manner it is anticipated that the heater will require less than 10 watts per gyro to maintain the proper temperature. The main consideration in the design of the inverter is the maintenance of exact frequency control for the wheel power. This will be controlled to better than 0.01 percent by using a crystal as a frequency standard and countdown circuitry. This factor is important since the frequency determines the wheel speed and hence the sensitivity of the gyro loop.

The output of the gyro is integrated to provide an indication of angular position. An obvious method of providing this function is to use an electronic analog integrator. This can be instrumented by using a dc-operational amplifier with a capacitor in the feedback loop. The chief consideration in this type of design is the drift of the integrator. The requirements of the system are such that the integrator cannot contribute more than 0.1 deg/hr of error. The scale factor on the integrator will determine the feasibility of accomplishing this. The scale factor will be a function of the maximum turning angle required. For instance, if the maximum turning angle in any axis is 100 degrees and the maximum integrator voltage is 50 volts, the integrator sensitivity will be 0.5 volt/degree. This would require that the integrator output would not change by more than 50 millivolts in one hour due to drift considerations.

This scaling will be accomplished with chopper stabilized amplifiers which are trimmed prior to operation and/or operated in a controlled environment.

An alternate method of accomplishing favorable scaling is to use an integrator such as that described above, but operated in a limited range. This is made possible with a pulse rebalance technique. In this way a count of the rebalance pulses provide a measure of angular position while maintaining a variable scale factor on the analog integrator. However, this does require precision rebalancing pulses and a counter or register to sum the pulses. Both approaches to the integration will be investigated to determine the best method of accomplishing the objectives.

In either approach it would prove advantageous to maintain the circuitry in a temperature controlled environment to reduce the temperature affects. This can be accomplished by maintaining all of the electronics and gyros in a closed container. This will in effect be a controlled environment by virtue of the gyro temperature control and the insulating effect of the cover. The output of the integrator is summed with the output of the rate gyro to provide the required error signals to the appropriate reaction control valve. This is accomplished by using a dc-feedback amplifier for summing the signals. The amplifier then feeds a Schmitt trigger that is appropriately biased for the correct firing level. The output of the Schmitt trigger feeds a power stage that controls the reaction control valves. The gain of the amplifier is adjusted to meet the control system requirement. The hysteresis of the Schmitt trigger is also adjusted to approximately 10 percent for system stability.

The summing amplifier provides a means of inserting commands for reorientations. This command is furnished by the CC&S unit; it provides programmed inputs, ground commanded inputs, or computer inputs to each axis.

The power stage is sized for the control valves of the reaction control system, which require approximately 1.5 amperes at 28 volts dc. The frequency response of this trigger circuit is sufficiently high (100 cps) to eliminate any contribution by it to system response.

All electronics will be microelectronics where possible. However, some of the high-power requirements may require the use of hybrid circuits. A weight and volume summary of the sensors and electronics is presented in Table IV.

TABLE IV  
WEIGHT AND VOLUME SUMMARY OF SENSORS AND ELECTRONICS  
(INTEGRATED CIRCUITS)

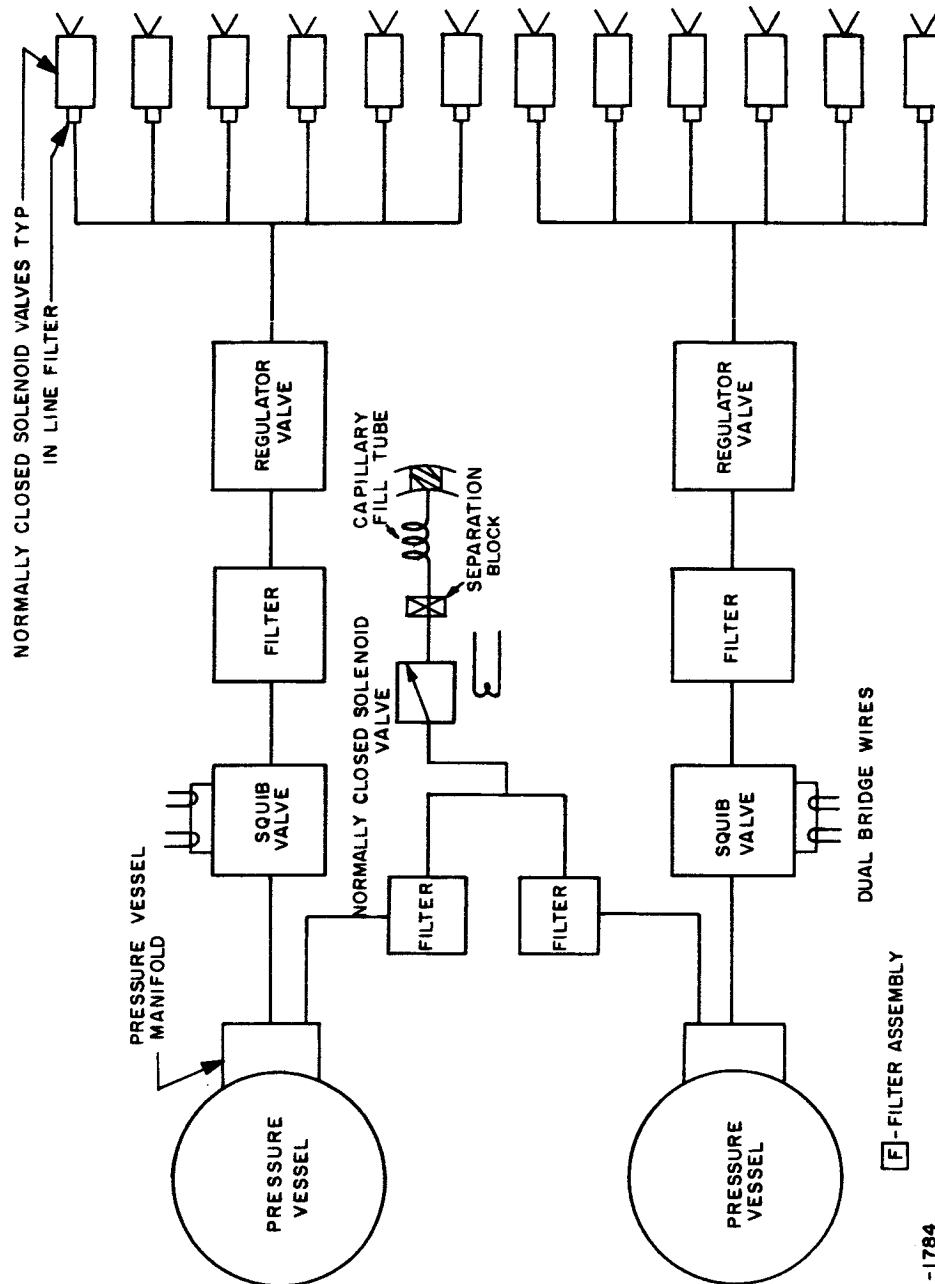
Component	Weight (pounds)	Volume (in. <sup>3</sup> )
Inverter	1.0	40
Gyro Package	4.0	50
Control Electronics	2.0	80
Integrator Subsystem	1.0	40
Mounting, Cables	2.0	--
Total	10.0 pounds	210 in. <sup>3</sup>

Note: Battery not included

#### 4.3 REACTION CONTROL SUBSYSTEM

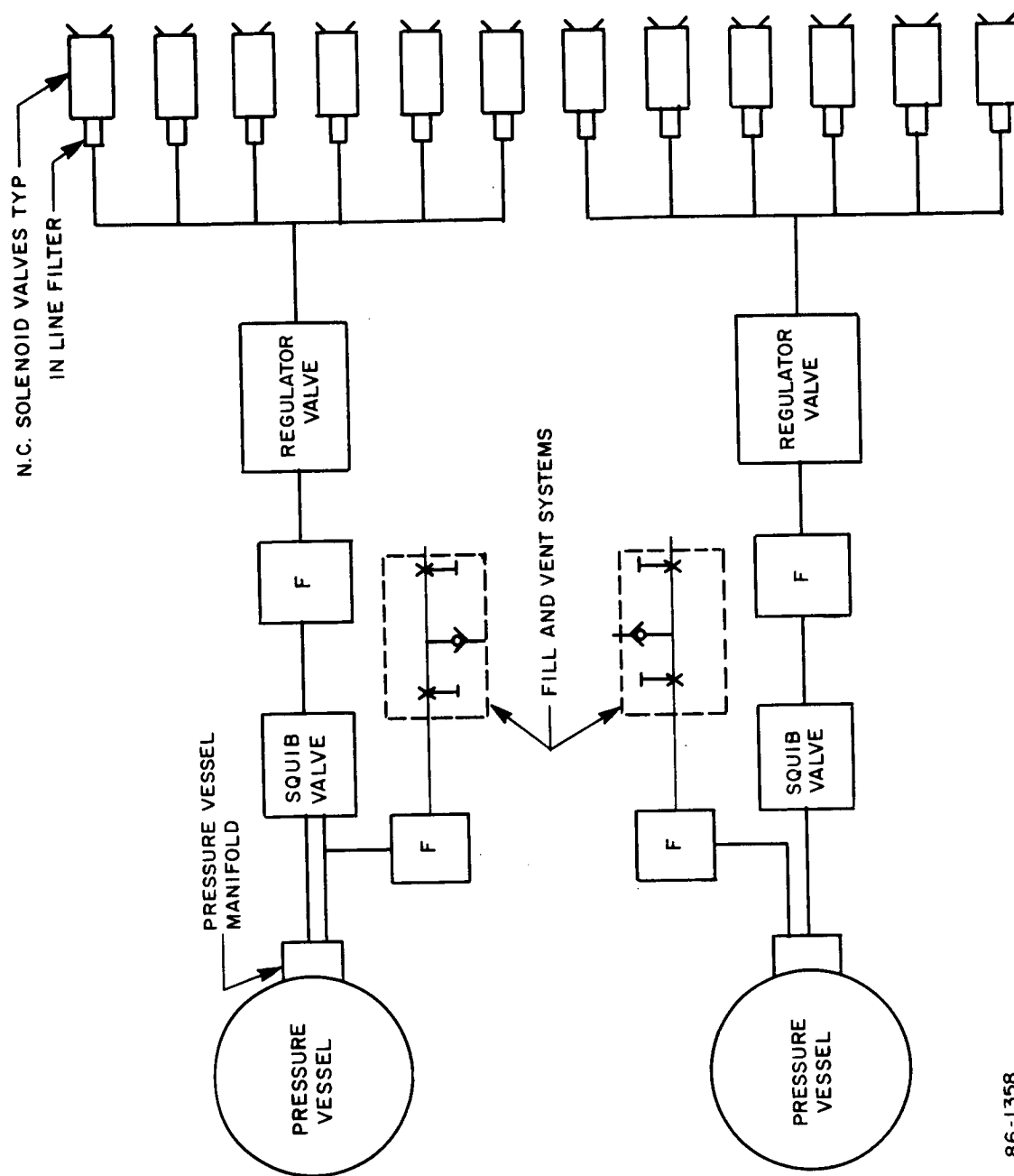
The reaction control system is basically a cold-gas system utilizing gaseous nitrogen as the propellant. Two identical independent subsystems as depicted in Figure 11 are proposed, each consisting of a vent and fill assembly, squib valve, filter, regulator valve, and six nozzle-solenoid assemblies with integral filters. The central regulator concept has been adopted for each subsystem. This two system approach provides the necessary safety margin against all failure modes, including the valve-open failure mode.

The use of conventional vent-fill systems utilizing a complex of valves, Figure 12, would necessitate filling the system prior to the sterilization cycle, thereby imposing a pressure vessel weight penalty since the vessel material strength is substantially degraded while the internal gas pressure rises significantly at this elevated temperature. Hence to avoid this weight penalty a fill system has been devised that allows filling the tanks after sterilization. This fill system, depicted in Figure 11 consists of a filter, a normally closed solenoid valve and a capillary tube sealed at the sterilization canister outlet and attached to a sterile propellant supply. Following the sterilization cycle the pressure



85-1784

Figure 11 COLD-GAS REACTION CONTROL SYSTEM



86-1358

Figure 12 CONVENTIONAL VENT-FILL SYSTEM

vessel is filled, after which the solenoid valve is closed and the tube is pinched and weld sealed outside the sterilization canister allowing redundancy in the seal.

The system is activated by simultaneously imposing a voltage on the squib initiators of both subsystems. Each regulator then supplies the nozzle valves with constant pressure gas. Actuating currents are simultaneously applied to two valves, one in each of the two systems, to produce the desired torque about a given axis.

The total impulse required to be delivered  $I_{st}$ , is summarized on Table V.

TABLE V

SUMMARY OF REQUIRED IMPULSE

Stabilization after separation	71 lb-sec
Orientation (2 maneuvers)	10 lb-sec
Stabilization while thrusting	131 lb-sec
Limit cycling	20 lb-sec
Total	232 lb-sec

Additional impulse is required as safety margin to account for the following modes of failure and performance degradation:

4.3.1 Leakage

A pressure vessel, line or component leak in one of the two systems will require that the non-leaking system do all the torquing; hence, the quantity of gas must be doubled. Defining the safety margin multipliers by the letter  $N$ , the multiplier for this case is  $N_1 = 2$ .

4.3.2 Valve Failures

A valve failing to open would result in the loss of a pure couple in one sense only on one axis; hence, no gas contingency is required since the valves are located in planes passing through the principal axes. However, should a

valve in one system fail to close, then one other valve in the same system will operate in conjunction with a third valve from the second system to cancel the torque until the failed valve drains its system down.

Since each of the systems contributes one-half of the cancelling torque, then each system must have an extra 50 percent of cold gas to accommodate this failure mode. Thus, the safety margin factor,  $N_2$ , is 1.5.

#### 4.3.3 Impulse Degradation

A portion of the available impulse is lost during short term reorientation and limit-cycle operations. Experience on other programs has shown that the multiplier for this effect should be approximately  $N_3 = 1.1$ .

The total stored impulse for the system,  $I_t$ , becomes, therefore:

$$I_t = I_{st} \times N_1 \times N_2 \times N_3 = 3.3 I_{st}$$

Gaseous nitrogen was selected as the propellant. A reasonable system weight can be realized utilizing nitrogen as indicated on Figure 13 which relates system weight as a function of molecular weight and impulse. Other propellants may have volume advantages for comparable system weights; however, their use is not warranted since the volume constraint does not appear limiting and additional cost and handling complexities are imposed by their use.

To obtain the required useable impulse, the required weight of propellant is determined and tank volume is computed taking into account the residual gas remaining in the tank at final gas temperature and pressure, using real-gas tables and a polytropic process for gas discharge.

The operating time of the RCS is estimated at 15 minutes and since a large portion of the gas is emitted during  $\Delta V$  thrusting, a polytropic exponent  $n = 1.05$  was assumed.

The pressure vessel design is contingent upon:

1. The quantity of propellant required, which is in turn based on the propellant selected, the impulse desired and the safety margin.
2. The selected storage pressure.
3. Design criteria including safety factors, environmental requirements, material selection and fabrication procedures.

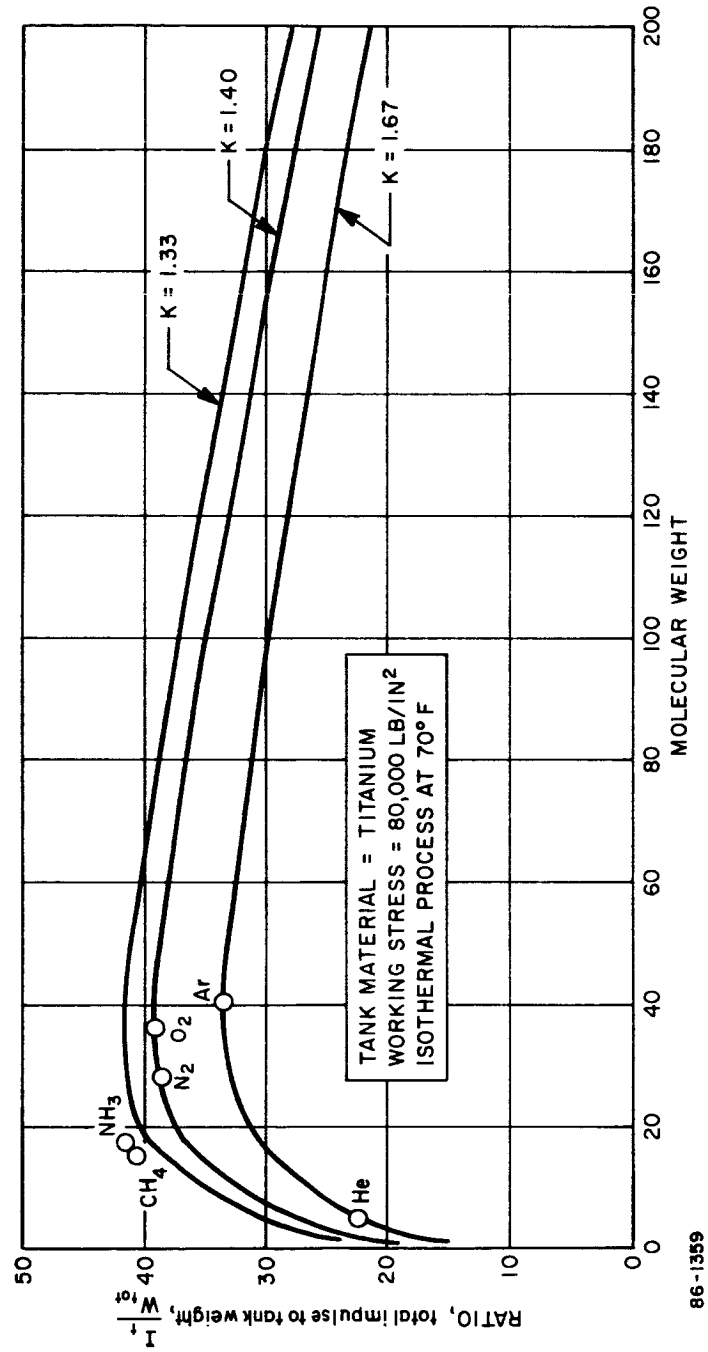


Figure 13 TOTAL IMPULSE/TANK WEIGHT VERSUS MOLECULAR WEIGHT

The pressure vessel is sized using 6-4 titanium alloy with a yield strength of 160,000 lb/in and a safety factor of two.

The pitch and yaw nozzles were sized at a 6-pound thrust level to counteract the disturbing torques due to rocket motor firing arising from these error sources:

- a. C.G. location error
- b. Rocket location error
- c. Rocket thrust misalignment

The disturbing torques in roll are negligible, so the roll nozzles were sized at a 0.3-pound thrust level solely to meet stabilization requirements for nulling separation rates.

The design of the remaining components is relatively straightforward, with the exception of the high vacuum requirement which necessitates the use of all metal valve seats. Also, special consideration must be given to material stability since the components will be subjected to elevated sterilization temperatures.

Contamination of the system by foreign matter and particles from the squib valve when it is ruptured is a most important problem, particularly since all metal valve seats are proposed and leakage is critical. Particular attention must be given to handling, assembly techniques and material cleanliness, especially the components, lines and the gas used as the propellant. Filtration is designed into the system at all critical locations. Consideration was given to both the filter functional and structural design since system initiation by squib detonation exposes all filters downstream to pressure fronts capable of blowing out improperly fixed filter elements.

A weight summary for the nozzles, tanks, gas, and associated equipment for the reaction control subsystem is presented in Table VI.

TABLE VI

## REACTION CONTROL SYSTEM WEIGHT SUMMARY

Component	Weight Each (lbs)	Number	Total (lbs)
Nozzle valves	1.3	12	15.6
Pressure vessels	6.1	2	12.2
Gas (GN <sub>2</sub> )	12.6	--	12.6
Squib valves	1.5	2	3.0
Vessel manifolds	0.3	2	0.6
Fill solenoid and capillary	0.8	1	0.8
Line coupler	6.0	2	12.0
Regulators	5.5	2	11.0
Filters	0.5	4	2.0
Total Weight			69.8 pounds

## 4.4 SPIN SUBSYSTEM

Spin stabilization is provided by 10 solid propellant rockets. The spin rockets will be arranged in two groups. In the case of failure of one group the other will be used for spin up to 10 rpm. Both sets of spin rockets will be used in the case of ACS failure in order to provide a higher spin rate for stabilization while thrusting. (In this failure mode it is necessary for the spacecraft to perform the orientation maneuver prior to separation in order to achieve the attitude required for thrusting.) In this case an additional eight rockets are required to despin to 10 rpm at entry.

The spin rockets are solid propellant Scout spin motor MARC-4B2 (Atlantic Research), modified. The primary modification is the replacement of the presently used propellant with a sterilizable propellant. A spin rocket performance summary is shown in Table VII and a design summary in Table VIII.

TABLE VII  
SPIN ROCKET VACUUM PERFORMANCE SUMMARY

Parameter	Value
<u>Impulse</u> Total per rocket	45 lb-sec
<u>Impulse</u> Specific	205 seconds
<u>Thrust</u> Average	82 pounds
<u>Burn Time</u>	0.55 seconds
<u>Temperature Limits</u>	
Operation	-35 to + 140 °F
Storage	-65 to + 140 °F

TABLE VIII  
NOMINAL SPIN ROCKET DESIGN SUMMARY

Parameter	Value
Envelope	1.53 inch diameter x 6.83 inch length
Weight	0.80 lb
Propellant	0.22 lb
Mass ratio, $W_p/W_t$	0.25

#### 4.5 PACKAGING

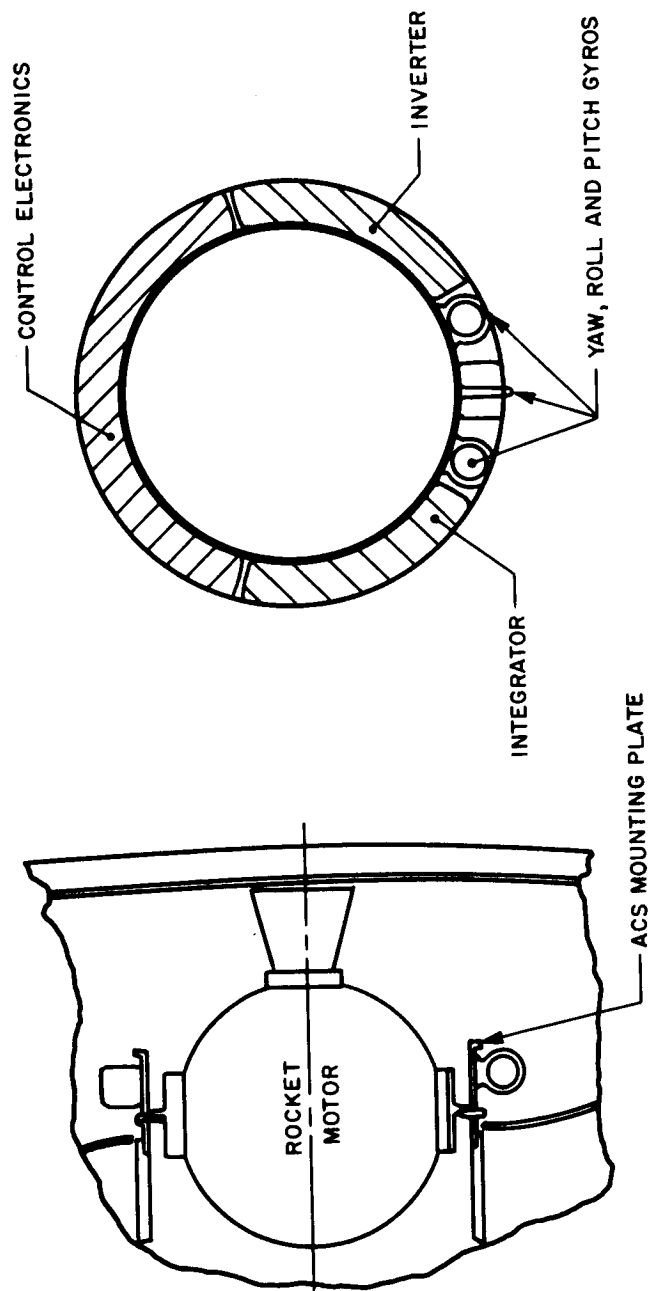
The following design requirements must be satisfied by the packaging configuration chosen for the ACS electronic package. The package must be mounted such that the ejection mechanism for the rocket motor shall also eject the ACS package. The location of the ACS package should be such as to minimize blocking of the VHF communication antenna with respect to the spacecraft. The c.g. of the package must be aligned with the c.g.'s of the vehicle and rocket motor.

Two major packaging requirements are that the axes of the gyros be aligned (within an allowable angular error) to the reference axes of the spacecraft and that the thrust vector be aligned (within an allowable angular error) with respect to the gyro package. The latter can be accomplished by combined use of optics and a rate table at the level of assembly at which the gyro package is mated to the rocket motor. The first requirement is considerably more involved since it involves initial alignment error plus errors due to distortion of the vehicle as a function of time. Allowable misalignment of the gyro package with respect to the spacecraft reference at the time of vehicle separation from the spacecraft is 0.2 degree (1 sigma).

The heating of the gyro package by radiation from the rocket motor must be considered in the packaging design. Calculations for heat transferred by radiation indicate that by silver plating the gyros and the rocket motor, the radiation heating of the gyro will be only 0.25 watt. Heating by conduction as a function of time will require analysis when the design has progressed beyond the preliminary phase. The ACS package could be further insulated by placing additional reflecting shields polished on both sides in a sandwich fashion between the shield and the rocket motor. The heat transfer will be decreased by the factor  $\frac{1}{n+1}$  where  $n$  is the number of additional shields. The axial length of the vehicle is restricted; therefore the ACS package cannot be located between the landed capsule and the rocket motor. The rocket nozzle achieves a high temperature; therefore, it would be unwise to attempt to locate the package in the vicinity of the nozzle. Since it is desirable to eject the ACS package (to increase the allowable payload entry weight) by the same mechanism that ejects the rocket motor, a logical location is around the rocket motor in a ring configuration. This is illustrated in Figure 14.

The aft part of the Marman clamp that attaches to the rocket motor will be a casting with provision for mounting gyros and associated electronics and will be a webbed construction to provide adequate support. The ejection spring will thus eject both the rocket motor and ACS package.

The center of gravity of the package may not be in alignment with the c.g. of the vehicle and the c.g. of rocket motor. This is because the gyros, which will



86-1360

Figure 14 ATTITUDE CONTROL SYSTEM PACKAGE

weigh up to 4 pounds, are clustered close together within about 90 degrees of the ring, while the electronics, which will weigh up to 4 pounds, will occupy about 270 degrees of the ring. Thus, the c.g. of the package is shifted toward the gyros. More accurate information on weights will be required before the package can be balanced realistically.

#### 4.6 ALIGNMENT SUBSYSTEM

To achieve acceptable levels of performance for the ACS, the alignment of the spacecraft and capsule attitude reference systems at the time of separation must be maintained to an accuracy of 0.2 degrees (1 sigma). Any degradation of this figure directly affects the ACS accuracy. This includes the alignment of the capsule thrust axis with respect to the capsule gyro reference axes and the alignment of the gyro reference axis with respect to the spacecraft reference axes. Unless an in-flight alignment is employed, the alignment must be maintained after the flight capsule is assembled and sterilized, attached to the flight spacecraft, during launch, transit, and separation. The ability to maintain this alignment up to separation appears to be questionable. Therefore, it is possible that an in-flight alignment may be required to ensure proper ACS performance. The present design does not incorporate such a system. However, if one is required, an optical alignment technique would be the best choice to reduce the dependence on mechanical rigidity. This approach imposes the requirement that an optical path must be provided between the spacecraft reference and the capsule gyro package. However, an optical alignment technique can easily meet the 0.2-degree (1-sigma) requirement.

## ATTITUDE CONTROL PROBE, ENTRY FROM ORBIT

### 5.0 INTRODUCTION AND SUMMARY

#### 5.1 SCOPE OF STUDY

The attitude control system requirements were determined for the various mission phases from separation to impact. The effects of other mission parameters (orbital parameters; location of the deorbit point; landing point) on the ACS requirements were evaluated as well as the intersystem requirements. These intersystem ACS tradeoffs included: the effect of maintaining communications between spacecraft and capsule; heat shield and structure penalties due to large angles of attack; and the effect on TV camera operation. Alternate design concepts were prepared and evaluated in terms of their ability to meet performance criteria and system constraints. From these alternatives a reference design was selected, and prepared in sufficient detail to establish size, weight, power, performance, development status, reliability, and ability to meet environmental criteria.

#### 5.2 MISSION PROFILE AND ATTITUDE CONTROL REQUIREMENTS

The attitude control system requirements vary for the various phases of the mission. For attitude control system considerations, the mission can be separated into five phases; each phase will now be described.

##### 5.2.1 Separation to Thrusting

After the flight spacecraft is injected into Mars orbit, separation occurs and a deorbit velocity increment is applied to the capsule to place it on an impact trajectory. The capsule can be placed in the proper thrusting attitude either by maneuvering the spacecraft prior to separation or by maneuvering the capsule by means of an active attitude control system. The time between separation and thrusting will be approximately one-half hour to allow sufficient separation distance between the spacecraft and the capsule. This separation distance is required to ensure that the rocket motor firing will not compromise the spacecraft operation.

##### 5.2.2 Thrusting

The attitude control system must maintain the proper attitude of the vehicle while the thrust rocket is firing since the required velocity increment must be obtained to provide the correct entry angle and landing site. The vehicle thrust vector is pointed by either spin stabilization or active attitude control of the capsule, or by gimbaling the rocket motor.

### 5.2.3 Thrusting to Entry

It is desirable to maintain communications between the spacecraft and the capsule from separation to impact. Therefore, proper orientation during this cruise phase is required if this is to be accomplished. However a more important consideration is the limitation of the angle of attack to small values and/or the achievement of low angular rates at entry to minimize the vehicle structure and heat shield design problems. The ACS would ideally provide a favorable communications attitude during this phase as well as provide favorable entry conditions.

### 5.2.4 Entry to Parachute Deployment

During this phase of the mission, the capsule will be aerodynamically stable and an ACS is not required. However, the instrumentation or sensor portion of the ACS may provide data during this phase for measuring entry phenomena for scientific purposes and for controlling discrete events. In addition, if an active ACS is selected, it can be used to prevent buildup of excessive roll rates due to aerodynamic torques resulting from vehicle asymmetries.

### 5.2.5 Parachute Descent

An active ACS could be used during this phase to stabilize the Suspended Capsule against disturbing forces. The more practical alternative would be the use of the sensor subsystem of the ACS to provide stabilization control signals to the scientific instrumentation (TV camera) requiring this control. Further, the ACS sensors could in themselves provide scientific data.

## 5.3 ALTERNATIVES CONSIDERED

Five ACS concepts were synthesized and evaluated.

### 5.3.1 Spin Only System

With this system, the capsule is oriented to the thrusting attitude by the spacecraft, and is spin stabilized after separation for thrusting and cruise; the spin rate is decreased prior to entry. This is the simplest and lightest system but requires a maneuver by the spacecraft which is the primary disadvantage. Performance is adequate for the entry from orbit mission.

### 5.3.2 Active ACS with Spin

This system uses an active ACS for orientation after separation. Spin stabilization is used to maintain attitude during thrusting and to entry. Adequate pointing accuracy can be achieved. It does not require a spacecraft maneuver and is more flexible; however, it is heavier than a spin only system.

### 5.3.3 Active ACS - Cold Gas

This system is the same as that previously described except that no spin stabilization is used. Control during thrusting and cruise is accomplished by a cold-gas reaction system. Due to the high thrust levels required to overcome the disturbance torques occurring during thrusting, the total impulse requirements make system weight excessive.

### 5.3.4 Active ACS with Gimballing

This concept also uses a cold-gas reaction control system except that gimballing of the rocket engine provides pitch and yaw control during thrusting. The thrust levels of the reaction control nozzles can therefore be sized to be compatible with orientation and limit cycle requirements, bringing the weight down. Lower reliability and increased complexity, due to the engine gimbal and its associated mechanism, are the major disadvantages.

### 5.3.5 Active ACS - Cold Gas and Hot Gas

This system utilizes a separate hot-gas reaction control system for use during the thrusting phase. Thus, weight requirements are not excessive. In addition, the system is flexible, has growth potential, and reliability and complexity features are improved. Because of its higher specific impulse, large c. g. offsets and thrust vector misalignments can be tolerated, thus easing concern over variations in these parameters during the heat sterilization process.

## 5.4 REFERENCE DESIGN SUMMARY

The design selected is the active ACS with cold gas and auxiliary hot gas; the control system actively maintains attitude from separation to entry. Attitude orientation maneuvers and initial stabilization are accomplished by a cold-gas reaction control system, control while thrusting for the  $\Delta V$  correction is provided by a hot-gas system. Commands to control the operation of the nozzle valves are generated in the Inertial Reference System (IRS) which includes a computer and a four-gimbal inertial platform. The inertial reference is established prior to separation. These command signals are a function of vehicle

angular error and its time rate of change. The reaction control system provides three-axis control in couples by means of twelve nozzles. Eight hot-gas nozzles provide control in pitch and yaw during the thrusting mode. Roll disturbances arising during this phase are handled by the cold-gas roll nozzles. Upon completion of the thrusting phase, the ACS maintains the attitude of the capsule with the cold-gas system. It may reorient the vehicle to optimize communication performance. An orientation will be performed prior to entry to an attitude which minimizes the angle of attack.

During early entry, the reaction control system pitch and yaw control will be disabled and roll control will be used only to limit roll rates. The IRS will remain operative and will provide acceleration data during the entry phase for the purpose of event control and also for entry wind and atmospheric density measurements. Upon parachute deployment, the IRS will provide the television camera gimbal system with commands required to maintain the optical axis of the cameras along the local vertical.

The IRS also includes a Sentry System consisting of body-mounted rate gyros which deactivate the reaction control system in case a failure of the inertial platform or any other component causes a control torque to be applied to any axis which results in a high angular rate, above 6 deg/sec. The roll rate gyro is also used as the sensor for roll-rate limiting during entry.

Some of the significant characteristics of the ACS are presented in Table IX. The sequence of operation is shown in Table X.

TABLE IX

ATTITUDE CONTROL SYSTEM CHARACTERISTICS

Performance	
During thrusting	0.5 deg (1 sigma)
At entry	1.0 deg (1 sigma)
Maximum Operating Times	
Separation to thrusting	30 minutes
Thrusting	35 seconds
Cruise	60 minutes
Weight	92 pounds
Stored Impulse	
Cold gas	248 lb-sec
Hot gas	3500 lb-sec
Limit Cycle Amplitude	
Yaw and pitch	0.5 degree
Roll	1.0 degree
IRS Performance After Entry	
Orientation uncertainty	1.0 deg (1 sigma)
Operating time	30 minutes

TABLE X

SEQUENCE OF OPERATION

Prior to Separation

Verify ACS operation

Align platform

Establish angular commands

Separation to deorbit -- 0.5 hour maximum

Nullify separation rates

Orient and maintain attitude for thrusting

Cold-gas reaction system active

Thrusting -- 35 seconds maximum

Maintain Attitude

Hot gas and cold-gas reaction systems active

Thrusting Termination to Entry -- 1.0 hour maximum

Maintain attitude for communications and entry conditions

Cold-gas reaction system active

Entry to Parachute Deployment

Disable pitch and yaw reaction system -- 0.1 g

Roll control limits roll rate

Provide accelerometer data

Parachute Deployment to Impact

Provide control signals for camera gimbals

Provide accelerometer data

## 6.0 PERFORMANCE REQUIREMENTS AND ANALYSIS

### 6.1 $\Delta V$ ACCURACY REQUIREMENTS

The accuracy which must be achieved in the direction and magnitude of the de-orbit velocity vector is determined by two factors. The first is the desire to minimize range dispersion in order to achieve particular landing sites; the second is the need to control the entry angle within specified limits to simplify vehicle design considerations. The accuracy of the direction of the imparted velocity is a function of ACS performance, while the accuracy in its magnitude depends on the propulsion system.

#### 6.1.1 Entry Range Dispersions

The effect of the thrusting angle error on the range at entry is shown in Figure 15. The top half of the figure shows entry-range dispersion as a function of periapsis altitude for apoapsis altitudes between 4000 and 20,000 km. Results are shown for de-orbit with a fixed-thrust rocket at the true anomaly and thrust application angle ( $\theta_{OP}$ ) which produces the optimum communications geometry for each orbit. That is, for each orbit there is a combination of de-orbit point and thrust application angle which gives the most satisfactory communications geometry between capsule and spacecraft, for a specified entry angle and de-orbit velocity. The entry angle is nominally -15 degrees, the value used in Figure 15, and the de-orbit velocity is fixed in all cases at 1400 ft/sec. A more detailed discussion of these relationships is contained in paragraph 7.1, Vol. V, Book 1. The curves are plotted for a fixed uncertainty in velocity magnitude of 0.33 percent and show that there is considerable variation in range dispersion over the range of parameters considered. If the error in thrust application angle ( $\Delta\theta_{OP}$ ) is 0.5 degree, the range dispersion is less than 25 km in all cases, whereas an error of 1.0 degree results in dispersions up to 40 km for the orbits considered.

#### 6.1.2 Entry Angle Dispersion

The lower half of Figure 15 illustrates the effect of the thrust application angle error ( $\Delta\theta_{OP}$ ) on the entry angle dispersion ( $\Delta\gamma_e$ ) for errors of 1.0 and 0.5 degree for the range of orbits considered. A 0.33-percent velocity magnitude error was also included in this calculation. It is evident from the plot that if the ACS accuracy is 0.5 degree the maximum dispersion in entry angle is 0.25 degree. If the one-sigma ACS accuracy is 1.0 degree, the entry dispersion is nearly 0.5 degree. The capsule design must accommodate performance variation of  $\pm 3$  sigma; that is, it must be designed for a variation of entry angle of  $\pm 1.5$  degrees (3 sigma) if the ACS accuracy is 1.0 degree (1 sigma). To provide reasonable vehicle design criteria, this has been selected as the design requirement of the ACS, with an accuracy of 0.5 degree (1 sigma) preferred.

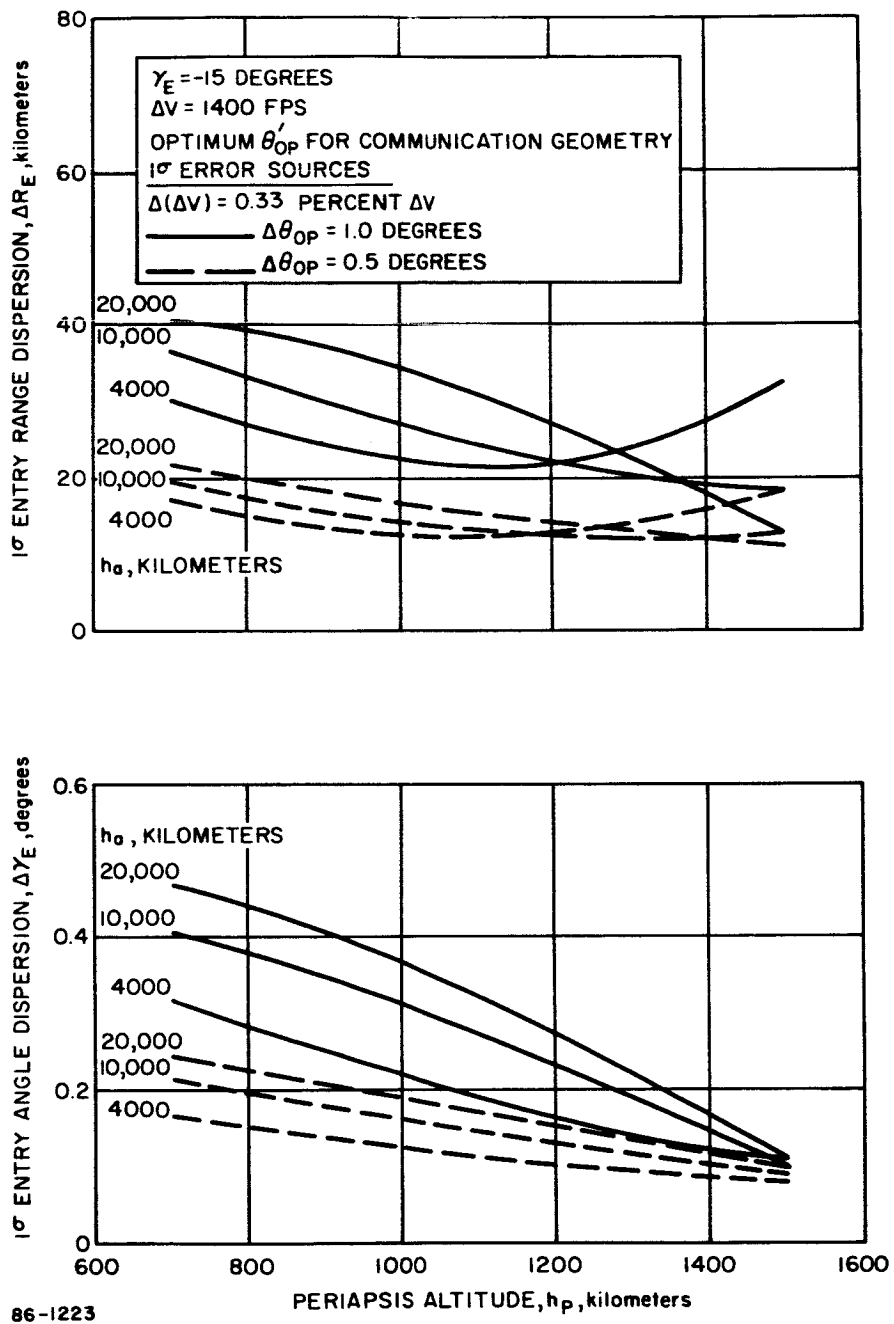


Figure 15 PERFORMANCE OF ACS

### 6.1.3 Effect of Velocity Magnitude

The results presented here are for a velocity magnitude error of 0.33 percent, since it is shown in Section 9.0 that this performance is achievable with existing propulsion systems. However, it is shown in paragraph 7.1, Book 1, Volume V, that even if the total impulse (hence velocity magnitude) uncertainty is increased by a factor of 3 to 1 percent, that the dispersion increases at most by about 50 percent. In summary, on the basis of the trajectory studies of dispersion, the total impulse uncertainty of the propulsion system should be 1 percent (1-sigma) with 0.33 percent (1-sigma) desirable.

## 6.2 TV CAMERA ORIENTATION REQUIREMENTS

The capsule is equipped with a TV camera which must be oriented so that the camera optical axis is aligned with the local vertical during the parachute descent phase. Satisfactory camera performance requires that this be accomplished with an uncertainty of 1.0 degree (1 sigma) in orientation with respect to the vertical at the nominal impact point. It is also necessary to minimize angular rates of the camera for satisfactory operation. The rates must be less than 0.01 deg/sec.

## 6.3 DESCENT ACCELERATION MEASUREMENT REQUIREMENTS

Accelerometer data will be used to reconstruct the profile of the Mars atmosphere. The problems of reconstructing the atmospheric profile will be greatly reduced if the data is available in a stabilized frame, thus eliminating the need for complex computation and eliminating the possible bias effects of accelerations due to angular body rates; the accelerometers then will measure only linear accelerations on the average. The atmospheric profile can adequately be reconstructed if the accelerometer data error is less than 0.1 percent of full scale. Full scale for the entry conditions under consideration need only be 15 g. The allowable error is therefore 0.015 g.

## 6.4 WIND MEASUREMENT REQUIREMENTS

A requirement exists to measure the velocity of surface wind gusts on Mars to  $\pm 20$  percent for gust velocities in excess of 50 ft/sec. The parachute assembly assumes a terminal velocity due to a wind force in approximately 20 seconds. Therefore the accelerometer measurements cannot contribute an error of more than 10 ft/sec in a 20-second interval. This requires that the accelerometer be accurate to at least  $0.5 \text{ ft/sec}^2$ , or 0.016 g.

## 6.5 ALTERNATE APPROACHES

Possible alternate approaches for design of the ACS can be conveniently discussed by examining the operation required during each phase of the mission and considering the candidate techniques which are suitable. Major ACS combinations can then be synthesized and evaluated against criteria.

### 6.5.1 Candidate Techniques by Mission Phase

#### 6.5.1.1 Orient Capsule to Thrust Attitude

The capsule can be placed in the proper attitude for thrusting either by maneuvering the spacecraft prior to separation or by maneuvering the capsule by means of an active ACS.

#### 6.5.1.2 Maintain Attitude During Thrust

The attitude of the capsule can be maintained during thrusting by spin stabilization; by means of an active ACS, or by gimbaling the rocket engine.

#### 6.5.1.3 Reorient for Proper Entry Attitude

The capsule dynamic performance during entry will be improved if the angle of attack is nominally zero. If an active ACS is employed, it can perform the reorientation. If only spin stabilization is used, this cannot be achieved since the stabilized attitude is determined by the required thrust direction and this will in general not result in a zero-angle of attack. However, the spin rate should be reduced so angle of attack convergence is not hindered. Convergence can further be improved if rate damping of the capsule is effected.

#### 6.5.1.4 Maintain Attitude During Cruise

The attitude of the capsule can be maintained during cruise by spin stabilization or by an active ACS.

#### 6.5.1.5 Maintain TV Camera Orientation

The TV camera may be fixed to the Suspended Capsule or gimbal mounted. If it is fixed, the ACS must continue to provide stabilization of the capsule during parachute descent. If the camera is mounted on gimbals and free to rotate with respect to the capsule, then signals from the ACS sensor can be used to control the gimbals for proper orientation.

#### 6.5.1.6 Wind Measurements

The measurement of wind-induced accelerations is simpler if the accelerometers are mounted on a stable platform. This platform can either be the capsule itself, if it is stabilized, or an inertial reference platform which is gyro stabilized.

#### 6.5.2 Synthesis of Alternate Systems

From the candidate techniques just described for each phase of the mission, alternate systems can be synthesized which can perform the required functions. Five such systems have been considered and will be described. Paragraphs 6.6 through 6.8 give more details on the performance of those which were given more thorough investigation. In Section 7.0 the systems are evaluated and the reference design is selected. A matrix of the five ACS alternate systems is shown in Table XI.

TABLE XI  
MAJOR ACS COMBINATIONS

	ACS Combination				
Phase	1	2	3	4	5
Orient	Flight Spacecraft Maneuver	FC ACS	FCACS (cold gas)	FC ACS	FC ACS
Thrust	Spin	Spin	FC ACS (cold gas)	Gimbal Engine	FC ACS (hot gas)
Cruise	Spin	Spin	FC ACS (cold gas)	FC ACS	FC ACS (cold gas)
Entry	Despin	Design	FC ACS (cold gas)	FC ACS	FC ACS (cold gas)
	1B-Rate Damp 1C-Orient ACS	2B-Rate Damp 2C-Orient ACS			

#### 6. 5. 2. 1 Spin Only System

The simplest system listed in Table XI is given in column 1 and utilizes a spacecraft maneuver for orientation to the proper attitude for thrust application. The capsule is spin stabilized after separation for thrusting and cruise. Despin is desirable to minimize communication loss during entry and to reduce problems of parachute deployment and entry-shell jettison. There are variations on the spin-only system, listed under categories 1B and 1C, which incorporate options of rate damping or reorientation with an ACS after despinning. The purpose of these two options would be to reduce the possible loss in communications time after the despin process.

#### 6. 5. 2. 2 Active ACS with Spin

Column 2 is the same as column 1 except that the capsule reorients itself. Therefore, a capsule ACS must be incorporated for orientation to the de-orbit thrust attitude. Spin stabilization is used to maintain attitude during thrusting and to entry. Despin is accomplished as in the previous case.

#### 6. 5. 2. 3 Active ACS - Cold Gas

This system uses active attitude control of the capsule for all phases. No maneuver of the spacecraft is required, and orientation to the thrusting and entry attitude is accomplished by the active ACS. Control during thrusting is also accomplished by the cold-gas system, which means that the reaction control thrust and impulse levels will be sized by the requirements during the de-orbit thrusting phase, resulting in a much heavier design, as will be seen.

#### 6. 5. 2. 4 Active ACS with Gimballing

This system uses an active cold gas ACS for all phases of the mission except during thrusting. To avoid the weight penalty associated with the use of cold-gas reaction control during the thrust period, as in the case of column 3. gimballing of the rocket motor is used instead.

#### 6. 5. 2. 5 Active ACS - Cold Gas and Hot Gas

The final system, column 5, also uses an active cold-gas ACS for all phases except thrusting. During thrust, a hot-gas reaction control system is used for thrust vector control in pitch and yaw.

## 6.6 ACHIEVABLE PERFORMANCE OF ACTIVE ACS PLUS SPIN CONFIGURATION

### 6.6.1 Description of Operation

The sequence of events for this system is:

- a. Nullify tipoff rates due to separation from the spacecraft and realign the capsule to the spacecraft reference attitude.
- b. Orient the capsule thrust axis into the proper attitude for thrusting.
- c. Spin the capsule for stabilization during thrusting and during cruise until entry.
- d. Despin during early entry (at 0.1-g deceleration)
- e. Inertial Reference System (IRS) serves as T. V. camera reference after despin.

Characteristics of the ACS are presented in Table XII. The system uses an inertially stabilized platform and a computer, which together comprise an Inertial Reference System (IRS). The attitude reference from the IRS is used by the closed-loop ACS and the T. V. camera pointing system. Twelve ACS cold-gas nozzles are used to provide reaction control couples about each axis. The platform system would not have been selected for ACS purposes if it were not required that it be on board anyway for the TV camera attitude reference. In the absence of the latter requirement a strapped-down gyro system would have been selected for the ACS reference system.

Characteristics of the spin system are also contained in Table XIII.

Ten spin rockets are provided for spin to 40 rpm and an additional 10 are provided for despin. Adequate spin performance can be obtained if 2-3 of the spin rockets fail to ignite. If that occurs the capsule will be over-despun at entry, but the final rate after despin (8-12 rpm) will not have serious effects.

If the spin rocket chain does not receive the initiating signal, the despin rockets will be used for spin-up. In this case despin cannot occur, so the entry-vehicle shell must be designed to handle the more severe angle of attack conditions which result.

TABLE XII

CHARACTERISTICS OF ACTIVE ACS PLUS SPIN SYSTEM

(Attitude Control System)

Parameter	Value
Limit cycle amplitude	<0.5 degrees
Limit cycle rate	0.1 deg/sec
Total impulse required	50 lb-sec
Total impulse stored	150 lb-sec
Maximum rate*	1 deg/sec
Thrust per nozzle	1 pound
Number of nozzles	12
Maximum operating time	15 minutes
IRS weight	18 pounds
Reaction Control System Weight	<u>25 pounds</u>
Total system weight	43 pounds

\*Rate limit during orientation

TABLE XIII

CHARACTERISTICS OF ACTIVE ACS PLUS SPIN SYSTEM

(Spin System)

Parameter	Value	
	Spin	Despin
Spin rate	+40 rpm	-40 rpm
Thrust per rocket	56.6 pounds	56.6 pounds
Burn time	1 second	1 second
Number of rockets	10	10
System weight	12 pounds	12 pounds

### 6.6.2 Error Analysis

A curve of  $\Delta V$  pointing error versus spin rate is presented in Figure 16. This figure indicates that a spin rate of 40 rpm will produce errors in the direction of the velocity vector equal to 0.8 degree ( $1\sigma$ ). To determine the overall system accuracy during thrusting this number must be combined with the errors existing before spinup, as determined by the following 1-sigma attitude errors:

FS sensor error	}	0.233 degree
FS limit cycle		
Alignment of IRS with respect to the spacecraft		
Drift of IRS (separation to spinup)		0.10 degree
Gimbal readout		0.10 degree
Computation		0.10 degree
Capsule limit cycle		0.289 degree

Assuming statistical independence of the error sources, the 1-sigma attitude error before spinup is 0.41 degree. Combining this with the errors due to spinup yields 0.9 degree as the 1-sigma  $\Delta V$  pointing accuracy during thrusting.

Since the spin stabilized capsule is not reoriented after de-orbit thrusting, the angle of attack at entry can be quite large (as high as 90 degrees or more) depending on the orbit, entry angle, thrust application angle, and other parameters.

Too large an angle of attack at entry causes the capsule, if it is not despin, to exhibit a coning motion during entry which would cause the capsule antenna pointing loss to exceed the allowable level for the communication range involved. Since angle of attack convergence takes longer with a spinning vehicle, despin of the capsule is indicated. Parachute and shell deployment problems also dictate despin of the capsule. Since despinning can cause tumbling in the absence of aerodynamic forces to provide righting moments and tumbling causes communications loss, despin should be delayed until the time when the aerodynamic forces become significant; i. e., at about 0.1 g.

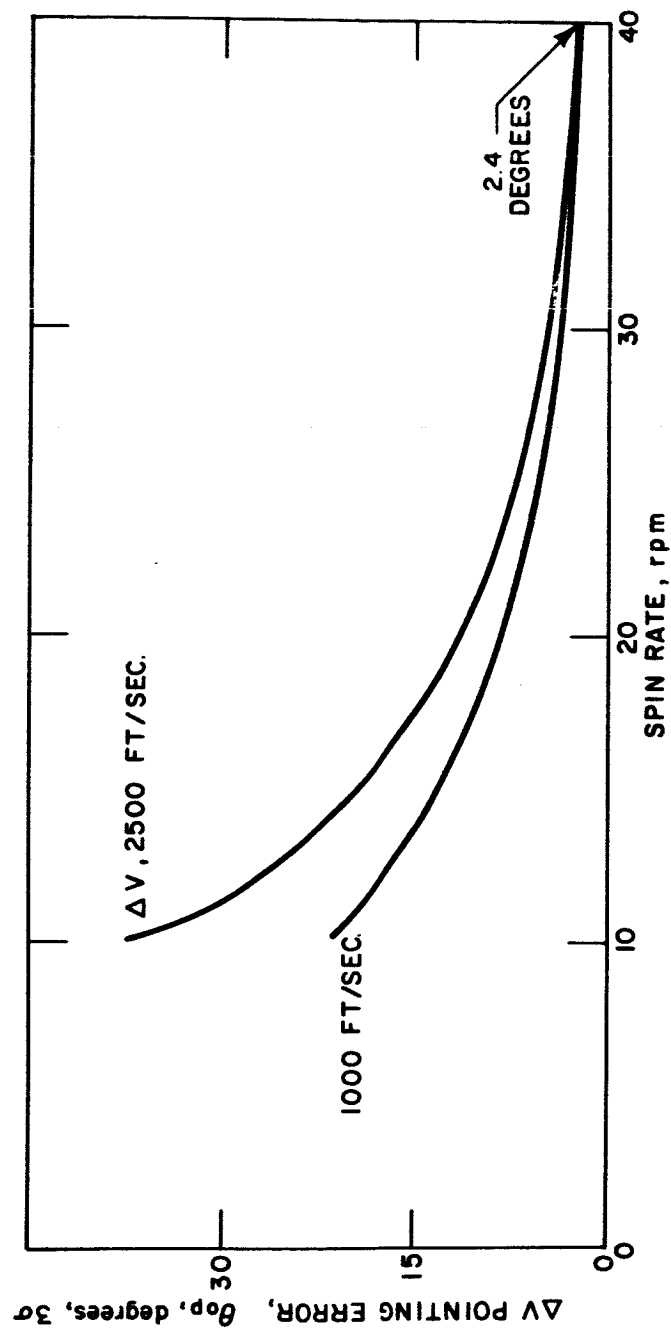


Figure 16 ΔV POINTING ERROR VERSUS SPIN RATE

25-1018

## 6.7 ACHIEVABLE PERFORMANCE OF ACTIVE ACS CONFIGURATION

### 6.7.1 Description of Operation

The sequence of events for the ACS using cold-gas and hot-gas reaction control is as follows:

- a. Nullify the separation rates and realign the capsule to the spacecraft reference attitude.
- b. Orient the capsule to the correct attitude for thrust application to de-orbit.
- c. Maintain the capsule attitude during the thrust application phase, using the hot-gas system.
- d. Orient the capsule to a preferred attitude during the cruise mode to optimize communications and entry conditions.
- e. Provide three-axis accelerometer data for controlling entry and descent events and to provide information for analyzing atmospheric characteristics including wind profiles.
- f. Provide control signals to maintain the two-axis television camera gimbal system aligned to the local vertical.

An attitude reference is established on the capsule by aligning a four-gimbal inertial platform with respect to the spacecraft attitude reference (Sun-Canopus). The required reorientation angles are stored in the CC & S memory system. At separation, the capsule platform will be operating in an inertial mode and the capsule will then be commanded, via the stored angle commands, to the required thrust application attitude. The attitude control system will orient the capsule to this attitude and maintain it until thrust application using cold gas. Just prior to thrust application, a hot-gas reaction system (yaw and pitch) will be activated to provide stabilization during thrust application. The cold-gas system will remain active during the thrusting phase and the cold-gas roll nozzles will provide roll stabilization during this phase.

Upon completion of the thrusting phase, the attitude control system using the cold-gas reaction system will maintain the attitude of the capsule. The ACS may reorient and hold the capsule to a preferred attitude for communication during the cruise mode. It will orient the capsule to a preferred attitude prior to entry to minimize the angle of attack. These angular commands will be stored in the CC & S and will be issued to the IRS computer at the correct time.

The ACS contains a Sentry subsystem that will disable the reaction control system during the cruise mode should the angular rate exceed 6 deg/sec. about any axis. This limits the tumble rate for entry load and heating considerations in case of an ACS failure.

During early entry, the reaction control of pitch and yaw will be disabled and the roll channel will provide roll-rate control to prevent high roll rates from building up. The Inertial Reference System will remain functioning and will provide acceleration data during the entry phase for scientific data and for event control purposes. Upon parachute deployment, the IRS will provide the TV camera gimbal system with the required commands to maintain the optical axis of the cameras along the local vertical. The characteristics of the IRS are summarized in Table XIV. The IRS provides the required orientation information for TV platform control. Other methods for providing TV stabilization or shutter control have been considered but found to be inadequate. Since the inertial system is required for TV control purposes, it seems logical to use the same system as the reference for the capsule attitude control. Further, once a stable platform is incorporated it is also logical to mount accelerometers on the stable element to measure entry decelerations in a non-rotating frame.

Characteristics of the cold-gas reaction system are summarized in Table XV. Twelve nozzles are used to provide reaction control couples about each of three axes. The reaction control system has a dual operating feature such that a failure of one nozzle will not cause a system failure. The cold-gas tanks are capable of withstanding sterilization after being fully charged.

Characteristics of the hot-gas reaction system are summarized in Table XVI.

#### 6.7.2 Error Analysis

With the performance of the IRS gyros and the ACS characteristics as specified and presented in Tables XIV and XVI the following 1-sigma attitude errors are the result:

TABLE XIV

SUMMARY OF INERTIAL REFERENCE SYSTEM CHARACTERISTICS

Item	Value
Accuracy	
Alignment (for ACS)	0.7 degree (3 sigma)
Drift (for TV gimbal control)	1.2 deg/hr (3 sigma)
Inertial Platform	
Gimbal	4-Full Freedom
Weight	10 pounds
Volume	400 in. <sup>3</sup>
Power	45 watts
Platform electronics	Included in Platform
Computer	
Weight	5 pounds
Volume	160 in. <sup>3</sup>
Power	10 watts
Sentry System	
Weight	2 pounds
Volume	50 in. <sup>3</sup>
Power	13 watts

TABLE XV

SUMMARY OF COLD GAS REACTION SYSTEM CHARACTERISTICS

Parameter	Value
Limit Cycle Amplitude	1.0 degree roll 0.5 degree pitch and yaw
Limit Cycle Rate	0.04 deg/sec
Total Impulse Required*	68 lb-sec
Total Impulse Stored	248 lb-sec
Maximum Rate During Orientation	1.0 deg/sec
Thrust Levels	0.5 pound
Number of Nozzles	12
Maximum Operating Time	90 minutes
System Weight	34 pounds

\*10 lb-sec of impulse required for TVC roll control.

TABLE XVI

SUMMARY OF HOT GAS REACTION SYSTEM CHARACTERISTICS

Solid Propellant Hot Gas System	Pitch and Yaw Control*
Limit Cycle Amplitude	0.5 degree
Limit Cycle Rate	0.3 deg/sec
Total Impulse	
Required	1225 lb-sec
Stored	3500 lb-sec
Number of Nozzles	8
Thrust per Nozzle	25 pounds
Number of Solid Propellant Generators	4
Burn Time	35 seconds
Total System Weight	40.0 pounds

\*Roll control during TVC accomplished with cold gas reaction control nozzles.

Flight Spacecraft Sensor Error	}	0.233 degree
Flight Spacecraft Limit Cycle		
Alignment of IRS with respect to Flight Spacecraft		

#### Drift of IRS

G Sensitive	0.003 degree
G Insensitive	0.20 degree
Gimbal Readout	0.10 degree
Computation	0.10 degree
Capsule Limit Cycle	$0.5\sqrt{3} = 0.289$ degree*

Assuming statistical independence of the error sources the standard deviation of the pointing error during thrusting is 0.445 degree. The maximum operating time is 90 minutes, at the end of which pointing accuracy will still be better than 2 degrees.

### 6.8 ACHIEVABLE PERFORMANCE WITH RATE DAMPING

#### 6.8.1 Description of Operation

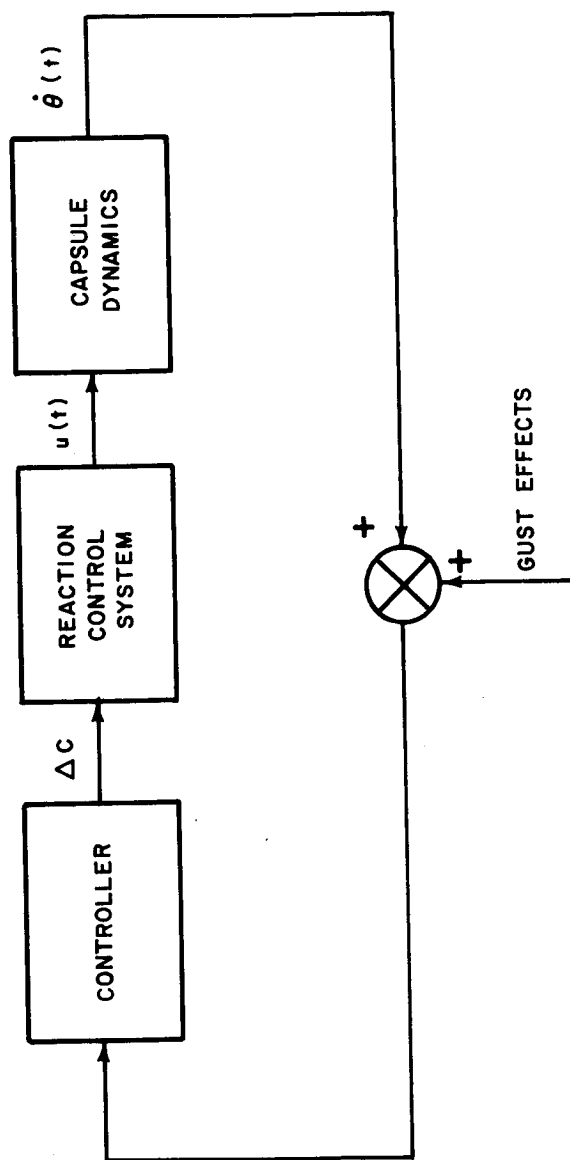
For the case of a spin system, performance can be improved by rate damping of the capsule during early entry after despin. Also, rate damping of the capsule during the parachute descent phase can improve stabilization of the optical axis of the television camera.

A block diagram of the rate damping system is shown in Figure 17. Control signals are generated such that whenever the angular rate is above a certain level torque is applied in a direction to reduce the rate. In this manner damping of the attitude angle and its rate of change is achieved.

#### 6.8.2 Performance and Error Analysis

The block diagram, depicted in Figure 17, illustrates the rate damping control loop for both the parachute descent phase and rate damping of the capsule during early entry. For the parachute descent phase, a simple pendulum model was chosen to represent the capsule dynamics. The equation of motion describing the response is

\* A uniform distribution is assumed.



86-1215

Figure 17 RATE DAMPING CONTROL LOOP

$$\ddot{\theta}(t) = -\omega_n^2 \theta(t) + u(t)$$

where  $\theta(t)$  = angular displacement (rad)

$u(t)$  = control acceleration (rad/sec<sup>2</sup>)

$\omega_n$  = undamped natural frequency (rad/sec)

( $\dot{\phantom{x}}$ ) = time rate of change of ( )

The dynamics of the controller - reaction control system combination, treated as a no-memory device, are presented in Figure 18. This model was subjected to initial rates corresponding to the maximum rate arising from a gust of wind. Typical values are presented in Table XVII.

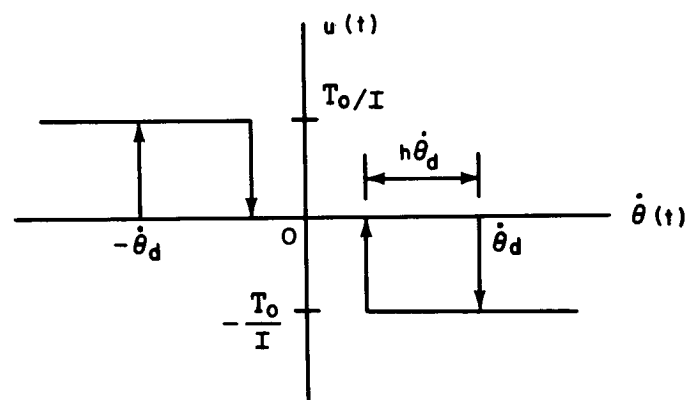
TABLE XVII

COMPARISON OF GUST VELOCITY TO MAXIMUM RATE

Gust Velocity (ft/sec)	Maximum Rate (deg/sec)
100	26.5
200	63.0
300	111.0
400	185.0

Results of this portion of the study are shown in Figures 19, 20, and 21, which illustrate nozzle-thrust requirements, total-impulse requirements, and reaction control system weight as a function of solution time. Since the intent here is rate cancellation for the purpose of camera pointing requirements, solution time is that time necessary to settle to and remain within a prescribed rate deadband, which in this case was 1 deg/sec.

As one might expect, for a given nozzle size the solution time increases with increasing gust velocity. Total impulse requirements for a given gust



$\dot{\theta}(t)$  = ANGULAR RATE  
 $h$  = HYSTERESIS FACTOR  
 $\dot{\theta}_d$  = RATE DEAD ZONE  
 $T_0/I$  = TORQUE TO INERTIA RATIO  
 86-1214

Figure 18 DYNAMICS OF CONTROLLER AND REACTION CONTROL SYSTEM

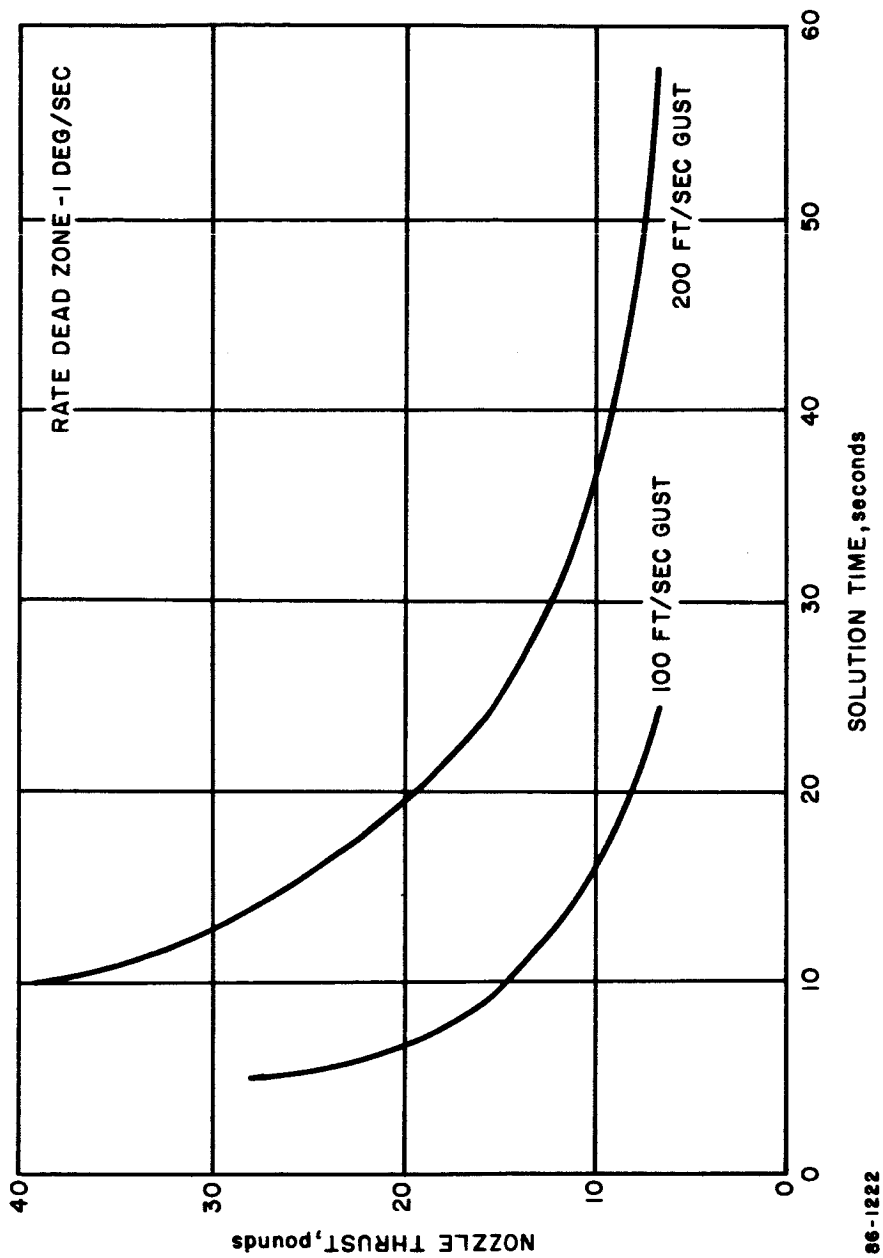
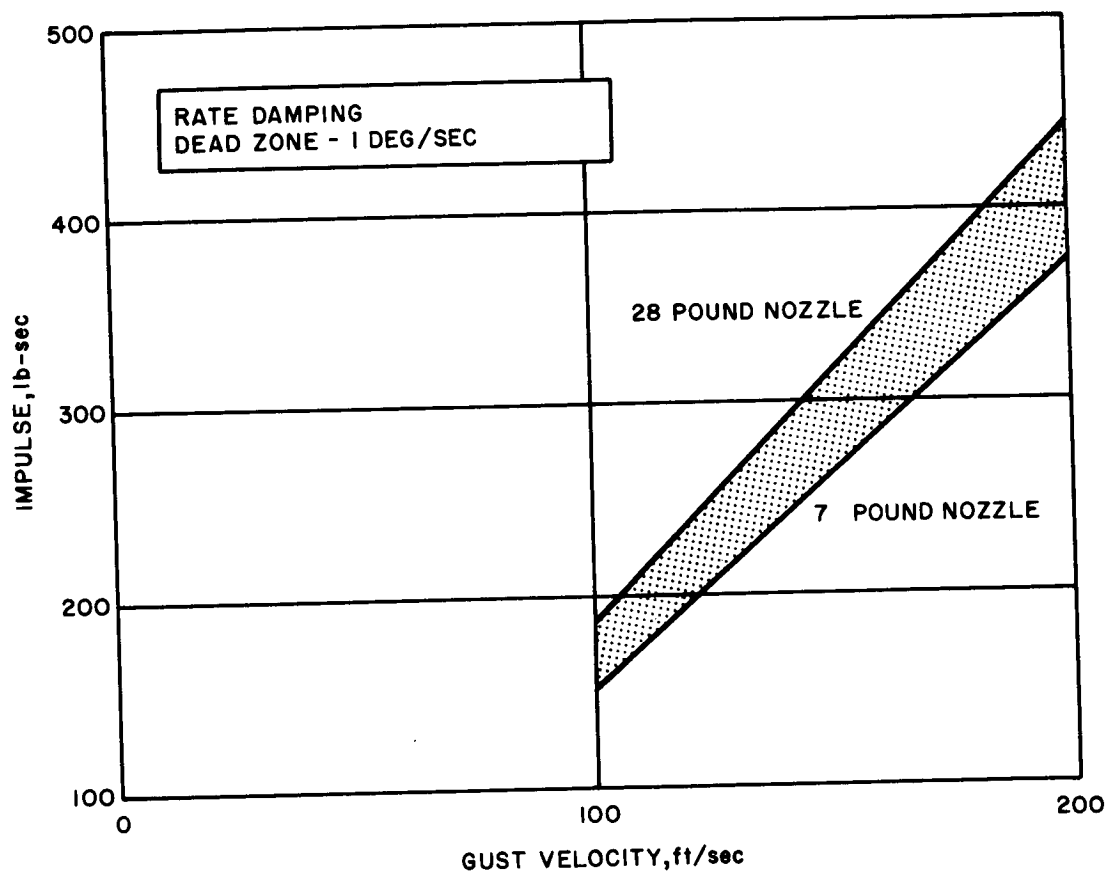
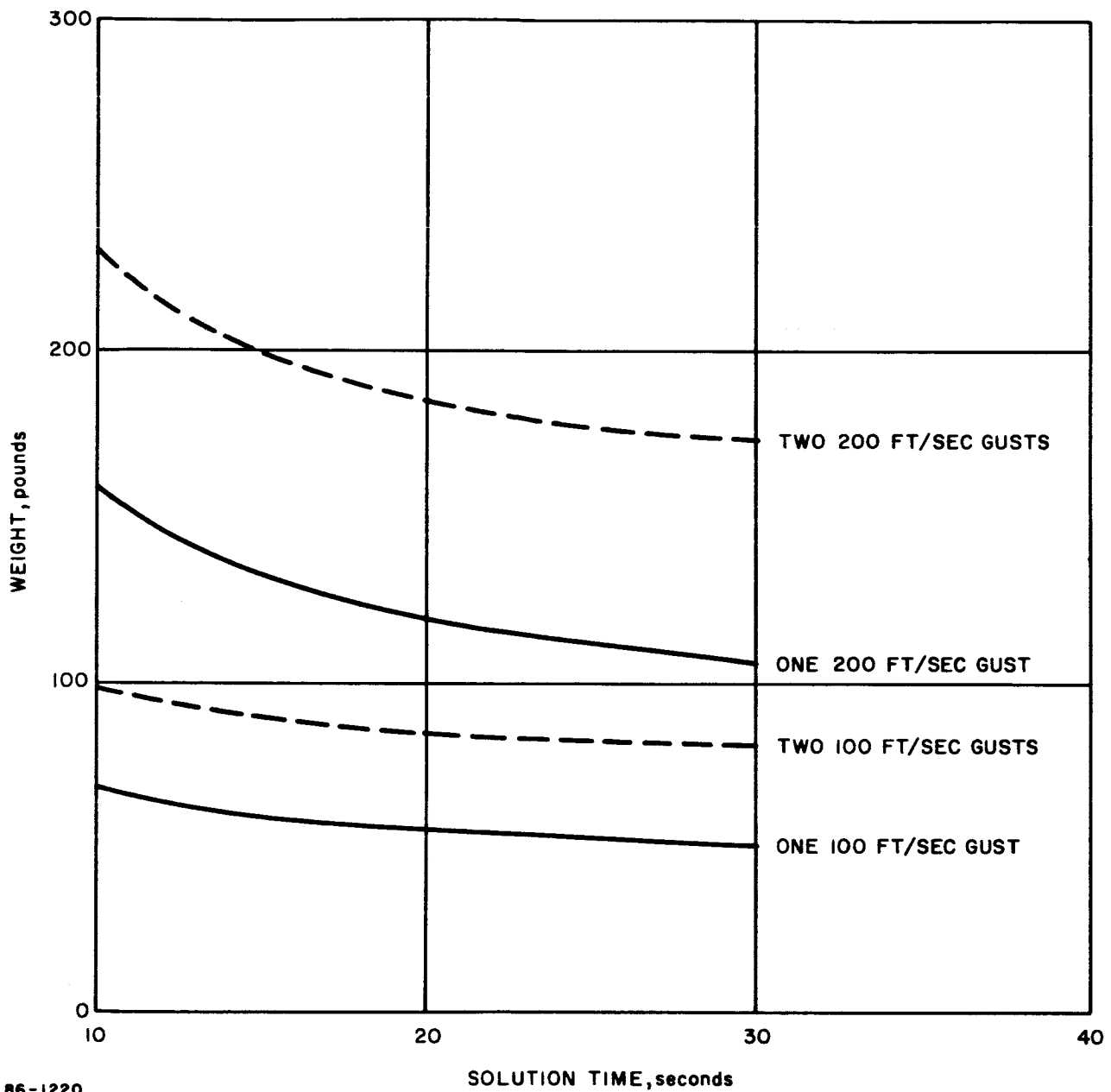


Figure 19 NOZZLE THRUST REQUIREMENTS VERSUS SOLUTION TIME (RATE DAMPING OF CAPSULE ON PARACHUTE)



86-1221

Figure 20 IMPULSE REQUIREMENTS VERSUS GUST VELOCITY (PER GUST) (RATE DAMPING OF CAPSULE ON PARACHUTE)

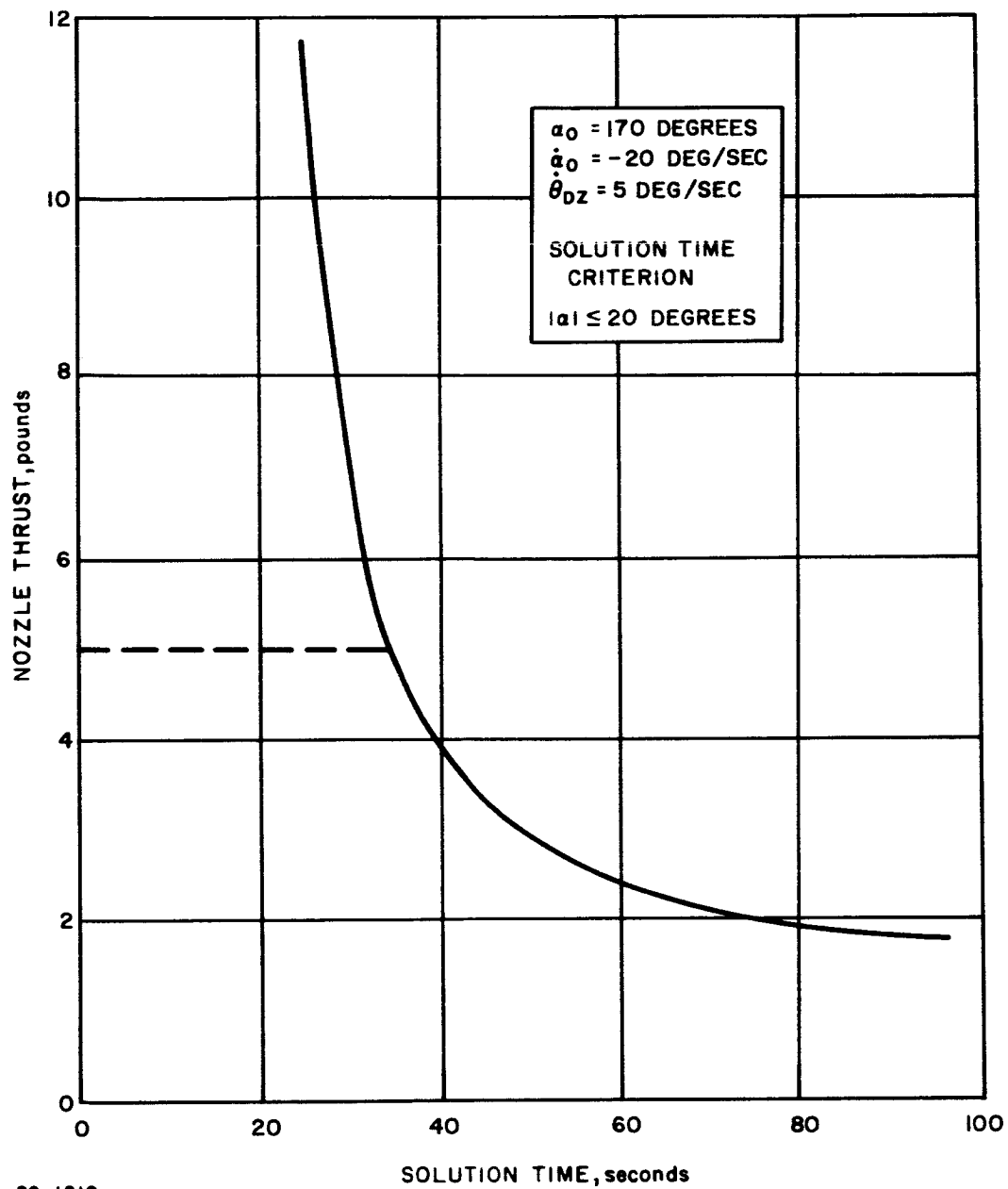


86-1220

Figure 21 REACTION CONTROL SYSTEM WEIGHT VERSUS SOLUTION TIME (RATE DAMPING OF CAPSULE ON PARACHUTE)

velocity are seen to increase with nozzle thrust. Figure 21 shows the effect of the number of gusts on reaction control system weight. Curves are presented for one and two gusts of 100 and 200 ft/sec. The other case analyzed was rate damping in pitch and yaw during early entry to improve angle of attack convergence. Figures 17 and 18 are again applicable, however, now one has an aerodynamic restoring torque present. System response was investigated for various combinations of initial angle of attack and rate. Results for a "worst" case of  $\alpha_0 = 170$  degrees and  $\dot{\alpha}_0 = 20$  deg/sec are contained in Figures 22 through 24, where  $\alpha_0$  and  $\dot{\alpha}_0$  are the initial values of angle of attack and its rate of change, respectively. The criterion for solution time is now that the magnitude of  $\alpha$  shall have damped to and remained less than or equal to 20 degrees. For a solution time of 34 seconds, 5-pound nozzles are required. Total impulse per axis is 148 lb-sec, and the reaction control system weight is 87 pounds. A weight summary is shown in Table XVIII including the weight of the active ACS for initial orientation of the capsule after separation from the spacecraft. It is interesting to note that after 60 seconds the total impulse per axis and the system weight become asymptotic to 140 lb-sec and 75 pounds, respectively. In the limit, then, the weight of the reaction control system with rate damping is 50 pounds heavier than the weight for no damping (25 pounds). For the nominal solution time of 34 seconds the weight differential is 62 pounds.

Controlling with an active ACS all the way to entry provides a nominally zero-angle of attack at entry. Hence, rate damping is not required with this form of control.



86-1219

Figure 22 NOZZLE REQUIREMENTS VERSUS SOLUTION TIME (RATE DAMPING DURING EARLY ENTRY)

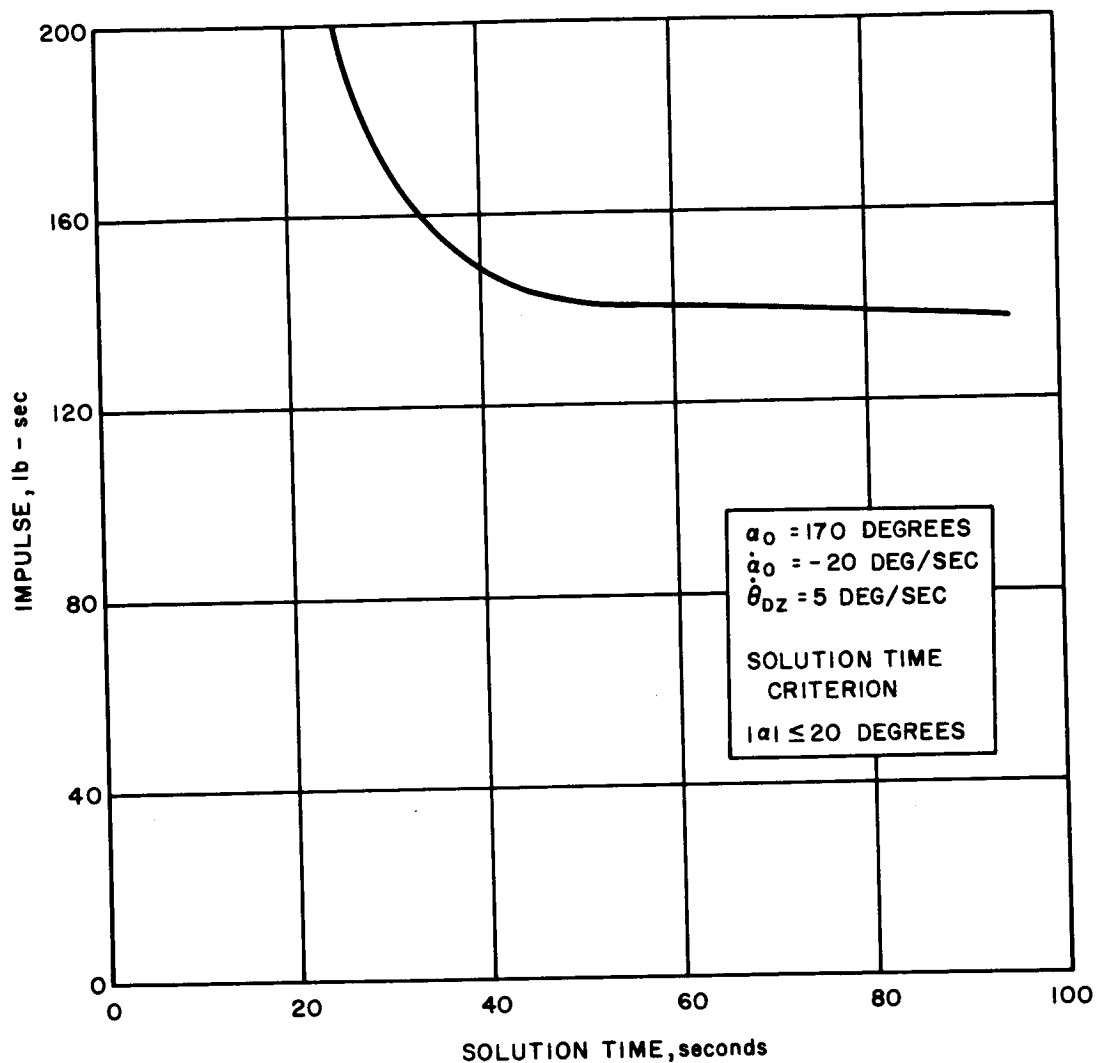


Figure 23 IMPULSE REQUIREMENTS PER AXIS VERSUS SOLUTION TIME (RATE DAMPING DURING EARLY ENTRY)

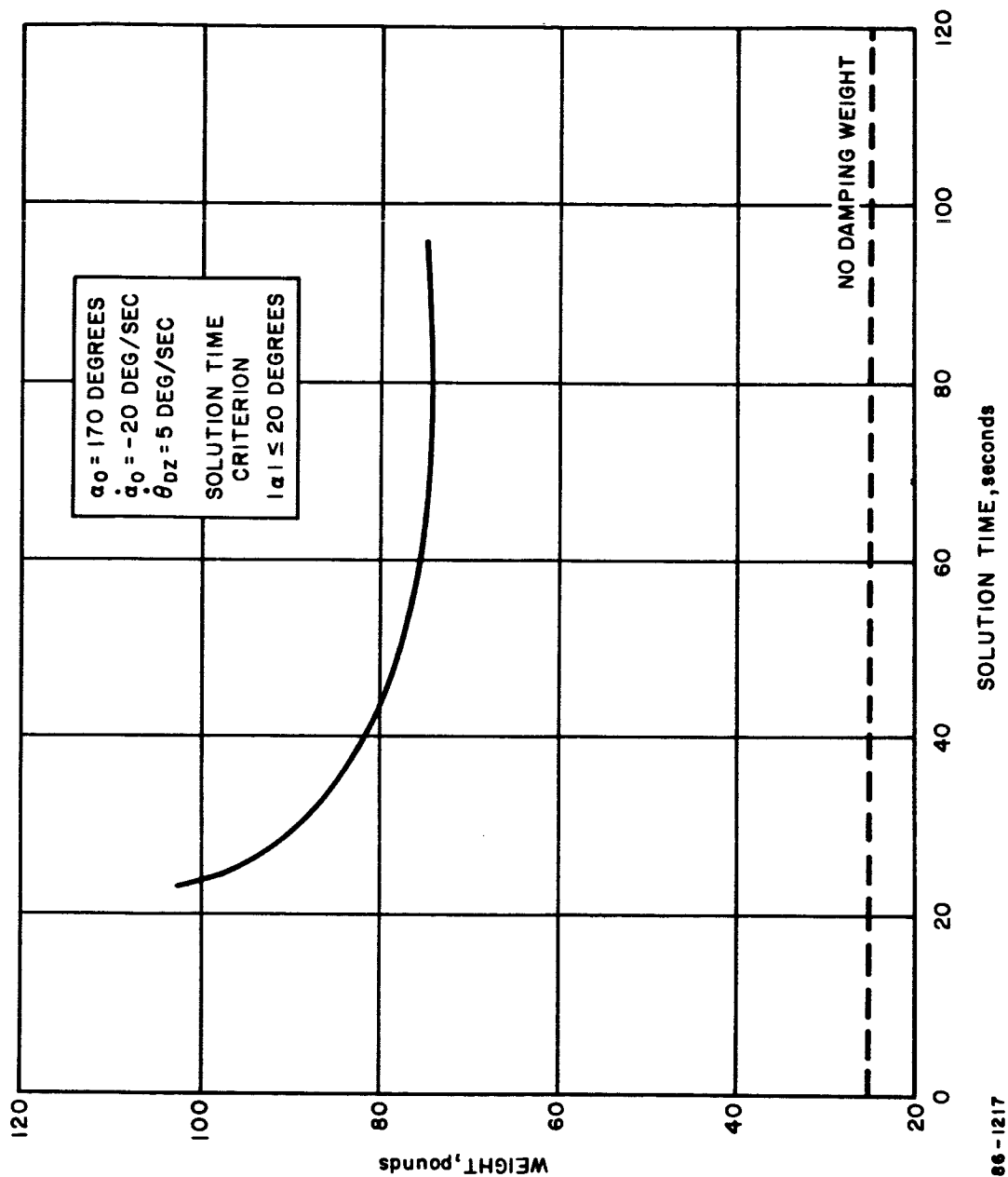


Figure 24 REACTION CONTROL SYSTEM WEIGHT VERSUS SOLUTION TIME (RATE DAMPING DURING EARLY ENTRY)

TABLE XVIII  
WEIGHT SUMMARY FOR RCS USED FOR RATE DAMPING  
DURING EARLY ENTRY

	Weight Each (lbs)	No.	Total Weight (lbs)
Nozzle Valves	1	12	12.0
Pressure Vessel	17.3	2	34.6
Gas (N <sub>2</sub> )	19.3	--	19.3
Squib Valves	1	2	2.0
Vessel Manifold	0.25	2	0.5
Line Complex	3	2	6.0
Regulators	5.5	2	11.0
Filters	0.5	4	<u>2.0</u>
			87.4 pounds

Initial Conditions:

$$a_0 = 170 \text{ degrees}$$

$$\dot{a}_0 = -20 \text{ deg/sec}$$

Assumptions:

$$\text{Dead Zone} = 5 \text{ deg/sec}$$

Assuming 2.5 lb Nozzles in Couples

Required Impulse    330 lb-sec

Stored Impulse       1155 lb-sec

Solution Time         34 seconds

## 7.0 SELECTION OF REFERENCE DESIGN CONCEPT FOR 1971 MISSION

### 7.1 CRITERIA AND CONSTRAINTS

#### 7.1.1 Basic Function

The ACS is required to perform the following basic functions:

- a. Orient the capsule thrust axis in the proper attitude for application of the separation velocity.
- b. Stabilize the capsule during thrusting.
- c. Reorient the capsule after thrusting to maintain proper attitude for communications or entry.
- d. Provide roll-rate damping during entry.
- e. Provide acceleration measurements during entry.
- f. Provide an attitude reference for the TV cameras, either by controlling the attitude of the capsule or by gimbaling the camera.

Some of these basic functions may not be required, depending on the detailed flight capsule design concept, or some may be desirable but not essential. Specifically, the orientation of the capsule is not required if the orientation is performed by the spacecraft before separation. Stabilization of the capsule during thrusting is required in all cases. Reorientation and maintenance of proper attitude before entry is not essential, but if not done, may place additional demands on other subsystems, and is therefore a proper function for a tradeoff evaluation. The roll-rate damping during entry is also not a firm requirement but is desirable in that it minimizes the difficulties which might occur at the time of parachute deployment.

#### 7.1.2 Criteria

In performing the basic functions the ACS should meet certain criteria as follows:

##### 7.1.2.1 Performance

The control of the thrust application angle should be such as to permit entry angle dispersion of less than 0.5 degrees (1-sigma), and the ACS should perform other orientation maneuvers as required. This requires attitude control during thrusting with an accuracy of at least 1.0 degree (1-sigma) for the design range of deorbit and entry conditions.

#### 7.1.2.2 Reliability

Backup failure modes should be provided in the event of failure of a critical part of the subsystem. Existing qualified rockets and components will be used where applicable.

#### 7.1.2.3 Environmental Criteria

The ACS must withstand:

- a. Flight capsule static accelerations of 15-g axial and 7.5-g lateral. Capsule dynamic loads which can be simulated by a 3-g rms axial and 2-g rms lateral vibration input to a flight configuration on a hard mount using a sine sweep 1 minute/octave from 2 to 100 cps.
- b. Nominal earth transportation and handling loads.
- c. Earth storage at  $80^{\circ}\text{F} \pm 30^{\circ}\text{F}$  for 2 years.

#### 7.1.2.4 Sterilization

The system must undergo three high temperature sterilization cycles within a period of 3 months. Sterilization conditions of  $295^{\circ}\text{F} \pm 2^{\circ}\text{F}$  for 24-hours duration are to be attained inside the motor where temperature lag is greatest. No inspection by disassembly is permitted after sterilization.

#### 7.1.2.5 Other Desirable Criteria

Other criteria may be desirable, but not at the expense of those already presented. The system should be light in weight. It should be flexible in its use; that is, it should readily accommodate changes in other subsystems or changes in requirements or mission details. The subsystem should have a minimum effect on design requirements of other subsystems. It should have growth potential for use on later more sophisticated missions.

#### 7.1.3 Basic Constraints

Design requirements include the following basic constraints:

- a. The capsule c. g. location will be within 0.167 inch (1 sigma).
- b. The  $\Delta V$  thrust rocket will be located to within 0.02 inch (1 sigma).

- c. The  $\Delta V$  thrust misalignment will be no greater than 0.167 degree (1 sigma).
- d. The de-orbit velocity sequence shall be accomplished within 30 minutes after separation.
- e. Exhaust products from ACS thrust nozzles or rockets must be gaseous only.
- f. Flight spacecraft sensor error is 0.053 degree (1-sigma) from the spacecraft reference axes.
- g. Flight capsule mounting accuracy is 0.167 degree (1-sigma) with respect to the reference axes of the spacecraft.

## 7.2 COMPARISON OF CONCEPTS AND SELECTION OF REFERENCE CONCEPT

Five ACS combinations, as shown in Table XI were described in paragraph 6.5. These are: (1) the spin-only configuration, (2) active ACS with spin, (3) active ACS - cold gas, (4) active ACS with gimbaling, (5) active ACS - cold gas and hot gas. An evaluation of the concepts against various criteria is presented in this section in order to illustrate the tradeoffs involved in the selection of the reference scheme.

### 7.2.1 Spin Only System

The pointing accuracy of 1.0 degree is achievable with the spin system at 30 - 40 rpm. At these spin rates, despin is required prior to or during early entry. The use of rate damping or reorientation with an ACS after despinning was considered to reduce the possible loss in communication time after the despin process. However, the reduction in loss of communications time is so minimal, that the adoption of these options is not warranted, since they are heavy and complicated. Although this is the simplest and lightest system, it necessitates a spacecraft maneuver, which is its major disadvantage.

### 7.2.2 Active ACS with Spin

Adequate pointing accuracy can be achieved with this configuration. It does not require a spacecraft maneuver and it possesses greater flexibility. However, it does not permit maneuvers after thrusting to improve communication or entry conditions, and lacks growth potential for later more demanding missions. Rate damping or reorientation with an ACS after despinning, if used, will increase system weight and complexity.

### 7.2.3 Active ACS (Cold-Gas Reaction System)

This system has the flexibility for performing additional orientations if required, and has a pointing accuracy which is better than the spin systems by a factor of 2 (0.5 degree compared to 1.0 degree.)

Its reliability is degraded somewhat by the longer operating time, although should still be acceptable. The system suffers a considerable weight disadvantage, however, because the cold-gas reaction system must be sized to overcome the disturbance torques occurring during the rocket thrust interval.

### 7.2.4 Active ACS with Gimballing

Thrust level of the reaction control nozzles can be sized on the basis of orientation and limit-cycle requirements, since TVC is provided by gimballing the rocket engine. Weight requirements are therefore reduced. Reliability and complexity, however, are major disadvantages.

### 7.2.5 Active ACS (Cold Gas and Hot Gas)

Since the hot-gas system is operative during the thrusting phase (35 seconds), the cold-gas nozzles need be sized only to meet orientation and cruise requirements. Thus, weight requirements are not excessive. In addition, the system is flexible, has growth potential, and reliability and complexity features are improved. Because of its efficiency large c. g. offsets and thrust vector misalignments can be tolerated, thus easing concern over variations in these parameters during the heat-sterilization process.

### 7.2.6 Selection of Reference Concept

The design configuration which has been selected is the active ACS with cold gas and hot gas for TVC. This system uses an IRS which is required to furnish an attitude reference for orientation of the TV camera and which also furnishes the ACS attitude information. The inertial platform provides an appropriate mount for the accelerometers used for wind and density measurements.

An evaluation of the alternate concepts is presented in Figure 25. On a relative basis the system selected is seen to be superior. The spin-only system was not selected because of the requirement for a spacecraft maneuver. The active ACS plus spin was rejected because it did not offer the maneuver capability of the capsule after thrusting. The remaining choices were all for active ACS with the selection of the method of thrust vector control being the key factor. The use of cold gas is in many respects the most attractive approach since it would permit a single reaction control system to be used for the entire mission. However, the

SYSTEM CRITERION	1 Spin Only	2 Active ACS Plus Spin	3 Active ACS (Cold Gas)	4 Active ACS Plus Gimbal	5 Active ACS (Cold Gas & Hot Gas)
Performance	Fair	Fair	Good	Good	Good
Complexity-Reliability	Good	Good	Fair	Poor	Fair
Weight	Good	Good	Poor	Fair	Good
Maneuvering Flexibility	Poor	Fair	Good	Good	Good
Effect on FS and Other Subsystems	Poor	Fair	Good	Fair	Good
Growth Potential	Poor	Poor	Good	Good	Good
Failure Modes	Good	Good	Fair	Poor	Fair
Communications Maintenance	Poor	Poor	Good	Good	Good

Figure 25 EVALUATION OF CANDIDATE SYSTEMS

76-0157P

weight penalty of approximately 150 pounds was considered to be too large to accept. If this weight penalty is tolerable, the all-cold gas system would be the preferred choice on the basis of simplicity of design and a minimum number of components. The gimbal system was clearly unattractive from a weight standpoint, as well as the complexity and interface problems associated with incorporating it into the capsule design. The hot-gas system selected is simple in design, reliable, and relatively light in weight. Several hot-gas systems were compared (monopropellant, bipropellant, and solid propellant), and the last was chosen. They were also compared with the cold-gas and gimbal systems to provide a firm basis for selection. The results of these comparisons and the details of the systems compared are contained in the tradeoff sections which follow.

### 7.3 INTRASYSTEM TRADEOFFS FOR REFERENCE CONCEPT

For the active ACS with cold and hot gas, there were various tradeoffs made within the design of the ACS itself. Particular attention was given to the selection of a technique for thrust vector control, considering three hot-gas systems and comparing them with cold gas and gimbaling.

#### 7.3.1 Sensor and Electronics Subsystem

Basically there were two approaches possible for the IRS once an active ACS system was decided upon. A strapped-down gyro approach or a gimballed platform approach. Complicated star and planet trackers were excluded from consideration since a conventional gyro approach provides adequate performance for the required operating time.

Once it was determined that the reference coordinate frame must be maintained until impact for T.V. camera stabilization considerations, the strapped-down approach was eliminated. This is due to the limitations imposed by available gyro torque motors. State of the art gyro torque motors limit input rates to 60 deg/sec while a platform approach can easily accommodate 1000 deg/sec. Since the reentry rates may exceed 60 deg/sec, the strapped-down approach cannot be considered.

#### 7.3.2 Reaction Control Subsystem for Attitude Control

The mission for attitude control requires an impulse of 68 lb-sec, used intermittently over a period of approximately 1.5 hours. These requirements preclude the use of a solid propellant system because at its present state of the art, solid propellants do not have start-stop capabilities and therefore, have to burn over the entire operating period. This would result in a considerable weight penalty. State of the art systems such as monopropellants and bipropellants, although competitive with cold-gas systems on the basis of weight, are unattractive because of their

complexity. A cold-gas system is most suitable for this vehicle application considering size, weight, cost, availability of flight proven hardware, low thrust applications and thrust response characteristics.

The reference design uses a central pressure regulator which feeds the thrust nozzle valves. Because the required thrust levels are very low, a central regulator affords minimum system complexity and weight since it may easily pass the required low rates of gas flow. Further, the low gas-flow rates result in minimal pressure loss in gas tubing as well as low cross coupling effects when different groups of nozzle valves are opened simultaneously. The availability of flight qualified regulators and nozzle solenoid valves testifies to the popularity of this system type for low-thrust, low-total impulse systems.

Reasonable cold-gas system weights can be realized utilizing gaseous nitrogen as the propellant. The results of a weight tradeoff considering several gaseous propellants are presented on Figure 26 showing system weight as a function of gas molecular weight and impulse. Propellants other than nitrogen may have volume advantage for comparable system weights; however since volume is not a limiting factor, the additional cost and handling complexities of the other fluids are not warranted.

Long time exposure to high vacuum radiation conditions of the deep-space environments have deteriorating effects on elastomers and lubricants in general. Consequently, regulators and solenoid valves incorporating metal seats are proposed for the reference design. Valves and regulators of this type, manufactured by Sterer, have been developed for similar missions.

Charging the pressure vessels prior to high temperature sterilization results in a 75 percent increase in vessel weight,\* because the elevated temperature lowers the material strength and increases the internal pressure in the vessel. Filling the vessels after sterilization may be accomplished with a fill system scheme as depicted in Figure 27. This fill system consists of a filter, normally closed solenoid and a capillary tube sealed at the canister outlet. This system concept adds considerable complexity to sterilization canister separation, since the capillary tube must also be separated during this phase. The vessel weight saving (approximately 2.0 pounds) does not warrant imposition of additional separation complexities and hence, the conventional vent-fill system depicted on Figure 28 was adopted for the reference design.

---

\* Detailed computations are presented in Appendix D.

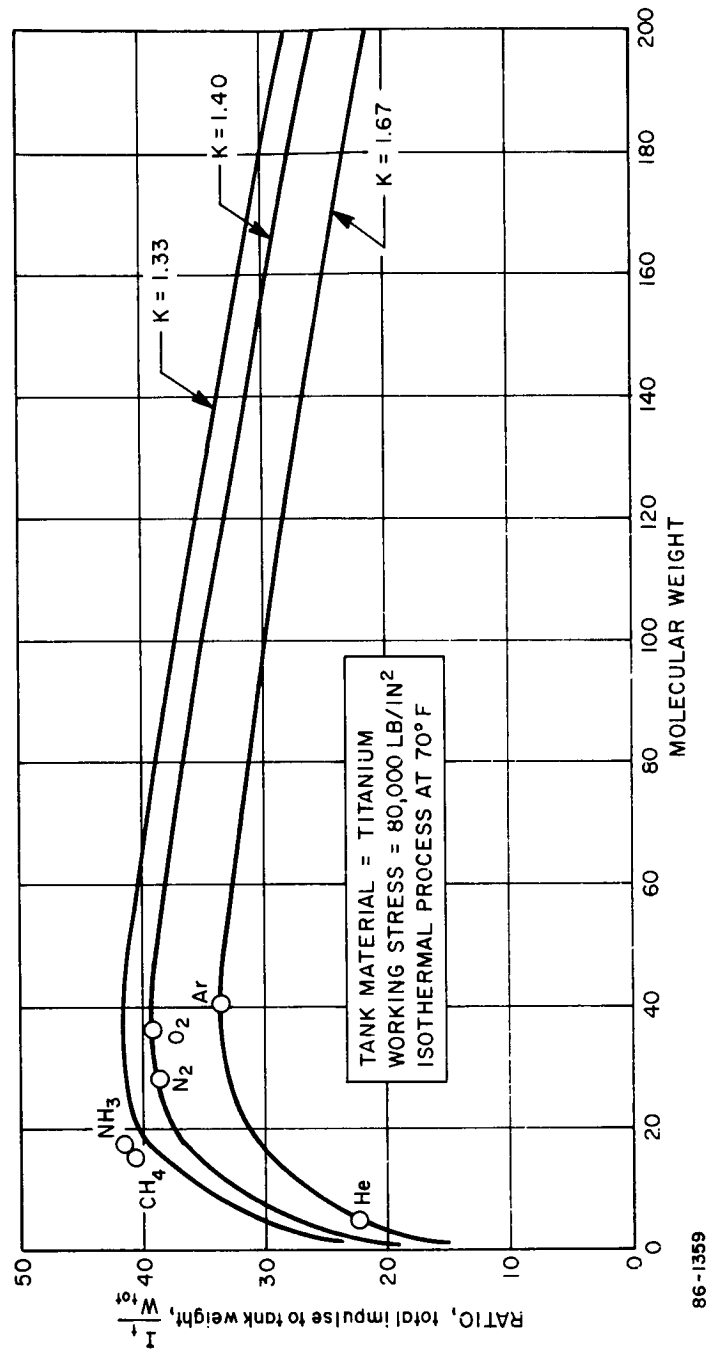


Figure 26 TOTAL IMPULSE/TANK WEIGHT VERSUS MOLECULAR WEIGHT

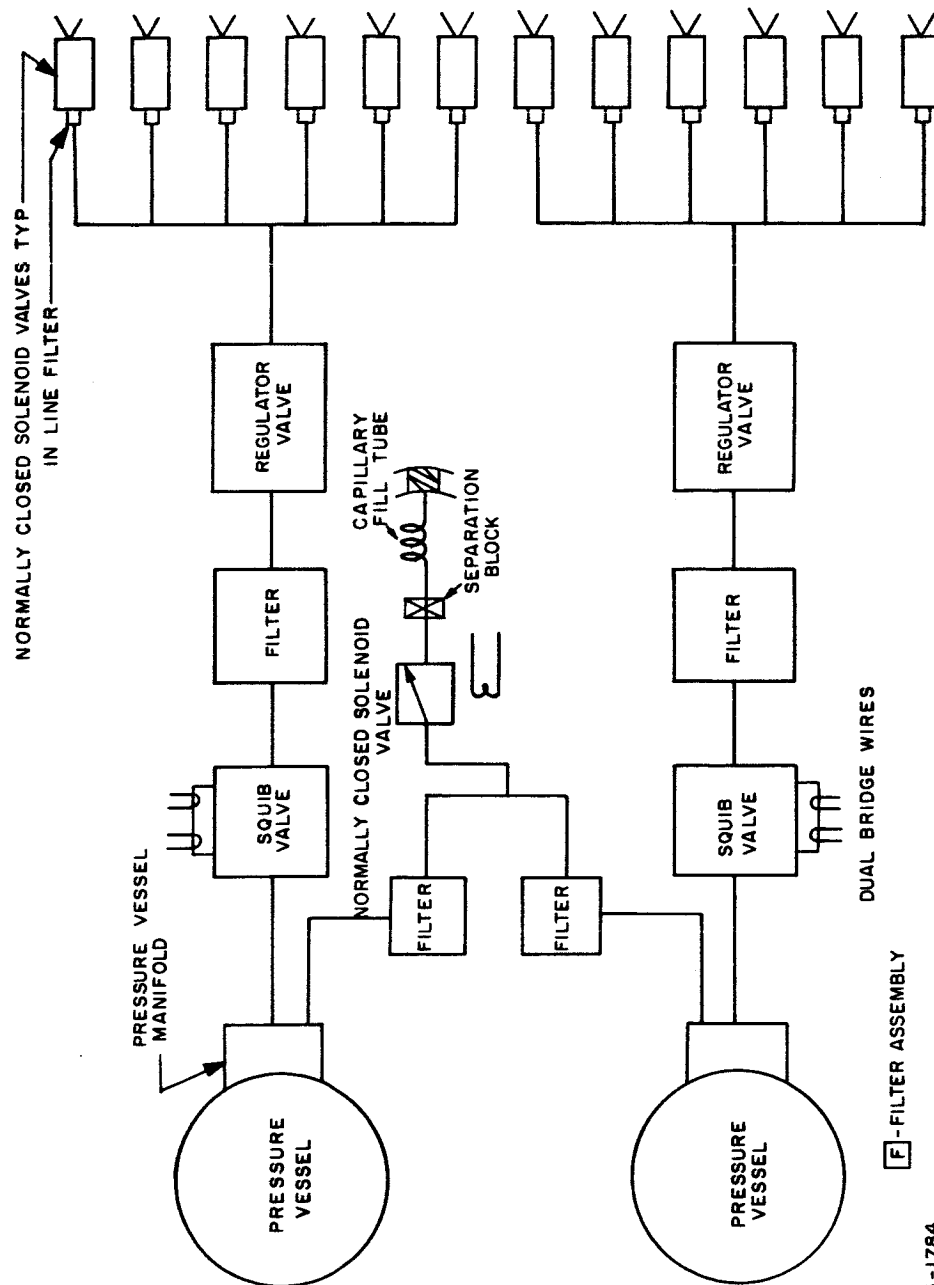
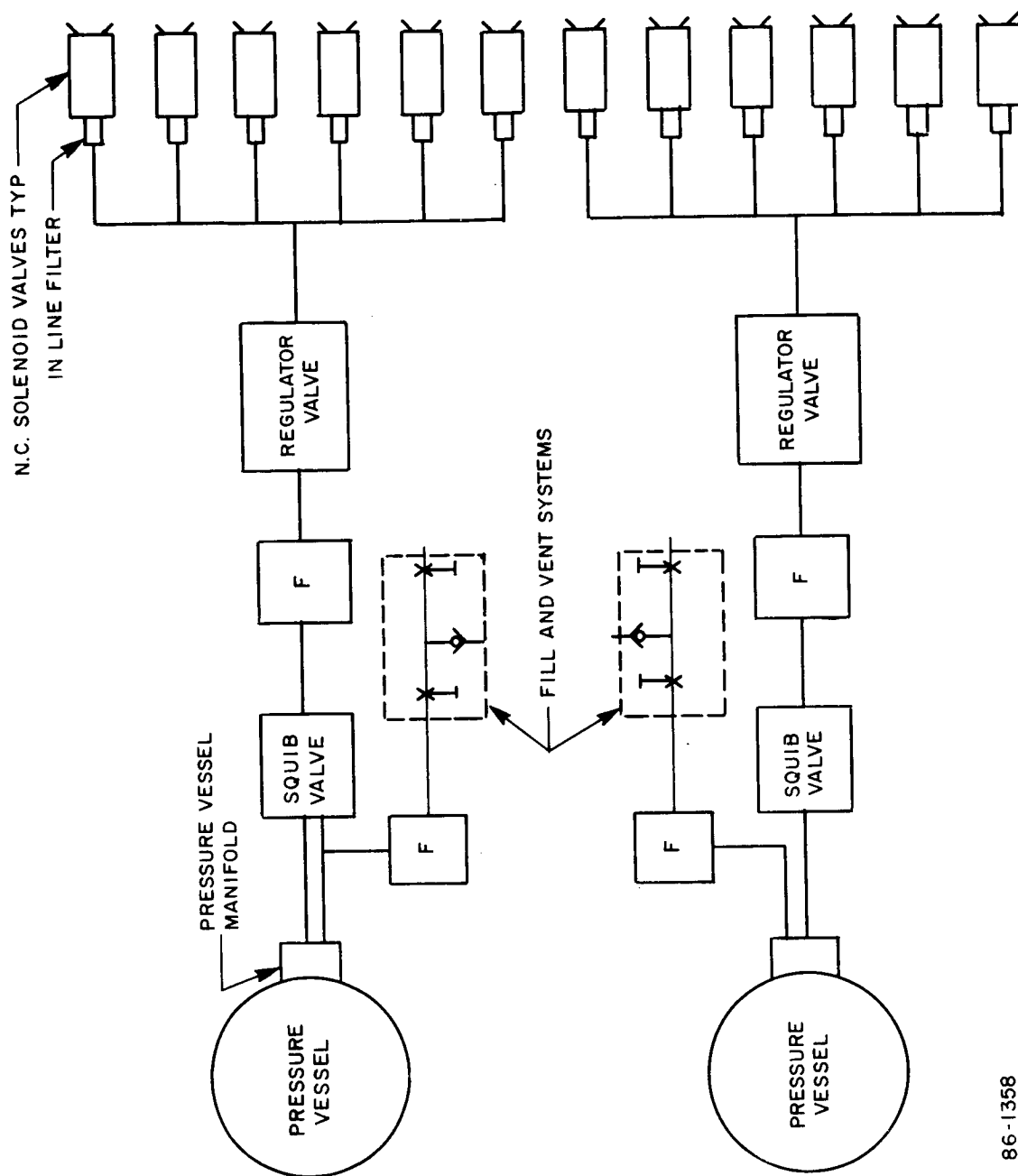


Figure 27 COLD-GAS REACTION SYSTEM

85-1784



86-1358

Figure 28 CONVENTIONAL VENT - FILL SYSTEM

### 7.3.3 Thrust Vector Control System

#### 7.3.3.1 Method of Approach

The selection of a TVC system design was based on a detailed tradeoff study of the variety of available state of the art design configurations. The most desirable system is defined as the system which exhibits the largest degree of compliance with the mission requirements of greatest relative importance.

Principal configuration and performance criteria, collectively referred to as the "mission requirements," were established. Representative criteria would include weight, complexity, and reliability.

A weighted scoring technique permitted a judicious comparative evaluation of alternate systems. Each criteria was assigned a weighted maximum score value i. e., weight, 12; complexity, 6; etc. Candidate systems were then tested against each criteria and scored according to the relative degree of compliance exhibited. That system possessing the greatest total score was identified as the most desirable system. Preparation of preliminary candidate system designs afforded a quantitative comparison for such criteria as weight and size, while comparison of the more subjective criteria such as complexity and cost, required considerable engineering judgement.

#### 7.3.3.2 Performance

For purposes of comparison of each of the candidate systems, a uniform set of performance requirements were established. These requirements are used in this section, but do not correspond to the final system design criteria which were established for the reference design. Consequently the designs described in this tradeoff discussion differ in detail from the reference design. The comparison between systems remain valid and the comparative results which would be obtained by using the final design criteria would be the same.

The system must operate for 35 seconds and provide control torques about the pitch and yaw axes, in couples, to overcome a moment of 95 foot-pounds. It must be able to provide the required moment if one-half of the couple fails. That is, a single nozzle must be sized to provide the 95 foot-pounds, even though in normal operation the required torque will be provided by two nozzles. Since the moment arm is 7.3 feet, the thrust required is 13 pounds. A total of eight thrust nozzles are required to produce negative and positive couples about each of two axes. The required torque is determined as that necessary to counteract the disturbing torques imposed by the thrust of the de-orbit

propulsion system and to provide satisfactory dynamic response. These disturbance torques are produced by the error in location of the rocket-thrust axis relative to the c. g., of the vehicle and the thrust vector misalignment, assumed to be 0.25 inch and 0.25 degree, respectively. It will be seen in the reference design that these tolerances are doubled (see paragraph 7.1.3) and accordingly the thrust levels in the reference design are nearly doubled (25 pounds), but the results of the tradeoff study are still applicable.

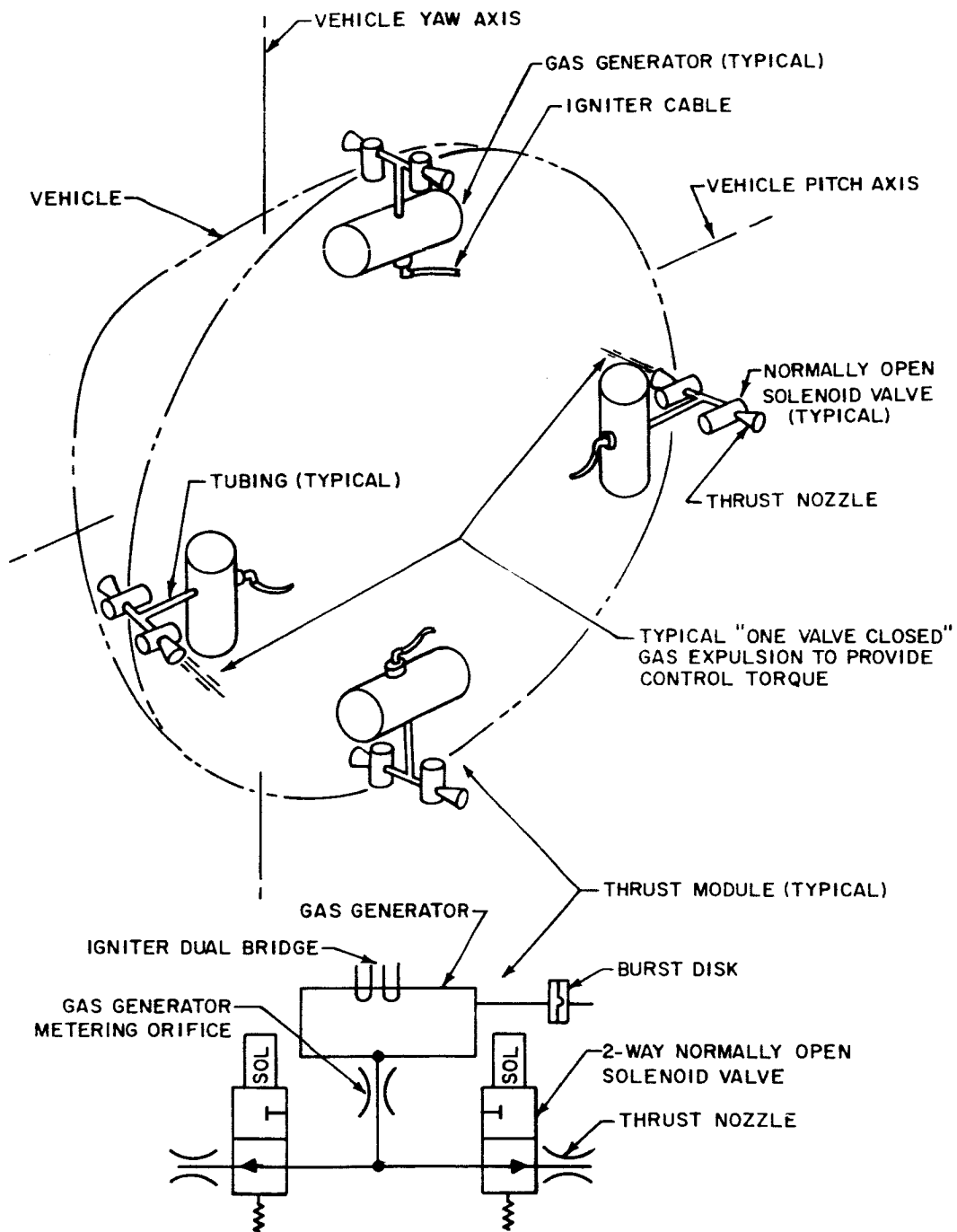
For all systems compared, the total impulse required is computed on the basis that a failure of any single component, such as a valve stuck open or closed, failure of the propellant supply, etc., will not cause the system to fail. For stored gaseous or liquid propellant systems, this requires that the stored propellant have a total impulse which is 3.3 times the required impulse. (See Appendix D.) For a solid propellant system, the same criteria are met, but the amount of stored impulse is dependent on the details of the configuration chosen, specifically, the thrust required, the operating time of the system, and the necessity of redundant elements to furnish a failure mode safety margin. (See paragraph 8.3.2).

Systems considered are solid propellant hot gas, hydrazine monopropellant, a bipropellant, a flexure gimbal system, and a cold-gas system. Jet vanes were considered impractical because of the weight and complexity due to the high temperature of the solid propellant exhaust gases, and conventional gimbal techniques were found to be noncompetitive in terms of complexity and weight, so these alternatives are not described here.

#### 7.3.3.3 Solid Propellant System

Figure 29 illustrates the solid propellant system design considered in the tradeoff study. Each of the four solid propellant hot-gas generators supply two normally open solenoid nozzle valves. Each thrust nozzle is of the same thrust rating. Four nozzles are located in each of the vehicle principal axis planes and normally operate in pairs to provide control torque couples.

System operation is begun by simultaneous application of an excitation voltage to each of the gas generator igniters to initiate combustion of the solid propellant. In the absence of command signals to the normally open solenoid valves, the products of combustion are expelled through the axially opposed nozzles yielding zero net torque applied to the vehicle. Control torques about either the pitch or yaw axes are commanded by closing opposed nozzles as illustrated for example in Figure 29 for the pitch axis.



86-1213

Figure 29 SOLID PROPELLANT OPEN CENTERED TVC SYSTEM

Utilization of two independent thrust modules (i. e., gas generator and two valves) per axis permits the complete loss of one module per axis as a result of failures. Each module is designed to provide the minimum required torque when acting as the sole control torque source for a given axis. System degradation as the result of failure is thereby limited to loss of pure torque couples for an axis incurring loss of one module.

Table XIX presents a breakdown of the system weight for a representative nozzle thrust magnitude of 13 pounds and a total operating time of 35 seconds. Each gas generator would occupy the volume enclosed by a right circular cylinder approximately 3.6 inch diameter by 6.1 inches long while each solenoid nozzle valve would require the volume of a right circular cylinder approximately 3.0 inches in diameter by 3.0 inches in length. Appendix E describes the calculations of the component weights and size.

This system has the advantages of:

- 1) Minimum weight, size, and complexity
- 2) No critical dynamic or static seals
- 3) No sliding metallic surfaces in contact with each other
- 4) Least problems associated with sterilization

TABLE XIX

SOLID PROPELLANT SYSTEM WEIGHT BREAKDOWN

Item	Nomenclature	Unit Weight (lbs)	No. Required	Total Weight (lbs)
1	Gas Generator	4.30	4	17.2
2	Solenoid Valve	0.52	8	4.2
3	Mounting Hardware	3.0	1	3.0
4	Tubing and Fittings	2.0	1	<u>2.0</u>
Total System Weight =				26.4 lbs.

#### 7.3.3.4 Monopropellant System

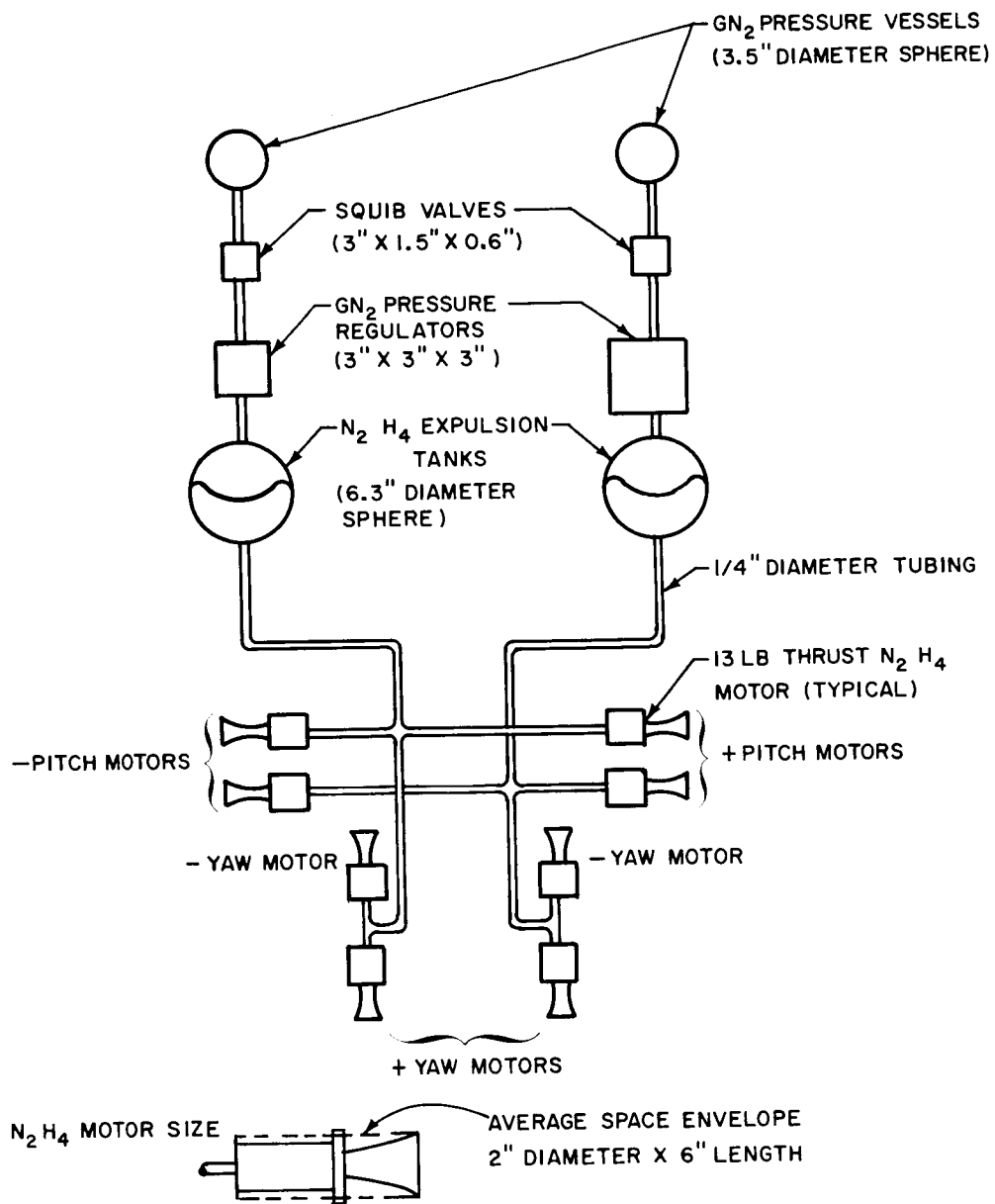
Figure 30 depicts the schematic layout of a monopropellant hydrazine TVC system. Hydrazine is supplied to catalytic decomposition motors by the conventional pressurized bladder expulsion tanks shown. System operation is begun by firing the normally closed squib valves applying a regulated nitrogen pressure on the expulsion tank bladders and in the liquid hydrazine at each motor fuel solenoid valve inlet. Thrust is commanded by electrical actuation of any fuel solenoid valve.

The component envelope dimensions noted in Figure 30 and the system weight breakdown given in Table XX represent "state of the art" monopropellant system components. Appendix F describes the procedures employed in sizing the system components.

TABLE XX

#### MONOPROPELLANT HYDRAZINE SYSTEM WEIGHT BREAKDOWN

Item	Nomenclature	Unit Weight (lbs)	No. Required	Total Weight (lbs)
1	Rocket Motor	1.63	8	13.04
2	N <sub>2</sub> H <sub>4</sub> Fuel	4.52	2	9.04
3	N <sub>2</sub> H <sub>4</sub> Expulsion Tank	1.34	2	2.68
4	GN <sub>2</sub> and pressure vessel	0.87	2	1.74
5	Pressure Regulator	1.50	2	3.00
6	Squib Valve	0.7	2	1.40
7	Tubing, Fill Valves, etc.	4.0	1	<u>4.00</u>
Total System Weight =				34.90



86-1212

Figure 30 MONOPROPELLANT HYDRAZINE SYSTEM

### 7. 3. 3. 5 Bipropellant System

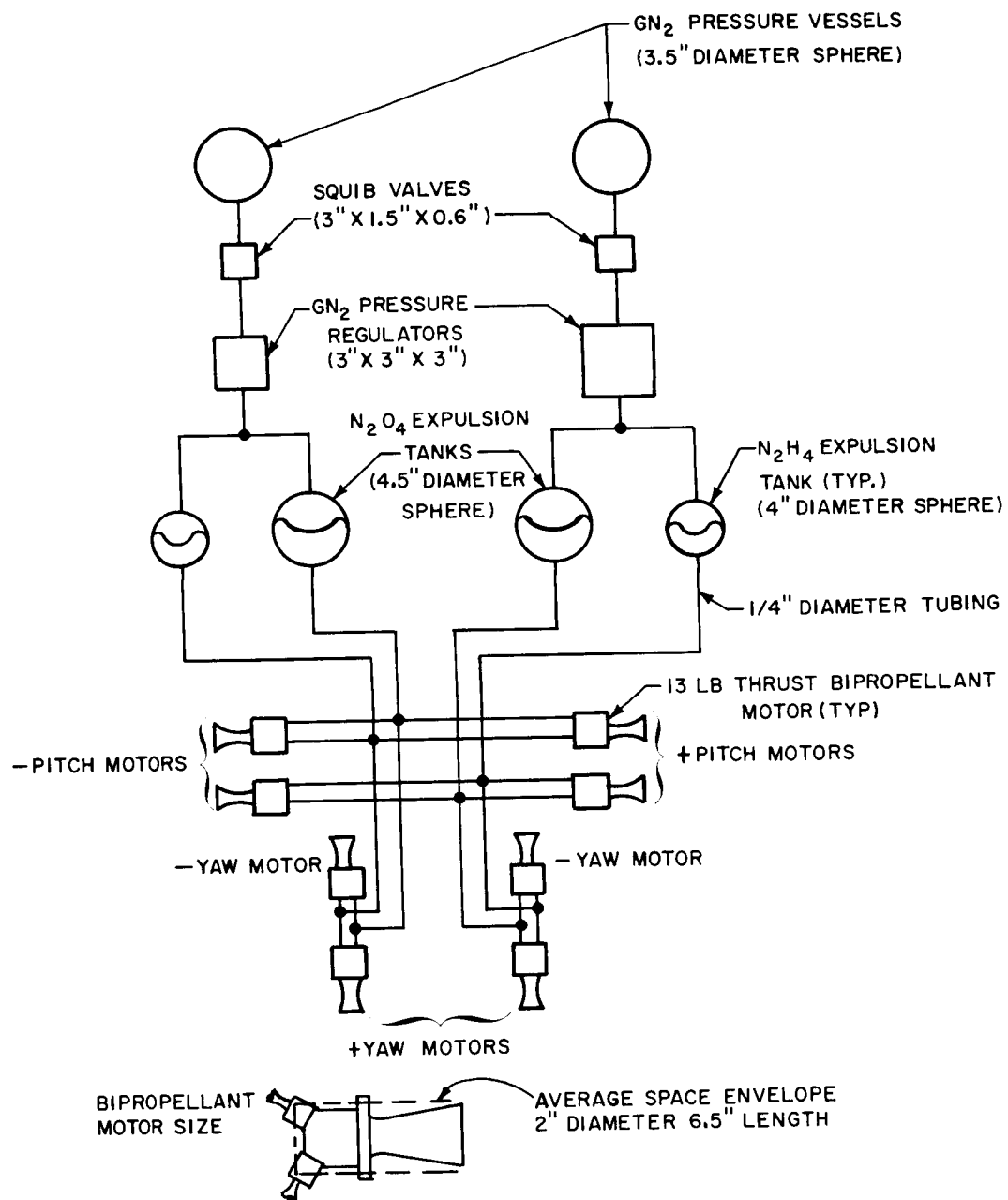
Figure 31 illustrates the schematic layout of a bipropellant hydrazine and nitrogen tetroxide TVC system. The hypergolic combination of hydrazine (fuel) and nitrogen tetroxide (oxidizer) is obtained by synchronized actuation of the respective solenoid valves on a thruster commanded to provide thrust. Both the fuel and the oxidizer supply subsystems consist of the same pressurized expulsion bladder design described for the monopropellant system.

Component sizes and weights are given in Figure 31 and Table XXI respectively. Appendix G delineates the procedures used in sizing the system components.

TABLE XXI

BIPROPELLANT  $N_2H_4$ - $N_2O_4$  SYSTEM WEIGHT BREAKDOWN

Item	Nomenclature	Unit Weight (lbs)	No. Required	Total Weight (lbs)
1	Rocket Motor	1.00	8	8.00
2	$N_2H_4$ Fuel	1.12	2	2.24
3	$N_2H_4$ Expulsion Tank	0.75	2	1.50
4	$N_2O_4$ Oxidizer	2.42	2	4.84
5	$N_2O_4$ Expulsion Tank	1.00	2	2.00
6	$GN_2$ and pressure vessel	0.54	2	1.08
7	Pressure Regulator	1.50	2	3.00
8	Squib Valve	0.70	2	1.40
9	Tubing, Fill Valves, etc.	8.00	1	<u>8.00</u>
Total System Weight = 32.06				



86-1211

Figure 31 BI-PROPELLANT N<sub>2</sub>H<sub>4</sub> - N<sub>2</sub>O<sub>4</sub> SYSTEM

#### 7.3.3.6 Gimbaled System

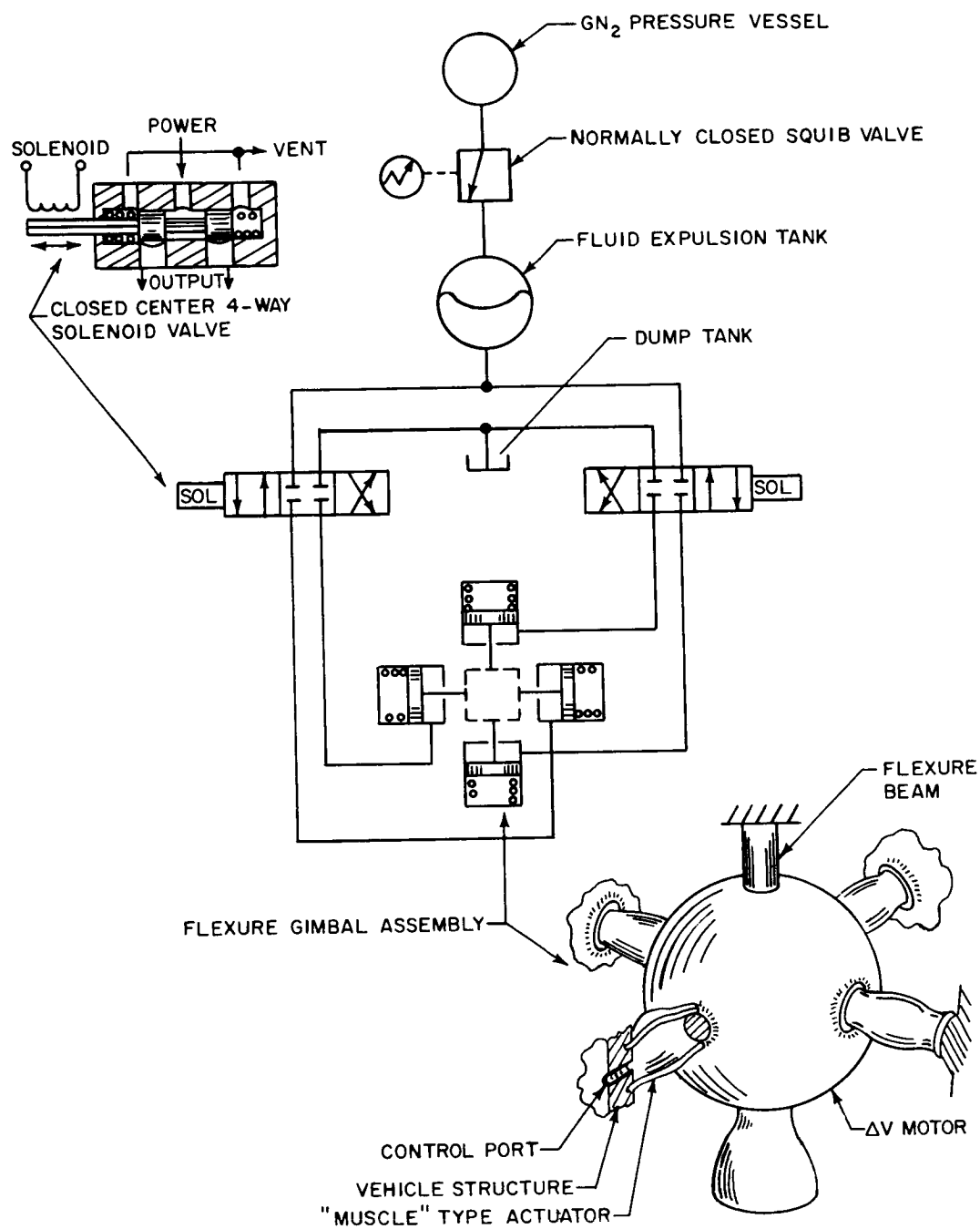
The principal components of a flexure gimbal TVC system are shown in Figure 32. The schematic represents the minimum number of components required to achieve thrust vector control and serves to describe the basic mode of operation associated with the system concept.

Angular displacement of the  $\Delta V$  thrust vector results from controlled bending of the motor flexure beam mount shown in Figure 32. Bending moments are created by pairs of "human muscle" type actuators located in the planes of the vehicle pitch and yaw axes. Application of fluid pressure to a given actuator causes elastic deformation of the transverse section diameter with introduction of an associated force along the actuator axis tending to pull the motor case toward the actuator vehicle mount. Since the actuator is incapable of exerting a force in more than one direction, opposed pairs are employed with fluid power control provided to simultaneously apply and relieve fluid pressure on the respective actuators of an opposed pair.

The fluid power source is comprised of a pressurized nitrogen vessel and bladder type fluid expulsion tank. The two closed-center, 4-way solenoid valves control selective pressurization and venting of actuators. Fluid exhausted from the actuators is collected in a dump tank.

Figure 33 illustrates the flexure gimbal TVC system proposed for consideration in the trade off study. The basic configuration of Figure 32 was amplified to provide the necessary margin of safety required against failure modes. Comparison of the basic configuration with Figure 33 indicates the use of identical redundant subsystems with the use of parallel control valves. Redundant actuators and fluid power supplies anticipate loss of the control fluid pressure in one of the subsystems through leakage. Parallel control valves provide protection against one of the subsystems failing in a "locked" position. Normal operation requires the two members of each pair of parallel valves to act in unison. Failure of one valve or an electrical command circuit failure causes the complementary valve to vent the affected subsystem power supply to the dump tank.

Table XXII tabulates the system weight breakdown of the flexure gimbal TVC system shown in Figure 33. Appendix H describes the procedures employed in determining the data of Table XXII.



86-1210

Figure 32 FLEXURE GIMBAL TVC BASIC CONFIGURATION

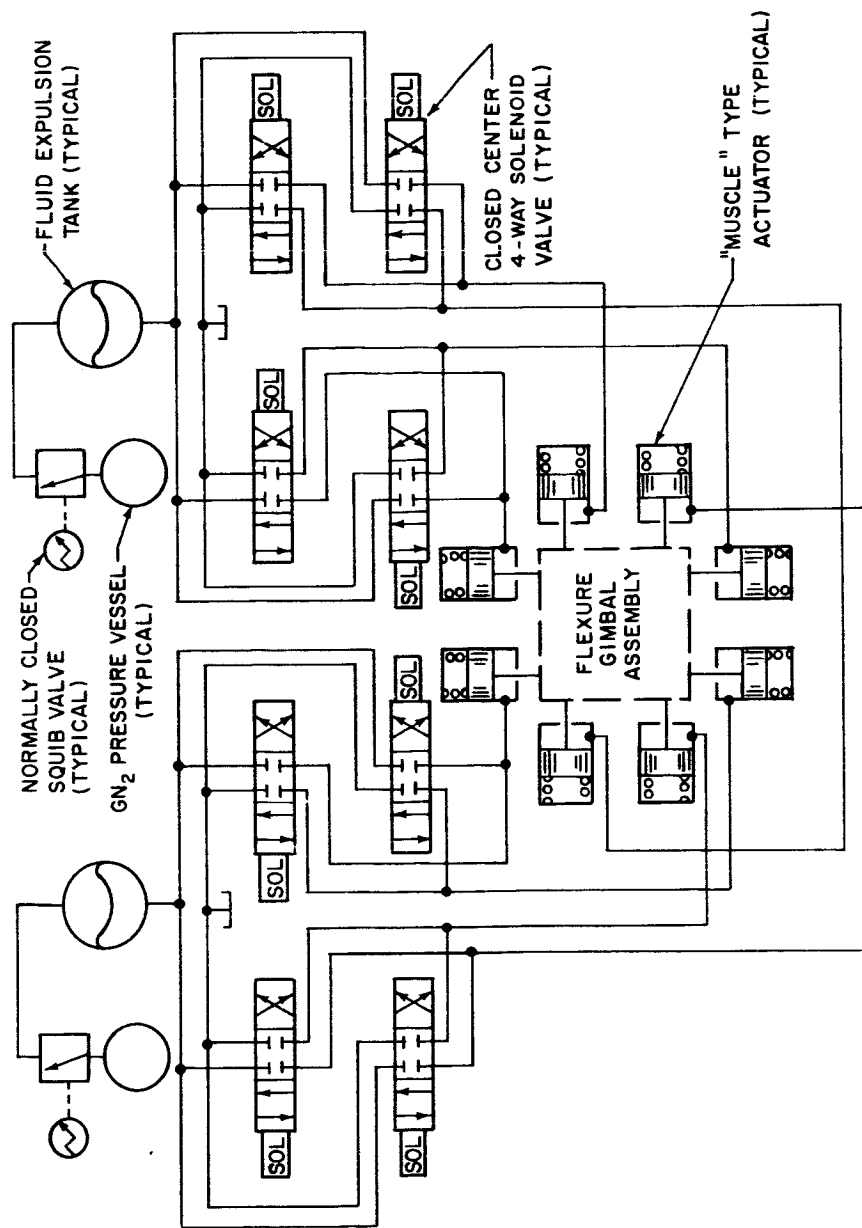


Figure 33 FLEXURE GIMBAL TVC SYSTEM

86-1209

TABLE XXII

## FLEXURE GIMBAL TVC SYSTEM WEIGHT BREAKDOWN

Item	Nomenclature	Unit Weight (lbs)	No. Required	Total Weight (lbs)
1	Actuator	0.66	8	5.28
2	Squib Valve	0.37	2	0.74
3	GN <sub>2</sub> Pressurant	0.7	2	1.40
4	GN <sub>2</sub> Pressure Vessel	1.0	2	2.00
5	Vessel Manifold	0.25	2	0.50
6	Fluid	1.20	2	2.40
7	Fluid Expulsion Tank	0.6	2	1.20
8	Filter	0.25	4	1.00
9	Control Valve	0.75	8	6.00
10	Tubing Complex	5.60	2	11.20
11	Dump Tank	0.6	2	<u>1.20</u>
Total System Weight =				32.92

## 7.3.3.7 Cold Gas System

Figure 34 shows the schematic layout of a cold gas nitrogen TVC system. Consideration of the same system type as employed for the ACS reaction control system permits utilization of a single dual-purpose system capable of meeting the requirements of either TVC or attitude control.

Redundant subsystems maintain the required safety margin against failure modes. The subsystems are identical and are of the conventional central regulator cold-gas design. Gaseous nitrogen propellant is stored under pressure in the pressure vessels by means of the fill and vent valves shown in series with filters and the vessel manifold. Normally closed squib valves serve to contain the propellant until

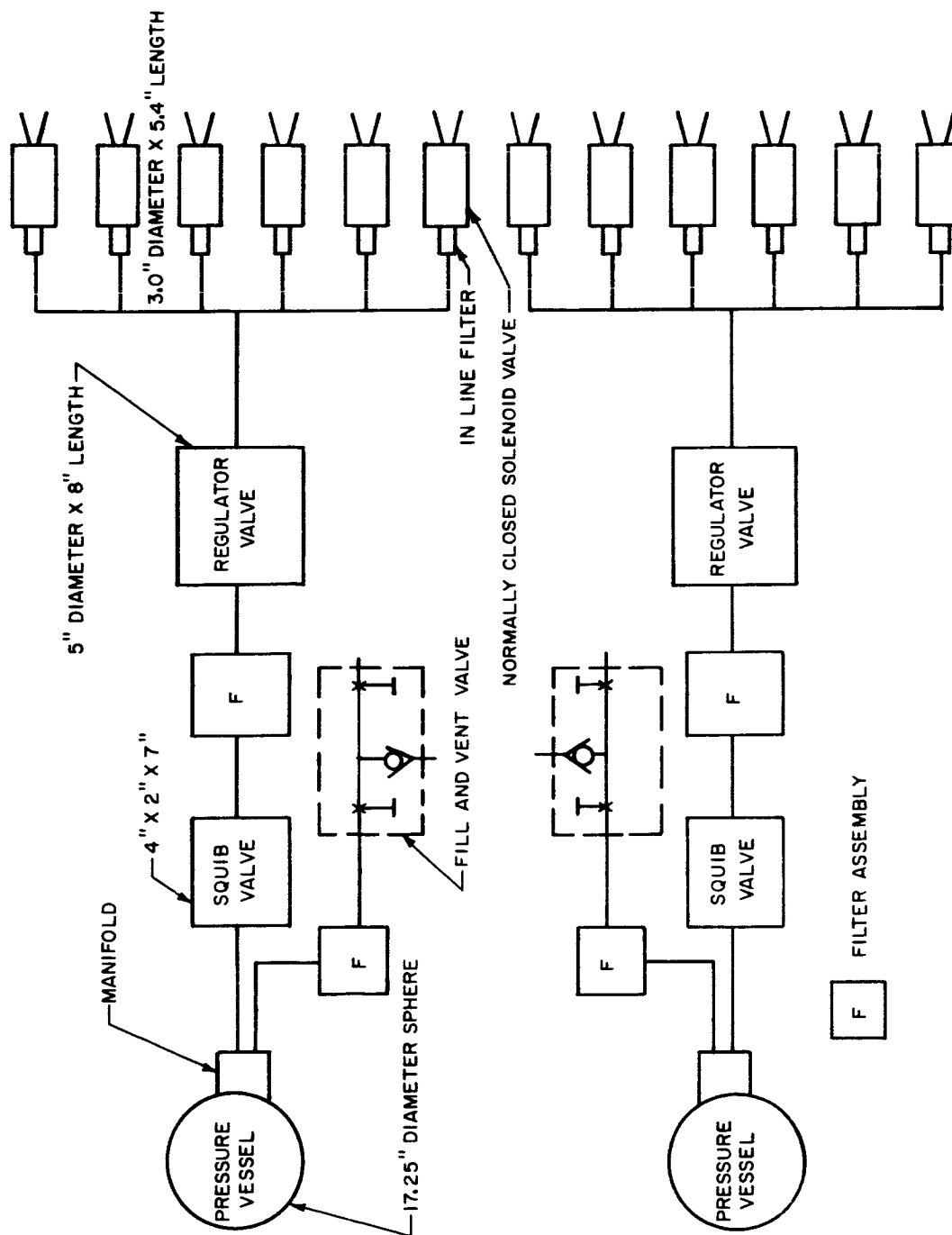


Figure 34 COLD GAS (NITROGEN) TVC SYSTEM

86-1208

system activation. Each pressure vessel supplies propellant to a pressure regulator and six normally closed solenoid valves. The ACS reaction control system roll control thrust is designed to counteract rocket motor roll axis disturbance torques. Since the subject system is both the ACS and TVC reaction control system, a total of 12 nozzle valves are shown in Figure 34 for torque couples about the three vehicle axes.

Table XXIII presents the system weight breakdown of the cold-gas TVC system. Appendix I delineates the procedures followed in determining the data of Table XXIII.

TABLE XXIII

COLD GAS GN<sub>2</sub> TVC SYSTEM WEIGHT BREAKDOWN

Item	Nomenclature	Unit Weight (lbs)	No. Required	Total Weight (lbs)
1	Solenoid Valve	1.8	12	21.6
2	Pressure Vessel	48.95	2	97.9
3	GN <sub>2</sub> Propellant	20.5	2	41.0
4	Squib Valve	1.3	2	2.6
5	Tubing Complex	3.0	2	6.0
6	Regulator	6.2	2	12.4
7	Filter	0.7	4	2.8
8	Manifold	0.35	2	<u>0.70</u>
Total System Weight = 185				

For comparison with the other tradeoff systems, the weight of the cold-gas reaction control system should be reduced by 25 pounds, which is the portion of the weight attributable to ACS functions other than TVC. The requirement for dry-heat sterilization of the pressure vessel and its contents under pressure is responsible for about 40 pounds of the system weight. However, if the c. g. offset (which is the main factor in sizing the TVC system) were increased by a factor of 2, the weight of the cold-gas system would be increased by over 100 pounds for a system in which the pressure vessel is charged after sterilization.

### 7.3.3.8 Comparison of TVC Systems

Figure 35 presents the results of applying the weighted scoring technique discussed earlier to the TVC system tradeoff study. The relative weights of the criteria were selected to emphasize the most critical mission requirements.

The factors considered in scoring are reviewed in the following discussion. For each criterion the relative merits and disadvantages of the candidate systems are discussed in general, while the numerical scores are contained in Figure 35.

1. System Weight -- The system weights shown earlier, are summarized below.

<u>System</u>	<u>Total Weight</u> (pounds)
Solid Propellant	26
Monopropellant	35
Bipropellant	32
Flexure Gimbal	33
Cold Gas	185*

The solid propellant system clearly offers the best weight.

2. Packaging -- Figures 31 and 33 indicate the complexity of the packaging problems associated with the bipropellant and flexure gimbal systems. The remaining systems are about equal with the monopropellant system regarded as slightly less desirable because of tubing required.

\*Weight attributable to TVC is 160 pounds; other attitude control functions require 25 pounds, for a total of 185 pounds.

FLEXURE GIMBAL	MODIFIED REORIENTATION COLD GAS	MONO-PROPELLANT SYSTEM	SOLID PROPELLANT SYSTEM	BI-PROPELLANT SYSTEM	RELATIVE WEIGHT OF CRITERIA	(25)
						CONFIGURATION AND PERFORMANCE CRITERIA
6	1	6	12	6	12	SYSTEM WEIGHT
1	3	2	3	1	3	PACKAGING
4	4	3	5	2	6	COMPATIBILITY WITH LAUNCH ENVIRONMENTS
4	4	3	5	2	6	COMPATIBILITY WITH SPACE ENVIRONMENTS
2	2	1	6	1	6	COMPATIBILITY WITH CONTAMINANTS
1	9	5	9	2	10	FAILURE MODES
1	6	3	6	1	6	COMPLEXITY
1	3	2	3	3	3	TEST DATA AVAILABILITY
5	5	1	4	3	5	RESPONSE TIME ADJUSTMENT
2	4	4	1	4	4	CONTROL TORQUE ADJUSTMENT
6	5	2	4	4	6	INHERENT RESPONSE CHARACTERISTICS
3	3	5	5	5	5	CROSS COUPLING OF AXIAL CONTROL TORQUES
4	10	4	10	6	10	PROVEN HARDWARE AVAILABILITY
3	5	2	5	1	5	HANDLING AND PREFLIGHT PREPARATION
8	10	4	10	1	10	STERILIZATION COMPATIBILITY
1	3	1	2	1	3	COST
52	77	48	90	43	100	POINT TOTAL

86-1191

Figure 35 ALTERNATE TVC SYSTEM PARAMETRIC EVALUATION

3. Compatibility with Launch Environments -- The bipropellant system is most susceptible to the severe dynamic environments during powered flight because of pressurized vessels and mechanisms involving moving parts. The remaining systems have fewer parts with the solid propellant system requiring no precision mechanisms such as regulators or fuel valves and no pressurized vessels.

4. Compatibility with Space Environments -- The bipropellant system is the least desirable in view of the many critical static and dynamic seals as well as the precision mechanisms utilizing closely fitted mechanical parts such as valves and regulators. These particular design features necessitate suitable design precautions to ensure insensitivity against space "vacuum welding" of mating metallic elements and distortion of precision parts due to thermal gradients.

The long-term mission duration imposes strict seal requirements on pressurized vessels. The other systems are rated progressively better with reduction of the number of seals and moving parts described above. The solid propellant system possesses no seals of a critical nature, no closely mated precision mechanical parts, and requires no long-term storage of pressurized fluid or gas.

5. Compatibility with Contaminants -- The solid propellant system definitely has the advantage over all the other systems which demand extreme care with respect to cleanliness of propellant and elimination of particulate contamination during fabrication. The alternate systems all employ items easily impaired by the smallest amount of foreign solid particles, i. e., regulators, fuel metering valves, and fluid pressure control valves.

6. Failure Modes and Complexity -- Both of these criteria are covered under a single discussion since they are mutually dependent. Examination of the system schematics indicates the increasing complexity and susceptibility to failure modes starting with the bipropellant design as the worst case and ending with cold gas and solid propellant as the most desirable. The flammable bipropellant and monopropellant liquids pose obvious disadvantages when considering failure modes while the flexure-gimbal system demands a very complex mechanization layout with the attendant susceptibility to failures.

7. Test Data Availability -- All the systems represent more or less "state-of-the-art" designs with the flexure gimbal being the sole "unique" approach. The scarcity of data on the monopropellant catalyst results in a slightly lower rating for that system.

8. Response Time Adjustment and Inherent Response Characteristics -- The cold-gas and solid propellant systems are the most flexible of the mass expulsion systems since the response of the valves on either system is strictly a question of tailoring the valve design to suit requirements. The bipropellant system has a definite limitation due to the well known ignition delay characteristic. Similarly, the monopropellant system catalyst possesses a finite ignition delay as a limit to the speed of response attainable. The flexure-gimbal design permits easy adjustment of response through proper design of the fluid pressure control valves.

9. Control Torque Adjustment -- The bipropellant, monopropellant, and cold-gas systems are easily modified for thrust level changes within reasonable limits. Variation of a nozzle throat section diameter and/or propellant pressure is easily accomplished. The flexure-gimbal system is restricted as to control torque adjustment since the muscle-type actuators are restricted to a finite maximum displacement. The solid propellant design requires major modifications of gas generator parameters to vary the output flow rate (i. e. thrust). Modification in this area entail corresponding changes in burning time and pressure levels which must be compatible with the operating characteristics of the nozzle valves.

10. Cross Coupling of Axial Control Torques -- With the exception of the cold-gas and flexure-gimbal systems, all the systems are inherently free from axial cross coupling. Each of the solid propellant thrust modules is completely independent thereby limiting cross coupling to the accuracy obtainable in the mechanical location of the thrust nozzles in the principal axis planes. The bipropellant and monopropellant systems require low liquid flow rates of high energy propellants. Pressure variations due to frictional losses at the motor valve inlets are correspondingly small yielding minimal cross coupling. Conversely, the cold-gas system requires relatively large flow rates necessitating the design precaution of balancing the frictional pressure losses in each tubing length in order to reduce cross coupling. The flexure-gimbal system has obvious disadvantages. To avoid cross coupling, the flexure pivot must be articulated in a single plane. Considering that all of the  $\Delta V$  motor supports are elastic members, the difficulty of planar displacement becomes apparent.

11. Proven Hardware Availability -- The cold-gas and solid propellant designs are definitely qualified concepts as attitude control systems. The bipropellant system has been utilized to a lesser degree while use of the Shell catalyst monopropellant system is still under development. The unique flexure-gimbal design is unproven and requires complete development.

12. Handling and Preflight Preparation -- The safety measures required to prepare the bipropellant and monopropellant systems place these designs as the least desirable. The necessity of handling both fluid and gas in the flexure gimbal causes this design to be regarded as somewhat easier to handle. Cold-gas and solid propellant are the most easily prepared configurations with previous program experience favoring the former and the lack of any pressurization enhancing the latter.

13. Sterilization Compatibility -- The bipropellant and monopropellant systems are ranked lowest due to the question of high temperature susceptibility of the propellant. Little is actually known at this time concerning possible chemical structure changes associated with prolonged heating. The flexure-gimbal system is somewhat better but would still require caution in heating the critical seal areas of the expulsion tank and muscle-type actuators, as well as the precision machined pressure control valves.

The cold-gas and solid propellant designs are the least troublesome when considering sterilization. Extra pressure vessel strength designed into the cold-gas system would take care of the increased pressure incurred at higher temperatures. The research applied to the problem of sterilizing a solid propellant for the  $\Delta V$  motor would be directly usable in the solid propellant system.

14. Cost -- Development cost would be highest on those systems having the least prior usage. Although both the cold-gas and solid propellant systems were cited earlier as being common concepts, the cold gas is given a slight edge since the solid propellant design employs "one-shot" devices necessitating higher development materials cost.

Evaluating the total scores accumulated by each system, it is seen that the solid propellant system possesses an outstanding margin. In general, the tradeoff study may be summarized by a comparison of the outstanding features of each system. Between the monopropellant and bipropellant systems, the latter has no weight or performance advantage. The added complexity of the bipropellant design is a justifiable cause for rejection compared to the monopropellant. In addition to the low total score achieved, the question of the technical feasibility of the flexure-gimbal system constitutes reason for rejection compared to the monopropellant design. A comparison between the monopropellant and solid propellant systems leads directly to the selection of the solid propellant design. In each critical criteria, a definite advantage is seen, i. e. weight, complexity, sterilization, compatibility, etc.

Comparing the solid propellant system with the cold gas system shows an overwhelming disadvantage due to the high weight of the cold-gas system. However, if weight were not a factor the cold-gas system would be very nearly equal to the solid propellant system in terms of all other important criteria. Furthermore, the weight of the cold-gas TVC system could be reduced to 120 pounds by using a capillary fill technique to charge the pressure vessels after sterilization (see paragraph 7.3.2). At this weight level, the cold-gas system appears more attractive, although the additional weight penalty of 100 pounds which would be imposed if the c. g. tolerance were doubled is still a strong factor weighing against the choice of cold gas. The hot-gas system, on the other hand, must pay a weight penalty of only 14 pounds if the same increase in c. g. tolerance is permitted.

Because of the importance of weight, the solid propellant system was selected.

## 8.0 REFERENCE ATTITUDE CONTROL SYSTEM DESCRIPTION

### 8.1 INTRODUCTION

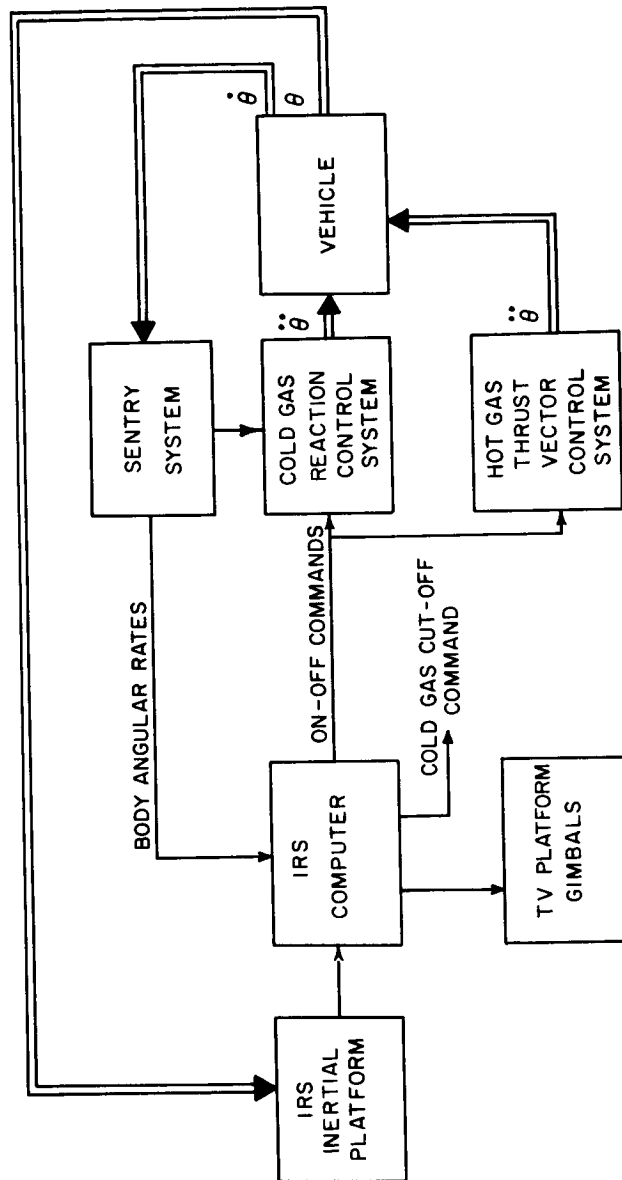
A block diagram of the attitude control system is shown in Figure 36. It differs from the system described for entry from the approach trajectory in that an inertial platform provides the reference for the ACS at separation. The platform also serves as a reference for the television camera and as a backup for wind measurements. A digital computer program uses the inertial platform gimbal angle data to generate commands for the reaction control system. An active ACS (cold gas) is used for orientation to the proper attitude for  $\Delta V$  thrusting. During thrusting an ancillary hot-gas system provides control over the disturbing torques in pitch and yaw. Upon completion of thrusting the cold-gas system provides control during cruise and performs any subsequent reorientations prior to entry into the Martian atmosphere. Failure of the inertial reference system (IRS) could result in erroneous commands to the reaction control system which would cause high pitch or yaw angular rates. Since such a tumbling motion at entry would be highly undesirable, a so-called "Sentry System" (consisting of body-mounted rate gyros) is provided to deactivate the reaction control system if high angular rates are encountered. The pitch and yaw reaction control is deactivated early during entry to allow the vehicle to assume an aerodynamically stable attitude during its trajectory in the atmosphere. Roll control is maintained in a rate-limiting mode to prevent roll resonance, a phenomenon in which aerodynamic torques due to vehicle asymmetries produce a rolling moment and possible high roll rates. The Sentry gyros furnish the control signals to the reaction control roll nozzles during entry in this mode. The following sections will discuss the sensor and electronics subsystem, consisting of the IRS and Sentry gyro systems, the reaction control subsystem, consisting of the cold-gas and hot-gas systems, the packaging arrangement, and the T.V. gimbaled platform.

### 8.2 SENSOR AND ELECTRONICS SUBSYSTEM

The inertial reference system (IRS) provides the required information for controlling the vehicle attitude. An auxiliary rate sensing (Sentry) system is provided to prevent a high tumble rate of the capsule in the event of an ACS failure.

#### 8.2.1 Inertial Reference System

The inertial reference system will establish and maintain an inertial reference by using a four-gimbal inertial platform. The four-gimbal mechanization permits full freedom about the three axes without the possibility of gimbal lock; i.e., that condition in which one of the gimbal



86-1192

Figure 36 ATTITUDE CONTROL SYSTEM BLOCK DIAGRAM

axes becomes aligned parallel to a second gimbal axis, causing the stable element to lose one of its degrees of freedom. To avoid this situation, the outer (redundant) gimbal torquer is controlled by a pickoff on the inner gimbal so as to maintain the remaining two axes mutually orthogonal at all times.

Prior to separation, the platform reference is established with respect to the spacecraft reference by caging the platform gimbals to the platform mounting surface or at a fixed angle with respect to this surface. The platform remains in the caged position until separation. At that time, the platform maintains the established inertial reference with three gyros mounted on the inner gimbal assembly. The readout from the platform is in the form of gimbal angles or signals proportional to some function (sine, cosine, etc.) of the gimbal angles. This information will be provided to the IRS computer for processing. During the attitude control phases of the mission, the computer will provide command signals to the reaction control subsystems to allow vehicle control. All logic functions and computations are performed within the computer to ensure proper operation of the ACS. These include the combination of angular errors and the rates of change of these errors in the proper proportions, and the inclusion of deadzone, hysteresis, and limiting, as required. The platform and computer also provide the command signals to the T.V. camera gimbal system during the parachute descent phase. The computer transforms the gimbal angle information into the proper reference frame for controlling the optical axis of the T.V. cameras along the local vertical. (See paragraph 8.5 and Appendix J).

#### 8.2.1.1 Inertial Reference System Performance

The vehicle stabilization error must be less than 0.5 degree (1-sigma) from separation until after thrusting. This accuracy includes alignment and spacecraft errors. The contribution of the IRS to this error is presented in paragraph 6.7.2. Specifically the IRS has the following error sources:

g-insensitive drift	0.4 deg/hr (1-sigma)
g-sensitive drift	0.3 deg/hr/g (1-sigma)
Readout error	0.1 degree (1-sigma)
Computation error	0.1 degree (1-sigma)

As a result of these sources, the error contribution from the IRS from separation until after thrusting is less than 0.25 degree (1-sigma) since the operating time is less than one-half hour.

The attitude requirements after thrusting are fairly modest and an IRS capable of maintaining attitude accuracy for thrusting can easily meet the entry attitude requirements and camera pointing requirements of 1 degree (1-sigma).

Since the IRS must provide stabilization information to impact, it must be capable of maintaining its inertial attitude reference during the entry phase by isolating the platform from vehicle body motion. As a result, the design selected is capable of maintaining the attitude reference in the presence of body angular rates as large as 1000 deg/sec.

#### 8.2.1.2 Physical Characteristics

The IRS proposed is similar to systems available today for missile and spacecraft applications. An example of an IRS system that meets the performance requirements is the new series of inertial platforms available from General Precision Incorporated (Model PD-205). Its physical characteristics are as follows:

	Weight (pounds)	Volume (cubic inches)	Power (watts)
Inertial platform	10	400	45
Computer	5	160	10

The inertial platform has its gimbal control electronics in micro-electronics form mounted directly on the gimbal assemblies. This minimizes the slip-ring requirements. The gyros are floated single-degree-of-freedom gyros, similar to those employed in various space programs. Those available on the General Precision platform are sub-miniature floated gyros, Model C70-2543-001. The computer is completely solid state and employs integrated circuit design. The only exception to the integrated circuitry is in the power stages which control the reaction control valves. The computer has a memory capability for storing commands issued from the vehicle CC&S. It also contains all the required logic for the attitude control system computations and T.V. platform gimbal angle transformations.

#### 8.2.1.3 Auxiliary Data

Besides the control functions described above, the IRS has the capability of providing accelerometer data. By mounting accelerometers on the inner gimbal, inertially-fixed accelerometer data is directly available from the IRS. The platform provides three-axis accelerometer data by using three single-axis accelerometers. The accelerometers have the capability of measuring accelerations of  $10^{-4}$  g to the

highest anticipated g levels during the entry phase. This accelerometer data can be used to control various mission functions during entry. This accelerometer data will provide a means of determining atmospheric characteristics during entry and the wind characteristics during the parachute phase.

#### 8.2.2 Sentry Gyro System

The rate gyro system consists of three spring-restrained rate gyros. Gyros available for this application include Honeywell's model M-100, Nortronic's model G-R-G-5; General Precision's model C-70-2021. The gyros will provide signals proportional to body angular rates. The accuracy of the information from the gyros is  $\pm 5$  percent and they are capable of sensing rates up to 20 deg/sec.

The information from the body-mounted rate gyro package is provided to the IRS computer. If the body rates exceed 6 deg/sec  $\pm 5$  percent, the IRS computer will issue a disable signal to the CC&S. The CC&S will then disable the ACS reaction control system by actuating a squib valve to shut off the cold-gas supply to the reaction control valves.

The Sentry system will not be armed until the thrusting maneuver is complete. It is unnecessary to arm the Sentry system prior to this event, since any ACS failure prior to thrusting results in a total mission failure. However, after the vehicle has been placed on an impact trajectory, and an ACS failure results, the mission objectives can virtually all be met if the vehicle rates are limited, thus providing acceptable entry conditions. The only loss is the possible lack of communications during the cruise mode. By limiting the tumble rate to 6 deg/sec about all axes, the vehicle will stabilize aerodynamically at entry. The data gathering portions of entry will not be affected by this failure, unless the cause is a failure of the inertial platform. If that occurs, the T.V. camera experiment would be compromised since the camera would not be stabilized.

When a deceleration of 0.1 g is sensed during entry, the pitch and yaw commands from the IRS computer are discontinued and the ACS operates in a roll-rate mode. In this mode, commands are furnished to the cold-gas roll valves to oppose roll angular rates whenever these rates exceed 6 deg/sec.

The Sentry rate gyro package will weigh less than 2 pounds; require 13 watts of power, and occupy a volume of 50 cubic inches.

### 8.3 REACTION CONTROL SUBSYSTEM

#### 8.3.1 Cold-Gas System for Attitude Control

##### 8.3.1.1 Introduction

The reaction control system for use during the orientation, stabilization, and limit cycle modes is a cold-gas system utilizing gaseous nitrogen as the propellant. Torque is produced in couples about all axes, so that no translational velocity is produced. Stability is enhanced by providing an error signal proportional to vehicle attitude and attitude rate in conjunction with on-off control logic.

The total impulse required is 68 lb-sec of which 10 lb-sec is required for roll control during the rocket thrust interval. To provide for redundancy and contingency 248 lb-sec will be stored. The thrust levels per nozzle are 0.5 pound in pitch, yaw, and roll. Control accelerations are then

- a.  $0.40 \text{ deg/sec}^2$  about the roll axis
- b.  $0.62 \text{ deg/sec}^2$  about the pitch and yaw axis

Response of the cold-gas system is characterized by a time delay of 0.020 second and a rise time of 0.005 second.

A total impulse summary is shown in Table XXIV. Detailed analysis and calculation of thrust and impulse requirements is contained in Section 1.0 of Appendix K.

TABLE XXIV

#### TOTAL IMPULSE SUMMARY

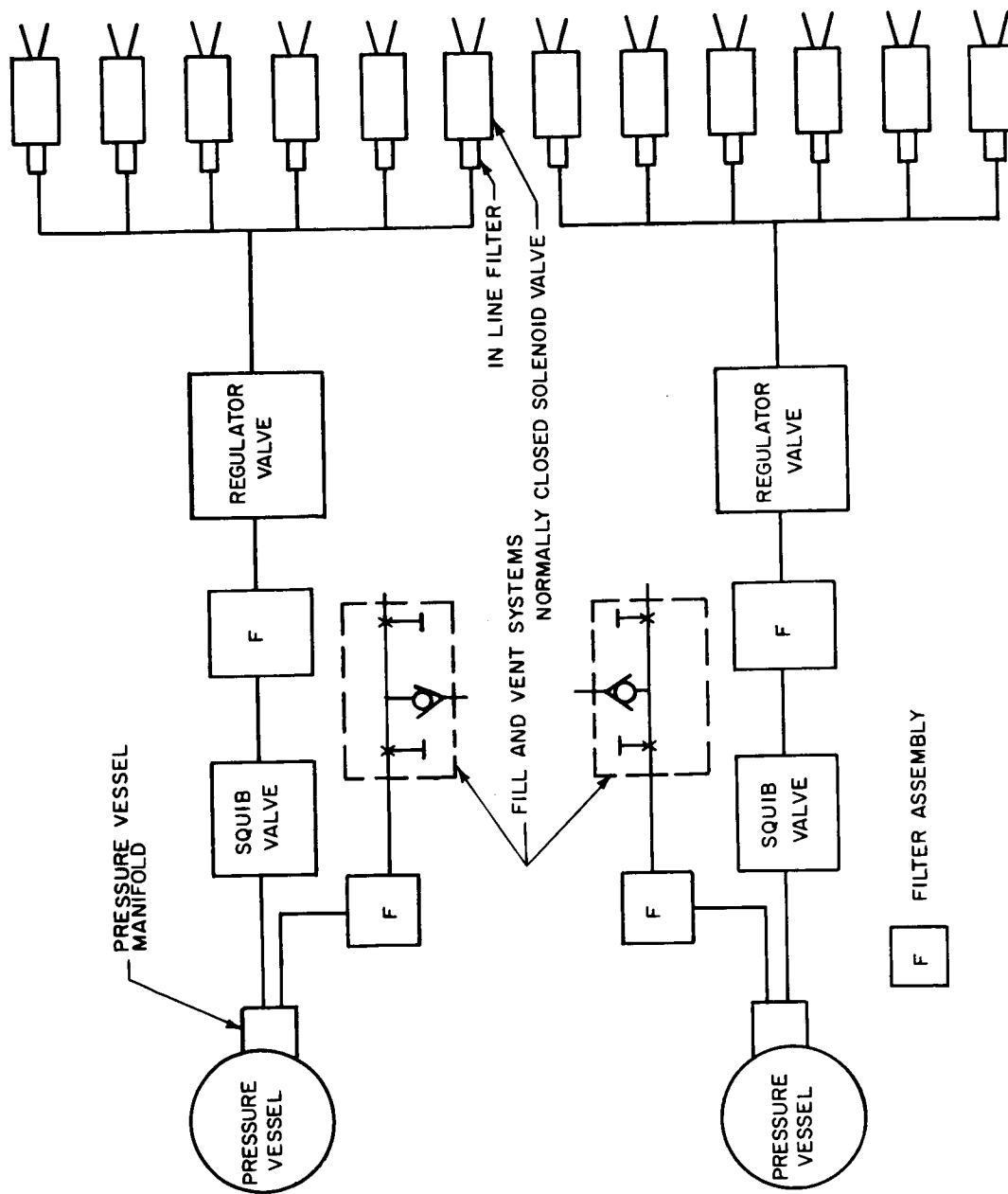
Mode of Operation	Impulse (lb - sec)
Stabilization	34
Orientation	16
Limit Cycle	8
Roll control during thrusting	10
Total	68

#### 8.3.1.2 Description

Figure 37 depicts the schematic layout of the ACS cold-gas reaction control system, which utilizes pressurized nitrogen as the propellant. Two identical independent subsystems are provided to give the component redundancy necessary to maintain the required safety margin against all failure modes. A detailed discussion of failure mode requirements and component sizing is presented in Appendix D. The pressure vessels are charged by means of the fill and vent assembly consisting of a complex of valves, filters, and vessel manifolds. Normally closed squib valves are used to seal the pressure vessels until system activation is desired. The conventional central regulator design concept was adopted for each subsystem to reduce the number of components required and to minimize axis cross coupling. Each regulator supplies constant pressure gas to six normally closed solenoid nozzle valves. The 12 nozzles are located on the vehicle in a manner to provide torque about the principal axes as couples. A torque couple for each axis (plus or minus) is generated by use of one nozzle from each subsystem. Each of the nozzles was designed to a thrust rating of 0.5 pound and has the capability of individually providing the maximum required torque for a given axis. Therefore, control is maintained even with the loss of an entire subsystem. The roll control nozzles are also used during thrusting to counteract any roll disturbance torques generated during this phase.

The system is activated by applying a voltage to the initiator of each squib valve. The desired torques are obtained by opening opposing nozzle valves. The components of the system will be subjected to long periods of exposure to deep space environments. This exposure to high vacuum conditions necessitates the use of metal seats in the valves and regulators. Propellant filtering is therefore a critical requirement since components designed with metal seats are particularly susceptible to leakage. Filtration was designed into the system at all critical locations. A filter has been located immediately downstream of the squib valves to contain any particles released when the valve is initiated. In addition, filters are placed immediately ahead of each nozzle to contain any particles released from the line complexes. Also, special procedures will be used to maintain component cleanliness during assembly. High sterilization temperatures necessitate temperature-stabilized materials for the valve and regulator components to minimize distortion and component failure.

A weight summary for the cold-gas reaction control subsystem is presented in Table XXV.



86-1193

Figure 37 REACTION CONTROL SYSTEM SCHEMATIC LAYOUT

TABLE XXV

## COLD GAS NITROGEN REACTION CONTROL SUBSYSTEM WEIGHT SUMMARY

<u>Item</u>	<u>Nomenclature</u>	<u>Unit Weight (lbs)</u>	<u>No. Required</u>	<u>Total Weight (lbs)</u>
1	Solenoid Nozzle Valve	0.185	12	2.2
2	Pressure Vessel	5.9	2	11.8
3	GN <sub>2</sub> Propellant	5.04	--	5.0
4	Squib Valve	0.37	2	0.7
5	Tubing Complex	2.85	2	5.7
6	Regulator	3.00	2	6.0
7	Filters	0.25	4	1.0
8	Manifolds - Fill and Vent Valve	1.0	2	<u>2.0</u>
Total System Weight =				34.4

8.3.2 Hot Gas System for TVC

## 8.3.2.1 Introduction

A solid propellant hot-gas system is used during thrusting to provide control over the disturbing torques in pitch and yaw. Roll control will be maintained by the cold-gas reaction control nozzles. The total impulse required is 1225 lb-sec, but to provide for redundancy and contingency 3500 lb-sec is stored. The thrust levels are 25 pounds per nozzle in pitch and yaw.\* The system is sized to maintain an accuracy of 0.5 degree (1-sigma) while overcoming the disturbing torque of the main propulsion system. Since the disturbing torque is unidirectional, the system will exhibit essentially soft limit cycle operation; i.e., one pulse per cycle.

\*Details of thrust and impulse calculations are contained in Section 2.0, Appendix K.

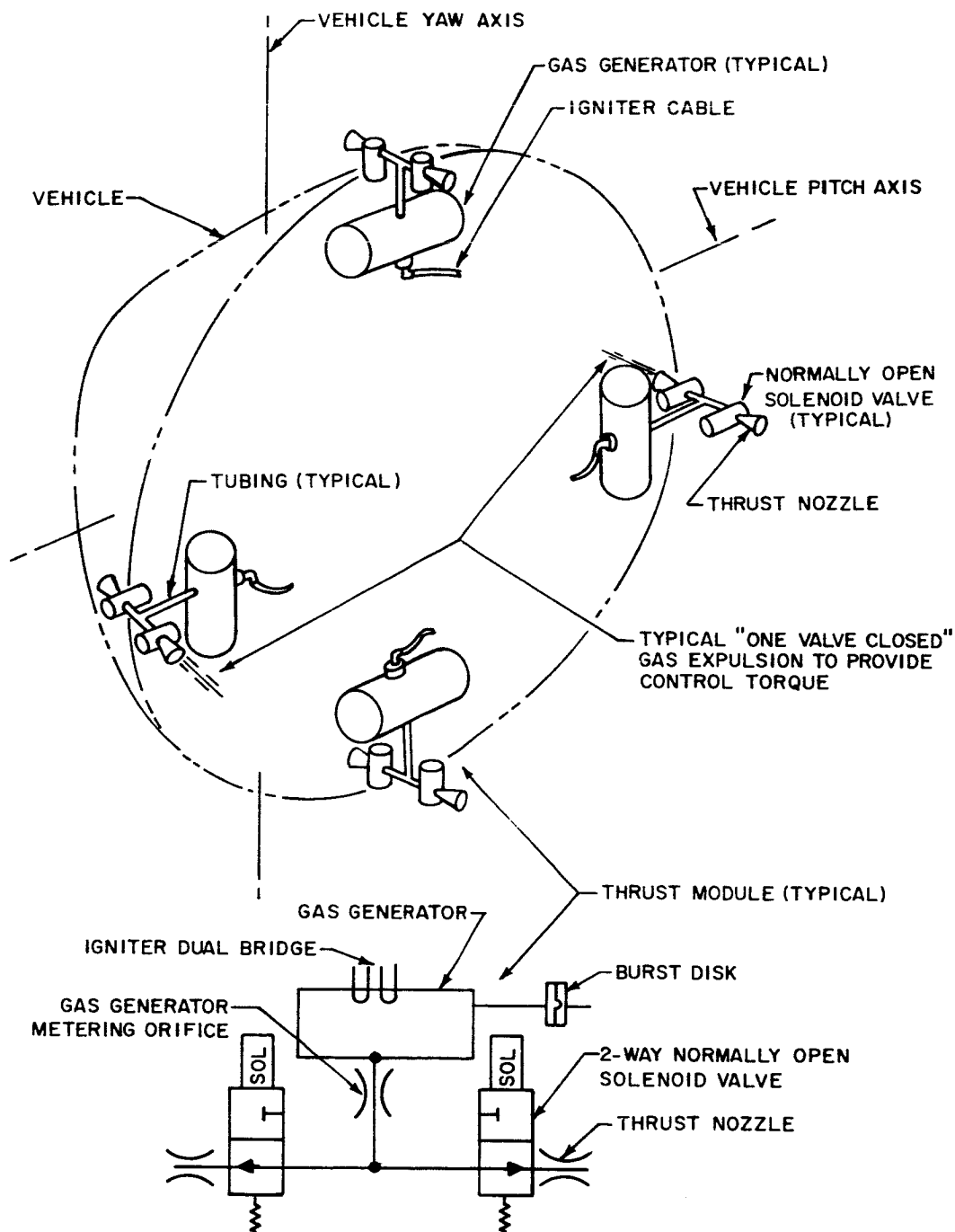
The pitch and yaw nozzles were sized to counteract the disturbing torques due to rocket motor firing arising from three error sources:

- a. Center of gravity location error (0.5 inch, 3-sigma)
- b. Rocket location error (0.06 inch, 3-sigma)
- c. Rocket thrust misalignment (0.5 degree, 3-sigma)

For an engine thrust of 3175 pounds, the required reaction control system torque is 133 ft-lb. The total control thrust from a single nozzle at a 7.3-foot moment arm required to produce this torque is 18 pounds. To improve dynamic response this value is increased by a factor of 1.4 to 25 pounds. A redundant set of nozzles is provided, so that under normal operation more than twice the required torque is available, but if one system fails the other can furnish the necessary control torque.

#### 8.3.2.2 Description

The solid propellant reaction control system selected to counteract disturbance torques during thrusting is depicted schematically in Figure 38. Each of the four solid propellant hot-gas generators supply two normally open solenoid nozzle valves. The gas generator and metering orifice provide a constant subsonic mass flow rate of generator products of combustion to the tubing leading to the solenoid valves. The flow path presented by either one or both of the solenoid valves in the open position is designed to maintain a choked flow condition at the metering orifice. Utilization of an equivalent sharp-edged metering orifice ensures a subsonic flow velocity downstream of the metering orifice. With both valves in the open position, the flow of hot gas is divided equally by the identical flow paths leading to the inlets of converging-diverging expulsion nozzles of the same size. It may be shown that the resultant reaction thrust at each nozzle is proportional to the mass flow rate, the temperature of the stream at the nozzle inlet, the nozzle geometry, and the environmental atmospheric pressure. Since the mass flow rate from the metering orifice is divided equally and equivalent flow paths produce the same gas temperature at each nozzle inlet, the thrusts are each equal to one half the available magnitude of 25 pounds implied by the total generator output flow rate. Location of the nozzles on a common axis of symmetry causes a net thrust cancellation. Closure of one valve causes the entire generator output to be expelled by the remaining



86-1213

Figure 38 SOLID PROPELLANT OPEN CENTERED TVC SYSTEM

open-valve nozzle yielding the total thrust as a net value of 25 pounds.

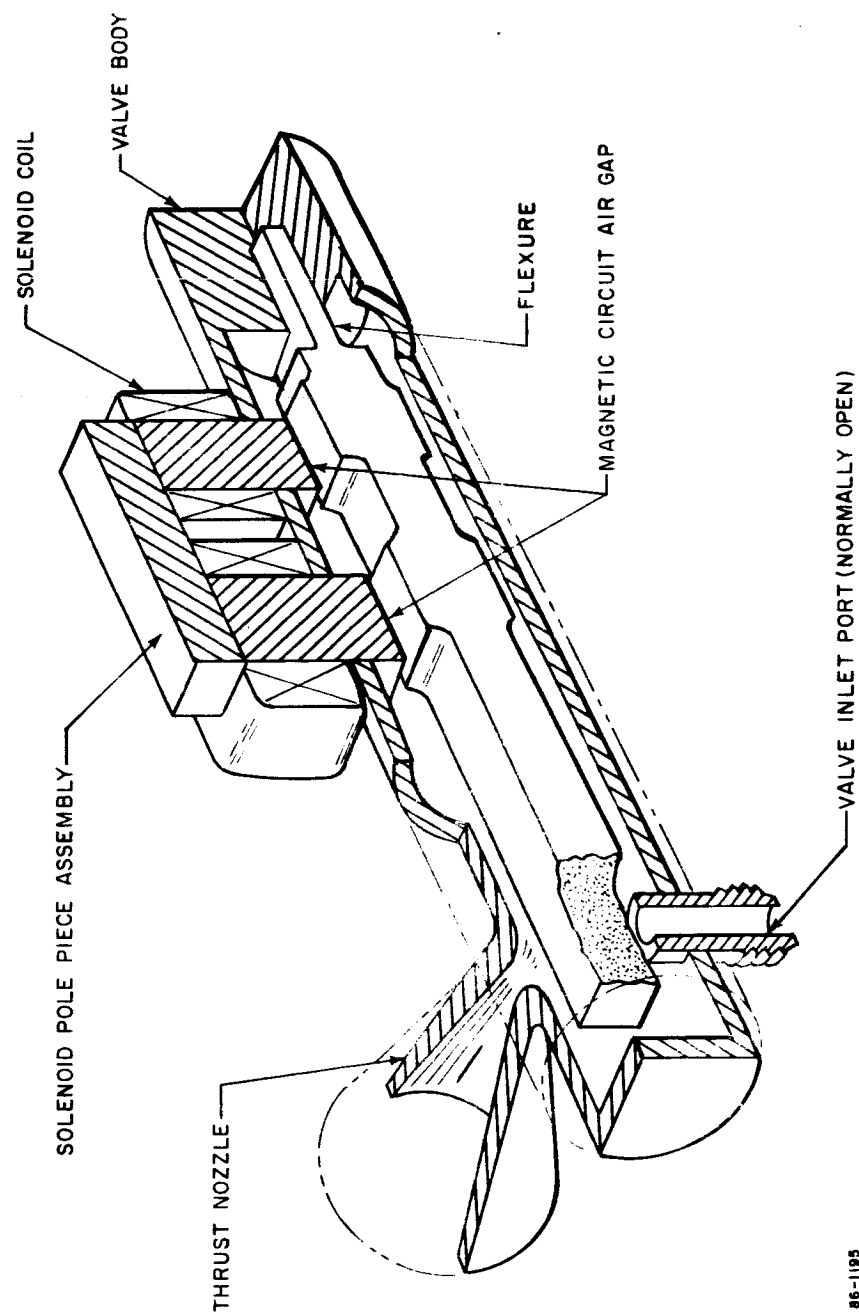
The system is activated by simultaneously applying a voltage to the ignitors of each gas generator to initiate combustion of the solid propellants. In the absence of command signals to the normally open solenoid valves, the hot-gas flow is expelled through both nozzles as described previously to produce zero net torque on the vehicle. Control torques about either the pitch or yaw axes are commanded by closing opposed solenoid valves on two thrust modules as illustrated for example in Figure 38 for the pitch axis.

Utilization of two independent thrust modules (each containing a gas generator and two solenoid nozzle valves) per axis permits the system to operate with the complete loss of one module per axis, as a result of failures. Each module is designed to provide the minimum required torque when acting as the sole control torque source for a given axis. System degradation as a result of failure is thereby limited to loss of a pure control torque couple for an axis if one module for that axis should fail.

The failure modes anticipated as capable of causing loss of a thrust module are described as follows. Each gas generator is protected against bursting when both valves are in the closed position by incorporation of a pressure release burst disk designed to vent the combustion chamber. The loss of pressure will rapidly extinguish the combustion process. If one valve should fail in the closed position (an unlikely failure mode for this type of normally open valve), an unbalanced torque will result which will cause angular motion, which will be detected by the control system sensor (the IRS). The IRS computer will then command the appropriate valves to close to oppose this motion.

This will result in the closure of two valves: one is the second valve on the failed module; the other is the opposing valve on the other module on the same axis as the failed module. Both valves having closed on the failed module, the burst disc will fracture as previously described. In other words, if a valve fails closed, the end result will be loss of that module. If one valve should fail in the open position, the net result will be loss of a pure torque couple for a torque command wherein the failed valve would have normally been commanded to close by the IRS.

The schematic representation of Figure 39 is the two-way solenoid valve proposed for this system design. The valve is a modified



86-1195

Figure 39 TWO-WAY SOLENOID VALVE

Philco Minuteman Roll Control Valve, Part SK 20230. This valve utilizes a flexure mounted flapper which eliminates the need for sliding parts and therefore minimizes dirt sensitivity and failure by sticking.

An aerodynamic cover is placed over the hot-gas modules to reduce drag. To avoid the transfer of large quantities of heat to these enclosed areas, the generators have been internally insulated to limit the case temperature to 100° F. maximum.

Size and weight calculations are presented in detail in Appendix L, Table XXVI represents the solid propellant weight summary.

TABLE XXVI  
SOLID PROPELLANT SYSTEM WEIGHT SUMMARY

<u>Item</u>	<u>Nomenclature</u>	<u>Unit Weight</u>	<u>No. Req'd</u>	<u>Total</u>
1.	Gas Generator	7.77	4	31.1
2.	Solenoid Valve	0.52	8	4.2
3.	Mounting Hardware			
	Tubing and Fittings			<u>5.0</u>
TOTAL SYSTEM WEIGHT				40.3

#### 8.4 PACKAGING

Packaging of both the hot-and cold-gas reaction control system is straightforward and does not present critical design problems. The cold-gas thrust nozzles are assembled directly to the solenoid valves and these assemblies are mounted on the circumference of the entry shell. The remaining components are connected by a tube complex which allows considerable component location flexibility on the vehicle.

The hot-gas thrust nozzles are also assembled directly to the solenoid valves and these assemblies are closely coupled to the gas generators. The generators and nozzle valves are separately mounted on the circumference of the entry shell and connected by short lengths of tubing. Critical mounting problems are not anticipated since low component temperatures are maintained (100-200° F).

Consideration was given to the use of two solid propellant generators in place of the four generators finally selected. The two-generator design concept requires a complex of hot tubes routed through the vehicle. The differential expansion and distortion due to these hot lines cause major vehicle design problems. The design concept utilizing four solid propellant generators closely coupled to the nozzles minimizes the expansion and distortion problem and therefore, was selected as the reference design.

Although the physical placement of the IRS on the vehicle is not critical, it is desirable for it to be placed reasonably near the mass center. Optical access for alignment during assembly is required. It is also necessary that the mounting location have sufficient structural rigidity so that the alignment will be maintained within specification values during sterilization, launch, cruise, de-orbit, and entry phases of the mission. The critical components (gyros and accelerometers) are temperature controlled and all electronic components are potted to provide protection from adverse environments during launch, de-orbit, and entry.

#### 8.5 TV STABLE PLATFORM

Some method of controlling the TV camera is required to reduce the effects of the capsule parachute dynamics. With the method selected, the TV cameras are mounted on a two-axis gimballed platform controlled by the inertial reference system. This approach is superior to the alternative concept of controlling the TV camera shutter when the look angle with respect to the vertical, and swing rates, are within acceptable limits.

With the alternative approach, the performance of the TV system is critically dependent on the magnitude of the wind gusts and the parachute and attachment harness design. When capsule motion about all three axes is considered, it is unlikely that all three body rates would ever be simultaneously less than the required 3 deg/sec. Thus shutter control technique results in marginal performance at best.

As previously mentioned, the reference design is far less sensitive to capsule parachute dynamics, and permits higher resolution pictures to be taken even in the presence of severe wind gusts.

Figure 40 shows a pictorial of the three boresighted cameras mounted on a 2-degree-of-freedom gimbal arrangement which allows motion in the pitch and yaw directions. The three cameras are contained in a cylindrical environmental canister for thermal control. A thin optical quartz window at one end provides camera viewing. This canister is mounted on the inner gimbal inside the yoke of the outer gimbal. Electrical connection between the cameras and the TV electronics, housed in the aft end of the outer cylindrical structure, is provided by circular loops around each of the gimbals. This arrangement

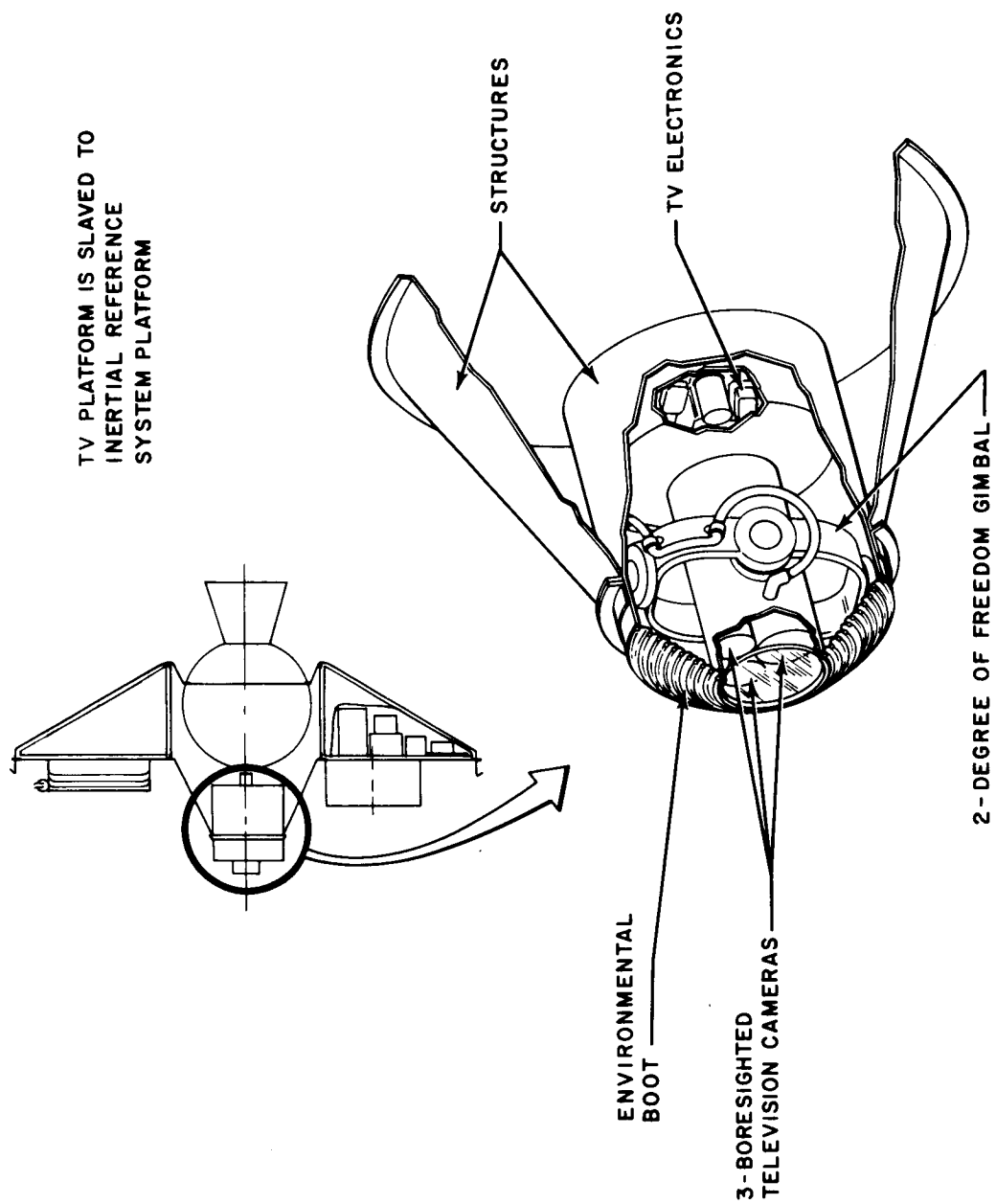


Figure 40 TV CAMERA PLATFORM

minimizes cable bending and allows maximum movement of the camera. Each gimbal is actuated by electrical torque motors which are commanded by the IRS computer.

The gimbals are of conventional design similar to that used in inertial reference platforms, and are made of magnesium castings. They are supported by Barden bearings (A500 and SFR Series) which are specifically treated for use in a space environment. Vernitron VCX-20 Synchros are used to readout the gimbal angles and inland direct drive torque motors (T-2157 and T-2804) are used for the gimbal drives. The power required is under 10 watts and the total gimbal assembly weighs under 10 pounds, excluding the camera system.

The function of the gimbal system is to align the optical axis of the TV camera with the local vertical; rotation about the line of sight is permitted. This makes possible the use of a two-gimbal system for the camera. The transformation required to convert the IRS platform gimbal angles to the two gimbal angles required to control the TV camera is performed in the IRS computer. The required equations are given in Appendix J where it is also shown that two gimbals for the camera are sufficient.

The camera pointing system must maintain the line of sight within 1 degree (1-sigma) of the vertical for satisfactory camera performance. It must also maintain the angular rates of the camera axis below 0.01 deg/sec. Although the IRS platform has full freedom, the camera platform will have limited freedom ( $\pm 45$  degrees on each axis). This simply means that the cameras may be displaced with respect to local vertical (greater than 1 degree) if the capsule is displaced (by a wind gust) more than 45 degrees from the local vertical. However, the IRS will maintain the correct reference and realign the cameras once the swing angle decreases.

## 9.0 PROPULSION SYSTEM

### 9.1 INTRODUCTION AND SUMMARY

#### 9.1.1 Scope

This section discusses the design of the propulsion system for the Flight Capsule. Both the entry from the approach trajectory and the entry from orbit mission concepts require a propulsion system to impart the necessary velocity change to the capsule to place it on an impact trajectory.

The impulse required is different for each mission but the basic propulsion system performance and design requirements are the same. Using these requirements as a baseline, an investigation was conducted to determine the type propulsion system best suited for the application. As part of this investigation, a tradeoff between solid and liquid propellant systems was conducted.

The results of this effort led to the selection of solid propellant systems for both mission applications with the systems differing in particular design characteristics. The propulsion system selection for each mission approach is discussed below in three parts: (1) performance and design requirements, (2) choice of solid versus liquid systems, (3) description of the reference system design.

#### 9.1.2 Primary Performance and Design Constraints

Even though the two propulsion systems require different total impulse levels, the primary performance and design constraints are the same. The requirement that had the largest impact on design was that only one firing cycle was necessary, and in conjunction with the one firing cycle was the requirement for a system of high reliability. This latter requirement was further amplified by the program requirement that only those subsystems should be considered for use in the flight capsule that would be consistent with the state-of-the-art existing in September, 1966.

The primary design constraints are imposed by sterilization and long term storage in space. Sterilization imposes new requirements on the design and assembly concepts now in use for propulsion systems, and material evaluation will be required to determine compatibility with sterilization environments. Space storability is not new in itself but the length of time (one year) exceeds that presently required of developed propulsion systems.

### 9.1.3 Design Summary

#### 9.1.3.1 Entry From the Approach Trajectory Design

The propulsion subsystem consists of a solid propellant rocket motor, which is fired to cause the capsule to impact the planet. The rocket firing is controlled by the capsule CC&S, which stores the start time and duration commands, updated as needed, through the DSIF-Flight Spacecraft-Flight Capsule communication link. After the attitude control system has positioned the capsule in the correct firing attitude, the rocket is ignited, at the prescribed time by an electrical signal originating in the Flight Capsule CC&S. Thrust termination is controlled by the flight capsule accelerometers, which measure the  $\Delta V$  attained, and is backed up by flight capsule CC&S with an electrical signal, when the commanded burning time has been realized. Thrust termination is followed by the jettisoning of the expended motor.

A solid propellant rocket motor was selected over a liquid propellant system because of higher reliability, easier sterilizability, easier packaging, better space storability, no requirement for restart, and cost.

The rocket motor is a modified Titan vernier motor (TE-M-345). The primary modification consists of replacing the present propellant with a sterilizable propellant (TP-H-3105). The motor has a total impulse capability of any value between 255 lb-sec minimum, and 16,320 lb-sec maximum, due to its thrust termination feature. The required total impulse of 4850 lb-sec nominal results in a  $\Delta V$  of 100 ft/sec, while the total impulse available results in a  $\Delta V$  capability of 290 ft/sec. The rocket motor operates at an average thrust level of 808 pounds with a specific impulse of 255 seconds.

The Titan vernier motor is spherical in shape, 13.5 inches in diameter, and 18.6 inches long, having a TH-1050 stainless steel case. The exhaust nozzle is partially submerged with an area ratio of 18.7, and is made of vitreous silica phenolic. The nozzle is retained in the motor case by a split flange, which is held together by two explosive bolts so that on receipt of an electrical signal the bolts are released, the flange separates, and the nozzle is blown free of the case resulting in a sudden drop in chamber pressure, which terminates thrust. The motor is mounted in the flight capsule using the mounting flanges presently existing on the Titan vernier motor. The total loaded weight of the propulsion subsystem is 81.0 pounds, which is a propellant mass ratio of .788.

#### 9.1.3.2 Entry From Orbit Design

The propulsion subsystem consists of a solid propellant rocket motor, which is fired to alter the capsule orbit such that the capsule impacts the planet. The rocket firing is controlled by the flight capsule CC&S, which stores the start time, and is updated as needed through the DSIF-to-Planetary Vehicle-to-Flight Capsule communication link. After the attitude control system has positioned the capsule in the correct firing attitude, the rocket is ignited at the prescribed time, by an electrical signal originated in the flight capsule CC&S. The rocket burns for 33.5 seconds to exhaust the total propellant loading.

A solid propellant rocket motor was selected over a liquid propellant system because of reliability, sterilizability, packaging, space storability, no restart requirement, and cost.

The rocket motor consists of a new design and propellant, but is similar to the Surveyor main retrorocket in design concept. The propellant (TP-H-3105) is sterilizable, and the motor total impulse is 101,600 lb-sec. This total impulse is that required to give the Separated Vehicle a  $\Delta V$  capability of 1400 ft/sec. The rocket motor operates at an average thrust level of 3000 pounds with a specific impulse of 254 sec.

This motor is spherical in shape, 22.3 inches in diameter, and 24 inches long, having a 6Al 4V titanium case. The exhaust nozzle is completely submerged with an area ratio of 18.7, and is made of vitreous silica phenolic. The total loaded weight is 432 pounds, which is a propellant mass fraction of 0.925.

An exhaust nozzle extension has been added to the basic motor to facilitate exhaust gas ducting away from the structure and other equipment. The extension is made of dielectric materials to prevent antenna attenuation.

### 9.2 PROBE, ENTRY FROM THE APPROACH TRAJECTORY

#### 9.2.1 Performance Requirements

The primary objective of the propulsion system is to alter the capsule approach trajectory to impact the planet.

In meeting this primary objective there are three system constraints that must be satisfied. The first is to have the capsule enter with an angle of -30 to -50 degrees. The second is to accelerate the capsule to provide sufficient lead time for communication. The third constraint is to accomplish separation at a specified range and time from encounter.

To meet the above system objectives and to follow a design philosophy of simplicity and conservatism, performance requirements were established for the propulsion subsystem. The capsule requires a  $\Delta V$  of 100 ft/sec which in turn requires a total impulse of 4850 lb-sec for the established capsule weight. This total impulse is to be accomplished by a single firing (no restart) and the system is to have a reliability goal of 0.990. The specific impulse requirement was established at a minimum of 250 seconds which is very satisfactory and results in a low propellant weight, since the total impulse requirement is low. The propellant weight reduction due to a higher specific impulse would not be a significant factor in the vehicle total weight.

The only requirement on thrust level is that it does not impart an axial acceleration to the capsule of more than 3 g.

The operational temperature requirement is a range of 20°F to 130°F and this somewhat narrow range was due to the fact that the propulsion system is within the Flight Capsule Sterilization Canister which in turn is shielded by the flight spacecraft during transit to the planet. Also, the motor is to be fired within 15 minutes after the capsule has completed the separation sequence.

#### 9.2.2 Design Requirements and Constraints

Sterilization is the one constraint that is new to the propulsion industry; therefore it has the largest impact on the design, and applies to the propulsion system in its entirety.

Variable total impulse capability was established as a requirement because the flight capsule mission profile has a fixed separation range from the planet. Using the mission profile established, the periapsis altitude of the planetary vehicle varies with respect to the errors resulting from the first and second midcourse corrections made by the planetary vehicle. Because the periapsis altitude may vary, the necessary  $\Delta V$  required to impact the planet must vary accordingly. In conjunction with the variable total impulse requirement is the additional requirement for a highly repeatable shutdown impulse. The requirement is 1 percent (1-sigma).

The propulsion system installation envelope constraints are a cylinder 14 inches in diameter by 19 inches long. Also, there is the requirement that the engine be jettisoned after firing. The jettisoning system is to be part of the flight capsule and not part of the propulsion subsystem.

The propellant mass ratio is not critical to the design but it should be as large as possible, keeping within the state-of-the-art or employing an existing system.

### 9.2.3 Solid versus Liquid Propellant Engines

The tradeoff study conducted was approached in a somewhat different manner than most such studies. Because of the desire for a propulsion subsystem that employed a simple design concept, was conservative from a performance viewpoint as to the state-of-the-art, and did not require restart, a solid propellant engine was chosen as the baseline design early in the flight capsule design study. Therefore, the tradeoff study was conducted to determine if a liquid propellant engine would result in a better choice for the application. The statement can be made almost categorically that if only a single firing is required, a solid propellant engine should be used for the propulsion system. It is readily apparent that the solid propellant system is the simplest and its inherent reliability is much higher than for liquid systems. For these reasons there has been widespread use of solids in space applications. The various propulsion subsystem requirements are discussed in the subsequent paragraphs to evaluate the effect they have on solid and liquid propellant systems, and the system which best fulfills each requirement is noted.

#### 9.2.3.1 Sterilization

Because the sterilization requirement is the one requirement that is new to propulsion system design and has to be met for the Mars probe program it was looked at first to determine its effect on the choice of a propulsion system. In the area of solid propellants, Thiokol Chemical Corporation has been working with propellants able to withstand the sterilization requirements. This work has been done over a period of more than 2 years and has resulted in a propellant (TP-H-3105) compatible with the required sterilization cycle and procedures. Work is continuing on this propellant under a contract with JPL; therefore, a sterilizable solid propellant does exist and meets the program requirement that it be developed by September, 1966.

Two liquid propellant systems were studied; (1) hydrazine as a mono-propellant and (2) hydrazine derivatives as the fuel and nitrogen tetroxide and its derivatives as the oxidizer for bi-propellant systems. It was readily apparent from the outset that very little work had been done in determining the compatibility of the above propellants with the sterilization environment and procedures. Some testing has been done with hydrazine and hydrazine derivatives and blends at the sterilization temperatures and the results have been unsatisfactory.

Decomposition of the hydrazine has been noted along with excessive vapor pressures. Decomposition of hydrazine has resulted in an explosive condition in many past instances so this condition is very unsatisfactory. The oxidizer propellants have a higher vapor pressure

at ambient conditions than fuels, thus sterilization would result in excessive propellant tank pressures. The two problem areas noted might be overcome by sterilizing the propellants before putting them aboard the flight capsule after the flight capsule has gone through its sterilization cycle, but this approach is not currently acceptable sterilization practice. Therefore, the propellant investigation with respect to sterilization led to the conclusion that liquid propellant systems are not sufficiently developed to meet this requirement. Even though liquid propellant systems do not meet the state-of-the-art requirement, an extensive effort could be put forth to accelerate their development to the required status if the advantage of liquid systems warranted such an effort. Therefore, other system requirements were evaluated to determine if other advantages of liquid systems outweigh the sterilization disadvantages.

#### 9.2.3.2 Variable Total Impulse

The requirement of a variable total impulse is one that suggests liquid systems, but there are also existing solid propellant rocket motors with thrust termination capability. Because there is no re-start requirement, the liquid system does not offer any advantage over the solid propellant system. The solid propellant system shutdown impulse is well within the flight capsule system requirements and with thrust termination it actually improves. From a variable impulse and shutdown impulse repeatability viewpoint, the solid propellant system is equal to the liquid system.

#### 9.2.3.3

Because the sterilizable propellant used in the solid system has a lower specific impulse than that obtained by liquid systems, the effect of specific impulse was studied. A specific impulse of 255 seconds\* is attainable with a nozzle area ratio of approximately 20 using the TP-H-3105 sterilizable propellant. With the same area ratio and an ablative chamber and exhaust nozzle (required because of packaging) and employing the bi-propellant combinations in use by Gemini or Apollo, a specific impulse of 280 seconds is attainable for low thrust engines. To meet the total impulse requirement approximately 20 pounds of propellant is required and the difference in specific impulse would result in a saving of 9 percent or about 2 pounds of propellant. This weight saving in propellant is not sufficient to compensate for the additional hardware weight of the liquid system tankage. Here again a liquid system does not offer sufficient advantage over the solid propellant system selected.

---

\* All values of specific impulse are for in vacuum performance.

#### 9.2.3.4 Thrust

There was no specific thrust requirement except that it had to be such that 3-g axial acceleration was not exceeded. In achieving a given thrust level, a solid propellant permits more compact packaging, since the size of the exhaust nozzle is dependent upon chamber pressure; the higher the chamber pressure the smaller the exhaust nozzle. The liquid systems that could be used for this application have chamber pressures on the order of 100 - 200 lb/in<sup>2</sup> while the solid systems of like size range around 400 to 600 lb/in<sup>2</sup>. So the liquid system is at a disadvantage.

#### 9.2.3.5 Space Storability

The 1-year space storability requirement is another one like sterilization that is relatively new to the propulsion industry. The requirement for space storage alone is not new, but 1-year storage is longer than previous requirements. No real experience exists with either the solid or liquid systems at this time, but from some space storage tests done on solid propellants of the same basic family as TP-H-3105, no problems are anticipated. Also, the solid propellant TP-H-3105 has shown satisfactory operating performance at -40°F. The liquid propellants considered for this application freeze at temperatures around 20°F and have frozen in some recent space flights. The oxidizer can have its freezing temperature lowered by adding mixed oxides of nitrogen, but this in turn raises the vapor pressure which creates a greater problem during sterilization. From the work done to date the solid propellant system has the advantage from a space storability standpoint.

#### 9.2.3.6 Development Status

A solid propellant motor, Titan vernier, exists. It is spherical in shape and meets the packaging requirement. It has been developed, and requires only a change in propellant to the sterilizable propellant which is also developed. Because of the existence of an available solid motor, a liquid propulsion system offers no advantage. Minimum cost for development and deliverable units is always a program requirement, and in both cases the solid propellant system will have the lower cost. This is apparent from the preceding discussion.

#### 9.2.3.7 Summary

The solid versus liquid propellant engine study concluded that the solid propellant motor selected for the baseline system was the best choice and that there were not sufficient advantages in a liquid system to justify an extensive development program to obtain liquid systems compatible with the sterilization requirement.

#### 9.2.4 Reference System Design

The propulsion subsystem selected consists of a solid propellant rocket motor which is fired to alter the capsule approach trajectory to impact the planet. The rocket firing is controlled by the flight capsule CC&S which stores the start time and duration commands, updated as needed through the DSIF-to-Planetary Vehicle-to-Flight Capsule communication link. After the attitude control system has positioned the separated vehicle in the correct firing attitude, the rocket is ignited at the prescribed time, by an electrical signal originated in the flight capsule CC&S. Thrust termination is controlled by the flight capsule accelerometers which measure the  $\Delta V$  attained and backed up by flight capsule CC&S with an electrical signal when the maximum burning time has been reached. The thrust termination is followed by the jettisoning of the expended motor.

The rocket motor is a modified Titan vernier motor (T-M-345). The primary modification consists of replacing the present propellant with a sterilizable propellant (TP-H-3105). The motor is spherical in shape, 13.5 inches in diameter and 18.6 inches long having a TH-1050 stainless steel case. The exhaust nozzle is partially submerged with an area ratio of 18.7 and is made of vitreous silica phenolic. The nozzle is retained in the motor case by a split flange which is held together by two explosive bolts so that on receipt of an electrical signal the bolts are released, then the flange separates and the nozzle is blown free of the case, resulting in a sudden drop in chamber pressure which terminates thrust.

The motor is mounted in the flight capsule using mounting flanges presently existing on the Titan vernier motor. The total loaded weight of the propulsion subsystem is 81.0 pounds which is a propellant mass fraction of 0.788.

To contribute to the reliability design goal of 0.990 the dual ignitors of the Titan motor are retained; each has a minimum firing current of 5 amperes.

The Titan vernier motor using sterilizable propellant has a total impulse capability of any value between 255 lb-sec minimum and 16,320 lb-sec maximum due to its thrust termination feature. The required total impulse of 4850 lb-sec nominal results in a  $\Delta V$  of 100 ft/sec while the total impulse available results in a  $\Delta V$  capability of 290 ft/sec for the Separated Vehicle. The total impulse capability may be reduced by off-loading propellant which would lower the rocket motor total weight by approximately 30 pounds. The resulting  $\Delta V$  capability would be 145 ft/sec.

In addition to the variable total impulse characteristic it was necessary to have a highly repeatable shutdown impulse. The Titan motor has a total

impulse repeatability for any one time period of less than 1 percent (3-sigma). When thrust termination is used the repeatability is improved because of the faster shutdown. A large pressure spike for a fraction of a second (40 milliseconds) accompanies the shutdown, but it will dissipate through the mounting joint sufficiently due to joint design so there will be no detrimental effect on the vehicle or subsystems.

The propellant specific impulse is 255 seconds which does not impose any large restriction on the performance because of the small propellant quantities.

The requirement that only gaseous exhaust products shall result from the combustion process prevents at this time improving the specific impulse by using metal additives to the propellant.

The average thrust level is 808 pounds and offers no problems for the capsule due to acceleration loads because the thrust to weight ratio is less than  $1/2g$ .

The characteristics of the propulsion system are summarized in Table XXVII.

### 9.3 PROBE, ENTRY FROM ORBIT

#### 9.3.1 Performance Requirements

The primary objective of the propulsion subsystem is to alter the Separated Vehicle orbit such that the vehicle impacts the planet. To accomplish this objective four types of mission approaches were studied.

##### 9.3.1.1 Minimum $\Delta V$

The first mission approach studied was to use the minimum  $\Delta V$  to de-orbit the capsule for the orbit and entry conditions required. The result of this study indicated that a different motor total impulse would be required for each orbit selected. The total impulse requirements were sufficient to require a different size motor, thus making it necessary to select the mission orbit very early in the program or develop and qualify a series of different size motors.

##### 9.3.1.2 Minimum Entry-Angle Dispersion

The second approach studied was to select deorbit conditions and de-orbit velocity which resulted in minimum entry-angle dispersion. The results were very similar to those in the first case studied in that a different motor total impulse would be required for each orbit selected. Therefore, this approach was not pursued further.

TABLE XXVII

SUMMARY OF PROPULSION SYSTEM CHARACTERISTICS  
(Entry from the approach trajectory)

. Total Impulse	16,320 lb-sec $\pm$ 1% (3- $\sigma$ )
. Specific Impulse	255 Seconds (vacuum)
. Thrust	808 pounds (average)
. Temperature Limits	
Operation	20 to 130° F
Storage	10 to 130° F
. Envelope	
Spherical	13.5 inch diameter by 18.6 inches long
. Weight	
Loaded	81 pounds
Propellant	63.9 pounds
. Mass Ratio $W_p/W_t$	0.788
. Burn Time	Variable
. Thrust Termination	On signal/blowoff nozzle
. Exhaust Nozzle Area Ratio	18.7
. Propellant Type	Solid-TP-H-3105
. Engine Assembly	Sterilizable

#### 9.3.1.3 Variable Total Impulse

The third approach studied was to consider using a rocket motor with variable total impulse capability to accomplish the requirement for different  $\Delta V$ 's for each orbit. It was determined that the range of impulses was so large that a motor designed for the maximum de-orbit velocity would have an excessive burn out weight if the minimum  $\Delta V$  was used. The leftover weight is not detrimental to the propulsion system, but, if it could not be jettisoned, the additional weight would have a detrimental effect on the vehicle  $m/C_D A$  for entry. It was not desired to impose the restriction that the propulsion subsystem must be jettisoned, therefore, it was decided that the variable impulse approach would not be pursued.

#### 9.3.1.4 Fixed Impulse

The fourth approach was to determine the feasibility of employing a fixed impulse de-orbit engine and to investigate the range of orbital altitudes over which the entry angle and communication geometry constraints could be satisfied with this concept. This analysis indicated that for orbits with periapsis altitudes of 700 km, 1000 km, and 1500 km and apoapsis altitudes of 4000 km, 10,000 km, and 20,000 km, the de-orbit velocity requirements are between 1300 ft/sec and 1500 ft/sec for de-orbit true anomalies in the vicinity of 260 degrees. Therefore, a fixed  $\Delta V$  of 1400 ft/sec can be employed to satisfy the flight capsule de-orbit requirements for all orbits considered by selecting the proper de-orbit true anomaly for the particular orbital altitudes. Further details on this study are contained in Section 8.0, Volume V, Book 1.

#### 9.3.1.5 Summary

To meet the above system objectives and to follow a design philosophy of simplicity and conservatism, performance requirements were established for the propulsion subsystem. The Separated Vehicle requires a  $\Delta V$  of 1400 ft/sec which in turn requires a total impulse of 101,600 lb-sec  $\pm$  1 percent (1-sigma) for the established vehicle weight. This total impulse is to be accomplished by a single firing and the system is to have a reliability goal of 0.990. The specific impulse requirement was established at a minimum of 250 seconds which is very reasonable considering the fact that the exhaust products are to be gaseous only, thus no metal additives may be employed in solid propellant motors to improve specific impulse.

A thrust level of 3,000 pounds nominal was established as a maximum. This was done to reduce the thrust level requirement on the attitude control jets.

The operational temperature requirement is a range of -40 to 175°F and appears to be reasonable from work that has been done with solid propellant systems.

#### 9.3.2 Design Requirements and Constraints

Sterilization is a new constraint for the propulsion industry; therefore, has the largest impact on the design, and applies to the propulsion system in its entirety.

The propulsion system installation envelope constraints are a cylinder 24 inches in diameter and 25 inches long. There is no requirement for jettisoning the system when the firing cycle is completed. As part of the packaging concept the thrust vector misalignment shall have a 3-sigma variation of less than a 0.5-degree cone angle.

The propellant mass ratio is to be greater than 0.90 because 400 pounds of propellant is required to give the necessary total impulse. This propellant weight is such that mass fraction contributes sufficiently to weight saving.

#### 9.3.3 Solid versus Liquid Propellant Engines

The requirements are not significantly different from those in paragraph 9.2, therefore, the discussion in paragraph 9.2.3 applies except in the case of the effect of specific impulse difference. A specific impulse of 280 seconds was used for the previous comparison. An engine has been developed that will give a 310-second specific impulse using the noted liquid propellants, and this impulse would save about 65 pounds in propellant weight, but the thrust chamber weight alone, not considering tankage, would consume the 65 pounds saved. Also, because of the lower chamber pressure than that possible with a solid propellant engine the allowable envelope would be exceeded. The tradeoff study done in paragraph 9.2.3 was applied to the propulsion system selection conducted herein, and the results were the same. A solid propellant engine was selected for the application.

#### 9.3.4 Reference System Design

The propulsion subsystem selected consists of a solid propellant rocket motor which is fired to alter the capsule trajectory, such that the vehicle impacts the planet. The rocket firing is controlled by the flight capsule CC&S which stores the start time and is updated as needed through the DSIF-to-Planetary Vehicle-to-Flight Capsule communication link. After the attitude control system has positioned the capsule in the correct firing attitude the rocket is ignited at the prescribed time, by an electrical

signal originated in the flight capsule CC&S. The rocket burns for 33.5 seconds to exhaust the total propellant loading.

The rocket motor consists of a new design and propellant but is similar to the Surveyor main retrorocket in design concept and the new propellant (TP-H-3105) is sterilizable. The motor is spherical in shape 22.3 inches in diameter and 24 inches long having 6 Al-4V titanium case. The exhaust nozzle is completely submerged with an area ratio of 18.7 and is made of vitreous silica phenolic. An exhaust nozzle extension has been mounted to the basic motor to facilitate exhaust gas ducting away from the structure and other equipments. The extension is made of dielectric materials to prevent antenna attenuation. This extension is 11 inches long, mounted to the motor nozzle exit with machine screws into heli-coil inserts in such a way that the established nozzle contour is continued. The extension structure is fiberglass coated with Teflon on both the interior and exterior surfaces. The rocket motor without nozzle extension weighs 432 pounds loaded, which is a propellant mass fraction of 0.925 and the nozzle extension adds 9 pounds to the total weight.

The motor is mounted in the flight capsule by bolting its flange to a matching one on the flight capsule structure. The motor is buried within the flight capsule structure and is not jettisoned after firing. The buried installation was employed instead of jettisoning because if the motor failed to jettison it would remain in the antenna field thus disrupting communication.

To contribute to the reliability design goal of .990, dual ignitors are used, and each has a minimum firing current of 4 amperes. The rocket has a total impulse of 101,600 lb-sec which is that required to give the capsule a  $\Delta V$  capability of 1400 ft-sec. This total impulse is repeatable within  $\pm 1$  percent (3-sigma) which is well within the trajectory design tolerance of 1 percent (1-sigma).

The propellant specific impulse is 254 seconds which does not impose any large restriction on the subsystem or capsule performance. The requirement that only gaseous exhaust products shall result from the combustion process and the fact that the propellant is to be sterilizable prevents at this time improving the specific impulse by using metal additives to the propellant. The above specific impulse does not take into consideration the performance increase obtainable from the nozzle extension because of the greater area ratio, 53 instead of 18.7. This would increase the effective specific impulse by approximately 7 percent an equivalent increase in specific impulse of 18 units.

The average thrust level is 3,000 pounds and offers no problems for the capsule due to acceleration loads because the thrust to weight ratio is approximately 1 g. The thrust level was designed to be as low as possible

to reduce thrust vector control thrust levels. The 3,000-pound level was the lowest that could be obtained for the type and quantity of propellant being used because of propellant burning rate.

The characteristics of the propulsion system are summarized in Table XXVIII.

TABLE XXVIII

SUMMARY OF PROPULSION SYSTEM CHARACTERISTICS

(Entry from orbit)

. Total Impulse	101,600 lb-sec $\pm 1\%$ (3- $\sigma$ )
. Specific Impulse	254 seconds (vacuum)
. Thrust	3000 pounds (Nominal)
. Temperature Limits	
Operation/Storage	-40 to + 175° F
. Envelope	
Spherical	22.3 inch diameter by 24 inches long
. Weight	
Loaded	432 pounds
Propellant	400 pounds
Mass Ratio $W_p/W_t$	0.925
Burn Time	33.5 seconds
Exhaust Nozzle Area Ratio	18.7
Propellant Type	Solid - TP-H-3105
Engine Assembly	Sterilizable

## APPENDIX A

### SEPARATION DYNAMICS

The situation analyzed herein is that of a body being pushed off from a much more massive body by a set of N springs arranged in a circle about the nominal center-of-mass of the body (see Figure A-1). It is assumed that the resultant of the spring forces passes through a point a distance  $f$  from the center of the spring circle, due to errors in strength and positioning of the springs. It is also assumed that the actual center-of-mass of the body is displaced by a distance  $e$  from the center of the spring circle. These two errors give a total offset of the spring force from the center-of-mass of the distance  $d$  shown on Figure A-1.

The separation force is assumed to be impulsively applied to the body. The total impulse,  $\bar{I}$ , is designed to give

$$\bar{I} = m V \quad (1)$$

However, due to the errors noted above, angular impulse is applied to the vehicle, given by

$$\bar{I}d = I \omega \quad (2)$$

Therefore,

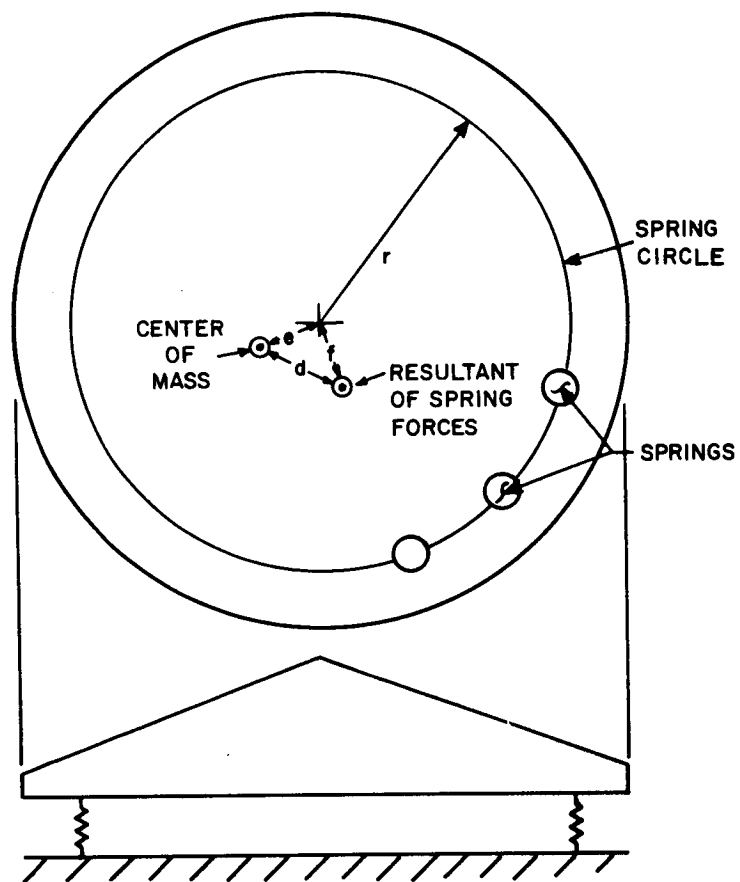
$$\omega = \frac{m V}{I} d \quad (3)$$

or integrating,

$$\theta = \frac{m s}{I} d \quad (4)$$

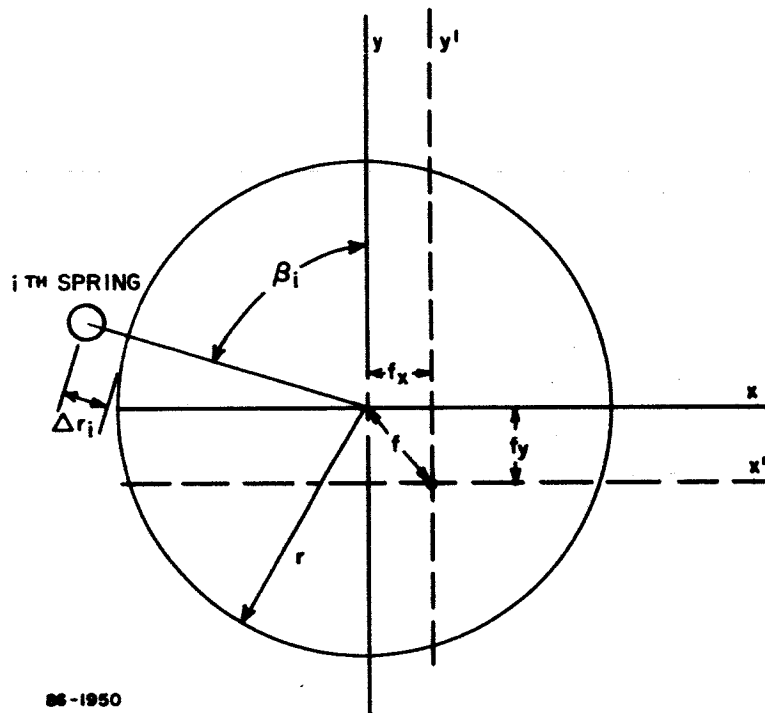
The next step in the analysis is the calculation of the spring force offset  $f$ . Figure A-2 shows the pertinent parameters. Errors in radial positions of the springs,  $\Delta r$ 's, are considered, but errors in angular position,  $\Delta \beta$ 's, are neglected.

Now, taking moments about the  $x'$  and  $y'$  axes shown on Figure A-2 yields



86-1949

Figure A-1 OFFSETS IN SEPARATION SYSTEM



88-1950

Figure A-2 OFFSETS IN RESULTANT SPRING FORCES

$$\sum_{i=1}^N F_i [(r + \Delta r_i) \sin \beta_i + f_x] = 0$$

$$\sum_{i=1}^W F_i [(r + \Delta r_i) \cos \beta_i - f_y] = 0 \quad (5)$$

where

$$\beta_i = \frac{2\pi}{N} i$$

or

$$f_x = - \frac{\sum_{i=1}^N F_i (r + \Delta r_i) \sin \beta_i}{\sum_{i=1}^N F_i}$$

$$f_y = \frac{\sum_{i=1}^N F_i (r + \Delta r_i) \cos \beta_i}{\sum_{i=1}^N F_i} \quad (6)$$

Now;

$$F_i = F_o \left[ 1 + \sum_{j=1}^J a_{ij} \right] \quad (7)$$

where

$F_o$  is nominal force

and

$a_{ij}$ 's are errors in  $F_0$  due to various sources at spring  $i$ .

If this expression is introduced into equations (6) then, by neglecting 2nd order terms, it can be shown that

$$\begin{aligned} f_x &= -\frac{r}{N} \left[ \sum_{i=1}^N \sum_{j=1}^J a_{ij} \sin \beta_i + \frac{1}{r} \sum_{i=1}^N \Delta r_i \sin \beta_i \right] \\ f_y &= +\frac{r}{N} \left[ \sum_{i=1}^N \sum_{j=1}^J a_{ij} \cos \beta_i + \frac{1}{r} \sum_{i=1}^N \Delta r_i \cos \beta_i \right] \end{aligned} \quad (8)$$

Let

$$\Delta r_i = a_i, \quad J+1$$

Then

$$\begin{aligned} f_x &= -\frac{r}{N} \sum_{i=1}^N \left( \sum_{j=1}^{J+1} a_{ij} \sin \beta_i \right) \\ f_y &= \frac{r}{N} \sum_{i=1}^N \left( \sum_{j=1}^{J+1} a_{ij} \cos \beta_i \right) \end{aligned} \quad (9)$$

At this point, the solution will proceed by root-sum-squaring the  $1\sigma$  error values:

$$\overline{a_{ij}} = 1\sigma \text{ value of } a_{ij}$$

then

$$\begin{aligned} f_x &= -\frac{r}{N} \left[ \sum_{i=1}^N \left( \sum_{j=1}^{J+1} \overline{a_{ij}}^2 \right) \sin^2 \beta_i \right]^{1/2} \\ f_y &= \frac{r}{N} \left[ \sum_{i=1}^N \left( \sum_{j=1}^{J+1} \overline{a_{ij}}^2 \right) \cos^2 \beta_i \right]^{1/2} \end{aligned} \quad (10)$$

Since the errors in each spring are independent of those in the other springs, the  $a_{ij}$  summation can be evaluated independently of  $i$  :

$$\sum_{j=1}^{J+1} \overline{a_{ij}}^2 \equiv A^2 \quad (11)$$

Then, since

$$\sum_{i=1}^N \sin^2 \left( \frac{2\pi}{N} i \right) = \sum_{i=1}^N \cos^2 \left( \frac{2\pi}{N} i \right) = \frac{N}{2} ,$$

$$f_y = -f_x = \frac{r A}{\sqrt{2N}} \quad (12)$$

and

$$f = \sqrt{f_x^2 + f_y^2} = \frac{r A}{\sqrt{N}} \quad (13)$$

This error value will be root-sum-squared with the error in center-of-mass position to yield the total offset,  $d$  . Thus,

$$d^2 = e^2 + f^2 \quad (14)$$

and so, using equations (3) and (4)

$$\omega = \frac{m V}{I} \sqrt{e^2 + \frac{r^2 A^2}{N}} \quad (15)$$

$$\theta = \frac{m s}{I} \sqrt{e^2 + \frac{r^2 A^2}{N}} \quad (16)$$

## APPENDIX B

### ANALYTICAL METHODS USED IN EVALUATION OF SPIN SYSTEM

A linearized statistical analysis was made of the spin - thrust system,  $\Delta V$  pointing accuracy, and precession cone characteristics. A description of the linearized analysis follows:

An axis-symmetrical vehicle is separated, spin-stabilized, and thrusting using body mounted reaction devices to achieve a perturbation velocity,  $\bar{V}_o$ . Due to errors in the system, an error,  $\Delta \bar{V}$ , in this velocity results, and after thrusting the stabilized vehicle exhibits precession cone motion. These effects are shown in Figure B-1. The variance,  $\sigma_{\Delta V_X}^2$ , in the in-line component of the error velocity is:

$$\sigma_{\Delta V_X}^2 = V_o^2 \left[ \sigma_{\Delta k_T}^2 + \frac{1}{m^2} \sigma_{\Delta m}^2 \right] \quad (1)$$

where

$\sigma_{\Delta k_T}^2$  = variance in the thrust rocket impulse (expressed as a fraction)

$\sigma_{\Delta m}^2$  = variance in the vehicle mass

$V_o$  = nominal perturbation velocity magnitude

$m$  = nominal vehicle mass

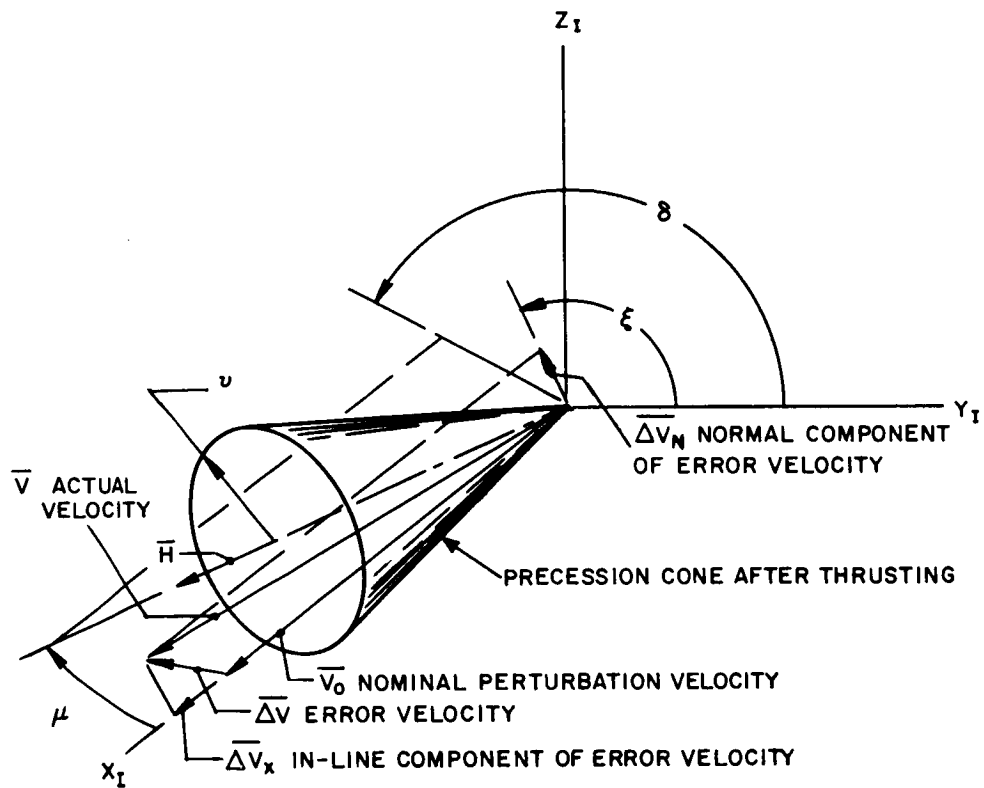
The variance,  $\sigma_{\Delta V_N}^2$ , in the normal component of the error velocity is:

$$\sigma_{\Delta V_N}^2 = V_o^2 (\sigma_{a_o}^2 + b_{\omega_o}^2 \sigma_{\omega_o}^2 + b_{\Delta l_S}^2 \sigma_{\Delta l_S}^2 + b_{\Delta l_T}^2 \sigma_{\Delta l_T}^2) \quad (2)$$

where:

$\sigma_{a_o}^2$  = variance in the separation attitude due to spacecraft deadband and bias.

$\sigma_{\omega_o}^2$  = variance in the deployed vehicle angular rate normal to the deployment direction immediately after separation from the spacecraft.



86-1364

Figure B-1 SPIN THRUST SYSTEM ERRORS

$\sigma_{\Delta'_S}^2$  = variance in the effective moment arm of the spin-up system.

$\sigma_{\Delta'_T}^2$  = variance in the effective moment arm of the thrust rocket.

$$b_{\omega_o}^2 = \frac{\beta^2}{\Omega_S^2 \left(\frac{\Omega_S T}{\beta}\right)^2} \left\{ 2 \left(1 - \cos \frac{\Omega_S T}{\beta}\right) + \left[ 1 + \left(\frac{\Omega_S T_1}{\beta}\right)^2 \right] \left(\frac{\Omega_S T}{\beta}\right)^2 \right. \\ \left. - 2 \frac{\Omega_S T}{\beta} \left\{ \frac{\Omega_S T_1}{\beta} \left[ \cos \frac{\Omega_S (T_2 + T)}{\beta} - \cos \frac{\Omega_S T_2}{\beta} \right] - \left[ \sin \frac{\Omega_S (T_2 + T)}{\beta} - \sin \frac{\Omega_S T_2}{\beta} \right] \right\} \right\}$$

$$b_{\Delta'_S}^2 = \frac{1}{2NR^2 \left(\frac{\Omega_S T}{\beta}\right)^2} \left\{ 2 \left(1 - \cos \frac{\Omega_S T}{\beta}\right) + \frac{\Omega_S T}{\beta} \left[ \frac{\Omega_S T}{\beta} + 2 \left( \sin \frac{\Omega_S (T_2 + T)}{\beta} - \sin \frac{\Omega_S T_2}{\beta} \right) \right] \right\}$$

$$b_{\Delta'_T}^2 = \frac{V_o^2 m^2}{I_T^2 \Omega_S^2 \left(\frac{\Omega_S T}{\beta}\right)^4} \left\{ \left(\frac{\Omega_S T}{\beta}\right)^2 + 2 \frac{\beta^4 - \beta^2 + 1}{\beta^2 (1 - \beta)^2} - \frac{2}{(1 - \beta)^2} \cos (1 - \beta) \frac{\Omega_S T}{\beta} \right. \\ \left. + \frac{2}{1 - \beta} \left[ (1 + \beta) \cos \frac{\Omega_S T}{\beta} - \frac{1 + \beta}{\beta^2} \cos \beta \frac{\Omega_S T}{\beta} + \beta \left(\frac{\Omega_S T}{\beta}\right) \sin \frac{\Omega_S T}{\beta} - \frac{1}{\beta} \left(\frac{\Omega_S T}{\beta}\right) \sin \beta \frac{\Omega_S T}{\beta} \right] \right\}$$

$$\beta = I_T/I_X$$

$\Omega_S$  = nominal spin rate

$T$  = thrust rocket nominal burning time

$T_1$  = time between separation and spin-up

$T_2$  = time between spin-up and thrust initiation

$N$  = number of spin rockets

$R$  = distance of spin rockets from vehicle center line

If  $T_2$  is large so that many spin revolutions occur before thrusting, then the worst case value for  $T_2$  should be used in the coefficients (that value of  $T_2$  which maximizes  $b_{\omega_o}^2$  and  $b_{\Delta'_S}^2$ ).

$$\text{If } \frac{\Omega_S T}{\beta} \gg 1 \quad \text{and} \quad \frac{\Omega_S T_1}{\beta} \gg 1, \text{ then:}$$

then:

$$b_{\omega_o}^2 \approx T_1^2 + \left( \frac{\beta}{\Omega_S} \right)^2$$

$$b_{\Delta l_S}^2 \approx \frac{1}{2NR^2}$$

$$b_{\Delta l_T}^2 \approx \left( \frac{V_o m \beta}{I_T \Omega_S^2 T} \right)^2$$

and

$$\sigma_{\Delta V_N}^2 = V_o^2 \left[ \sigma_{a_o}^2 + \left( T_1^2 + \frac{\beta^2}{\Omega_S^2} \right) \sigma_{\omega_o}^2 + \left( \frac{V_o m \beta}{I_T \Omega_S^2 T} \right)^2 \sigma_{\Delta l_T}^2 + \frac{1}{2NR^2} \sigma_{\Delta l_S}^2 \right]$$

Any direction of the normal component of  $\Delta \bar{V}$  in the  $y$ - $z$  plane in Figure B-1 is equally likely ( $\xi$  is uniformly distributed between 0 and  $2\pi$ ). This is exactly true if  $N > 2$  and conservative if  $N = 2$ .

Expressions for  $\sigma_{\Delta l_S}^2$  and  $\sigma_{\Delta l_T}^2$  are:

$$\sigma_{\Delta l_S}^2 = \sigma_{\Delta X_S}^2 + X^2 \sigma_{\Delta k_S}^2 + (R^2 + X^2) \sigma_{\Delta \xi_S}^2 \quad (4)$$

$$\sigma_{\Delta l_T}^2 = \sigma_{\Delta X_T}^2 + \sigma_{\Delta c_g}^2 + L^2 \sigma_{\Delta \xi_T}^2 \quad (5)$$

where:

$\sigma_{\Delta X_S}^2$  = variance in the location of any spin rocket.

$\sigma_{\Delta k_S}^2$  = variance in a single spin rocket impulse.

$\sigma_{\Delta \xi_S}^2$  = variance in the angular misalignment of a single spin rocket thrust vector.

$\sigma_{\Delta X_T}^2$  = variance in the location of the thrust rocket off the vehicle centerline.

$\sigma_{\Delta c_g}^2$  = variance in the vehicle c. g., location off the vehicle centerline.

$\sigma_{\Delta \xi_T}^2$  = variance in the angular misalignment of the thrust rocket thrust vector.

$X$  = distance of the plane of the spin rockets from the vehicle c. g.

R = radius of spin rocket circle.

L = distance of thrust rocket aft of vehicle c. g.

The variance of  $\mu$ , the angle which defines the center of the final precession cone, is approximately:

$$\sigma_{\mu}^2 = \sigma_{a_o}^2 + \left( T_1^2 + \frac{\beta^2}{\Omega_S^2} \right) \sigma_{\omega_o}^2 + \frac{1}{2NR^2} \sigma_{\Delta l_S}^2 + \left[ \frac{\beta(1-2\beta+5\beta^2)^{1/2} V_o m}{(1-\beta) \Omega_S^2 T I_T} \right]^2 \sigma_{\Delta l_T}^2 \quad (6)$$

A conservative estimate for the variance in the precession cone half angle is:

$$\sigma_v^2 = \left( \frac{\beta}{\Omega_S} \right)^2 \sigma_{\omega_o}^2 + \frac{1}{2NR^2} \sigma_{\Delta l_S}^2 + \left[ \frac{2\beta^2 V_o m}{(1-\beta) \Omega_S^2 T I_T} \right]^2 \sigma_{\Delta l_T}^2 \quad (7)$$

The expressions for  $b_{\omega_o}^2$  and  $b_{\Delta l_S}^2$  contain the time,  $T_2$ , between spin up and thrust initiation as a variable. For the case under investigation, this time is large so that many revolutions occur before thrusting. To maintain conservatism, that value of  $T_2$  which maximizes  $b_{\omega_o}^2$  and  $b_{\Delta l_S}^2$  is used. Maximization of these equations yield the following expressions

$$b_{\omega_o}^2 = \frac{\beta^2}{\Omega_S^2 \left( \frac{\Omega_S T}{\beta} \right)^2} \left\{ 2 \left( 1 - \cos \frac{\Omega_S T}{\beta} \right) + \left[ \left( 1 + \frac{\Omega_S T_1}{\beta} \right)^2 \right] \left( \frac{\Omega_S T}{\beta} \right)^2 \right. \quad (8)$$

$$\left. + 2 \frac{\Omega_S T}{\beta} \left[ 2 \left( 1 + \frac{\Omega_S^2 T_1^2}{\beta^2} \right) \left( 1 - \cos \frac{\Omega_S T}{\beta} \right) \right]^{1/2} \right\} \quad (9)$$

and

$$b_{\Delta l_S}^2 = \frac{1}{2NR^2 \left( \frac{\Omega_S T}{\beta} \right)^2} \left\{ 2 \left( 1 - \cos \frac{\Omega_S T}{\beta} \right) + \frac{\Omega_S T}{\beta} \left[ \frac{\Omega_S T}{\beta} + 2 \sqrt{2 \left( 1 - \cos \frac{\Omega_S T}{\beta} \right)} \right] \right\}$$

which were used in the analysis.

## APPENDIX C

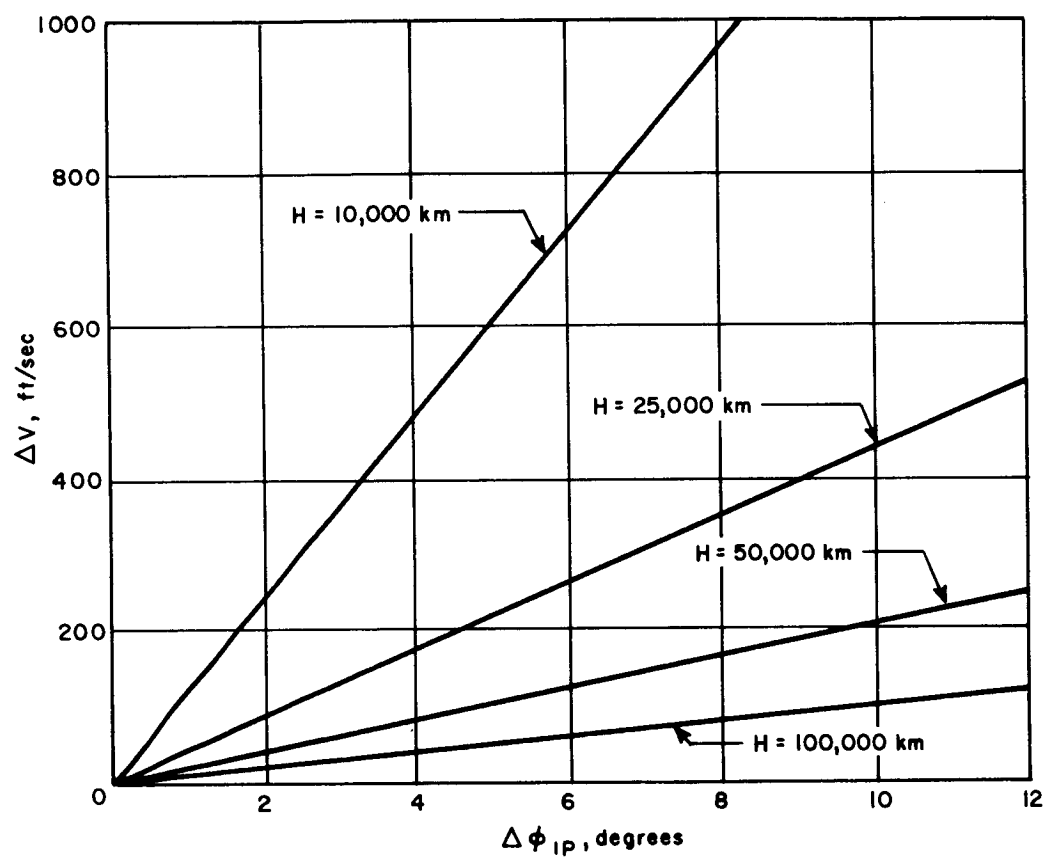
### DIRECT ENTRY TERMINAL GUIDANCE VELOCITY REQUIREMENTS

#### 1.0 INTRODUCTION

A terminal guidance system for the direct entry mission mode can be designed to correct either impact position errors or entry angle dispersions introduced by an uncertainty in the spacecraft position relative to Mars at the time of separation and uncertainties in the capsule velocity vector introduced during the application of the separation velocity. This present analysis was performed with the view toward reducing impact uncertainties; however, with the reduction in the surface pressure of the new postulated Martian atmosphere, entry angle control may take precedence over impact position control. The results of this preliminary analysis can be employed for either system since the variation in both range angle and entry angle are presented as a function of correction velocity and correction altitude.

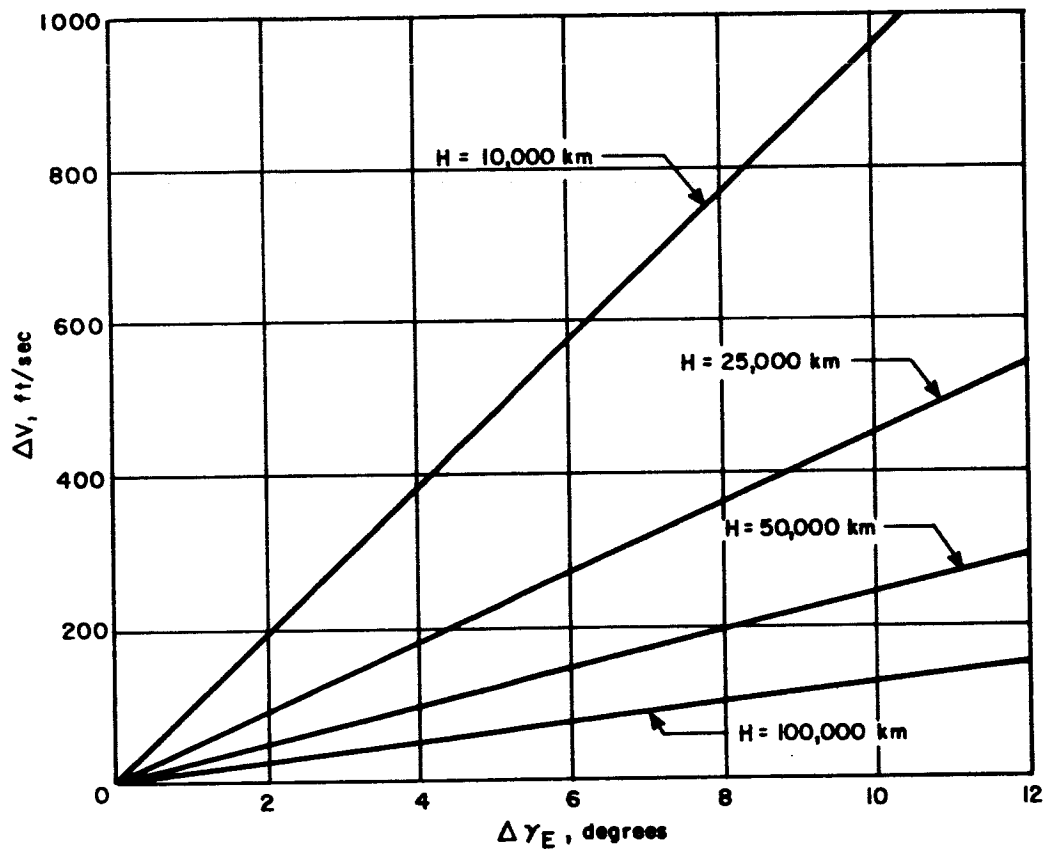
#### 2.0 RESULTS

In order to determine the implications on future capsule design requirements of a terminal guidance system, an analysis was performed to determine the magnitude of the velocity correction as a function of the correction altitude,  $H$ , required to vary the in-plane,  $\Delta\phi_{ip}$ , and out-of-plane,  $\Delta\phi_{op}$ , impact locations for entry angles of  $-50$  and  $-90$  degrees. For a range of correction altitudes between 10,000 km and 100,000 km, an approximate inverse relationship exists between the terminal guidance correction velocity and correction altitude, i.e., the correction velocity decreases from 1000 to 85 ft/sec as the correction altitude increases from 10,000 km to 100,000 km for a 500 km (8.33 degrees) variation in the impact point, a 90 degree entry angle, and a hyperbolic approach velocity of 3 km/sec. The variation in the magnitude of the correction velocity with hyperbolic approach velocity was not investigated. Throughout this analysis a thrust application angle of 90 degrees was maintained to produce the smallest velocity requirements for a given range displacement. These results are presented in Figure C-1. The application of the terminal correction maneuver to remove a dispersion in the in-plane impact point introduced by perturbations in the separation parameters also tend to remove a corresponding dispersion in the entry angle. The variation in the entry angle is presented in Figure C-2. These results indicate that the change in entry angle is dependent on the correction point. For correction velocities required to change the impact location by 500 km the change in entry angle decreases from 10.3 degrees to 6.8 degrees as the correction altitude increases from 10,000 km to 100,000 km.



86-1951

Figure C-1  $\Delta V$  VERSUS IN-PLANE DISPLACEMENT,  $\gamma_E = -90$  DEGREES,  $\Delta V$  APPLIED PERPENDICULAR TO CAPSULE VELOCITY VECTOR



88-1952

Figure C-2  $\Delta V$  VERSUS CHANGE IN ENTRY ANGLE,  $\gamma_E = -90$  DEGREES,  $\Delta V$  APPLIED PERPENDICULAR TO CAPSULE VELOCITY VECTOR

The magnitude of the correction velocity, in addition to being dependent upon the correction altitude, is also dependent upon the entry angle, and for entry angles other than 90 degrees, the in-plane and out-of-plane velocity requirements are significantly different. For a -50 degree entry angle the velocity requirements for an in-plane position change of 500 km are 765 and 70 ft/sec correction ranges of 10,000 km and 100,000 km, respectively, whereas for a similar correction normal to the orbit plane the velocity requirements have reduced to 600 fps and 55 fps. These results are presented in Figure C-3 and C-4.

As might be expected there is a significant reduction in the entry angle variation associated with out-of-plane correction maneuvers as compared with in-plane corrections for entry angles less than -90 degrees. In performing an in-plane maneuver to correct the impact location by 500 km for a -50 degree entry angle the entry angle variation decreases from 9.2 to 6.6 degrees as the correction range increases from 10,000 to 100,000 km. For a similar out-of-plane correction maneuver the variation in entry angle is approximately 0.63 degrees and essentially independent of correction range. The variation in the entry angle produced by out-of-plane maneuvers is essentially insignificant since in effect the trajectory is not being altered but simply rotated about the radius vector at the correction point. These results are presented in Figure C-5 and C-6. In order to impact at a specific location on a rotating planet the effects of the variation in time of flight from the correction point to entry must be considered. For an entry angle of -90 degrees with a correction maneuver of 500 km the time change is approximately 10 seconds and essentially independent of the correction range. For an entry angle of -50 degrees with an in-plane correction maneuver of 500 km the same trends are noted except that the time variation has increased by an order of magnitude from 10 to 100 seconds. For a similar out-of-plane maneuver the time variation is insignificant varying from 5 to 13 seconds as the correction point is increased from 10,000 to 100,000 km. Variation in the impact locations without introducing perturbation in the time of flight can be accounted for by employing thrust application angles slightly different than 90 degrees. The variation in time results are presented in Figures C-7 through C-9.

To determine the accuracy with which these terminal correction maneuvers must be made a simple error analysis was performed considering that the velocity errors could be spherically distributed. A coordinate system was established with one axis along the velocity vector at the correction point, the second axis normal to the velocity vector in the plane of motion defined by the position and velocity vectors and the third axis normal to both the velocity vector and the plane of motion. The results of this analysis are presented in Table C-I below for velocity errors along each of the three axes.

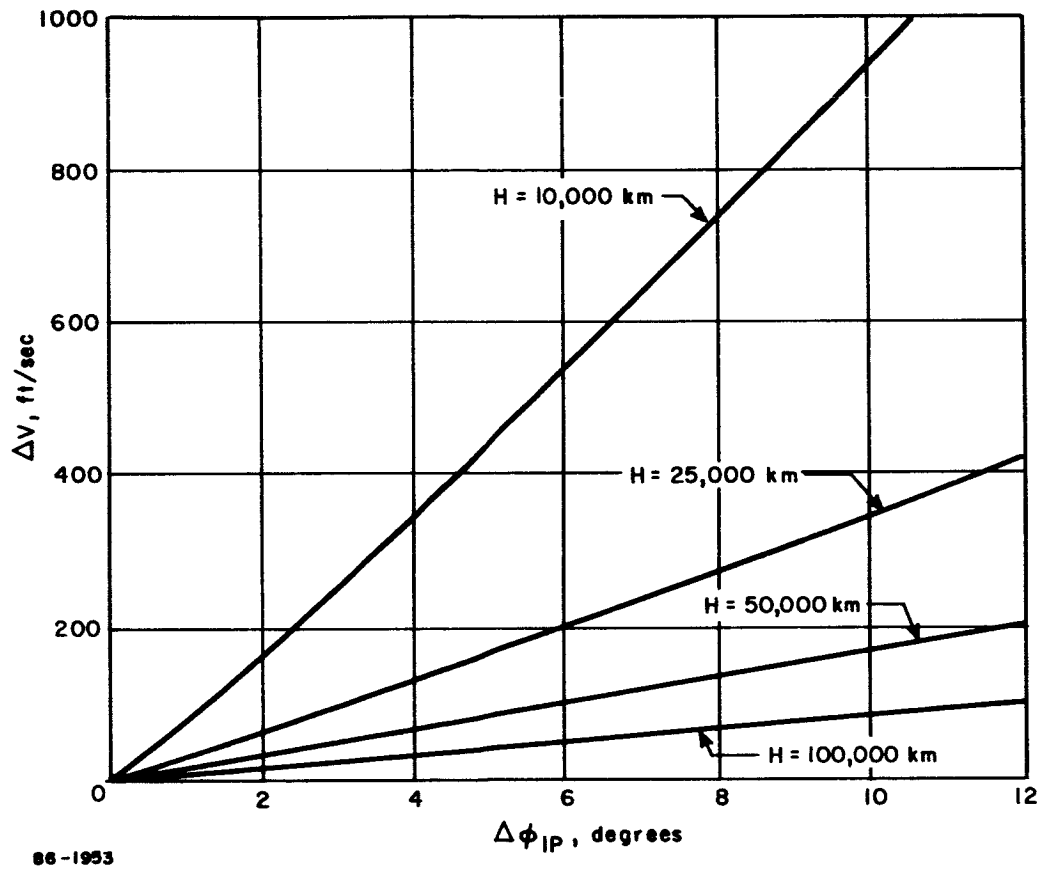
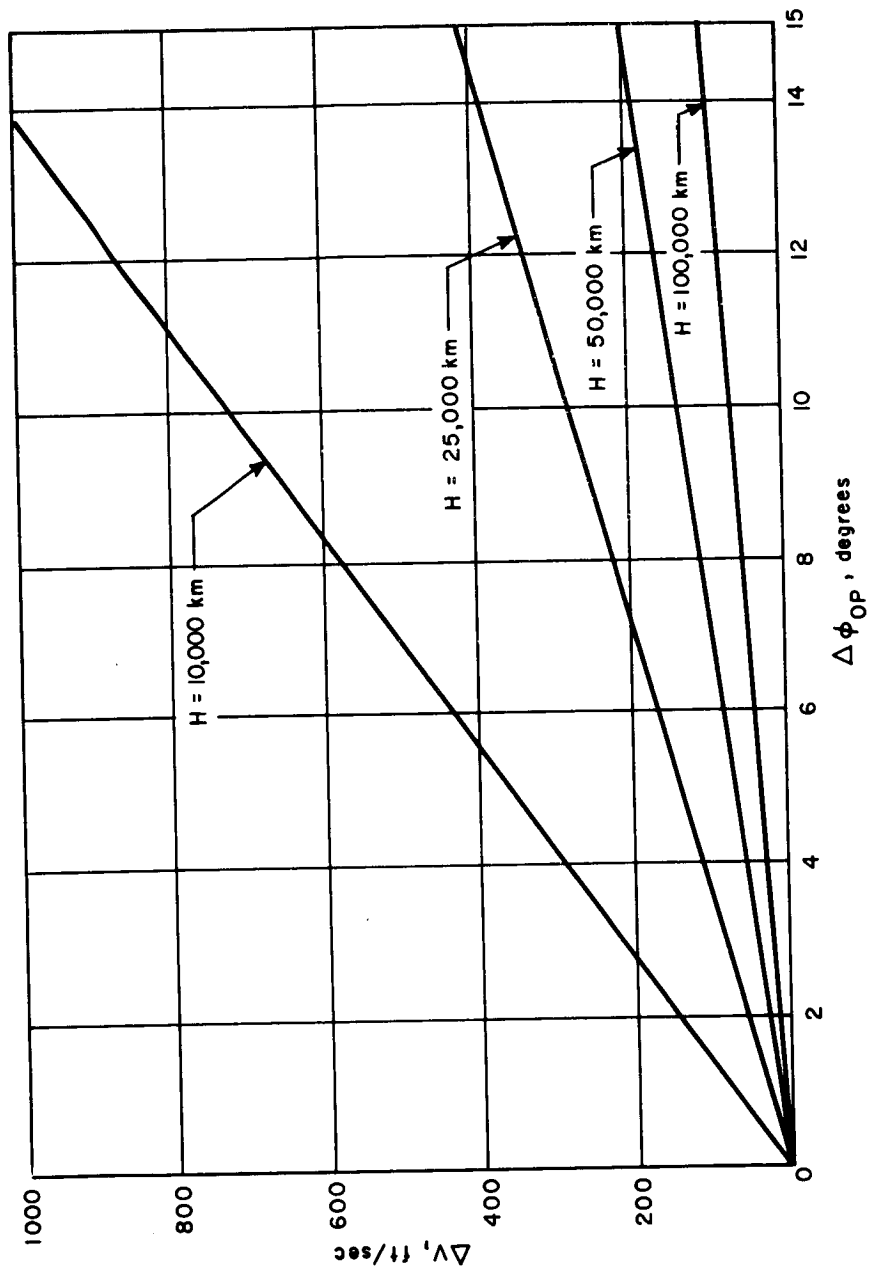


Figure C-3  $\Delta V$  VERSUS IN-PLANE DISPLACEMENT,  $\gamma_e = -50$  DEGREES  $\Delta V$  APPLIED PERPENDICULAR TO CAPSULE VELOCITY VECTOR



86-1954

Figure C-4  $\Delta V$  VERSUS OUT-OF-PLANE DISPLACEMENT,  $\gamma_e = -50$  DEGREES,  $\Delta V$  APPLIED PERPENDICULAR TO ORBITAL PLANE

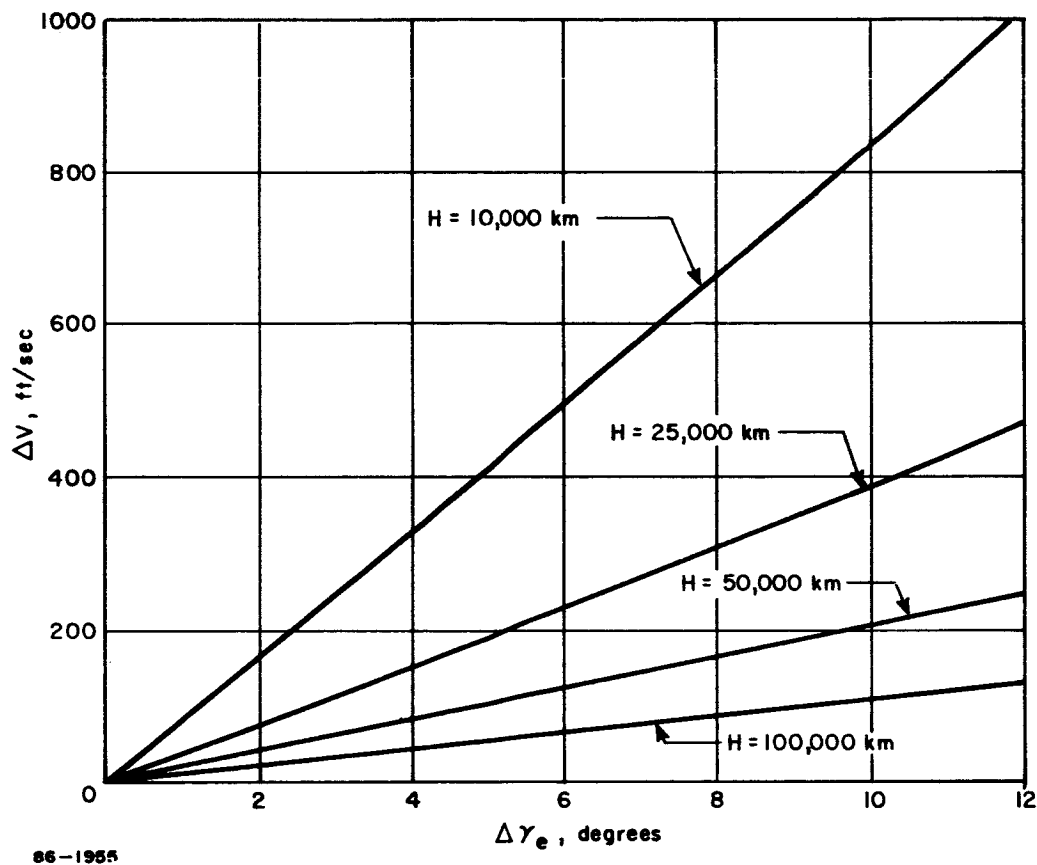


Figure C-5  $\Delta V$  VERSUS CHANGE IN ENTRY ANGLE,  $\gamma_e = -50$  DEGREES,  $\Delta V$  APPLIED PERPENDICULAR TO CAPSULE VELOCITY VECTOR

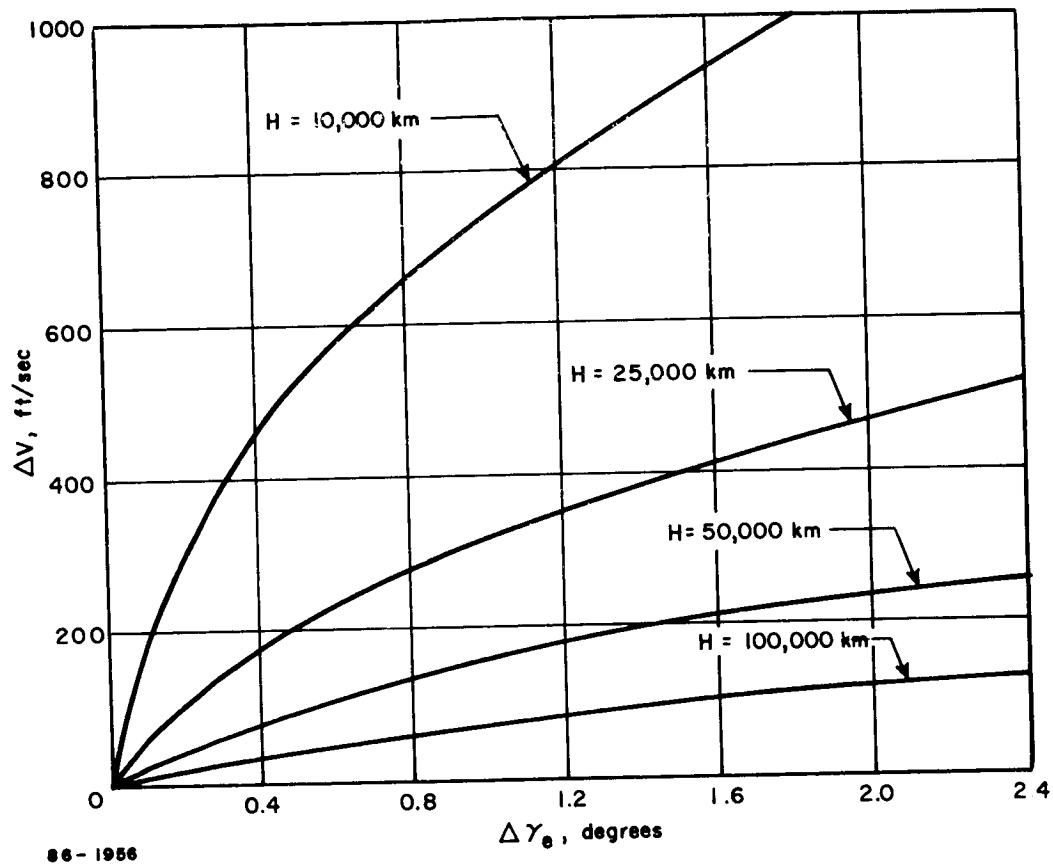


Figure C-6  $\Delta V$  VERSUS CHANGE IN ENTRY ANGLE,  $\gamma_e = -50$  DEGREES,  $\Delta V$  APPLIED PERPENDICULAR TO ORBITAL PLANE

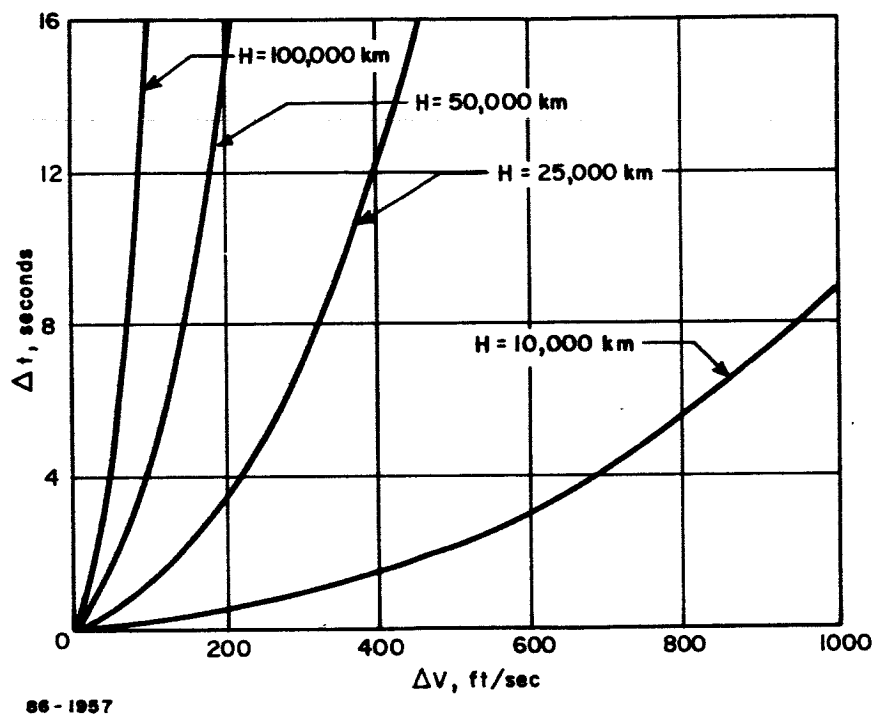


Figure C-7  $\Delta t$  VERSUS  $\Delta V$ ,  $\gamma_e = -90$  DEGREES,  $\Delta V$  APPLIED PERPENDICULAR TO CAPSULE VELOCITY VECTOR

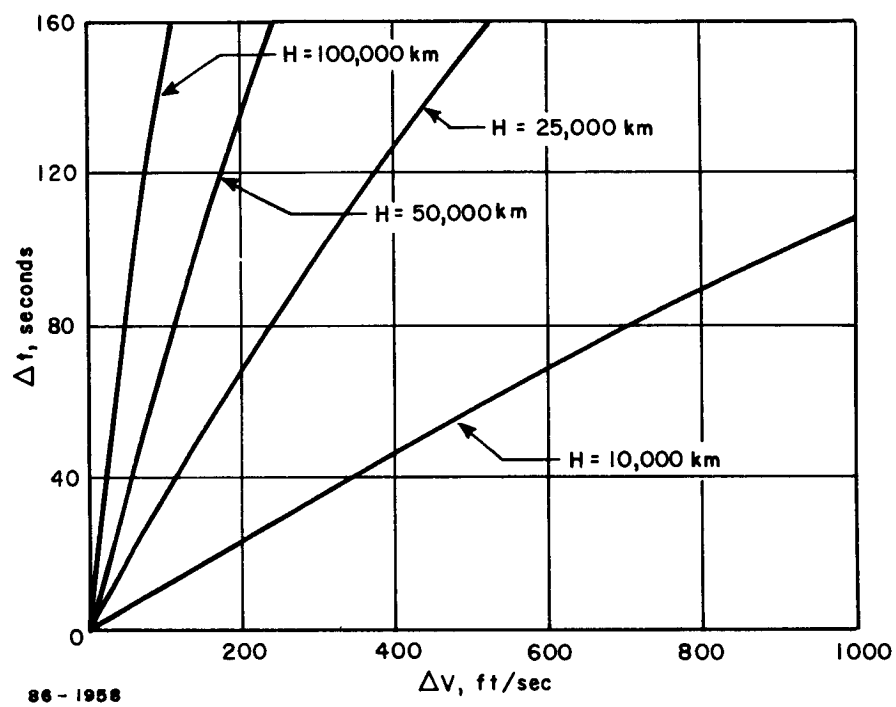


Figure C-8  $\Delta t$  VERSUS  $\Delta V$ ,  $\gamma_e = -50$  DEGREES,  $\Delta V$  APPLIED PERPENDICULAR TO CAPSULE VELOCITY VECTOR

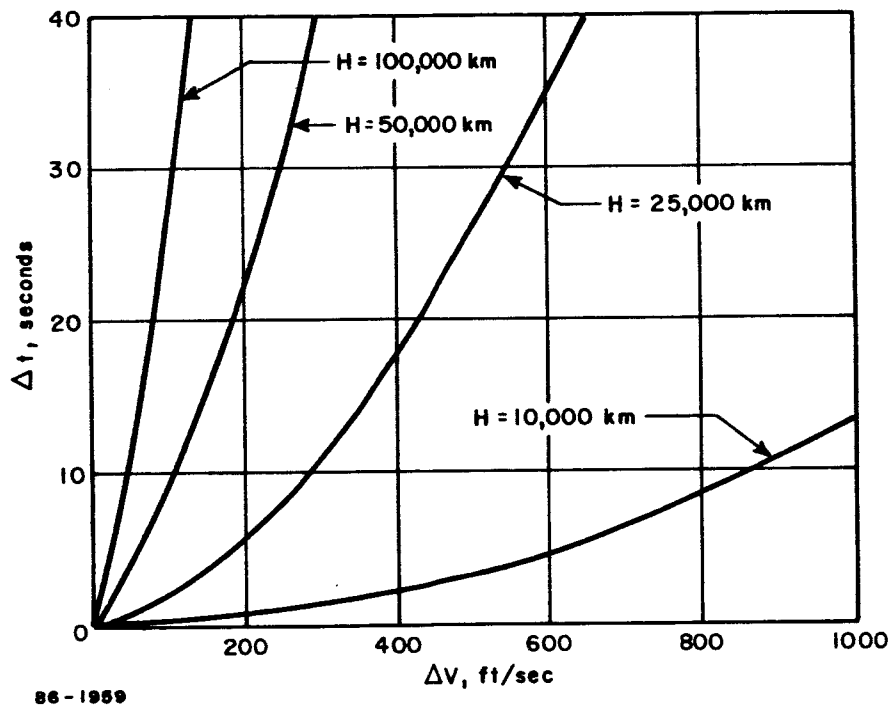


Figure C-9  $\Delta t$  VERSUS  $\Delta V$ ,  $\gamma_e = -50$  DEGREES,  $\Delta V$  APPLIED PERPENDICULAR TO ORBITAL PLANE

TABLE C-1  
TERMINAL GUIDANCE INFLUENCE COEFFICIENTS

$\gamma_E$ (deg)	Correction Altitude (km)	$\Delta(\Delta V) \perp$ to $V_c$		$\Delta(\Delta V)$ along $V_c$		$\Delta(\Delta V) \perp$ to $V_c$ out of plane		
		$\partial T / \partial \Delta V$ sec/ft/sec	$\partial \phi_{ip} / \partial \Delta V$ deg/ft/sec	$\partial T / \partial \Delta V$ sec/ft/sec	$\partial \phi_{ip} / \partial \Delta V$ deg/ft/sec	$\partial T / \partial \Delta V$ sec/ft/sec	$\partial \phi_{op} / \partial \Delta V$ deg/ft/sec	$\partial \phi_{ip} / \partial \Delta V$ deg/ft/sec
-50	100,000	1.43	0.119	2.41	0.004	0.26	0.097	0
	50,000	0.68	0.059	1.02	0.003	0.11	0.048	0
	25,000	0.32	0.029	0.43	0.002	0.04	0.023	0
	10,000	0.11	0.011	0.13	0.001	0.01	0.008	0
-90	100,000	0.150	0.097	2.44	0	0.150	0.097	0
	50,000	0.072	0.048	1.04	0	0.072	0.048	0
	25,000	0.030	0.023	0.43	0	0.030	0.023	0
	10,000	0.009	0.008	0.12	0	0.009	0.008	0

These results indicate that the influence coefficients are reduced by at least an order of magnitude as the separation range is reduced from 100,000 to 10,000 km and that velocity uncertainties on the order of 1 percent could be tolerated.

The terminal guidance system can be designed to correct either impact position or entry angle uncertainties. In view of the reduced surface pressures associated with the postulated Martian atmospheres, entry angle control may become a primary objective since entry angles between -30 and -50 degrees are required to insure adequate parachute deployment conditions with present vehicle design weights. The results of this analysis can be employed to determine the terminal guidance maneuver requirements as a function of correction altitude for a -50 degree entry angle (Figure C-5). For an entry angle of -50 degrees the velocity requirement to alter the entry angle by  $\pm 7.5$  degrees varies between 80 and 620 ft/sec as the correction altitude is reduced from 100,000 to 10,000 km. The corresponding change in the in-plane component of the impact position error is 9.5 and 6.8 degrees for the same correction altitudes. These results indicate that the correction of entry angle also tends to correct impact position errors and that for the higher correction altitudes the impact position error is overcorrected whereas for the lower altitudes the position error is undercorrected. This implies that an altitude may exist such that both in-plane parameters may be simultaneously corrected, i.e., at a correction altitude of 25,000 km the velocity correction to perturb the entry angle by 7.5 degrees also changes the impact position by 8.3 degrees (500 km).

## APPENDIX D

### REFERENCE DESIGN COLD GAS SYSTEM SIZING CALCULATION

A cold-gas reaction control system is used as the reference design for the Capsule for entry from orbit (see paragraph 8.3.1.2). This Appendix contains the calculations used to size that system based on impulse requirements presented in Appendix K. A summary of these requirements are:

<u>Mode</u>	<u>Impulse Requirements (lb-sec)</u>
Stabilization	34
Orientation	16
Limit Cycling	8
Roll Control During Thrusting	10
	<hr/>
Total Required	69 lb-sec

Additional impulse is required as safety margin to account for the following modes of failure:

1. Leakage: A pressure vessel, line or component leak in one of the two systems will require that the non-leaking system do all the torquing; hence, the quantity of gas must be doubled. Defining the safety margin multipliers by the letter N, the multiplier for this case is  $N_1 = 2$ .
2. Valve Failures: A valve failing to open would result in the loss of a pure couple in one sense only on one axis; hence, no gas contingency is required since the valves are located in planes passing through the principle axis. However, should a valve in one system fail to close, then one other valve in the same system will operate in conjunction with a third valve from the second system to cancel the torque until the failed valve drains its system down.

Since each of the systems contributes one-half of the cancelling torque, then each system must have an extra 50 percent of cold gas to accomodate this failure mode. Thus, the safety margin factor,  $N_2$ , is 1.5.

3. Impulse Degradation: A portion of the avialable impulse is lost during short term reorientation and limit cycle operations. Experience on other programs has shown that the multiplier for this effect should be approximately  $N_3 = 1.1$ .

The total stored impulse becomes, therefore:

$$I_{ts} = I_{st} \times N_1 \times N_2 \times N_3 = 3.3 I_{st}$$

The impulse required for each vessel ( $I_t$ ) is

$$I_t = \frac{3.3}{2} \times 68 = 113 \text{ lb.-sec.}$$

The temperature operating limits of the Reaction Control system have been established at  $-100^\circ\text{F}$  to  $300^\circ\text{F}$ . The average specific impulse for nitrogen as a function of absolute temperature may be obtained from

$$I_{sp(ave)} = \sqrt{\frac{2Rk}{g(k-1)}} \sqrt{T}$$

Where

$I_{sp(ave)}$  = average specific impulse (seconds)

$R$  = universal gas constant (ft/ $^\circ\text{R}$ )

$g$  = gravitational constant (ft/sec<sup>2</sup>)

$k$  = ratio of the specific heats ( $c_p/c_v$ )

$T$  = absolute temperature ( $^\circ\text{R}$ )

Based on previous experience an average specific impulse of 60 seconds for the  $60^\circ\text{F}$  point may be assumed, then:

$$I_{sp(60^\circ)} = K \sqrt{520} = 60 \text{ seconds and at } -100^\circ\text{F}$$

$$I_{sp(-100^\circ\text{F})} = K \sqrt{360}$$

Therefore the desired specific impulse is:

$$I_{sp(-100^\circ\text{F})} = \frac{K}{K} \frac{\sqrt{360}}{\sqrt{520}} \times 60 = 50 \text{ seconds}$$

The total weight of propellant to be expelled by one subsystem is obtained using the average specific impulse computed above, i. e.

$$\Delta W_{GN_2} = \frac{I_t}{I_{sp(ave)}} = \frac{113}{50} = 2.26 \text{ pounds}$$

In addition to the impulse degradation, a decrease in available pressure will be experienced when the temperature is lowered from the assumed fill temperatures of 60°F to the operating temperature of -100°F. For this constant volume process the operating pressure is obtained using:

$$P_o = \frac{P_a}{T_a} T_o$$

where:

$P_o$  = the desired operating pressure (lb/in<sup>2</sup>)

$T_o$  = operating temperature (°F)

$P_a$  = fill pressure (lb/in<sup>2</sup>)

$T_a$  = fill temperature (°R)

$$P_o = \frac{3015}{520} (360) = 2090 \text{ psia}$$

Expanding the gases from the operating pressure and temperature assumed above results in a temperature drop which may be calculated using the expression for a polytropic process as follows:

$$T_f = \left( \frac{P_o}{P_f} \right)^{\frac{n-1}{n}} (T_o)$$

where

$T_f$  = final temperature (°R)

$P_o$  = initial operating pressure (psia)

$n$  = polytropic exponent assumed (1.05)

$T_o$  = initial operating temperature (°R)

$P_f$  = final pressure (cutoff) = (psia)

$$T_f = \left( \frac{215}{2090} \right)^{\frac{1.05-1}{1.05}} \times 360 = 323^\circ\text{R}$$

The volume of each pressure vessel is determined from the relationship relating the amount of propellant used and the amount finally left in the vessel, which is

$$V_v = \frac{\Delta W_{GN_2}}{\rho_i - \rho_f}$$

where

$V_v$  = volume of the pressure vessel (in.<sup>3</sup>)

$\rho_i$  = initial  $GN_2$  density (lb/in.<sup>3</sup>)

$\rho_f$  = final  $GN_2$  density (lb/in.<sup>3</sup>)

The initial fill conditions are assumed at

$$p_i = 3015 \text{ psia}$$

$$T_i = 520^\circ R$$

and the density  $\rho_i$  (from the real-gas tables) is  $8.08 \times 10^{-3}$  lb/in.<sup>3</sup>

The final gas conditions are

$$p_f = 215 \text{ psia}$$

$$T_f = 323^\circ R$$

and the density, taken from the real-gas tables is

$$\rho_f = 0.84 \times 10^{-3} \text{ lb/in.}^3$$

Then

$$V_v = \frac{\Delta W_{GN_2}}{\rho_i - \rho_f} = \frac{2.26 \times 10^3}{(8.08 - 0.84)} = 312 \text{ in.}^3$$

The weight of  $GN_2$  stored initial in both vessels is

$$W_{GN_2} = 2 (V_v) \rho_i \text{ lbs.} = 2 \times 312 \times 8.08 \times 10^{-3} = 5.04 \text{ pounds.}$$

The inside radius of the vessel is:

$$r_i = \sqrt[3]{\frac{3}{4} \frac{V_v}{\pi}} = \sqrt[3]{\frac{(0.75) (312)}{\pi}} = 4.22 \text{ inches}$$

or the vessel I. D. = 8.44 inches.

The vessels will be subjected to the elevated sterilization temperatures of 300°F when pressurized. Entering the real gas data tables with 300°F and the gas density at the initial conditions ( $\rho_i$ ) as arguments, the internal pressures resulting from this sterilization temperature is found to be 4800 lb/in<sup>2</sup>. Vendor data indicates that the ultimate strength of the alloy at 300°F is 135,000 lb/in<sup>2</sup>. The vessel thickness may be computed by using the "hoop stress" formula as follows:

$$t = \frac{P_i r}{2S}$$

where

$$P_i = \text{maximum vessel pressure} = (3000 \text{ lb/in.}^2)$$

$$S = \text{maximum working stress level (lb/in.}^2)$$

$$t = \text{wall thickness} = (\text{inches})$$

Assuming a factor of safety = 2

$$t = \frac{4800}{135,000} \times 4.22 = 0.151 \text{ inch.}$$

The vessel outside diameter is then

$$d_o = d_i + 2t = 8.44 + 0.30 = 8.74 \text{ inches.}$$

The vessel weight may be computed with

$$W_V = 1/6 \pi \rho_V (d_o^3 - d_i^3)$$

where

$$W_V = \text{weight of the vessel (pounds)}$$

$$\rho_V = \text{density of the vessel material} = 0.16 \text{ lb/in.}^3 \text{ (Ti alloy)}$$

$$d_o = \text{vessel O.D. (inches)}$$

$$d_i = \text{vessel I.D. (inches).}$$

Substituting

$$W_{VS} = \frac{\pi (0.16)}{6} [(8.74)^3 - (8.44)^3] = 5.5 \text{ pounds.}$$

Adding 0.4 pound to allow for boss weight, the final vessel weight is then

$$W_V = 5.5 + 0.4 = 5.9 \text{ pounds}$$

The regulator size is based on an estimated output pressure of approximately 100 lb/in.<sup>2</sup> and the maximum required GN<sub>2</sub> weight flow rate.

Assuming a simultaneous pitch, yaw and roll thrust command, the total thrust supplied by the regulator is:

pitch thrust	=	1.0 pound
yaw thrust	=	1.0 pound
roll thrust	=	1.0 pound
		<hr/>
Total		3.0 pounds

the required flow is:

$$W_{GN_2} = \frac{F}{I_{sp}} = \frac{3}{50} = 0.06 = 0.06 \text{ lb/sec}$$

A representative regulator weight based on typical manufactured hardware is 3.0 pounds.

Each nozzle valve must handle a flow of approximately:

$$W_{GN_2} = \frac{0.5}{50} = 0.01 \text{ lb/sec}$$

A representative nozzle weight is 0.185 pound.

This system weight breakdown is:

Cold-Gas GN<sub>2</sub> ACS Reaction Control System Weight Breakdown

<u>Item</u>	<u>Nomenclature</u>	<u>Unit Weight</u>	<u>No. Required</u>	<u>Total</u>
1	Solenoid Valve	0.185	12	2.2
2	Pressure Vessel	5.9	2	11.8
3	GN <sub>2</sub> Propellant	5.04	--	5.0
4	Squib Valve	0.37	2	0.7
5	Vessel Manifold	0.25	2	0.5
6	Fill and Vent Valve	0.75	2	1.5
7	Tubing Complex	2.85	2	5.7
8	Regulator	3.00	2	6.0
9	Filter	0.25	4	1.00

Total System Weight = 34.4 pounds.

## APPENDIX E

### SOLID PROPELLANT SYSTEM SIZING CALCULATIONS\*

#### 1.0 GENERATOR REQUIREMENTS:

- (1) Total thrust rating = 13 pounds
- (2) Operating time = 35 seconds

#### 2.0 ASSUMPTIONS:

All nozzles and sonic orifices are ideal

$$p_g = \text{generator internal pressure} = 2500 \text{ lb/in}^2$$

$$T_g = \text{temperature of combustion} = 2460^\circ\text{R}$$

$$T_c = \text{gas temperature at nozzle inlet} = T_g/2$$

Propellant = OMAX 453D

#### 3.0 GENERATOR METERING ORIFICE SIZE:

The area of the generator metering orifice throat section is expressed as:

$$A_g = \frac{F}{p_g C_2} \sqrt{\frac{T_g}{T_c}}$$

where

$$A_g = \text{metering orifice throat area-in}^2$$

$$F = \text{generator thrust rating-pounds}$$

$$C_2 = \text{a constant} = k \sqrt{\frac{2}{k-1} \left( \frac{2}{k+1} \right)^{\frac{k+1}{k-1}}} = 1.97$$

$$k = \text{ratio of specific heats} = 1.3 \text{ for OMAX 453D}$$

\* The calculations in this Appendix are for the system compared in tradeoff studies (see Section 7.3.3.3). The reference design solid propellant system calculations are contained in Appendix L.

substituting:

$$A_g = \frac{13 \sqrt{2}}{2500 (1.97)} = 3.73 \times 10^{-3} \text{ in}^2$$

The metering orifice diameter is:

$$d_g = \sqrt{\frac{4 (3.73) 10^{-3}}{\pi}} = 0.069 \text{ inch.}$$

#### 4.0 PROPELLANT DIMENSIONS:

For OMAX 453D propellant initially at  $-100^\circ\text{F}$  and burning at  $2500 \text{ lb/in}^2$ , the following generator parameters are known:

$$\text{burn rate} = 0.08 \text{ in/sec}$$

$$\frac{\text{burn surface area}}{\text{metering orifice area}} = 5000$$

The burn surface area is, therefore,  $5000 A_g$  or  $5000 (3.73) 10^{-3} \text{ in}^2 = 18.65 \text{ in}^2$

Assume a cylindrical generator design with two diametral surfaces burning simultaneously. The area of the propellant transverse section is  $18.65/2 = 9.32 \text{ in}^2$ .

$$\text{Propellant diameter} = \sqrt{\frac{4 (9.32)}{\pi}} = 3.45 \text{ inch}$$

Each burn surface must be ignited for 35 seconds. The total propellant length is calculated as:

$$\text{Propellant length} = 2(35) (0.08) = 5.6 \text{ inches.}$$

#### 5.0 PROPELLANT WEIGHT

The volume of propellant is:

$$5.6(9.32) = 52.1 \text{ in}^3$$

and with a density of  $0.053 \text{ lb/in}^3$ , the propellant weight is:

$$52.1(0.053) = 2.76 \text{ pounds.}$$

## 6.0 PROPELLANT CASE WEIGHT

The weight of the generator case is written as:

$$W_c = \left[ \frac{\pi \rho p_g d_p}{4\sigma} + \frac{\pi \rho p_g l_p}{2\sigma} \right] d_p^2$$

where

$\rho$  = density of case material =  $0.28 \frac{\text{lb}}{\text{in.}^3}$  (steel)

$\sigma$  = working stress level of case material

$l_p$  = propellant length

$d_p$  = propellant diameter

$l_p$  is taken as 6 inches to allow 0.4 inch in addition to the actual propellant length of 5.6 inches to allow for igniter packaging.

$\sigma$  represents the "hoop stress" and is taken as 77,000 lb/in.<sup>2</sup> for maraging steel.

Substituting,  $W_c$  is calculated as:

$$W_c = \left[ \frac{3.45}{4} + \frac{6}{2} \right] \frac{3.14 (3.45)^2 (2500) (0.28)}{50,000} = 1.3 \text{ pounds.}$$

## 7.0 COMPLETE GENERATOR SIZE AND WEIGHT

The case wall thickness is expressed as:

$$t = \frac{W_c}{\left( \frac{\pi d_p^2}{2} + \pi d_p l_p \right) \rho}$$

$$t = 0.055 \text{ inch.}$$

The generator exterior dimensions are now found as:

$$\text{O. D.} = 3.45 + 2(0.055) = 3.56 \text{ inches}$$

$$\text{length} = 6.00 + 2(0.055) = 6.11 \text{ inches.}$$

Assuming that the igniter material weight is 10 percent of the propellant weight gives 0.28 pound as the igniter weight.

The total generator weight is found to be:

$$W_g = 0.28 + 2.76 + 1.3 \approx 4.3 \text{ pounds}$$

## 8.0 SOLENOID NOZZLE VALVE PARAMETERS

The nozzle solenoid valve must have an equivalent sharp-edged orifice size greater than the nozzle throat size to prevent excessive pressure drop. The relation between generator metering orifice area and nozzle throat area is given as:

$$\frac{A_n}{A_g} = \frac{p_g}{p_c} \sqrt{\frac{T_c}{T_g}}$$

assuming a nozzle inlet pressure of  $1000 \frac{\text{lb}}{\text{in.}^2}$

$$\frac{A_n}{A_g} = \frac{2500}{1000} \sqrt{0.5} = 1.765$$

substituting  $A_g = 3.73 \times 10^{-3} \text{ in.}^2$ ,  $A_n = 6.58 \times 10^{-3} \text{ in.}^2$

the diameter of the nozzle throat is:

$$d_n = \sqrt{\frac{4 (6.58) 10^{-3}}{\pi}} = 0.092 \text{ inch}$$

A valve with 0.20-inch diameter equivalent sharp-edged orifice should be adequate. The Philco Corporation, P/N SK 20230 (modified Minuteman Roll Control Valve), is taken as the reference design. The valve weight is given as 0.52 pound.

## 9.0 TOTAL SYSTEM WEIGHT BREAKDOWN

<u>Item</u>	<u>Nomenclature</u>	<u>Wt/unit (pounds)</u>	<u>No. Required</u>	<u>Total</u>
1	Gas Generator Assembly	4.3	4	17.2
2	Solenoid Nozzle Valve	0.52	8	4.2
3	Tubing, brackets etc.	estimated		5.0
				<u>26.4</u>

Total System Weight = 26.4 pounds.

## APPENDIX F

### MONOPROPELLANT HYDRAZIN SYSTEM SIZING CALCULATIONS

This Appendix contains the calculations for the system compared in the tradeoff studies, (see paragraph 7.3.3.4).

#### 1.0 SYSTEM REQUIREMENTS

- (1) Total impulse stored = 1062 lb-sec in each subsystem
- (2) Four 13-pound motors in each subsystem or a total of 8

#### 2.0 ROCKET MOTOR SIZE

From Figure F-1, assuming an area ratio = 70

$$\dot{w}/F = 0.00428 \quad C_F = 1.84$$

where

$$\dot{w} = \text{N}_2\text{H}_4 \text{ flow rate lb/sec}$$

$$F = \text{motor thrust pounds}$$

$$C_F = \text{thrust coefficient from } F = C_F A_t P_c$$

$$P_c = \text{chamber pressure}$$

The propellant flow rate is calculated as:

$$\dot{w} = 0.00428 (13) = 0.0556 \text{ lb/sec}$$

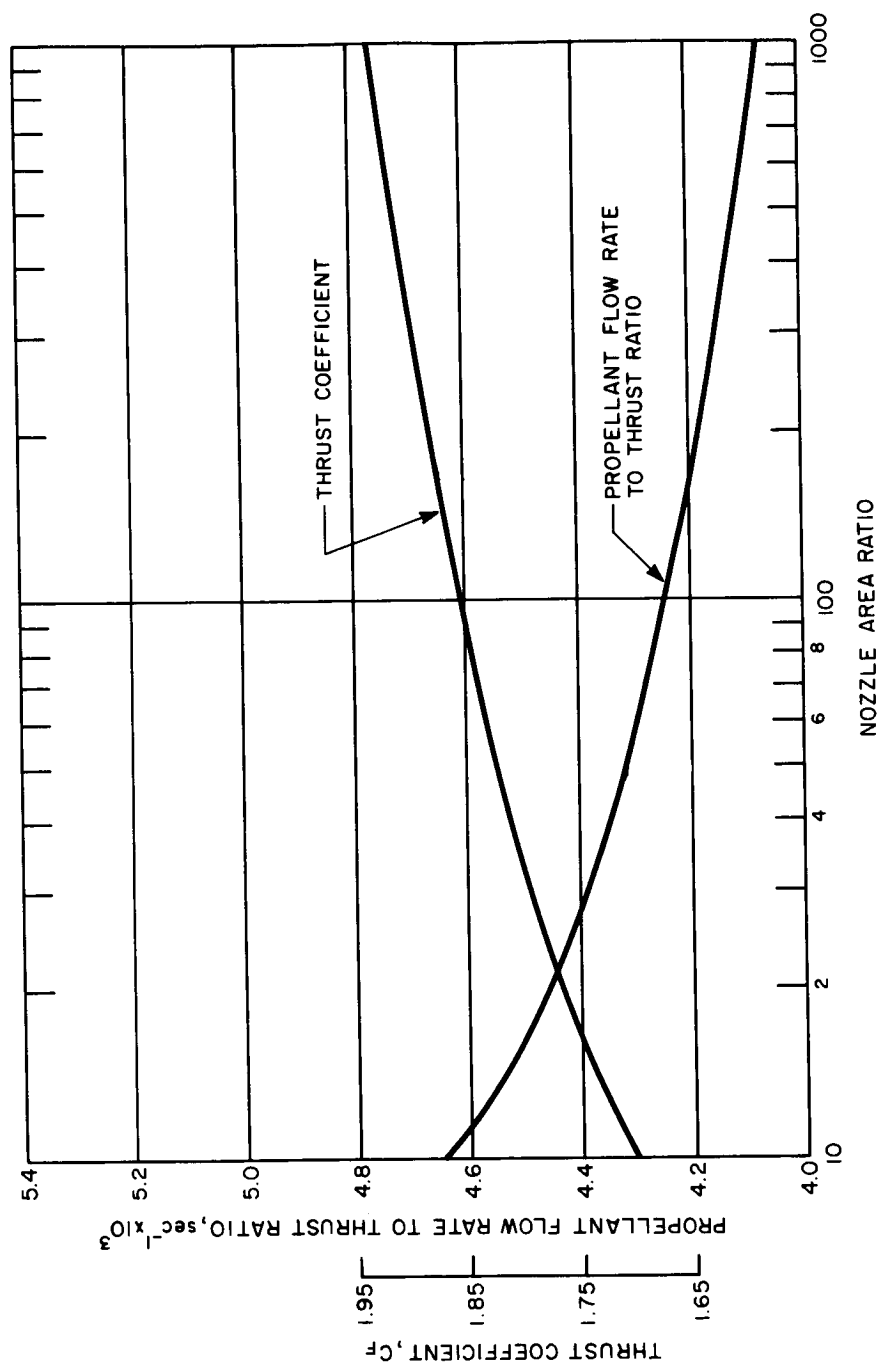
Assuming a value of  $p_c = 200 \text{ lb/in.}^2$  and entering Figure F-2 gives the nozzle section weight as:

$$w_n \approx 0.08 \text{ pounds (for } \dot{w} = 0.0556 \text{ lb/sec)}$$

Entering Figure F-3 with  $\dot{w} = 0.0556 \text{ lb/sec}$ , the weight of the catalyst chamber assembly is found as  $w_c$ .

$$w_c = 0.8 \text{ pound}$$

A survey of manufacturer's data indicates that a reasonable estimate for the solenoid valve weight is 0.5 pound. The total motor assembly weight is summarized as follows:



86-1196

Figure F-1 MONOPROPELLANT-HYDRAZINE PROPELLANT FLOW RATE TO THRUST RATIO  
VERSUS AREA RATIO, THRUST COEFFICIENT

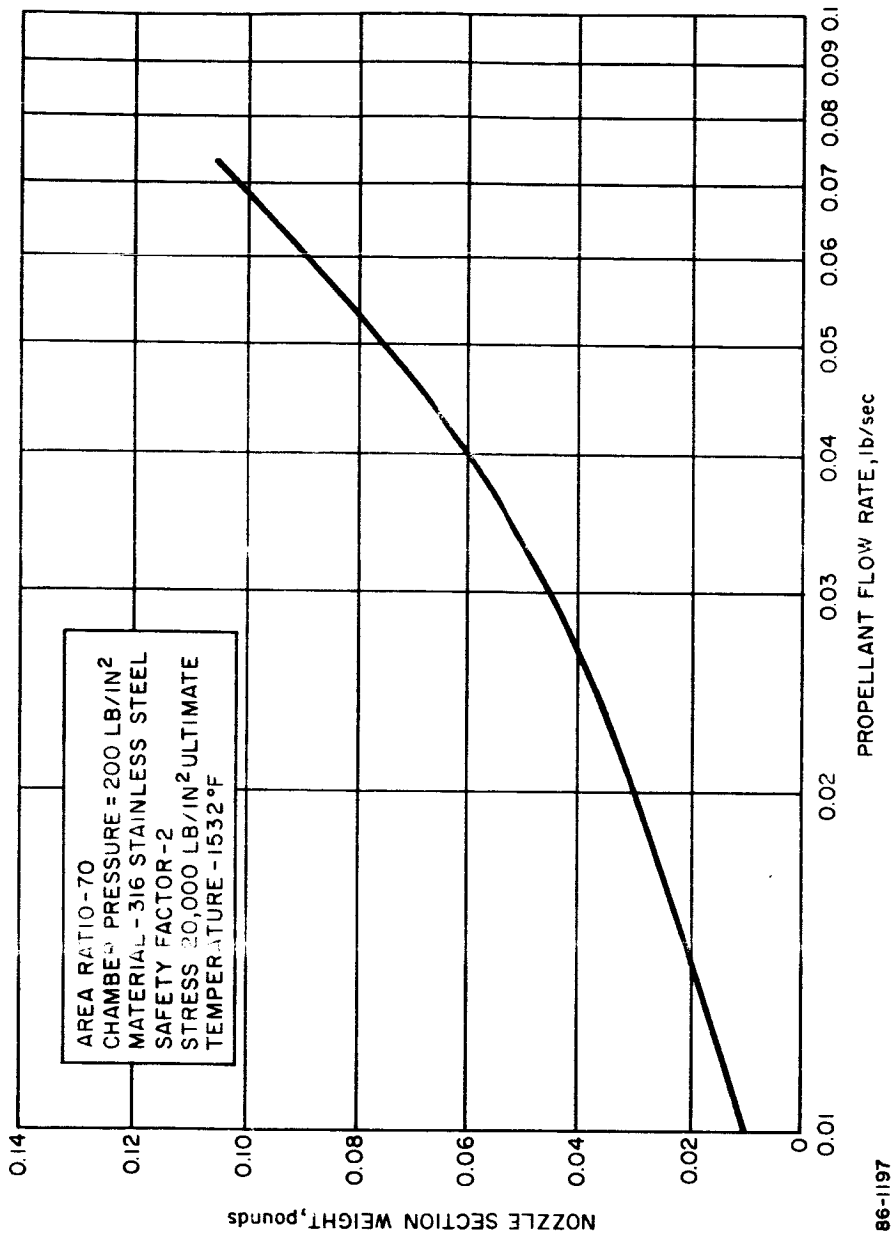


Figure F-2 MONOPROPELLANT-HYDRAZINE NOZZLE WEIGHT VERSUS PROPELLANT FLOW RATE

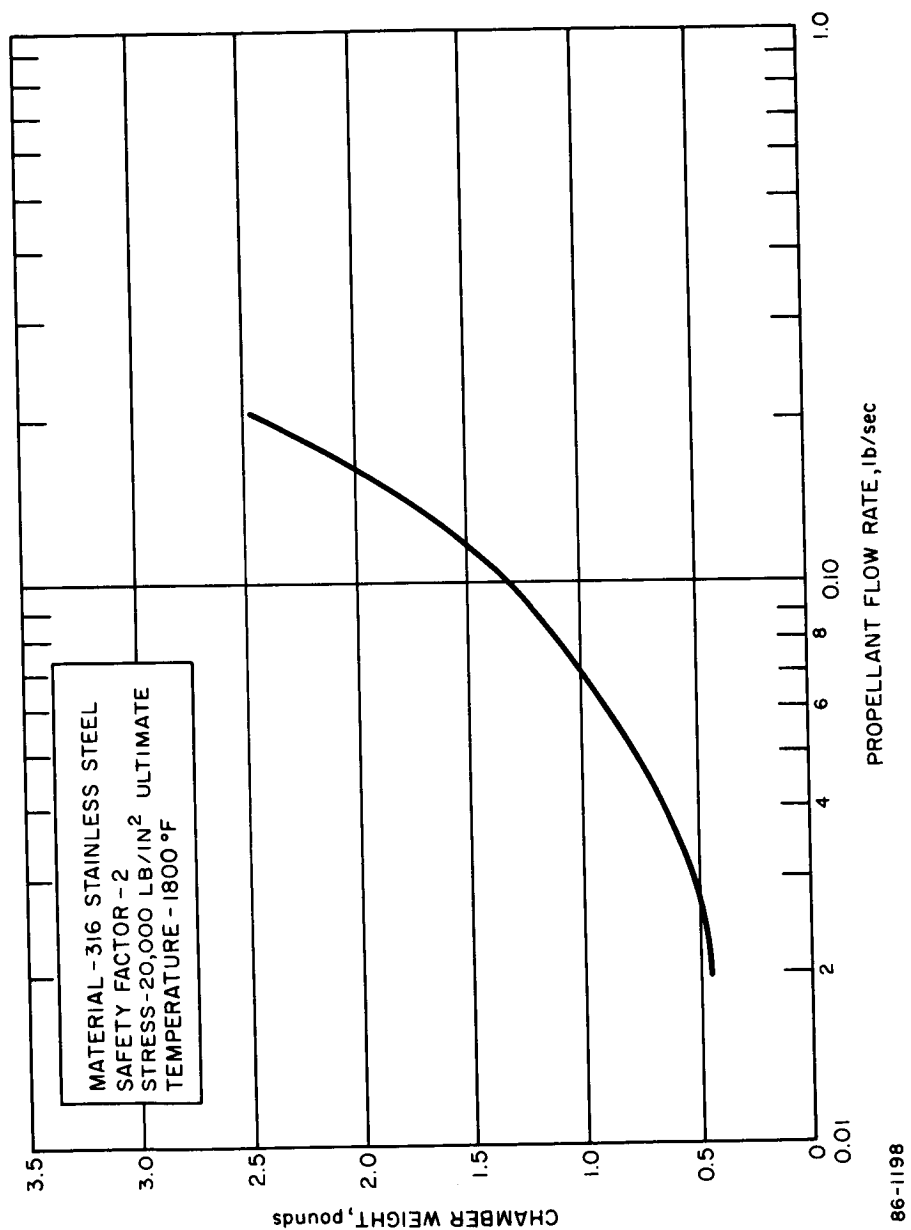


Figure F-3 MONOPROPELLANT-HYDRAZINE CHAMBER WEIGHT VERSUS PROPELLANT FLOW RATE

Nozzle Section = 0.08 pound

Catalyst Chamber = 0.8 pound

Solenoid Valve = 0.5 pound

Mounting Plate (est.) = 0.25 pound

Total Motor Assembly = 1.63 pounds

### 3.0 PROPELLANT STORAGE TANK SIZE

The weight of  $N_2H_4$  ( $W_f$ ) required in each tank is:

$$W_f = \frac{I_{total}}{I_{spec}} = \frac{1062 \text{ lb-sec}}{235 \text{ sec}} = 4.52 \text{ pounds}$$

where

$I_{total}$  = total impulse required

$I_{spec}$  = fuel specific impulse (235 seconds)

The volume of fuel ( $V_f$ ) is calculated using the fuel weight and specific volume ( $v_f$ ) as:

$$V_f = W_f v_f = (4.52)(27.5) = 124.2 \text{ in.}^3$$

The propellant tank weight is found from Figure F-4 assuming a 0.020-inch wall thickness

$$\frac{W_T}{V_f} = 0.0045$$

or

$$W_T = 0.0045 (124.2) = 0.56 \text{ pound}$$

Assuming that the bladder weight is 20 percent of the tank weight, the total propellant tank weight is calculated as

$$W_T = 1.2 (0.56) = 0.67 \text{ pound}$$

The above tank weight assumes a safety factor of 2 : 1. Assuming that sterilization will require twice the wall thickness, the weight of the tank is doubled.

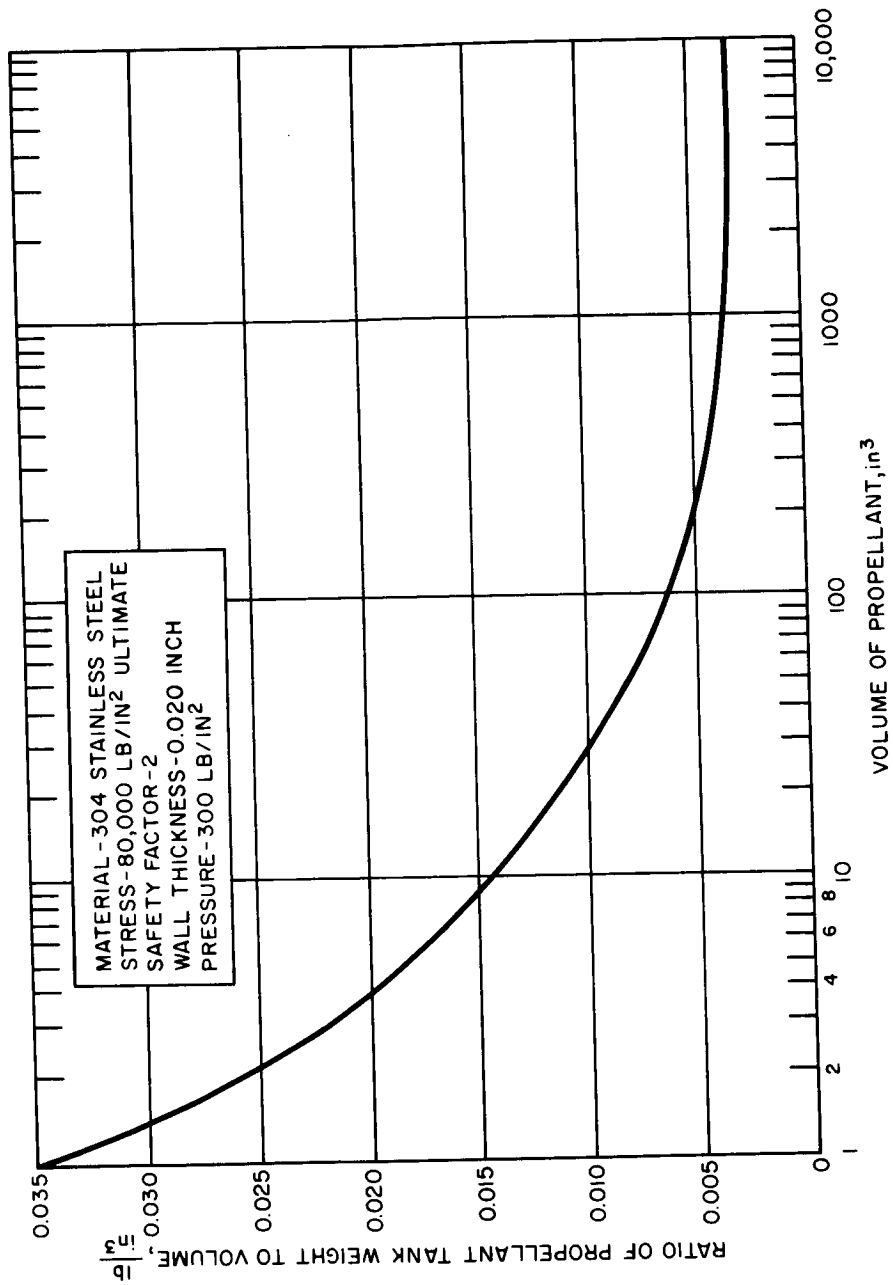


Figure F-4 PROPELLANT TANK WEIGHT TO VOLUME RATIO VERSUS PROPELLANT VOLUME

$$W_T = 1.34 \text{ pounds}$$

The approximate tank O. D. is calculated as 6.3 inches

#### 4.0 NITROGEN PRESSURE VESSEL SIZE

Figure F-5 gives the value of the ratio of pressure vessel plus nitrogen weight to propellant volume for any charging pressure greater than 1750 lb/in.<sup>2</sup> as:

$$\frac{W_{GN_2} + W_{GN_2 \text{ tank}}}{V_f} \approx 0.0035$$

or

$$W_{GN_2} + W_{GN_2 \text{ tank}} = 0.0035 (124.2) = 0.435 \text{ pound}$$

The above weight is doubled to anticipate sterilization pressures giving

$$W_{GN_2} + W_{GN_2 \text{ tank}} = 0.87 \text{ pound}$$

The volume of the spherical GN<sub>2</sub> pressure vessel ( $V_{GN_2}$ ) is calculated as:

$$V_{GN_2} = \frac{V_f k p_f}{P_1 - P_2} \quad (\text{adiabatic expulsion})$$

where

$$p_f = \text{fuel pressure} = 300 \text{ lb/in.}^2$$

$$P_1 = \text{initial GN}_2 \text{ pressure} = 3000 \text{ lb/in.}^2$$

$$P_2 = \text{final GN}_2 \text{ pressure} = 600 \text{ lb/in.}^2$$

$$k = \text{GN}_2 \text{ ratio of specific heats} = 1.4$$

$$V_f = \text{volume of propellant} = 124.2 \text{ in.}^3$$

substituting:

$$V_{GN_2} = 21.7 \text{ in.}^3$$

The approximate diameter of the vessel is calculated as 3.6 inches.

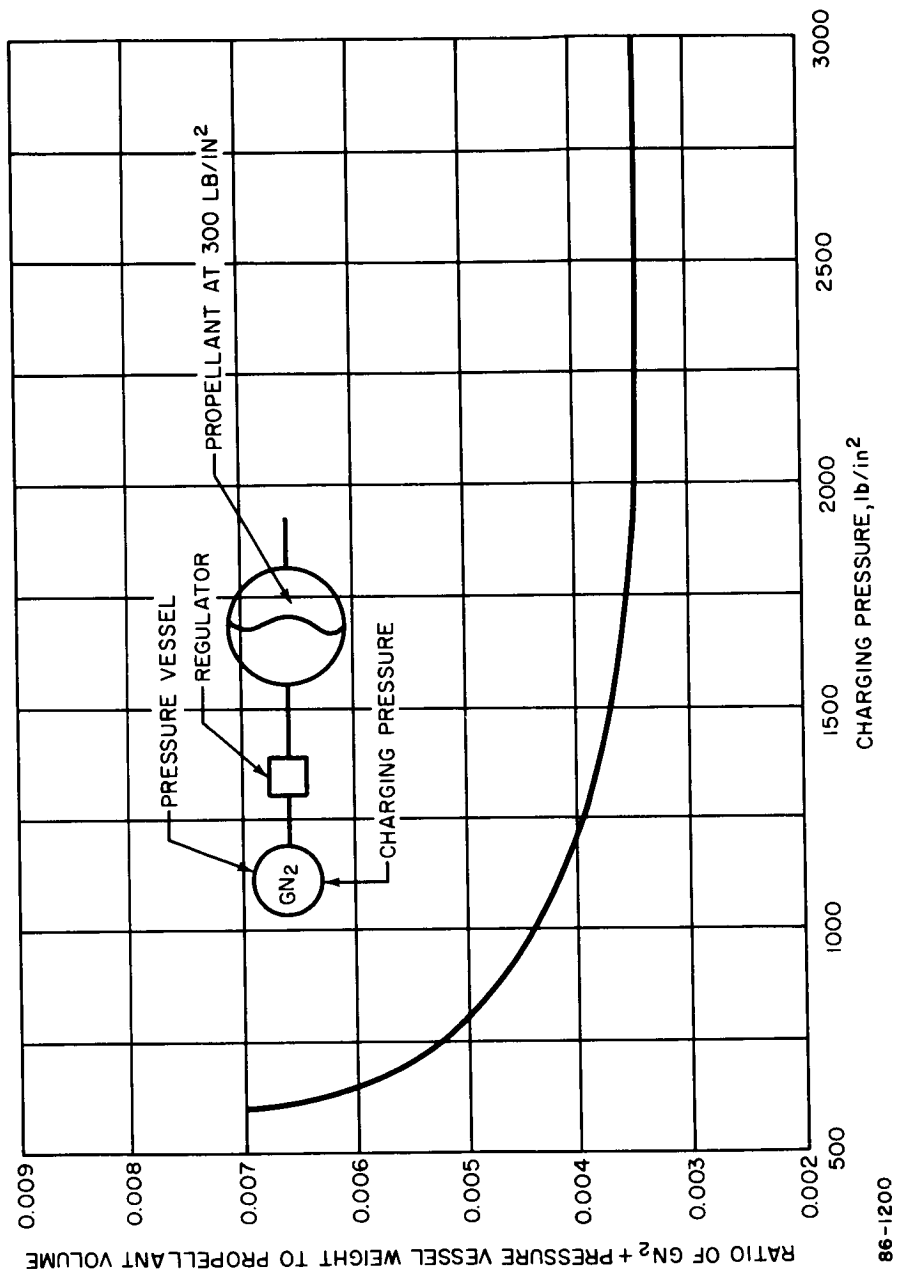


Figure F-5 ADIABATIC EXPULSION PROCESS RATIO OF GN<sub>2</sub> PRESSURE VESSEL WEIGHT TO PROPELLANT VOLUME VERSUS CHARGING PRESSURE

## 5.0 TOTAL SYSTEM WEIGHT BREAKDOWN

<u>Item</u>	<u>Nomenclature</u>	<u>Wt/unit (pounds)</u>	<u>No. Required</u>	<u>Total (pounds)</u>
1	Rocket Motor	1.63	8	13.04
2	Hydrazine Fuel	4.52	2	9.04
3	Propellant Storage Tank	1.34	2	2.68
4	GN <sub>2</sub> + pressure vessel	0.87	2	1.74
5	GN <sub>2</sub> pressure regulator	1.50*	2	3.00
6	Squib Valve	0.70*	2	1.40
7	Tubing, Fittings, etc.	estimated		4.00

Total system weight = 34.90

System Weight  $\approx$  35 pounds.

---

\* Estimates based on representative manufactured components.

## APPENDIX G

### BIPROPELLANT HYDRAZINE-NITROGEN TETROXIDE SYSTEM CALCULATIONS

#### 1.0 SYSTEM REQUIREMENTS

(1) Total impulse stored = 1062 lb sec in each subsystem

(2) Four 13-pound motors in each subsystem or total = 8

#### 2.0 PROPELLANT ( $N_2 H_4 + N_2 O_4$ ) WEIGHT AND VOLUME

Assuming a propellant specific impulse of 300 seconds, the propellant weight ( $W_p$ ) is:

$$W_p = \frac{1062 \text{ lb-sec}}{300 \text{ sec}} = 3.54 \text{ pounds.}$$

The fuel weight is calculated using the formula:

$$W_f = \frac{W_p}{R + 1}$$

where

$$W_f = N_2 H_4 \text{ weight}$$

$$W_p = N_2 H_4 + N_2 O_4 \text{ weight}$$

$$R = \text{mixture ratio (weight } N_2 O_4 / \text{weight } N_2 H_4) = 2.15$$

$$W_o = N_2 O_4 \text{ weight}$$

$$\therefore W_f = \frac{3.54}{2.15 + 1} = \underline{1.12 \text{ pounds}}$$

and

$$W_o = W_f R = 1.12 (2.15) = \underline{2.42 \text{ pounds.}}$$

The volume of fuel and oxidizer to be stored is calculated by multiplying weight by specific volume to find:

$$V_f = 1.12 (27.5) = 30.8 \text{ in}^3$$

$$V_o = 2.42 (19.3) = 46.7 \text{ in}^3$$

The respective tank diameters are calculated as approximately:

Fuel Tank O. D. = 4.0 inches

Oxidizer Tank O. D. = 4.5 inches.

### 3.0 FUEL STORAGE TANK SIZE

The fuel tank weight ( $W_{ft}$ ) is found from Figure F-4 of Appendix F assuming 0.020-inch wall thickness.

$$\frac{W_{ft}}{V_f} \approx 0.010 \text{ or } W_{ft} = 0.308 \text{ pound.}$$

Assuming sterilization pressure requires twice the wall thickness, the tank weight becomes 0.62 pound.

The final fuel storage tank weight is found by the assumption that the bladder weight is 20 percent of the tank weight giving:

$$W_{ft} = 1.20 (0.62) = \underline{0.75 \text{ pound.}}$$

### 4.0 OXIDIZER STORAGE TANK SIZE

The oxidizer tank weight ( $W_{ot}$ ) is found in a similar manner as described previously for the fuel tank.

$$W_{ot} = (0.009) (46.7) = 0.42 \text{ pound.}$$

With sterilization:  $W_{ot} = 0.84 \text{ pound}$

With the bladder:  $\underline{W_{ot} = 1.00 \text{ pound.}}$

### 5.0 NITROGEN PRESSURE VESSEL SIZE

From Figure F-5 Appendix F for an adiabatic expulsion process:

$$\frac{W_{GN_2} + W_{GN_2 \text{ tank}}}{V_p} = 0.0035$$

and

$$V_p = V_o + V_f = 77.5 \text{ in.}^3$$

$$W_{GN_2} + W_{GN_2} \tan K = (77.5) (0.0035) = 0.27 \text{ pound}$$

assuming a weight multiple of two for sterilization

$$W_{GN_2} + W_{GN_2} \tan K = 0.54 \text{ pound .}$$

The size of the spherical pressure vessel is calculated as follows:

Assuming an adiabatic expulsion process, the  $GN_2$  pressure vessel volume is expressed as:

$$V_{GN_2} = \frac{V_p k p_p}{p_1 - p_2}$$

where

$$p_p = \text{fuel pressure} = 300 \text{ lb/in.}^2$$

$$p_1 = \text{initial } GN_2 \text{ pressure} = 3000 \text{ lb/in.}^2$$

$$p_2 = \text{final } GN_2 \text{ pressure} = 600 \text{ lb/in.}^2$$

$$k = GN_2 \text{ ratio of specific heats} = 1.4$$

$$V_p = \text{propellant volume} = 77.5 \text{ in.}^3$$

$$V_{GN_2} = \frac{77.5 (1.4) (300)}{3000 - 600} = 13.5 \text{ in.}^3$$

The approximate O. D. is calculated as 3 inches.

## 6.0 ROCKET MOTOR SIZE

Reference to Figure G-1' shows that the weight of a 13-pound thrust motor is 1.0 pound.

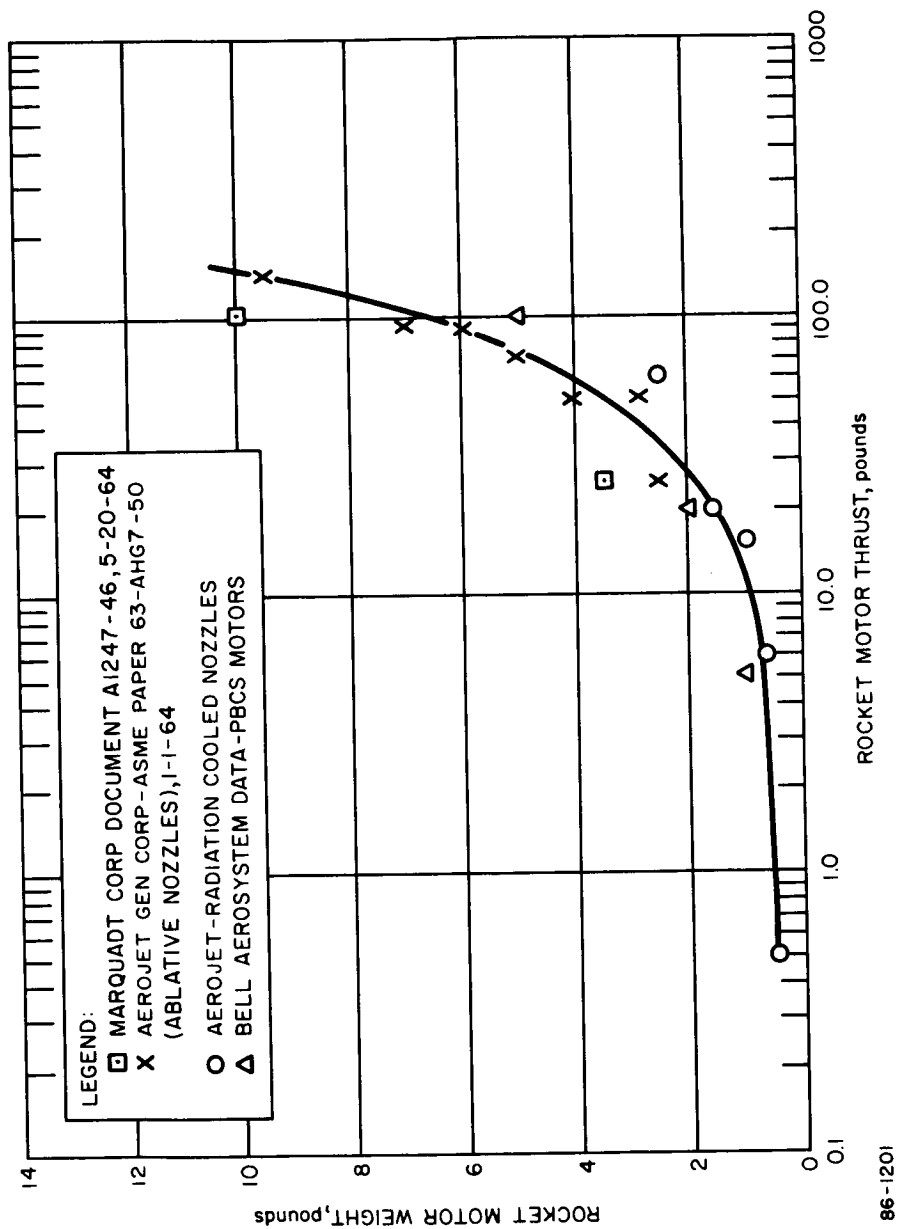


Figure G-1 BIPROPELLANT ROCKET MOTOR WEIGHT VERSUS THRUST

## 7.0 TOTAL SYSTEM WEIGHT BREAKDOWN

Item	Nomenclature	Weight Unit (pounds)	No. Required	Total Pounds
1.	Rocket Motor	1.0	8	8.00
2.	Hydrazine Fuel	1.12	2	2.24
3.	Hydrazine Tank	0.75	2	1.50
4.	Oxidizer	2.42	2	4.84
5.	Oxidizer Tank	1.00	2	2.00
6.	GN <sub>2</sub> + Pressure Regulator	0.54	2	1.08
7.	GN <sub>2</sub> Pressure Regulator	1.50*	2	3.00
8.	Squib Valve	0.7*	2	1.40
9.	Tubing, Fittings, etc.		estimated	<u>8.00</u>

Total Weight = 32.06

System Weight  $\cong$  32 pounds

---

\* Estimates based on representative manufactured components.

## APPENDIX H

### FLEXURE GIMBAL SYSTEM SIZING CALCULATIONS

This Appendix contains the calculations for the system compared in the trade-off studies, (see Section 7.3.3.6).

Figure H-1 illustrates the flexure-gimbal system geometry where representative values were chosen for the critical dimensions.

The assumptions taken are listed as:

- (1) The compliance of the flexure is negligible
- (2) Only small angular displacements of the  $\Delta V$  motor will be examined
- (3) The  $\Delta V$  thrust vector passes through the  $\Delta V$  motor center of mass "C".
- (4) The maximum operating frequency of the system shall not exceed 10 cps.

For small values of  $\theta$  the displacements  $CC'$  and  $AA'$  may be written as:

$$CC' = \theta OC \text{ and } AA' = \theta OA$$

The maximum required deflection is determined by the maximum disturbance torque to be counteracted. From the text, this value is given as:

$$(7.5)(13) = 97.5 \text{ ft-lb}$$

Equating the control torque and disturbance torques gives:

$$F_o \sin \theta_{\max}(1) = 97.5 \text{ ft-lb.}$$

where

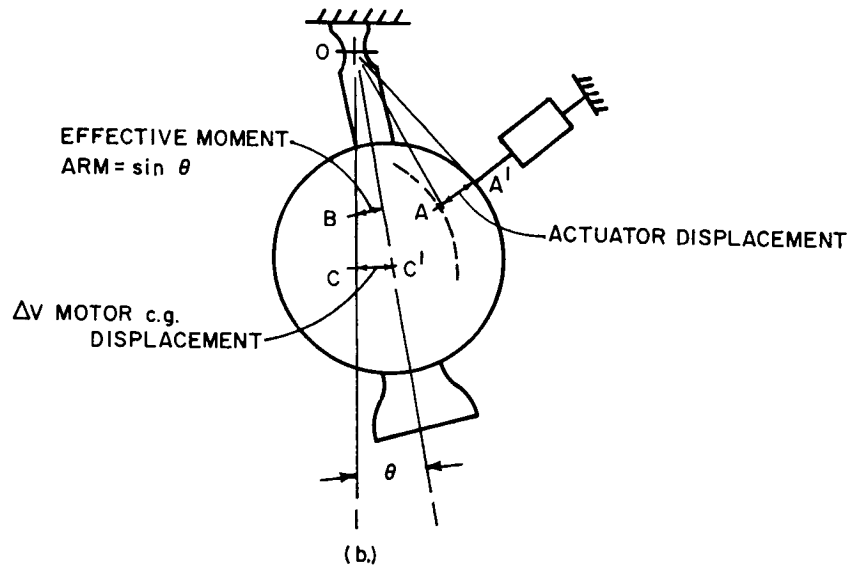
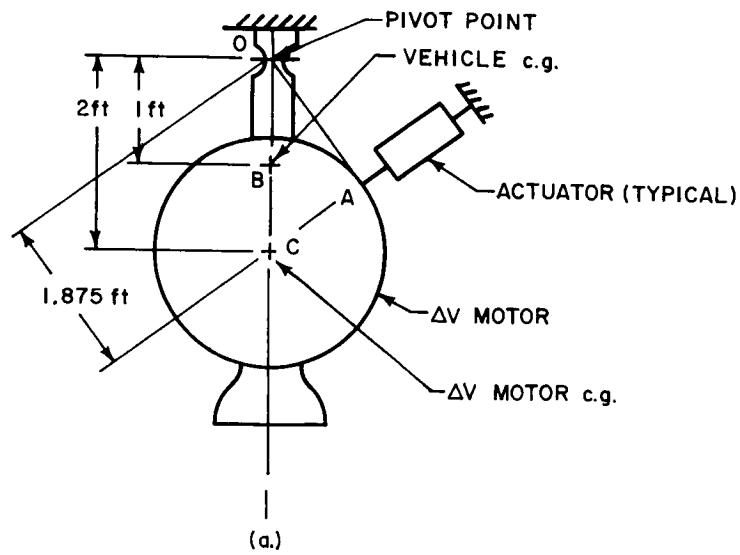
$$F_o = \Delta V \text{ motor thrust} = 3175 \text{ pounds}$$

$$\text{for small angles, } 3175 \theta_{\max} = 97.5$$

solving for  $\theta_{\max}$ ,

$$\theta_{\max} = \frac{97.5}{3175} \text{ radians} = 0.0307 \text{ rad.} = 1.76 \text{ degrees}$$

letting  $CC' = c$  and  $AA' = a$



86-1202

Figure H-1 FLEXURE GIMBAL DEFLECTION GEOMETRY

$$c_{\max} = OC \theta_{\max} = 2(0.0307) = 0.0614 \text{ foot} \cong 0.74 \text{ inch}$$

$$a_{\max} = OA \theta_{\max} = 1.875 (0.0307) = 0.0576 \text{ foot} \cong 0.69 \text{ inch}$$

Assuming that peak displacements are 10 percent of maximum values with sinusoidal operation, peak values are written as:

$$C_o = 0.1 c_{\max} = 0.074 \text{ inch or } 0.00614 \text{ foot}$$

$$A_o = 0.1 a_{\max} = 0.069 \text{ inch or } 0.00576 \text{ foot}$$

Equating the torques applied to the  $\Delta V$  motor gives:

$$F_a (OA) = (OC) M \ddot{c} \quad (1)$$

where

$$F_a = \text{force exerted by an actuator on the motor (pounds)}$$

$$M = \Delta V \text{ motor mass} - 18.65 \frac{\text{lb-sec}^2}{\text{ft}}$$

Furthermore, for sinusoidal motion:

$$\ddot{c} = -\omega^2 C_o \sin \omega t \quad (2)$$

$$\ddot{a} = -\omega^2 A_o \sin \omega t \quad (3)$$

rearranging Equation (1) gives:

$$F_a = \frac{OC}{OA} M \ddot{c}$$

and substituting from Equations (2) and (3)

$$\ddot{c} = \ddot{a} \cdot \frac{C_o}{A_o} = \frac{\ddot{a} (OC) \theta_{\max} (0.1)}{(OA) \theta_{\max} (0.1)} = \ddot{a} \frac{OC}{OA}$$

giving:

$$F_a = \left( \frac{OC}{OA} \right)^2 M \ddot{a}$$

further substitution of  $\ddot{a}$  from Equation (3) gives:

$$F_a = - \left( \frac{OC}{OA} \right)^2 M \omega^2 A_o \sin \omega t$$

solving for  $F_a$  (max value)

$$F_a = - \left( \frac{2}{1.875} \right)^2 18.65 [10 (2 \pi)]^2 (0.00576) (1) = 483 \text{ pounds}$$

The effective area of an actuator  $A_a$  with an assumed supply pressure of 1000 lb/in.<sup>2</sup> is calculated as:

$$A_a = \frac{483}{1000} = 0.483 \text{ in.}^2$$

The volume of fluid required to operate the system is based on examination of the case where one pair of actuators must articulate the motor from the null position to a peak displacement of  $C_o$  sinusoidally for 35 seconds at 10 cps.

The total swept volume is:

$$2 A_a A_o (35) (10) \text{ in.}^3$$

or

$$2 (0.483) (0.069) (35) (10) = 23.3 \text{ in.}^3$$

For two pairs of actuators (pitch and yaw control) the required fluid is  $2(23.3)$  = 46.6 in.<sup>3</sup>

The required storage tank internal radius ( $r_i$ ) is:

$$r_i = \sqrt[3]{\frac{3 (46.6)}{4 \pi}} = 2.23 \text{ inches}$$

Applying the hoop stress formula with the assumptions of maximum pressure = 3000 lb/in.<sup>2</sup> and maximum stress = 80,000 lb/in.<sup>2</sup>, the wall thickness is found as:

$$t = \frac{P_{\max} r_i}{2 \sigma_{\max}} = \frac{3000 (2.23)}{160,000} = 0.042$$

The tank dimensions are therefore:

$$\text{O.D.} = 4.54 \text{ inches} \quad \text{I.D.} = 4.46 \text{ inches}$$

The tank weight is calculated as:

$$W_T = \frac{\pi \rho T}{6} [(O.D.)^3 - (I.D.)^3]$$

where

$W_T$  = tank weight

$\rho_T$  = density of tank material =  $0.16 \frac{\text{lb}}{\text{in.}^3}$  ( $T_i$  alloy)

substituting:

$$W_T = \frac{\pi (0.16)}{6} [(4.54)^3 - (4.46)^3] = 0.42 \text{ pound}$$

allowing 30 percent for bosses, bladder assembly, and mounting brackets:

$$W_T = 0.42 + 0.13 = 0.55 \text{ pound}$$

The weight of fluid is calculated using a fluid specific gravity of 0.7 as a representative value.

$$W_F = 0.7 \left( \frac{62.4}{1728} \right) \frac{\text{lb}}{\text{in.}^3} (46.6) \text{ in.}^3 \approx 1.2 \text{ pounds}$$

The  $\text{GN}_2$  pressurant vessel is sized assuming an isothermal process in expelling the fluid from the fluid storage tank.

Assuming pressure limits of 1500 and 1000 lb/in.<sup>2</sup> in the  $\text{GN}_2$  vessel the expression  $PV = \text{constant}$  gives:

$$P_i V_i = P_f V_f$$

where

$P_i$  = initial  $\text{GN}_2$  pressure = 1500 lb/in.<sup>2</sup>

$P_f$  = final  $\text{GN}_2$  pressure = 1000 lb/in.<sup>2</sup>

$V_i$  = the  $\text{GN}_2$  initial volume (volume of  $\text{GN}_2$  vessel)

$V_f$  = final  $\text{GN}_2$  volume =  $V_i + 46.6 \text{ in.}^3$

Solving for  $V_i$  :

$$V_i = \frac{1000}{1500} (V_i + 46.6)$$

or

$$V_i = 93.2 \text{ in.}^3$$

The inside radius required is:

$$r = \sqrt[3]{\frac{3(93.2)}{4\pi}} = 2.82 \text{ inches}$$

or the vessel I.D. = 5.64 inches

Assuming that the  $\text{GN}_2$  vessel is sterilized in a pressurized condition, the wall thickness is calculated for the corresponding higher pressure and lower material ultimate strength.

As a constant volume process the perfect gas equation of state gives:

$$\frac{P_1}{T_1} = \frac{P_2}{T_2}$$

where

$P_1$  = 1500 lb/in.<sup>2</sup> initial pressure

$T_1$  = 520°R initial temperature

$T_2$  = 760°R assumed sterilization temperature

$P_2$  = sterilization pressure

solving for  $P_2$  gives:

$$P_2 = \left( \frac{1500}{520} \right) 760 = 2190 \text{ lb/in.}^2$$

With the ultimate strength of  $T_i$  alloy at 300°F taken as 135,000, applying the hoop-stress formula gives the wall thickness  $t$  as:

$$t = \frac{2190(2.82)}{135,000} = 0.046 \text{ inch}$$

The vessel O.D. is, therefore,  $5.64 + 2(.046) = 5.73$  inches.

Calculating the vessel weight gives:

$$W_V = \frac{\pi(0.16)}{6} [(5.73)^3 - (5.64)^3] = 0.76 \text{ pounds}$$

Allowing 30 percent for bosses and mounting brackets:

$$W_V = 0.76 + 0.23 \approx 1.0 \text{ pound}$$

The weight of the  $\text{GN}_2$  stored initially in the pressure vessel is:

$$93.2 \text{ in.}^3 (0.007375 \text{ lb/in}^3) = 0.69 \text{ pound}$$

The fluid dump tank is assumed to be the same size as the storage tank.

The final system weight breakdown is:

Item	Nomenclature	Unit Weight (pounds)	No. Required	Total Weight
1	Actuator	0.66	8	5.28
2	Squib Valve	0.37	2	0.74
3	$\text{GN}_2$ Pressurant	0.7	2	1.4
4	Vessel Manifold	0.25	2	0.5
5	Fluid	1.2	2	2.4
6	Fluid Storage Tank	0.6	2	1.2
7	Filter	0.25	4	1.0
8	Control Valve	0.75	8	6.0
9	$\text{GN}_2$ Pressure Vessel	1.0	2	2.0
10	Tubing Complex	5.6	2	11.2
11	Dump Tank	0.6	2	<u>1.2</u>
Total System Weight =				32.92 pounds

Total Weight = 33 pounds

## APPENDIX I

### COLD GAS SYSTEM SIZING CALCULATIONS\*

#### 1.0 STORED IMPULSE REQUIREMENT

The system must store impulse for both the attitude and thrust vector control maneuvers. The minimum total impulse required is:

Assumed average value for the ACS = 50 lb-sec

TVC requirement = 644 lb-sec

Total Impulse Required = 694 lb-sec

Providing the necessary safety margin against failure modes, the impulse requirement for each pressure vessel ( $I_t$ ) is:

$$I_t = 694 \times 1.5 \times 1.1 = 1145 \text{ lb-sec}$$

Assuming an average specific impulse of 60 seconds the weight of  $\text{GN}_2$  expelled is found to be:

$$\Delta W_{\text{GN}_2} = \frac{1145 \text{ lb-sec.}}{60 \text{ sec}} = 19.1 \text{ pounds.}$$

The weight of  $\text{GN}_2$  expelled may be expressed as:

$$\Delta W_{\text{GN}_2} = V_V (\rho_i - \rho_f)$$

where

$V_V$  = volume of pressure vessel in. <sup>3</sup>

$\rho_i$  = initial  $\text{GN}_2$  density lb/in. <sup>3</sup>

$\rho_f$  = final  $\text{GN}_2$  density lb/in. <sup>3</sup>

Assuming an initial charge pressure of 3000 lb/in. <sup>2</sup> and a final pressure of 200 lb/in. <sup>2</sup>, real-gas data tables give the value of density as:

---

\* The calculations in this Appendix are for the system compared in the tradeoff studies, (See paragraph 7.3.3.7). The reference design cold-gas reaction system calculations are contained in Appendix D.

$$\rho_i = 8.08 \times 10^{-3} \text{ lb/in.}^3 \text{ at } 60^\circ\text{F}$$

$$\rho_f = 0.56 \times 10^{-3} \text{ lb/in.}^3 \text{ at } 60^\circ\text{F}^*$$

The volume of the pressure vessel is therefore found as:

$$V_V = \frac{\Delta W_{\text{GN}_2}}{\rho_i - \rho_f} = \frac{19.1 \times 10^3}{(8.08 - 0.56)} = 2540 \text{ in.}^3$$

The weight of  $\text{GN}_2$  stored initially in both pressure vessels is:

$$W_{\text{GN}_2} = 2 (V_V) \rho_i \text{ pounds}$$

$$W_{\text{GN}_2} = 2 (2540) (8.08 \times 10^{-3}) = 41 \text{ pounds.}$$

The inside radius of the vessel is:

$$r = \sqrt[3]{\frac{3 V_V}{4\pi}} = \sqrt[3]{\frac{0.75}{\pi}} (2540) = 8.45 \text{ inches}$$

or the vessel I. D. = 16.90 inches.

Applying the "hoop stress" formula gives the wall thickness:

$$t = \frac{P_i r}{2S}$$

where

$$P_i = \text{maximum vessel pressure} = 3000 \text{ lb/in.}^2$$

$$S = \text{maximum working stress level, assumed to be } 80,000 \text{ lb/in.}^2$$

$$t = \text{wall thickness inches}$$

substituting gives

$$t = \frac{3000 (8.45)}{160,000} = 0.158 \text{ inches.}$$

\* An isothermal process is assumed, since only a small density change will be experienced due to the temperature drop associated with the actual polytropic expansion for this system. The density refinement realized from polytropic considerations is therefore not warranted for these system tradeoff studies but should be, however, considered during the design of the reference system.

The vessel O. D. is therefore  $16.90 + 2(0.158) = 17.22$  inches.

The vessel weight is expressed as:

$$W_V = \frac{1}{6} \pi \rho_V [d_o^3 - d_i^3]$$

where

$W_V$  = weight of the vessel

$\rho_V$  = density of vessel material -  $0.16 \frac{\text{lb}}{\text{in.}^3}$  ( $T_i$  alloy)

$d_o$  = vessel O. D. = 17.22 inches

$d_i$  = vessel I. D. = 16.90 inches

substituting gives:

$$W_V = \frac{\pi(0.16)}{6} [(17.22)^3 - (16.9)^3] = 25 \text{ pounds}$$

adding 10 percent for the weight of bosses, the total pressure vessel weight becomes

$$W_V = 25 + 2.5 = 27.5 \text{ pounds.}$$

The prior vessel calculations must be modified to ensure an acceptable material stress level at the higher gas pressure caused by the sterilization temperature.

Assuming that  $300^\circ\text{F}$  is a representative sterilization temperature, the corresponding vessel pressure is found by entering the real-gas data tables at  $300^\circ\text{F}$  and the same gas density found for the vessel at  $3000 \text{ lb/in.}^2$  and  $60^\circ\text{F}$ .

The sterilization pressure found is  $4800 \text{ lb/in.}^2$ . In addition, the ultimate strength of the titanium alloy is reduced to  $135,000 \text{ lb/in.}^2$  at  $300^\circ\text{F}$ . The maximum working stress level is reduced to  $67,500 \text{ lb/in.}^2$  and again applying the hoop stress equation for the material thickness gives:

$$t = \frac{4800(8.45)}{135,000} = 0.30 \text{ inch.}$$

The vessel O. D. becomes  $16.90 + 2(0.30) = 17.50$  inches.

The vessel weight is calculated as:

$$W_{VS} = \frac{\pi (0.16)}{6} [(17.5)^3 - (16.9)^3] = 44.5 \text{ pounds.}$$

Again taking 10 percent to allow for boss weight, the final vessel weight is:

$$W_{VS} = 44.5 + 4.45 = 48.95 \text{ pounds.}$$

The regulator size is based on an estimated output pressure of approximately 100 lb/in.<sup>2</sup> and the maximum required GN<sub>2</sub> weight flow rate.

Assuming simultaneous pitch, yaw, and roll thrust commands, the total thrust supplied by a regulator is:

Pitch thrust = 13 pounds

Yaw thrust = 13 pounds

Roll thrust = 1 pound

Total = 27 pounds

the required flow rate is:

$$W_{GN_2} = \frac{27 \text{ lb}}{60 \text{ sec}} = \frac{F}{I_{sp}} = 0.45 \text{ lb/sec}$$

A representative regulator weight based on typical manufactured hardware is 6.2 pounds.

The system weight breakdown is given as:

Item	Nomenclature	Unit Weight (pounds)	No. Required	Total (pounds)
1	Nozzle Valve	1.8	12	21.6
2	Pressure Vessel	48.95	2	97.9
3	GN <sub>2</sub>	20.5	2	41.0
4	Squib Valve*	1.3	2	2.6
5	Tubing Complex	3.0	2	6.0
6	Regulator*	6.2	2	12.4
7	Filter*	0.70	4	2.8
8	Vessel Manifold*	0.35	2	0.7
Total System Weight = 185 pounds				185.0 pounds

\* Estimated values

## APPENDIX J

### GIMBAL ANGLE COORDINATE TRANSFORMATION FOR CAMERA POINTING

This appendix contains a discussion of aligning the optical axis of the television camera with the local vertical. Equations are derived which relate the camera gimbal angles to six known Euler angles. A two-gimbal system for the camera is seen to be sufficient.

The transformation from inertial  $(X_I, y_I, Z_I)$  to body coordinates  $(X_B, y_B, Z_B)$  is given in Figure J-1. A four-gimbal system with the rotation sequence  $\psi$  about  $Z_I$ ,  $\phi_i$  about  $X'$ ,  $\theta$  about  $y''$ ,  $\phi_o$  about  $X_B$  is assumed. One can readily show that the transformation matrix,  $\underline{A}$ , relating  $\{X_B, y_B, Z_B\}$  to  $\{X_I, y_I, Z_I\}$  is:

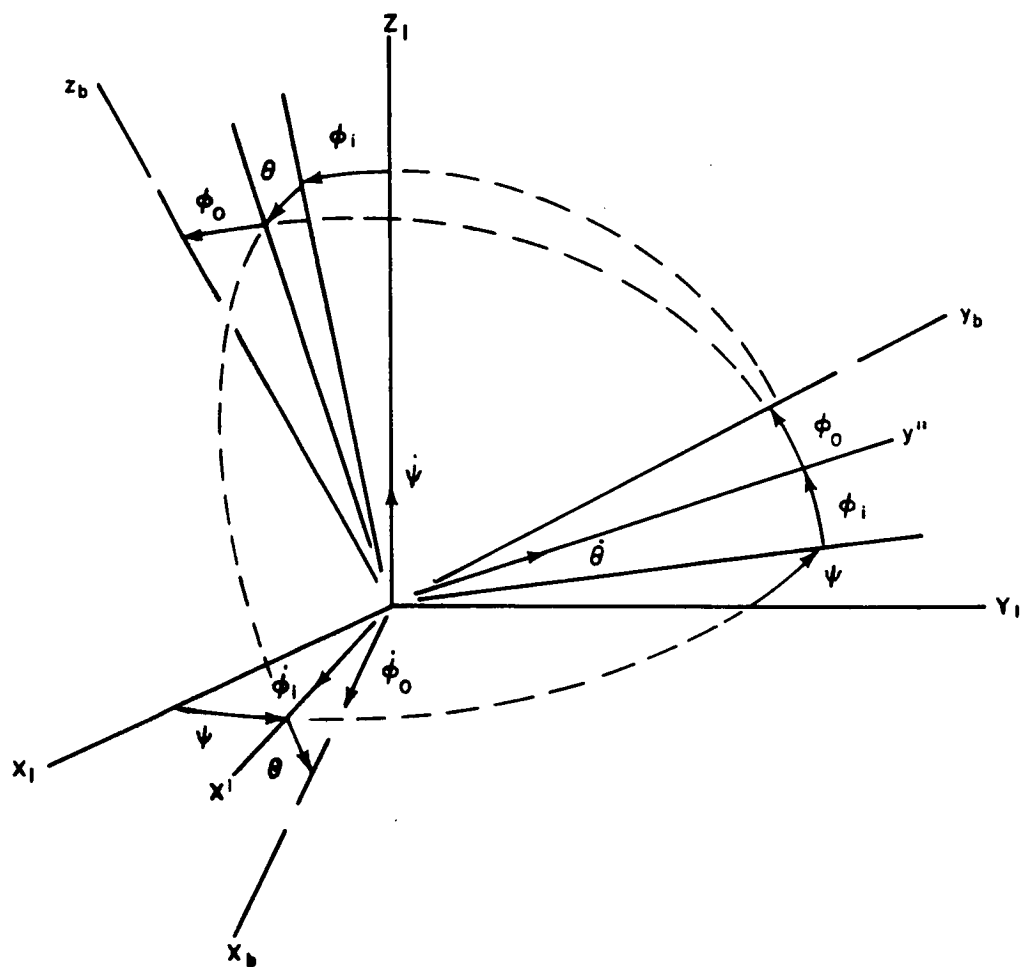
$$\underline{A} = \begin{bmatrix} \cos \theta \cos \psi - \sin \theta \sin \phi_i \sin \psi & \cos \theta \sin \psi + \sin \theta \sin \phi_i \cos \psi & -\sin \theta \cos \phi_i \\ \sin \phi_o \sin \theta \cos \psi - \cos \phi_o \cos \phi_i \sin \psi & \sin \phi_o \sin \theta \sin \psi + \cos \phi_o \cos \phi_i \cos \psi & \cos \phi_o \sin \phi_i \\ + \sin \phi_o \cos \theta \sin \phi_i \sin \psi & -\sin \phi_o \cos \theta \sin \phi_i \cos \psi & + \sin \phi_o \cos \theta \cos \phi_i \\ \cos \phi_o \sin \theta \cos \psi + \sin \phi_o \cos \phi_i \sin \psi & \cos \phi_o \sin \theta \sin \psi - \sin \phi_o \cos \phi_i \cos \psi & -\sin \phi_o \sin \phi_i \\ + \cos \phi_o \cos \theta \sin \phi_i \sin \psi & -\cos \phi_o \cos \theta \sin \phi_i \cos \psi & + \cos \phi_o \cos \theta \cos \phi_i \end{bmatrix}$$

From Figure J-2 it is seen that the camera line-of-sight coordinate is related to the body coordinates  $(X_B, y_B, Z_B)$  by the matrix.

$$\underline{B} = \begin{bmatrix} \cos \beta & \cos \alpha & \sin \beta & -\cos \beta & \sin \alpha \\ -\sin \beta & \cos \alpha & \cos \beta & \sin \beta & \sin \alpha \\ \sin \alpha & 0 & \cos \alpha \end{bmatrix} \quad (2)$$

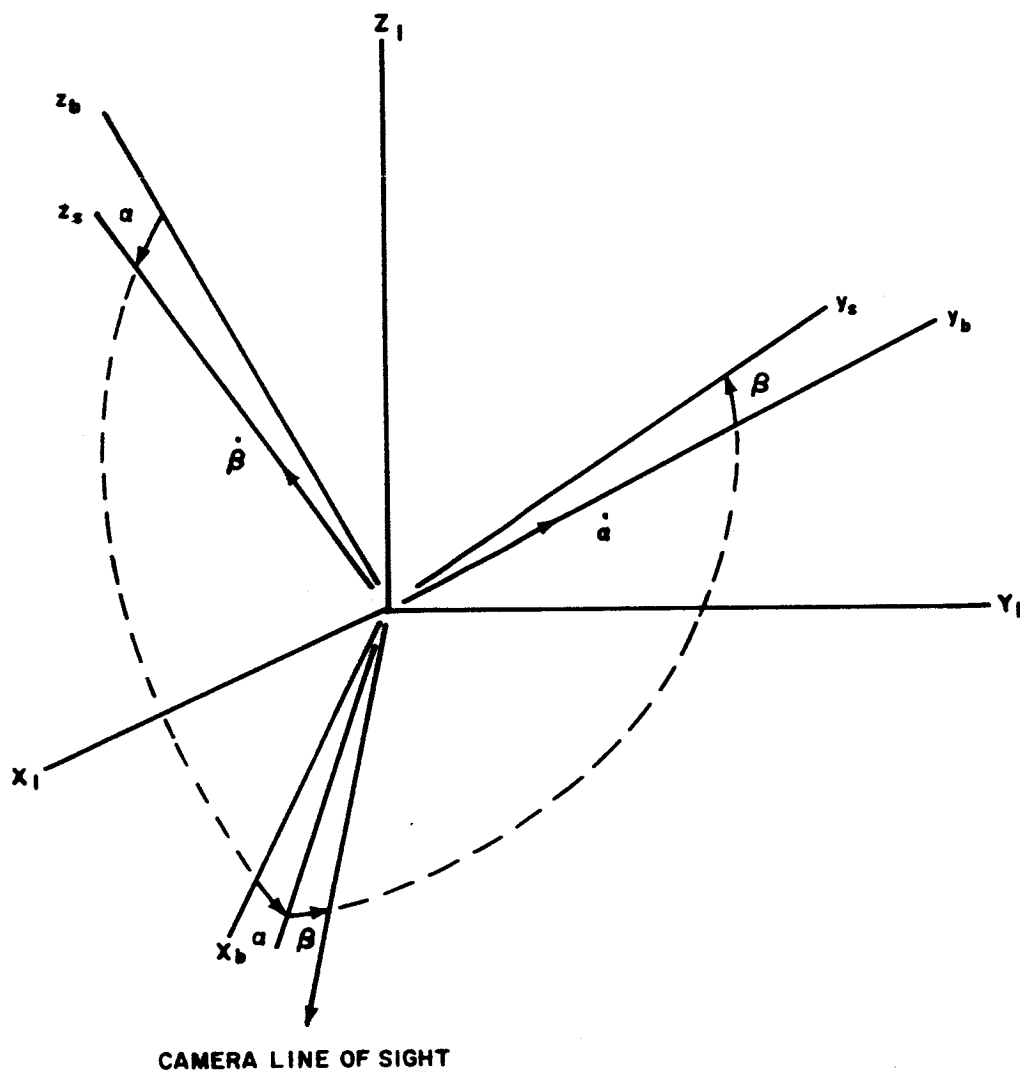
The orientation of the local vertical with respect to inertial coordinates  $(X_I, y_I, Z_I)$  is shown in Figure J-3. Similar to Equation (2) the matrix defining the relation between the local vertical coordinate system and inertial coordinates is:

$$\underline{C} = \begin{bmatrix} \cos \eta & \cos \gamma & \sin \eta & -\cos \eta & \sin \gamma \\ -\sin \eta & \cos \gamma & \cos \eta & \sin \eta & \sin \gamma \\ \sin \gamma & 0 & \cos \gamma \end{bmatrix} \quad (3)$$



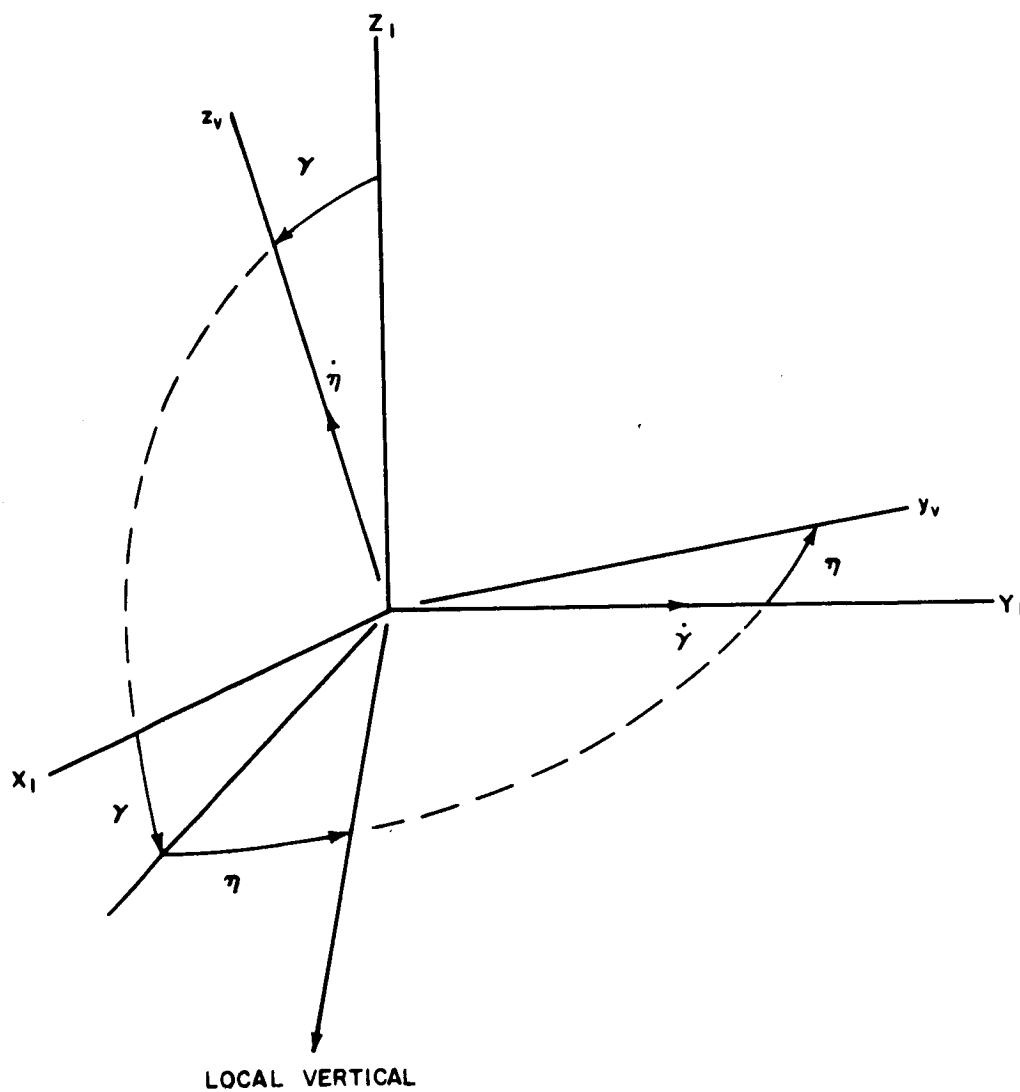
86-1203

Figure J-1 FOUR GIMBAL SYSTEM TRANSFORMATION



86-1204

Figure J-2 CAMERA LINE OF SIGHT TRANSFORMATION



86-1205

Figure J-3 LOCAL VERTICAL TRANSFORMATION

The following relations then exist:

$$\{LV, y_V, Z_V\} = \underline{C} \{X_I, y_I, Z_I\} \quad (4)$$

and

$$\{LS, y_S, Z_S\} = \underline{B} \underline{A} \{X_I, y_I, Z_I\} \quad (5)$$

Comparing Equation (4) with (5) it is seen that a necessary and sufficient condition for the camera line-of-sight to be aligned with the local vertical is that the elements of the first row of  $\underline{C}$  equal the corresponding elements of the product  $\underline{B} \underline{A}$ . Only the first row need be considered since rotations about the line-of-sight are permitted. Hence:

$$\begin{aligned} \cos \eta \cos \gamma &= (\cos \theta \cos \psi - \sin \theta \sin \phi_1 \sin \psi) \cos \beta \cos \alpha \\ &+ (\sin \phi_0 \sin \theta \cos \psi - \cos \phi_0 \cos \phi_1 \sin \psi + \sin \phi_0 \cos \theta \sin \phi_1 \sin \psi) \sin \beta \\ &- (\cos \phi_0 \sin \theta \cos \psi + \sin \phi_0 \cos \phi_1 \sin \psi + \cos \phi_0 \cos \theta \sin \phi_1 \sin \psi) \cos \beta \sin \alpha \end{aligned} \quad (6)$$

$$\begin{aligned} \sin \eta &= (\cos \theta \sin \psi + \sin \theta \sin \phi_1 \cos \psi) \cos \beta \cos \alpha \\ &+ (\sin \phi_0 \sin \theta \sin \psi + \cos \phi_0 \cos \phi_1 \cos \psi - \sin \phi_0 \cos \theta \sin \phi_1 \cos \psi) \sin \beta \\ &- (\cos \phi_0 \sin \theta \sin \psi - \sin \phi_0 \cos \phi_1 \cos \psi - \cos \phi_0 \cos \theta \sin \phi_1 \cos \psi) \cos \beta \sin \alpha \end{aligned} \quad (7)$$

$$\begin{aligned} -\cos \eta \sin \gamma &= -\sin \theta \cos \phi_1 \cos \beta \cos \alpha \\ &+ (\cos \phi_0 \sin \phi_1 + \sin \phi_0 \cos \theta \cos \phi_1) \sin \beta \\ &+ (\sin \phi_0 \sin \phi_1 - \cos \phi_0 \cos \theta \cos \phi_1) \cos \beta \sin \alpha \end{aligned} \quad (8)$$

Equations (6), (7), and (8) can be "solved" to yield expressions of the form

$$\cos \beta \cos \alpha = f \quad (9)$$

$$\sin \beta = g \quad (10)$$

$$\cos \beta \sin \alpha = h \quad (11)$$

where  $f, g, h$  are functions of the six known Euler angles.

Equations (9) - (11) while not uniquely defining the gimbal angles  $\alpha, \beta$  do yield one and only one orientation of the line of sight. Since there are three equations any ambiguity as to direction is resolved.

## APPENDIX K

### COMPUTATION OF REACTION CONTROL SYSTEM IMPULSE REQUIREMENTS

This appendix contains an estimate of the closed-loop reaction control system total impulse requirements for the Flight Capsule entry from orbit (see paragraphs 8.3.1 and 8.3.2). The analysis is divided into two portions. The first considers requirements during the orientation - limit-cycle mode of operation, while the second deals with stabilization during thrusting for the  $\Delta V$  correction.

#### 1.0 ORIENTATION - LIMIT-CYCLE MODE

##### 1.1 Stabilization of Initial Rates and Attitude Error

Assuming second-order dynamics, the minimum time to reduce the state of the system to zero is:

$$t_s = \frac{\dot{\theta}_o}{a} + 2 \sqrt{\frac{\theta_o}{a} + \frac{\dot{\theta}_o^2}{2a^2}} \quad (1)$$

where

$\theta_o, \dot{\theta}_o$  = initial attitude and rate errors (rad, rad/sec)

$a$  = control acceleration (rad/sec<sup>2</sup>)

The control acceleration using couples is given by:

$$a = \frac{2 F l}{I} \quad (2)$$

where

$F$  = thrust per nozzle (lb)

$l$  = control moment arm (feet)

$I$  = moment of inertia (slug-ft<sup>2</sup>)

The moments of inertia are

$$I_{XX} = 1063 \text{ slug-ft}^2$$

$$I_{YY} = I_{ZZ} = 673 \text{ slug-ft}^2$$

For a thrust level of 0.5 pound per nozzle on all axes and a moment arm of 88 inches, we then have

$$a_x = 0.40 \text{ deg/sec}^2$$

$$a_y = a_z = 0.62 \text{ deg/sec}^2$$

Letting  $\theta_o = 1$  degree and  $\dot{\theta}_o = 1$  degree per second about all axes, Equation (1) yields

$$t_{s_x} = 7 \text{ seconds}$$

$$t_{s_y} = t_{s_z} = 5 \text{ seconds}$$

Since we will not, in fact have optimum switching, the settling times are arbitrarily multiplied by two. With sequential stabilization the total time is

$$t = 10 + 10 + 14 = 34 \text{ seconds}$$

The total impulse required for stabilization is

$$I_t = 2 \times 0.5 \times 34 = 34 \text{ lb-sec}$$

## 1.2 Orientation

Two orientations are considered. The first is to attain the proper attitude for  $\Delta V$  thrusting. It is assumed that the vehicle will reorient 180 degrees in pitch and 90 degrees in roll from a zero rate initial state. The maneuver is rate limited to 1 degree per second. Orientation time is given by

$$t = \frac{\dot{\theta}_o}{a} + \frac{\dot{\theta}_L}{a} + \frac{\theta_o}{\dot{\theta}_L} + \frac{\dot{\theta}_o^2}{2 a \dot{\theta}_L} \quad (3)$$

where

$$\dot{\theta}_L = \text{limiting rate}$$

For pitch then, we have

$$t_y = 182 \text{ seconds}$$

and for roll

$$t_x = 93 \text{ seconds}$$

The total time is

$$t_{\text{total}} = 182 + 93 = 275 \text{ seconds} \approx 4.6 \text{ minutes}$$

The burn time for the rate limited maneuver is

$$t_b = \frac{\dot{\theta}_o + 2 \dot{\theta}_L}{a} \quad (4)$$

so

$$t_{b_x} = 5 \text{ seconds}, \quad t_{b_y} = 3 \text{ seconds.}$$

Total impulse =  $2 \times 0.5 \times 8 = 8 \text{ lb-sec}$  for the first orientation.

The second orientation is made in order to achieve a nominally zero angle of attack at entry. The configuration at entry is used; hence, the inertias are:

$$I_{xx} = 1055 \text{ slug-ft}^2$$

$$I_{yy} = I_{zz} = 597 \text{ slug-ft}^2$$

Then

$$a_x = 0.40 \text{ deg/sec}^2 \text{ (as before)}$$

$$a_y = a_z = 0.70 \text{ deg/sec}^2$$

For a pitch maneuver of 90 degrees and roll of 90 degrees,

$$t_y = 91 \text{ seconds}$$

$$t_x = 93 \text{ seconds}$$

so the total orientation time is 184 seconds or approximately 3 minutes.

The burn times are

$$t_{b_y} \approx 3 \text{ seconds}, \quad t_{b_x} = 5 \text{ seconds}$$

### 1.3 Limit Cycling

A pulse duration of 0.05 second is assumed. The impulse per cycle is given by:

$$I_{t_{LC}} = 2 \times 1 \times .05 = 0.1 \text{ lb-sec/cycle for all axes}$$

The limit cycle rate is

$$\dot{\theta}_{LC} = \frac{1}{2} a \Delta t \quad (5)$$

so

$$\begin{aligned} \dot{\theta}_{LC_x} &= 0.01 \text{ deg/sec} \\ \dot{\theta}_{LC_y} &= \dot{\theta}_{LC_z} = 0.018 \text{ deg/sec} \end{aligned}$$

The limit cycle period is

$$\tau_{LC} = \frac{4\theta_{LC}}{\dot{\theta}_{LC}} \quad (6)$$

$$\text{and } \theta_{LC_x} = 1 \text{ degree so } \tau_{LC_x} = 400 \text{ seconds}$$

$$\theta_{LC_y} = \theta_{LC_z} = 0.5 \text{ degree}$$

hence

$$\tau_{LC_y} = \tau_{LC_z} = 111 \text{ seconds}$$

The duration of limit cycling to entry is approximately 1 hour so the number of cycles are:

$$N_x = 9 \text{ cycles}$$

$$N_y = N_z \approx 32 \text{ cycles}$$

Total impulse for limit cycling during this phase is

$$I_t = 73 \times 0.1 = 7.3 \text{ lb-sec}$$

#### 1.4 Summary

A total impulse summary for this phase is shown in Table K-I

TABLE K-1

TOTAL IMPULSE SUMMARY

Mode	Impulse (lb-sec)
Stabilization	34
Orientation	16
Limit Cycling	8
Total	58 lb-sec

2.0 STABILIZATION DURING  $\Delta V$  THRUSTING

This section considers requirements imposed by disturbing torques developed by the  $\Delta V$  rocket motor. Due to the magnitude and durations of these torques an ancillary control system is used. Required thrust levels and total impulse are presented.

2.1 Pitch and Yaw Control

As developed in Reference 1, the variance of the disturbing torque in pitch and yaw is given by

$$\sigma_{\Delta T}^2 = F_e^2 (\sigma_{\Delta cg}^2 + \sigma_{\Delta R}^2 + L^2 \sigma_{\Delta \xi}^2) \quad (7)$$

where

$F_e$  = engine thrust (pounds)

$\sigma_{\Delta cg}$  = standard deviation of the vehicle c. g. location error (feet)

$\sigma_{\Delta R}$  = standard deviation of the rocket motor location error (feet)

$L$  = distance of rocket motor thrust application point from vehicle c. g. (feet)

$\sigma_{\Delta \xi}$  = standard deviation of the angular misalignment of the rocket motor thrust vector (radians)

---

Reference 1. Graves, E.C., Preliminary Disturbing Torque Analysis, TR GCCD-K220-607 27 October 1965.

The errors are

$$3\sigma_{\Delta R} = 0.06 \text{ inch}$$

$$3\sigma_{\Delta \xi} = 0.5 \text{ degree}$$

$$3\sigma_{\Delta c_g} = 0.5 \text{ inch}$$

and  $F_e = 3175$  pounds acting for 35 seconds. Since the rocket motor is located at the vehicle center of gravity,  $L \approx 0$ . From Equation (7) one obtains

$$3\sigma_{\Delta T} = 133 \text{ ft-lb}$$

for the 3-sigma value of disturbing torque in pitch and in yaw.

The control torque is given by

$$T_c = F_c l \quad (8)$$

where

$$F_c = \text{total control nozzle thrust (pounds)}$$

$$l = \text{control moment arm (7.3 feet)}$$

To simply balance the disturbing torque,  $F_{c_{\min}} = 18$  pounds. Multiplying this value by 1.4 to improve dynamic response, the thrust is 25 pounds total in pitch and in yaw, required for a single nozzle for control in each direction about each axis. If control redundancy is provided, an extra set of 25 pound nozzles to provide couples about each axis could be used.

Considering the case for which the disturbing torque acts at an angle of 45 degrees with respect to the pitch and yaw axes, components of disturbing torque whose magnitudes are  $(0.7) (3\sigma_{\Delta T})$  act about each axis. Assuming that on-time is proportional to the torque about each axis the required total impulse is

$$I_t = (25) (0.7 + 0.7) (35) = 1225 \text{ lb-sec}$$

## 2.2 Roll Control

The disturbing torque in roll is given by

$$T_{d\phi} = F_e l_\phi \sin \epsilon \quad (9)$$

where

$$l_{\phi} = 3\text{-sigma value of c. g. offset } (3\sigma_{\Delta_{cg}})$$

$$\epsilon = 3\text{-sigma value of angular misalignment } (3\sigma_{\Delta_{\xi}})$$

For the values stated in section 2.1 we have

$$T_{d\phi} = 1.2 \text{ ft-lb.}$$

To balance this requires a minimum thrust of 0.16 pound. Multiplying this value by 1.4 to improve dynamic response the thrust becomes 0.22 pound. This value is well under the thrust of the cold-gas roll nozzles, so they are used for roll control during thrusting.

The total impulse required is

$$I_t = 0.22 \times 35 = 7.7 \text{ lb-sec}$$

A value of 10 lb-sec is allowed in the impulse summary.

## APPENDIX L

### REFERENCE DESIGN SOLID PROPELLANT SYSTEM SIZING CALCULATIONS

This Appendix contains calculations for the hot-gas system used for the reference design Flight Capsule entry from orbit (see paragraph 8.3.2.2).

#### 1.0 GENERATOR REQUIREMENTS (EACH)

- (1) Total Thrust Rating = 25 pounds
- (2) Operating Time = 35 seconds
- (3) Impulse/Generator = 875 lb-sec

#### 2.0 ASSUMPTIONS

- (1) Generator operating pressure  $p_g = 2500 \text{ lb/in.}^2$
- (2) Combustion temperature  $T_g = 2460^\circ\text{R}$
- (3) Nozzle inlet gas temperature  $= T_c = T_g/2 = 1230^\circ\text{R}$
- (4) Propellant selected - OMAX 453D
- (5) Isentropic flow through the nozzles is assumed.

#### 3.0 GENERATOR METERING ORIFICE SIZE

The area of the generator metering orifice throat section is expressed as:

$$A_g = \frac{F}{p_g C_2} \sqrt{\frac{T_g}{T_c}}$$

where

$A_g$  = metering orifice throat area ( $\text{in.}^2$ )

$F$  = generation thrust rating (pounds)

$$C_2 = \text{a constant} = k \sqrt{\frac{2}{k-1} \left[ \frac{2}{k+1} \right]^{\frac{k+1}{k-1}}} = 1.97$$

$k$  = ratio of specific heats = 1.3 for OMAX 453D

Substituting:

$$A_g = \frac{25 \sqrt{2}}{2500 (1.97)} = 7.2 \times 10^{-3} \text{ in}^2$$

the metering orifice diameter is

$$d_g = \sqrt{\frac{4}{\pi} \times 7.2 \times 10^{-3}} = 0.0956 \text{ inch.}$$

#### 4.0 PROPELLANT DIMENSIONS

For OMAX 453D propellant initially at  $-100^\circ\text{F}$  and burning at  $2500 \text{ lb/in.}^2$ , the following generator parameters are known:

$$\text{burn rate} = 0.08 \text{ in./sec}$$

$$\frac{\text{burn surface area}}{\text{metering orifice area}} = 5000$$

The burn surface area is therefore  $5000 A_g$  or

$$5000 (7.2 \times 10^{-3}) \text{ in.}^2 = 36.0 \text{ in.}^2$$

Therefore a cylindrical generator design with two diametrical surfaces burning simultaneously will have a transverse section of:

$$36.0/2 = 18 \text{ in.}^2$$

$$\text{The propellant diameter} = \sqrt{\frac{4}{\pi} 18} = 4.78$$

Since each surface must burn for 35 seconds, the propellant length is calculated to be:

$$\text{Propellant length} = 2(35)(.08) = 5.6 \text{ inches.}$$

#### 5.0 PROPELLANT WEIGHT

The volume of propellant is:

$$5.6 \times 18 = 100.8 \text{ in.}^3$$

and with a density of  $0.053 \text{ lb/in.}^3$  the propellant weight is:

$$100.8 \times 0.053 = 5.35 \text{ pounds.}$$

## 6.0 PROPELLANT CASE WEIGHT

The weight of the generator case is written as

$$W_c = \left[ \frac{\pi \rho P_g d_p}{4\sigma} + \frac{\pi \rho P_g l_p}{2\sigma} \right] d_p^2$$

where

$$\rho = \text{density of the case material} = 0.28 \frac{\text{lb}}{\text{in}^3} \text{ (steel)}$$

$$\sigma = \text{working stress level of case material}$$

$$l_p = \text{propellant length}$$

$$d_p = \text{propellant diameter}$$

Let the propellant length equal 6 inches to allow for ignitor packaging.

A maraging steel with a maximum hoop stress of 77,000 lb/in.<sup>2</sup> is selected.

Substituting,  $W_c$  is calculated as:

$$W_c = \left[ \frac{4.78}{4} - \frac{6}{2} \right] \frac{(4.78)^2 (3.14) (0.28) (2500)}{77,000} = 2.0 \text{ pounds.}$$

## 7.0 COMPLETE GENERATOR SIZE AND WEIGHT

The case wall thickness is expressed as

$$t = \frac{P_g d_p}{2} = \frac{2500 \times 4.78}{2 \times 77,000} = 0.078 \text{ inch.}$$

The generator dimensions are now defined as:

$$\text{OD} = 4.78 + 2(0.078) = 4.94 \text{ inches}$$

$$\text{Length} = 6.00 + 2(0.078) = 6.16 \text{ inches.}$$

Assuming that the ignitor material weight is 0.37 pound, the total generator weight is found to be:

$$W_g = 0.37 + 5.40 + 2.00 = 7.77 \text{ pounds.}$$

## 8.0 SOLENOID NOZZLE VALVE PARAMETERS

The solenoid valve is sized with an equivalent sharp-edged orifice larger than the nozzle throat size to minimize pressure drops. The relation between generator metering orifice area and nozzle throat area is given:

$$\frac{A_n}{A_g} = \frac{P_g}{P_c} \sqrt{\frac{T_c}{T_g}}$$

Assuming a nozzle inlet pressure of 1000 lb/in.<sup>2</sup>

$$\frac{A_n}{A_g} = \frac{2500}{1000} \sqrt{0.5} = 1.765$$

Substituting

$$A_g = 7.2 \times 10^{-3} \text{ in.}^3$$

$$A_n = 1.765 \times 7.2 \times 10^{-3} = 12.7 \times 10^{-3} \text{ in.}^2$$

$$d_n = \sqrt{\frac{4}{\pi} \times 12.7 \times 10^{-3}} = 0.127 \text{ inch}$$

A valve with 0.3-inch diameter equivalent sharp-edged orifice should be adequate. The Philco Corporation, P/N SK20230 (modified Minuteman Control Valve), is taken as the reference design. The valve weight is given as 0.52 pound.

## 9.0 TOTAL SYSTEM WEIGHT BREAKDOWN

Item	Nomenclature	Unit Weight (pounds)	No. Required	Total Weight
1.	Gas Generator Assembly	7.77	4	31.1
2.	Solenoid Nozzle Valve	0.52	8	4.2
3.	Tubing, Brackets, etc.			5.0
Total				40.3 pounds